VIETNAM JOURNAL OF HYDRO - METEOROLOGY

ISSN 2525 - 2208

VIETNAM METEOROLOGICAL AND HYDROLOGICAL ADMINISTRATION

No 13
12-2022

Publishing licence
No: 166/GP-BTTTT - Ministry of Information and Communication dated 17/04/2018

Editorial office
No 8 Phao Dai Lang, Dong Da, Ha Noi
Tel: 024.39364963
Email: tapchikttv@gmail.com

Engraving and printing
Vietnam Agriculture Investment Company Limited
Tel: 0243.5624399

VIETNAM JOURNAL OF HYDROMETEOROLOGY
Volume 13 - 12/2022

TABLE OF CONTENT

VIETNAM JOURNAL OF HYDROMETEOROLOGY

Research Article

Microplastics and solutions to remove microplastics in wastewater from wastewater treatment plants in the Saigon–Dong Nai river basin, Vietnam

Huynh Phu[1*], Huynh Thi Ngoc Han[2], Nguyen Ly Ngoc Thao[1], Tran Thi Minh Ha[3]

[1] HUTECH University; h.phu@hutech.edu.vn
[2] Ho Chi Minh University of Natural Resources and Environment, Ho Chi Minh City, Vietnam; htnhan_ctn@hcmunre.edu.vn;
[3] Tay Nguyen University, Buon Ma Thuot – Dak Lak, Vietnam; ttmha@ttn.edu.vn

*Corresponding author: h.phu@hutech.edu.vn; Tel.: +84–966687548

Received: 05 October 2022; Accepted: 29 November 2022; Published: 25 December 2022

Abstract: The article studies the occurrence of microplastics in the inlet and outlet wastewater streams at wastewater treatment plants in the Saigon-Dong Nai river basin, Vietnam and provide a suitable removal solution. The sampling method is suitable for the actual conditions of Vietnam combined with the application of Fourier-transform infrared spectroscopy to analyze the microplastic composition in the sample. The results show that microplastics exist in many different shapes and colors. Density of microplastics in the inlet stream is from 10.188-15.074 gL^{-1}. Density of microplastics in the outlet stream is from 0.684-2.107 gL^{-1}. In which, filaments with an average length of 524.68 μm and an average radius of 100.4 μm; slender form with an average length of 229.49 μm and an average width of 101.3-120.6 μm; granules with an average radius of 113.81μm. The removal efficiency of microplastics in the wastewater stream at the surveyed wastewater treatment plants ranges from 85.4% to 93.7% through the following main processes: pre-settlement, flotation, moving bed biofilm reactor, sedimentation, filtration. Solutions for the removal of microplastics from wastewater treatment plants in the Saigon - Dong Nai river basin were proposed and discussed.

Keyword: Microplastic; Saigon–Dong Nai river; Wastewater; Wastewater treatment plant.

1. Introduction

Plastic waste has received a lot of attention over the years. The rest of this plastic waste through flows, leaks and discharges wastewater into rivers, seas and lakes, etc [1]. Plastic packaging products for food, beverage and medicinal items are often used only once, which contributes to 61% of the litter on global beaches [2]. Disposable single-use plastic products enter the waste stream shortly after use, contributing to the cumulative accumulation of more than 6.3 billion tons of plastic waste generated worldwide. Only 9% of plastic waste has been recycled globally. Meanwhile, the majority of global plastic waste is either landfilled or ended up polluting the environment (80%). This has resulted in an estimated 4 million to 12 million tons of plastic ending up in the oceans annually [3]. Since 2019, almost the whole world has been, is and will have to struggle with a global pandemic - Covid 19. The World Health Organization has requested a 40% increase in disposable PPE production [4]. If the average global population uses one disposable mask per day, this could lead to monthly global consumption and waste of 129 billion masks and 65 billion gloves [5]. The prolonged

Covid-19 pandemic has caused profound impacts on all aspects of social life, including plastic waste [6]. This pandemic has increased plastic waste [7].

Recent research has shown that in the top ten countries ranked for using plastic in daily life and production, there are eight countries originating from Asia, of which Vietnam ranks 4th [8]. In Vietnam, between 2000 and 13,000 tons of floating plastic debris is collected annually in the main urban canals [9].

Microplastics are persistent, non-biodegradable and cannot be recovered for recycling like large pieces of plastic. Once microplastics are introduced into the environment, they are very difficult to remove. Their classification depends on the intended use of the original plastic. There are many ways to classify. One of them is to classify them using different symbols, including the recycling symbol on the products [10]. Based on size, microplastics are classified as: Macroplastics, Microplastics and Nanoplastics [11].

Wastewater from domestic and industrial activities has been proven to have microplastic pollution. Industrial wastewater and water treatment plants are a major source of microplastic pollution in freshwater ecosystems. Water treatment plants are almost “collection points” of microplastic pollution that are released into the receiving water environment [12-16]. Currently, Vietnam has concluded about the presence of microplastics in the surface water environment and the results discussed about their risk to human health [17].

Wastewater flow under the active control of human is through many different treatment technologies. Following that process, microplastics will be removed. The study by Bayo et al demonstrated that microplastics are removed when the wastewater flows through the primary sedimentation chamber [18]. In addition, microplastics in the waste stream are also removed when going through the stages of flotation [19-20], coagulation, filtration processes such as sand filtration, activated carbon, membrane filtration [21-22], and sludge. activity [23] or membrane technology Membrane Bioreactor (MBR) [24]. To date, relevant evaluation studies have also been published such as the relationship of microplastics and the wastewater treatment system [25] and water ozonation [26]. In general, the removal of microplastics with each treatment technology is still not clear, but the analysis results of microplastics in the inlet and outlet streams of the wastewater treatment system have been published a lot.

Research on microplastic treatment in the world has been carried out by many countries with effective removal: Finland (99.4%), Sweden (99.9%), France (83%-95%), Netherlands (72%), American (99.9%), Germany (97%), Australia (99%), England (98%), Italy (84%), China (97.2%), Russia (95.6%) [27]. The efficiency of removing microplastics from the wastewater stream of some key processes in the wastewater treatment plant: level 1 treatment (58.6%), level 2 treatment (84.1%), level 3 treatment (93.8%) [28-29].

There have been a number of proposed technological schemes to remove microplastics in wastewater such as: diagram of flocculation settling process [30]; diagram of removing microplastics by Anaerobic tank, Anoxic tank, Aerobic tank and Sediment tank [31]; diagram of microplastic collection by pump and filter device [31] or flowcharts for removing microplastics from waste streams with level 1 treatment, level 2 treatment and level 3 treatment processes [24, 32-35]. The objectives of this study are to evaluate the occurrence of microplastics in some wastewater treatment plants in the Saigon - Dong Nai river basin and to propose technical process for removal microplastic.

2. Materials and methods

2.1. Sample collection

Currently, microplastic researchers usually take water samples by using plankton sampling nets to collect surface water samples containing microplastics based on NOAA’s Ocean microplastic sampling method [36]. The plankton net sampling method is very suitable

for the surface water environment of the ocean, the sampling space is large, the boat connected to the net with the required speed is easy to use. Nonetheless, with the condition of surface water inland rivers of Vietnam, the author takes the sampling method more suitable for the actual conditions as follows:

- At locations with open conditions in the river basin (about 20-50 m from the outlet of wastewater treatment plants in the river basin, depending on actual conditions), surface water samples were collected using a 1×1 m^2 Newton grid, 500 µm meshed meshes 3 meters long. The grids are placed side by side connected by aluminum bars at the top and bottom. The net is connected to the boat by steel wire and a large hook with a flow meter attached, which is used to measure the water velocity at the time of sampling.

- At collection pits or sewers that collect wastewater before entering treatment plants, we use Bucket with wide mouth design to easily scoop surface water (water level thickness is about 30-50 cm from water surface). The water sample consisting of microplastics, impurities and coarse garbage is poured through a sieve of size 0.6-5 mm with a diameter of 300 mm made of 304 stainless steel, passing through the funnel and into the sample containers.

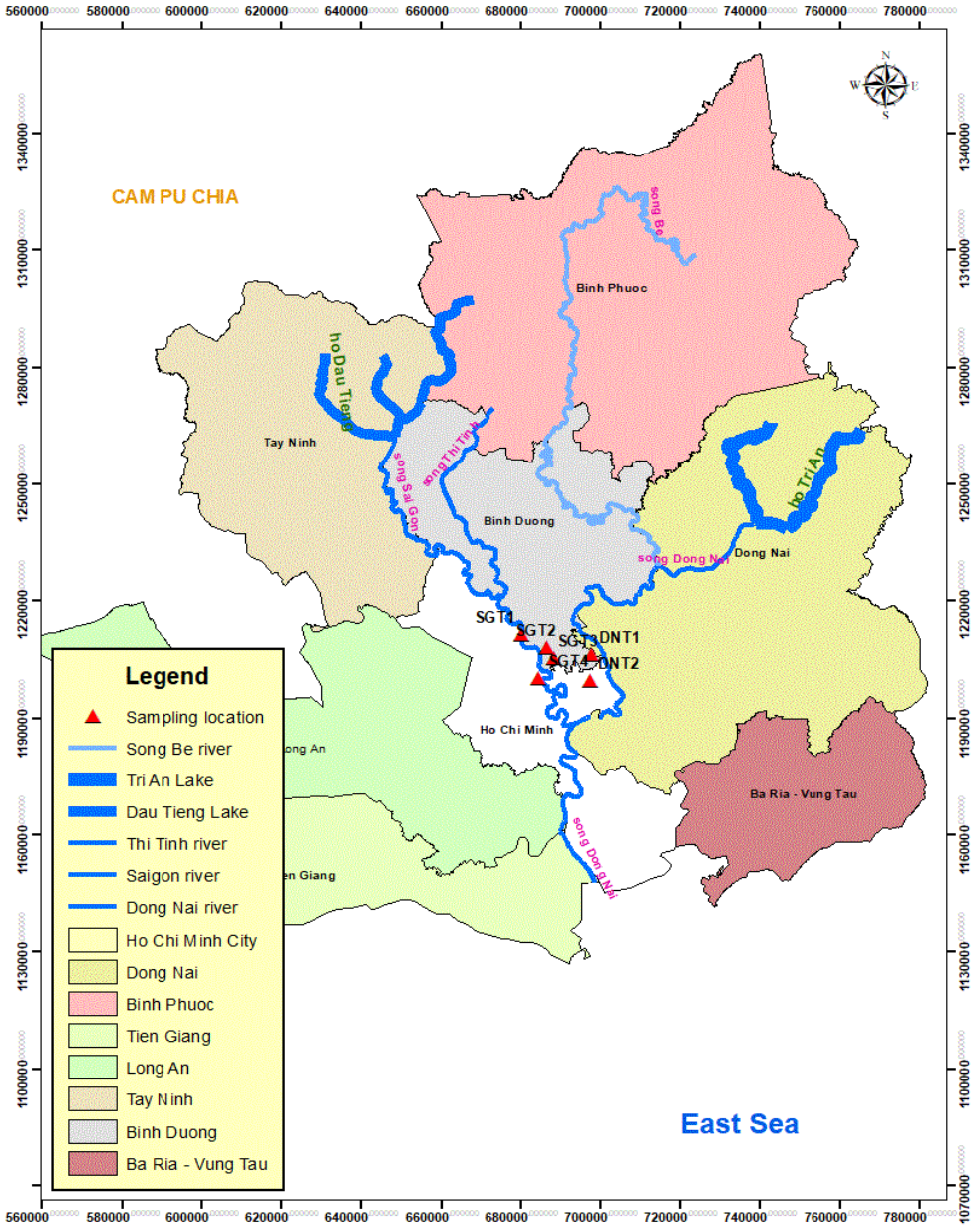

Figure 1. Location map of surveyed wastewater treatment plants.

These surface water sampling locations are flow locations that can carry large amounts of plastic waste from the upper Saigon river and Dong Nai river flowing through densely populated residential areas and industrial zones of Ho Chi Minh City and Binh Duong province. Survey and water sampling were carried out at 6 wastewater treatment plants in the Saigon - Dong Nai river basin, the symbols for the wastewater treatment plants are SGT1, SGT2, SGT3, SGT4, DNT1, DNT2 (Figure 1). The author selected the above 6 wastewater plants for sampling because these plants are located in the area near the end of the Saigon - Dong Nai river basin, at the confluence of 2 rivers. This area is densely populated. These treatment plants mainly treat domestic wastewater for residents of HCM and Binh Duong and have the receiving source in the Saigon-Dong Nai river basin.

Samples will be taken at 02 locations of 6 factories: at the pits and culverts collected before entering the plant and about 20-50m away from the outlet of wastewater treatment plants in the river basin, depending on actual conditions. Sampling time is about 30 minutes per site at low tide. The number of samples to be taken at each location is 2 samples. Sampling frequency is every 6 months in the dry and rainy seasons of the year. In Vietnam, the rainy season is from May to December and the dry season from January to April. Each sample collected at least 2 liters of wastewater containing microplastics. All samples were shipped to the laboratory of Nation Lab Ho Chi Minh City and Phu My Institute of Technology Development for Environment and Water Resources.

2.2. Process of analyzing microplastics in wastewater samples

The collected samples were carefully packed and preserved by the research team in Styrofoam containers before they were transported to the laboratory for analysis (Figures 2a–2b).

Figure 2. (a) Ba Bo canal – Binh Duong, where waste containing microplastics from wastewater treatment plants is discharged; (b) Water samples are ready to be sent to the microplastic analysis laboratory.

Water and sediment samples were coded and stored in Styrofoam and sent to the laboratory for analysis. The process of sample processing and microplastic observation was carried out by the research team according to the steps shown in Figure 3.

Samples after removing coarse impurities larger than 5 mm were dried at 60^{o}C for 24–48 hours. Samples after drying were sieved through 0.3 mm sieve to remove components smaller than 0.3 mm. Samples after 0.3 mm sieving were put into glass tubes (250 mL) and labeled to prepare for decomposition of organic compounds. 20 mL of 30 % H_2O_2 (hydrogen peroxide) solution and 0.05M $FeSO_4$ (Fe II) solution were added to the apparatus (beaker). Let the mixture sit at room temperature for 5 minutes before continuing. The mixture was stirred well, and gently heated on an electric stove 15 minutes (when air bubbles are observed on the surface, remove the beaker from the hotplate and place it in the fume hood until

reduced). The mixture was further heated for an additional 30 min. Continue adding another 20 mL of 30% hydrogen peroxide as the reaction changes color from amber to pale yellow.

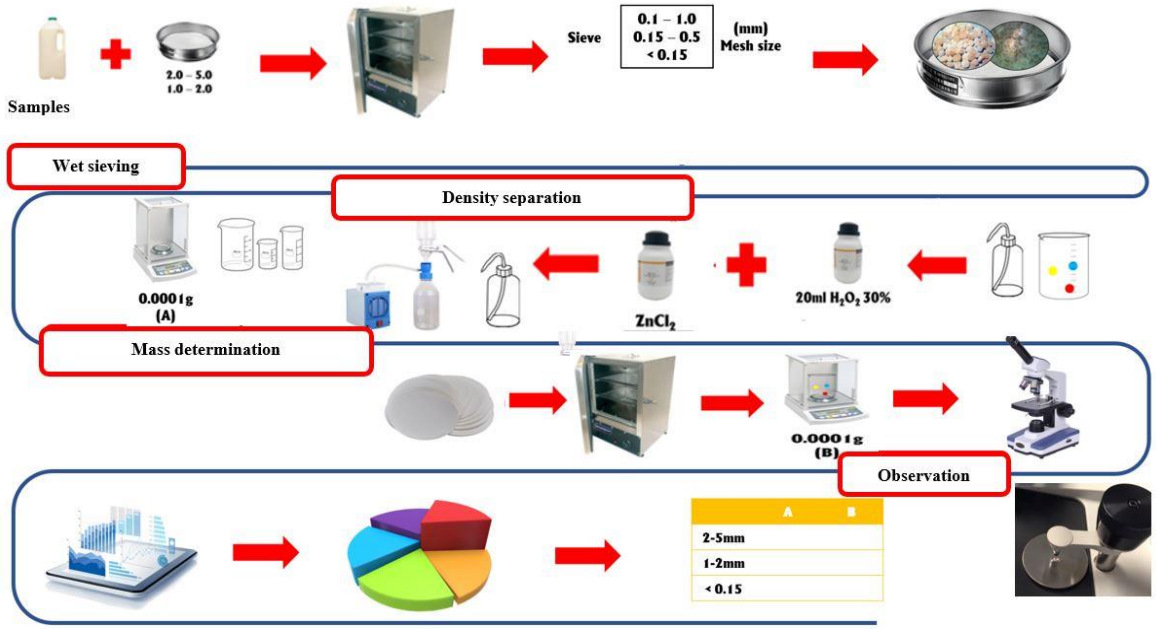

Figure 3. Process of analyzing microplastics in wastewater samples.

To separate minerals and metals: slowly add $ZnCl_2$ solution (d = 1.6 gmL^{-1}) to the sample mixture, stir well, then continue to add $ZnCl_2$ solution in the tube to increase the density of the sample solution. This mixture was put into a centrifuge with a rotational speed of 2500 RCF per min 03 times, for 5 minutes each time to separate microplastics from metals and minerals. Microplastics with a low density will float to the surface of the $ZnCl_2$ solution (minerals and metals with density larger than 1.4 gmL^{-1} will sink at the bottom of the mixture). The supernatant of the mixture was kept for further analysis. The $ZnCl_2$ solution containing microplastics floating above was filtered through the Nalgene vacuum filtration system and used a Milipore reticular filter with 47 mm diameter, 0.45 µm pore size, 3.1×3.1 mm per cell size. Filters were dried and weighed to the nearest 0.1 mg (A_1). The filter is then gently removed and wrapped in aluminum foil bags, dried for about 18–24 hours. The filter after drying is balanced with an accuracy of 0.1 mg (A_2).

Weight of microplastics:

$$A = A_1 - A_2 \quad (1)$$

The identification of microplastics was facilitated using a Fourier transform infrared (FTIR) spectrophotometer.

2.3. Microplastic analysis method by Fourier–transform infrared spectroscopy (FTIR)

FTIR microscopes are generally dedicated to measuring specified samples such as small contaminants on polymer films or microscopic samples transferred to infrared transparent windows. The obtained spectra are compared with internal spectral libraries to find the closest match and determine the chemical composition. A match of 70% or more is considered sufficient for confirmation. The research team applied the FTIR method to determine the microplastic composition in the sample through the spectral peak data obtained when running the sample.

For FTIR analysis, sample vials were washed and poured into a clean, dry, labeled petri dish (separated by size fraction) and placed in a 50°C oven until the petri dish and dry contents. The individual beads were then removed from the petri dish using a microscope (Leica EZ4HD, 8–40× zoom, built–in 3Mpixel camera) and placed on the FTIR (PerkinElmer

Spectrum Two ATR; 450/cm to 4000/cm, 64) scans, resolution 4/cm). The FTIR analysis procedure of the authors is carried out as shown in Figure 4.

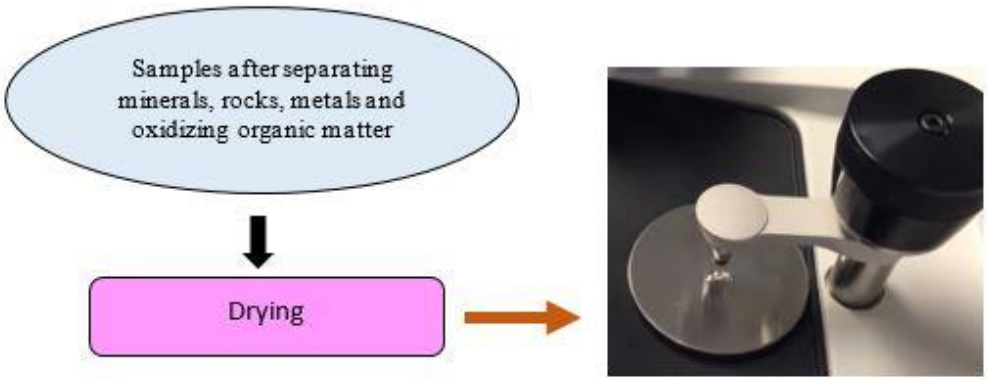

Figure 4. Microplastic analysis procedure by FTIR method.

2.4. Nile Red staining and identification of microplastics by fluorescence microscopy

Fluorescence microscope is a type of biological microscope, which helps to observe the fluorescent light from the specimen after being excited by light from a mercury lamp. When combined with additional equipment, brightfield microscopes can also perform fluorescence imaging. The Nile Red staining method is an alternative to solving the problem of small and transparent microplastics: using the fluorescent dye Nile Red (9–diethylamino5H–benzo[α]phenoxazine–5–one), a strong fluorescence for hydrophobic objects for staining microplastics. The purpose of the Nile Red staining method is to make the resin particles glow more clearly when viewed under a fluorescence microscope. This method helps us to determine the size and density of microplastics in the sample by counting and measuring the size of the luminous particles on the filter paper [35] (Figure 5).

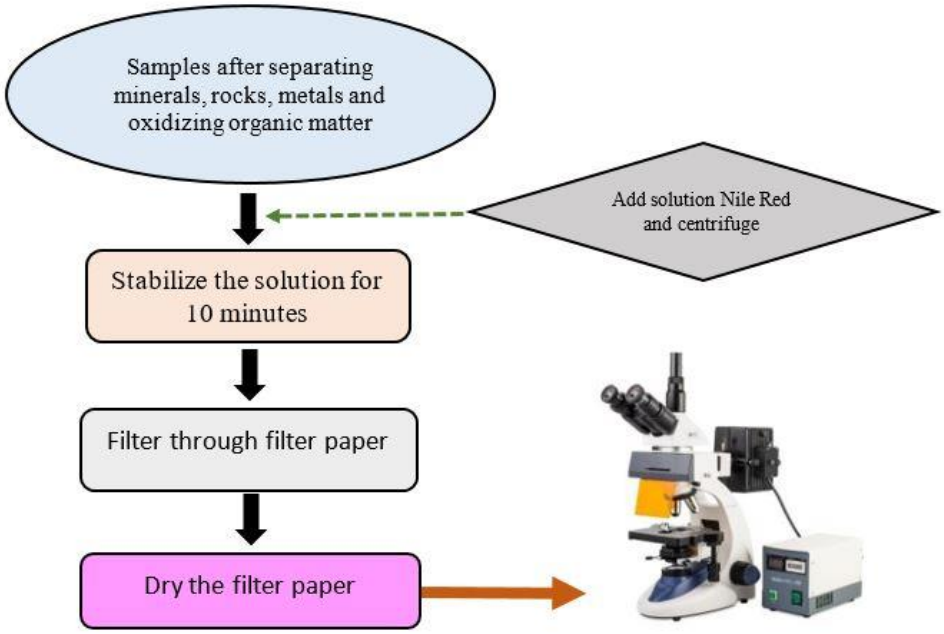

Figure 5. Procedure for analyzing microplastic samples by fluorescence microscopy.

2.5. Method of determining microplastics by stereomicroscopy

The stereo microscope allows for easy 3–D visualization of specimens in their natural state without the need to cut them out. Magnification is usually between 10 and 50 times. The purpose of applying a stereo microscope is that we can observe a 3–D image of the

specimen at low magnification. The shape and color of the microplastics were recorded (Figure 6).

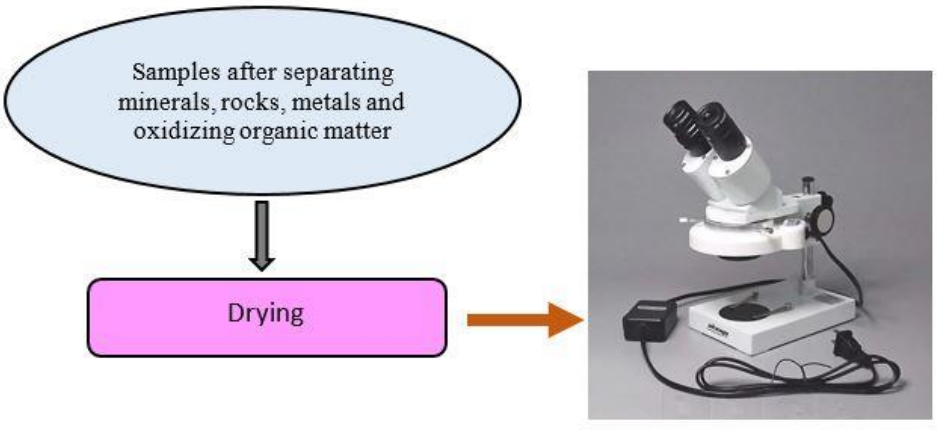

Figure 6. Microplastic analysis process by stereo microscope.

3. Results and discussion

3.1. The results of analysis of microplastics

The results of analysis of microplastics in the inlet and outlet effluents of the domestic wastewater treatment process of some factories in the Saigon–Dong Nai river basin are shown in Table 1.

Table 1. Microplastics in the inlet and outlet waste streams of domestic wastewater treatment in some factories in the Saigon–Dong Nai river basin.

No.	Wastewater plant	Sample symbol	Density of microplastics in the inlet stream (gL^{-1})	Density of microplastics in the outlet stream (gL^{-1})	Removal performance (%)
1	Nam Binh Duong wastewater treatment plant	SGT1	14.432	2.107	85.4
2	Wastewater treatment plant VSIP Industrial Park 1	SGT2	10.188	1.114	89.1
3	Ba Bo Water treatment station	SGT3	12.229	1.516	87.6
4	Tham Luong – Ben Cat wastewater treatment plant	SGT4	15.074	1.749	88.4
5	Di An wastewater treatment plant	DNT1	12.986	1.286	90.1
6	Wastewater treatment plant of Ho Chi Minh City Hi–Tech Park	DNT2	10.851	0.684	93.7
	Average performance				**89.1**

Apply a combination of modern microplastic identification methods to be able to more accurately determine microplastic components, more effectively for colorless, transparent, detectable microplastics including microplastics have small and microscopic sizes (Figures 7–10).

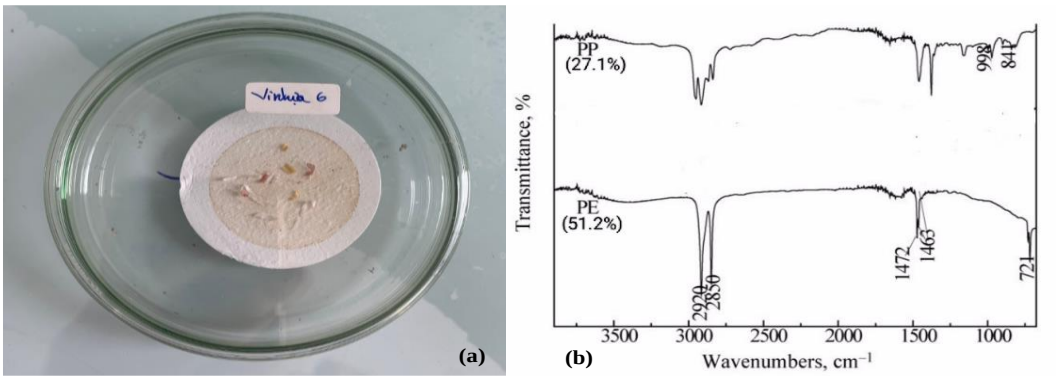

Figure 7. (a) Microplastics were found in the wastewater sample of one wastewater treatment plant (Di An wastewater treatment plant); (b) Spectrum of identification of Polypropylene (PP) and Polyethylene (PE) resins in water by FTIR.

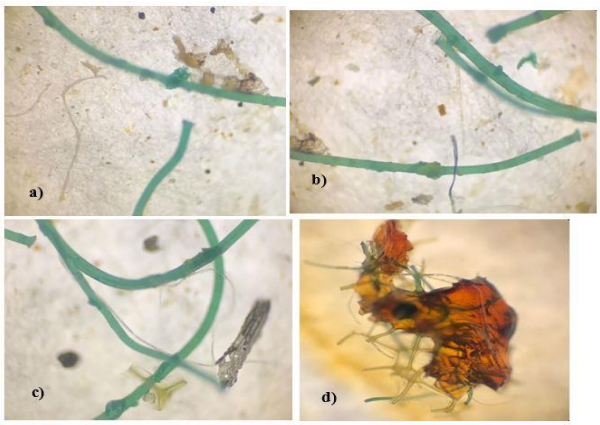

Figure 8. Microscopic filaments under the stereo microscope: (a) Fibrous microplastics are mostly blue > white; (b, c) Microplastics in the form of Fibers of different sizes, blue; d) Microplastic in the form of yellow filaments tangled.

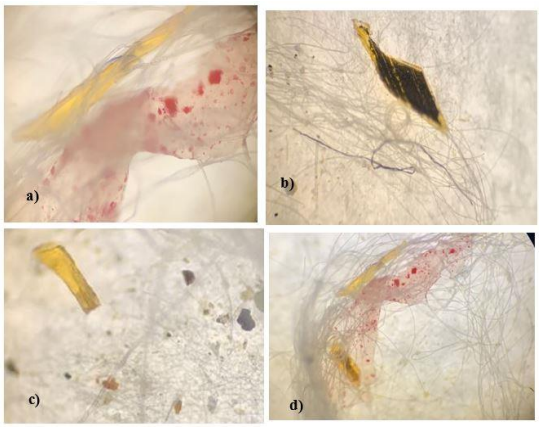

Figure 9. Microplastics in the form of a stereo microscope: (a, b, c) Microplastics of different sizes yellow > green > white; (d) Yellow microplastics surrounded by white fibers.

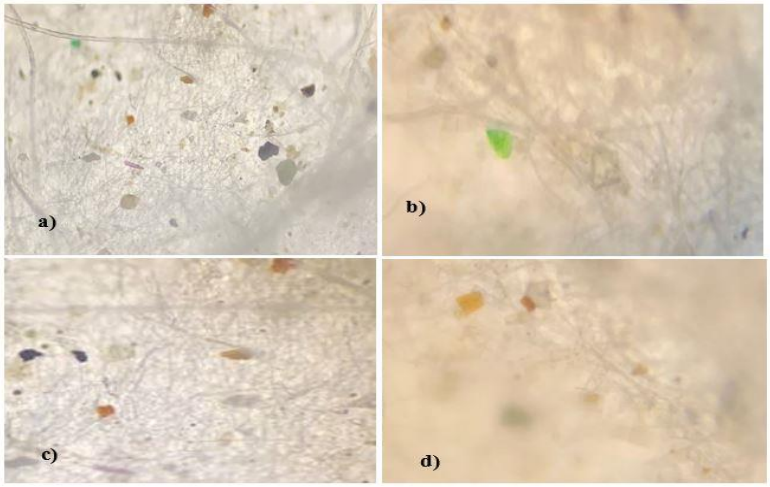

Figure 10. Microplastic granules under a stereo microscope: a) Microplastics with black> blue>white particles; b) Microplastics are green; c) Many microplastics are mixed in white filamentous microplastics; d) Microplastic particles are white.

- The filamentous microplastic has an average length of 524.68 μm and an average radius of 100.4 μm.

- Flake microplastics have an average length of 229.49 μm and an average width of 101.3–120.6 μm.

- Granular microplastics have an average radius of 113.81μm.

Microplastics in the output of domestic wastewater treatment at Sai Gon–Dong Nai river wastewater treatment plants are shown in Table 2.

Table 2. Microplastics in the output stream of domestic wastewater treatment at wastewater treatment plants on Saigon–Dong Nai river.

Number	Wastewater plant	Sample symbol	Fiber form (MPs/Sample)	Flake form (MPs/Sample)	Granular form (MPs/Sample)
1	Nam Binh Duong wastewater treatment plant	SGT1	13	15	12
2	Wastewater treatment plant VSIP Industrial Park 1	SGT2	187	11	15
3	Ba Bo Water treatment station	SGT3	13	55	12
4	Tham Luong – Ben Cat wastewater treatment plant	SGT4	410	13	73
5	Di An wastewater treatment plant	DNT1	10	20	0
6	Wastewater treatment plant of Ho Chi Minh City Hi–Tech Park	DNT2	4	11	2

After the samples were analyzed by the FTIR method, the microplastics in the samples showed that PE accounted for 51.2%, PP accounted for 27.1%, PVC accounted for 13.4% and 8.3% were other plastics. The results of applying analytical methods in Vietnamese conditions show that microplastics have many colors, shapes and very small sizes; microplastics in the form of thin granules, filaments and microplastics ranging in size from 0.1–5 mm.

3.2. Solution for removal microplastics

The technological diagram proposed by the authors to remove microplastics is shown in Figure 11. This diagram is proposed by the author to be applied to domestic wastewater treatment plants to remove microplastics in domestic wastewater; specifically, domestic wastewater of residents on both sides of the Saigon–Dong Nai river basin.

Wastewater containing microplastics from sources is collected into the sump, then transferred to a grease separation tank to remove the amount of grease floating on the water to avoid clogging the pump system and the rear pipeline (this process removes up to 95% microplastics). Wastewater continues to be directed to the conditioning tank to stabilize the flow, concentration and pH balance to suit the operating conditions of microorganisms. After regulating the flow and concentration, the wastewater is transferred to the moving bed biofilm reactor (MBBR) tank to treat organic substances in the water. The outstanding advantage of the MBBR tank is that it saves space and has the ability to handle very well the polluting criteria in wastewater (more than 99% of microplastics are removed). To treat BOD, wastewater is pumped through an aerotank, where an aerator is arranged to create favorable conditions for aerobic microorganisms to grow and increase BOD treatment capacity. Next, the wastewater is taken to a settling tank to settle microbial sludge, where the collected microbial sludge is transferred to a sludge tank and periodically treated by drying or then used as fertilizer. 98% of microplastics are removed as they bind to suspended solids and are separated by sedimentation. Part of the activated sludge will be recycled to the MBBR tank for further treatment.

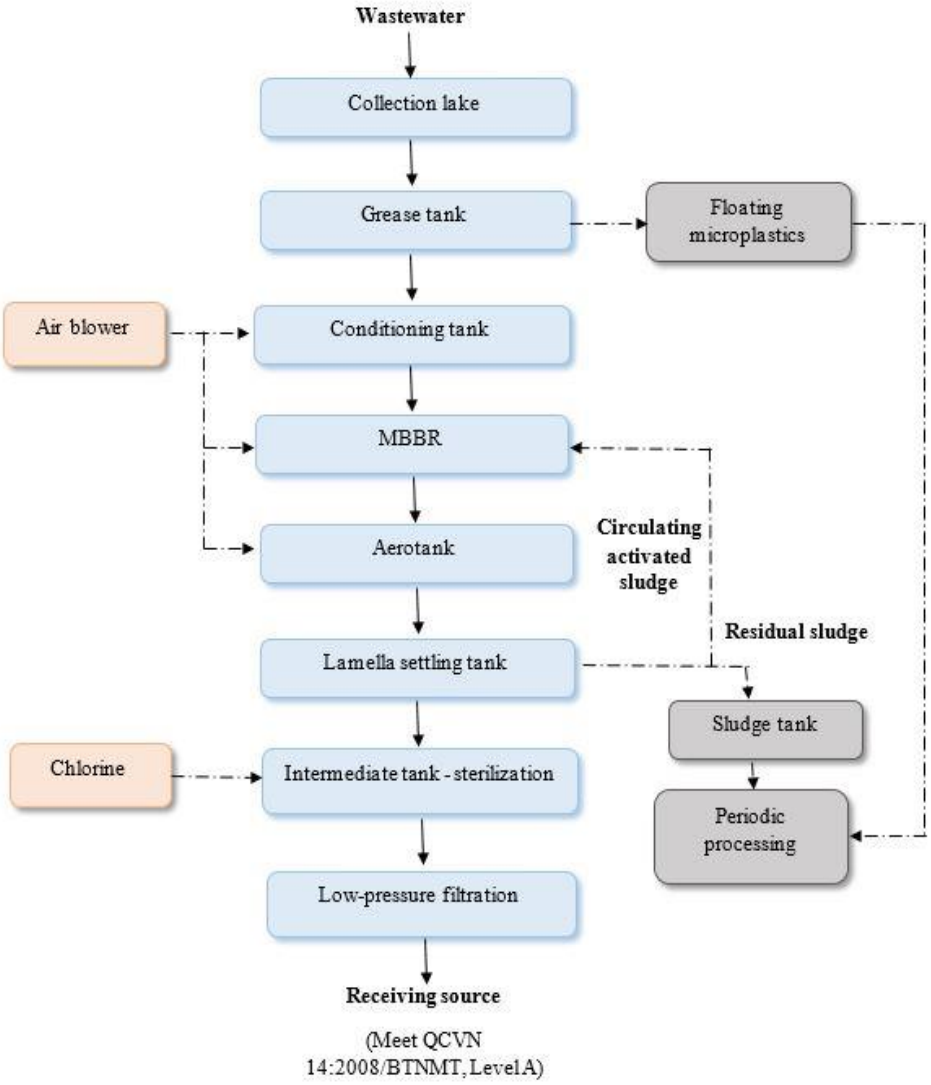

Figure 11. Flowchart of domestic wastewater treatment technology and microplastic removal in wastewater stream.

Wastewater after sludge separation is transferred to a disinfection tank to eliminate all harmful bacteria with chlorine chemicals, then to a pressure filter tank to remove the remaining small residues before being discharged to the receiving source; after being processed to meet QCVN 14:2008/BTNMT column A standards.

Some limitations:

- Requires operator experience;
- Sludge can occur behind the MBBR system according to the biofilm cycle, leading to reduced settling efficiency, reducing microplastic removal efficiency.

4. Conclusion

The average removal efficiency of microplastics in wastewater of treatment plants is from 85.4% to 93.7% through the following processes: pre-settlement, flotation, MBBR, settling and filtration. The development of techniques to remove microplastics from water is necessary to prevent some of the health problems stemming from microplastics. Although the unit works in wastewater treatment technology can partially remove microplastics from the waste stream, but the challenges of technology, minimum cost, efficiency of other components should also be considered in conjunction.

Nonetheless, the limitation of the study is that it is not possible to sample wastewater in each work of the wastewater treatment system. Therefore, the research results only stop at the general assessment of the microplastic removal efficiency of the whole processing when the wastewater flows in and out of the wastewater treatment plant.

Authors contribution. Construction research idea: H.P., H.T.N.H.; Select research methods: H.P., H.T.N.H., N.L.N.T.; T.T.M.H.; Data processing: H.P., H.T.N.H., N.L.N.T.; Sample analysis: H.P., H.T.N.H., N.L.N.T.; Take samples: H.T.N.H., N.L.N.T.; T.T.M.H.; Writing original draft preparation: H.P., H.T.N.H.; N.L.N.T.; T.T.M.H.; Writing review and editing: H.P., H.T.N.H.

Acknowledgments. This study was carried out under the sponsorship of the research project Microplastics in surface water and sediments of Saigon – Dong Nai rivers, of Phu My Institute of Technology Development for Environment and Water Resources.

Conflicts of interest. The authors declare that this article was the work of the authors, has not been published elsewhere, has not been copied from previous research; there was no conflict of interest within the author group.

References

1. Barnes, DK.A.; Galgani, F.; Thompson, R.C.; Barlaz, M. Accumulation and fragmentation of plastic debris in global environments. *Philos. Trans. Royal Soc. B: Biol. Sci*, **2009**, *364(1526)*, 1985–1998.
2. Brooks, A.L.; Wang, S.; Jambeck, J.R. The Chinese import ban and its impact on global plastic waste trade. *Sci. Adv.* **2018**, *4(6)*, 1–8. https://doi.org/10.1126/sciadv.aat0131.
3. Jambeck, J.R.; Geyer, R.; Wilcox, C.; Siegler, T.R.; Perryman, M.; Andrady, A.; Narayan, R.; Law, K.L. *Entradas de residuos plásticos desde la tierra al océano. Ciencia*, **2015**, *347(6223)*, 768–771. http://www.sciencemag.org/cgi/doi/10.1126/science.1260879%0Ahttps://www.sciencemag.org/lookup/doi/10.1126/science.1260352.
4. WHO. Shortage of personal protective equipment endangering health workers worldwide. World Healthy Organization, 2020. https://www.who.int/news/item/03-03-2020-shortage-of-personal-protectiveequipment-endangering-health-workers-worldwide.
5. Yudell, M.; Roberts, D.; DeSalle, R.; Tishkoff, S. NIH must confront the use of race in science. *Science* **2020**, *369(6509)*, 1314–1315. https://doi.org/10.1126/SCIENCE.ABD9925.
6. La, V.P. Policy response, social media and science journalism for the sustainability of the public health system amid the COVID–19 outbreak: The vietnam lessons. *Sustainability* **2020**, *12(7)*, 2931. https://doi.org/10.3390/su12072931
7. Peng, Y.; Wu, P.; Schartup, A. T.; Zhang, Y. Plastic waste release caused by COVID–19 and its fate in the global ocean. Proceedings of the National Academy of Sciences of the United States of America, 2021, 118(47). https://doi.org/10.1073/pnas.2111530118.
8. Jambeck, J.R.; Geyer, R.; Wilcox, C.; Siegler, T.R.; Perryman, M.; Andrady, A. Plastic waste inputs from land into the ocean. *Science* **2015**, *347(6223)*, 768–771.
9. Kieu Le, T.C.; Strady, E.; Perset, M. Life Cycle of Floating Debris in the Canals of Ho Chi Minh City (PADDI), 2016.
10. Phu, H.; Han, H.T.N. Report of the Workshop "Microplastics in water and sediments of Saigon–Dong Nai river and risks to people's health in Ho Chi Minh City". Hutech Institute of Applied Sciences. Ho Chi Minh City University of Technology, 2021.
11. Raymond, G.; Gireeshkumar, B.; Quentin, D.; Morgan, T.; Alessandro, M.; Maria, G.D.; Onofrio, M.M.; Marc, L.L.C.; Florent, C.; Fabienne, L.; Pietro, G. Gucciardi.

Raman Tweezers as a Tool for Small Microplastics and Nanoplastics Identification in Sea Water. *Environ. Sci. Technol.* **2019**, *53(15)*, 9003–9013. doi:10.1021/acs.est.9b03105.

12. Eerkes–Medrano, D.; Thompson, R.C.; Aldridge, D.C. Microplastics in freshwater systems: A review of the emerging threats, identification of knowledge gaps and prioritisation of research needs. *Water. Res.* **2015**, *75*, 63–82. https://doi.org/10.1016/j.watres.2015.02.012.
13. Mason, S.A.; Garneau, D.; Sutton, R.; Chu, Y.; Ehmann, K.; Barnes, J.; Fink, P.; Papazissimos, D.; Rogers, D.L. Microplastic pollution is widely detected in US municipal wastewater treatment plant effluent. *Environ. Pollut*. **2016a**, *218*, 1045–1054. https://doi.org/10.1016/j.envpol.2016.08.056.
14. Murphy, F.; Ewins, C.; Carbonnier, F.; Quinn, B. Wastewater treatment works (WwTW) as a source of microplastics in the aquatic environment. *Environ. Sci. Technol.* **2016**, *50*, 5800–5808. https://doi.org/10.1021/acs.est.5b05416.
15. Ziajahromi, S.; Neale, P.A.; Leusch, F.D. Wastewater treatment plant effluent as a source of microplastics: Review of the fate, chemical interactions and potential risks to aquatic organisms. *Water Sci. Technol.* **2016**, *74*, 2253–2269. Doi:10.2166/wst.2016.414.
16. Bui, X.T.; Vo, T.D.H.; Nguyen, P.T.; Nguyen, V.T.; Dao, T.S.; Nguyen, P.D. Microplastics pollution in wastewater: Characteristics, occurrence and removal technologies. *Environ. Technolo. Innovation* **2020**, 101013. https://doi.org/10.1016/j.eti.2020.101013.
17. Phu, H.; Han, H.T.N.; Thao, N.L. Plastic waste, microplastics in the Saigon – Dong Nai river basin, the risk of impacts on the health of people. *VN J. Hydrometeorol.* **2022**, *736(1)*,14–27. Doi:10.36335/VNJHM.2022(736(1)).14-27.
18. Bayo, J.; Olmos, S.; López–Castellanos, J. Microplastics in an urban wastewater treatment plant: The influence of physicochemical parameters and environmental factors. *Chemosphere* **2020**, *238*, 124593. http://dx.doi.org/10.1016/j.chemosphere.2019.124593.
19. Talvitie, J.; Mikola, A.; Koistinen, A.; Setälä, O. Solutions to microplastic pollution–Removal of microplastics from wastewater effluent with advanced wastewater treatment technologies. *Water Res.* **2017a**, *123*, 401–407. http://dx.doi.org/10.1016/j.watres.2017.07.005.
20. Talvitie, J.; Mikola, A.; Setälä, O.; Heinonen, M.; Koistinen, A. How well is microlitter purified from wastewater? A detailed study on the stepwise removal of microlitter in a tertiary level wastewater treatment plant. *Water Res.* **2017b**, *109*, 164 172. http://dx.doi.org/10.1016/j.watres.2016.11.046.
21. Hidayaturrahman, H.; Lee, T.G. A study on characteristics of microplastic in wastewater of South Korea: Identification, quantification, and fate of microplastics during treatment process. *Mar. Pollut. Bull.* **2019**, *146*, 696–702. http://dx.doi.org/10.1016/j.marpolbul.2019.06.071
22. Wang, Z.; Lin, T.; Chen, W. Occurrence and removal of microplastics in an advanced drinking water treatment plant (ADWTP). *Sci. Total Environ.* **2020**, *700*, 134520. http://dx.doi.org/10.1016/j.scitotenv.2019.134520.
23. Magni, S.; Binelli, A.; Pittura, L.; Avio, C.G.; Della Torre, C.; Parenti, C.C.; Gorbi, S.; Regoli, F. The fate of microplastics in an Italian wastewater treatment plant. *Sci. Total Environ.* **2019**, *652*, 602–610. http://dx.doi.org/10.1016/j.scitotenv.2018.10.269.
24. Lares, M.; Ncibi, M.C.; Sillanpää, M.; Sillanpää, M. Occurrence, identification and removal of microplastic particles and fibers in conventional activated sludge process

and advanced MBR technology. *Water Res.* **2018**, *133*, 236–246. http://dx.doi.org/10.1016/j.watres.2018.01.049.

25. Zhang, Z.; Chen, Y. Effects of microplastics on wastewater and sewage sludge treatment and their removal: A review. *Chem. Eng. J.* **2019**, 122955. http://dx.doi.org/10.1016/j.cej.2019.122955.
26. Chen, R.; Qi, M.; Zhang, G.; Yi, C. Comparative experiments on polymer degradation technique of produced water of polymer flooding oilfield. *IOP Conf. Ser.: Earth Environ. Sci.* **2018**, 012208. http://dx.doi.org/10.1088/1755-1315/113/1/012208.
27. Habib, R.Z.; Thiemann, T.; Kendi, R.A. Microplastics and wastewater treatment plants–A review. *J. Water. Resour. Prot.* **2020**, *12(1)*, 1–35.
28. Michielssen, M.R.; Michielssen, E.R.; Ni, J.; Duhaime, M.B. Fate of microplastics and other small anthropogenic litter (SAL) in wastewater treatment plants depends on unit processes employed. *Environ. Sci. Water Res. Technol*. **2016**, *2(6)*, 1064–1073.
29. Liu, X.; Yuan, W.; Di, M.; Li, Z.; Wang, J. Transfer and fate of microplastics during the conventional activated sludge process in one wastewater treatment plant of China. *Chem. Eng. J.* **2019**, *362*, 176–182. http://dx.doi.org/10.1016/j.cej.2019.01.033.
30. Lapointe, M.; Farner, J.M.; Hernandez, L.M.; Tufenkji, N. Understanding and improving microplastics removal during water treatment: Impact of coagulation and flocculation. *Environ. Sci. Technol.* **2020**, *54(14)*, 8719–8727. https://doi.org/10.1021/acs.est.0c00712.
31. Liu, W.L.; Wu, Y.; Zhang, S.J.; Gao, Y.Q.; Jiang, Y.; Horn, H.; Li, J. Successful granulation and microbial differentiation of activated sludge in anaerobic/anoxic/aerobic (A^2O) reactor with two–zone sedimentation tank treating municipal sewage. *Water Res.* **2020b**, *178*, 115825. https://doi.org/10.1016/j.watres.2020.115825.
32. Carr, S.A., Liu, J., Tesoro, A.G. Transport and fate of microplastic particles in wastewater treatment plants. *Water. Res*. **2016**, *91*, 174e182.
33. Murphy, F.; Ewins, C.; Carbonnier, F.; Quinn, B. Wastewater treatment works (WwTW) as a source of microplastics in the aquatic environment. *Environ. Sci.Technol.* **2016**, *50(11)*, 5800e5808.
34. Dris, R.; Gasperi, J.; Rocher, V.; Saad, M.; Renault, N.; Tassin, B. Microplastic contamination in an urban area: a case study in Greater Paris. *Environ. Chem.* **2015**. 12(5), 592–599.
35. Michielssen, M.R.; Michielssen, E.R.; Ni, J.; Duhaime, M. Fate of microplastics and other small anthropogenic litter (SAL) in wastewater treatment plants depends on unit processes employed. *Environ. Sci. Water Res. Technol.* **2016**, *2(6)*, 1064-1073.
36. NOAA. Methods for the Analysis of Microplastics in the Marine Environment Recommendations for quantifying synthetic particles in water and sediments. Technical Memorandum NOS–OR&R–48, 2015.

VIETNAM JOURNAL OF HYDROMETEOROLOGY

Research Article

Assessment of the vulnerability to flooding in industrial areas in Bac Ninh Province

Doan Quang Tri[1*], Quach Thi Thanh Tuyet[1], Nguyen Van Nhat[1]

[1] Vietnam Journal of Hydrometeorology, Viet Nam Meteorological and Hydrological Administration; doanquangtrikttv@gmail.com; tuyetkttv@gmail.com; vannhat.tv@gmail.com

*Corresponding author: doanquangtrikttv@gmail.com; Tel.: +84–988928471

Received: 5 September 2022; Accepted: 10 December 2022; Published: 25 December 2022

Abstract: The impact of climate change has become stronger in recent years, climate change has increased hydrometeorological disasters in which flooding is one of the natural disaster risks that have a strong impact on the economy. Bac Ninh province has a lot of industrial zones, thus, the study and assessment of flood damage to Bac Ninh industry is urgent. The study uses Analytical Hierarchy Process (AHP) method to estimate flood damage for industrial areas in Bac Ninh province. This study uses satellite images, land use map and flooded area of Bac Ninh province data to build a matrix to determine the weight of the vulnerability. The study results have calculated the vulnerability weight according to the land use situation, built a vulnerability map for the whole Bac Ninh province and assessment of industrial damage due to flooding for each district of Bac Ninh province.

Keywords: Vulnerability assessment; Industrial flooding; Bac Ninh.

1. Introduction

Flood is one of the natural disasters, regularly threatening people's lives and socio–economic development [1–5]. Flooding has left very heavy consequences, thousands of households were flooded, buildings were destroyed, socio–economic activities were interrupted [6–7]. The process of strong urbanization along with the impact of climate change and the situation of heavy rain causes flooding in urban areas with increasing frequency [8–9]. Inundation affects greatly the management of water drainage. Every the flood events, drainage companies have to work hard to pump and drain water, unclog drains and other response solutions. Annual funding for dredging reservoirs, canals and rainwater regulation, as well as dredging and clearing sewers also costs billions of VND each locality. Flooding also affects wastewater treatment facilities. When it rains heavily, the amount of water flowing to the wastewater treatment plant is greater than the allowed capacity, most factories have to use emergency discharge pipes to the environment, which cannot treat wastewater up to the output standards. Heavy rains make drainage works overloaded, and at the same time make it difficult for managers to find investment solutions to improve the drainage capacity of urban drainage systems. These solutions are often very expensive, and most cannot mobilize private capital, but must use the state budget.

For the assessment of this kind of vulnerability, indicators have proved essential in representing relevant variables and processes involved. Flooding is the result of a variety of factors that include environmental, social, and economic aspects [10]. In recent years, the importance of vulnerability has attracted significant scientific interest, reflecting the need for

a shift to new approaches within risk management [11]. Any approach regarding urban resilience to natural hazards such as coastal flooding should also incorporate features that include the norms, policies, and values that shape cities nowadays [12]. In risk perceptions, the understanding of vulnerability is both broad and subjective.

Bac Ninh is the smallest province in Vietnam, in the Red River Delta and located in the Northern key economic region, Vietnam. In 2019, Bac Ninh is Vietnam's 22nd largest administrative unit in terms of population, sixth in gross domestic product (GRDP), second in GRDP per capita, seventh in growth rate. GRDP growth with 1,378,592 inhabitants. Bac Ninh is one of the provinces affected by inundation caused by heavy rains and storms [13–14].

In this study, a framework for assessing the vulnerability to inundation to industrial urban areas in Bac Ninh Province, the AHP method was selected for this area. Vulnerability is assessed using an interdisciplinary approach based on identification of the socio–economic context, thereby identifying vulnerability patterns and determining exposure to physical threats. Currently, there are two commonly used methods, which are the method of constructing the weighted average (the average value method uses the method [15]; the method of unequal weighting uses the assessment of experts [16]; PCA multivariate statistics and AHP unequal weight method [17]). This study uses the unequal weighted method AHP to assess the flood damage for industrial urban areas in Bac Ninh Province.

2. Materials and Methodology

2.1. Description of study site

Bac Ninh is a province located in the Red River Delta, in the Northern Delta region. The geographical location is in the range from 20°58' to 21°16' north latitude and 105°54' to 106°19' east longitude. The North borders Bac Giang province; the East and Southeast borders with Hai Duong province; To the south, it borders Hung Yen Province; The West borders Hanoi (Figure 1). Rain data at meteorological stations in the region Satellite image of corresponding time of occurrence of heavy rains according to the vulnerability assessment scenarios Current map of land use in Bac Ninh Province.

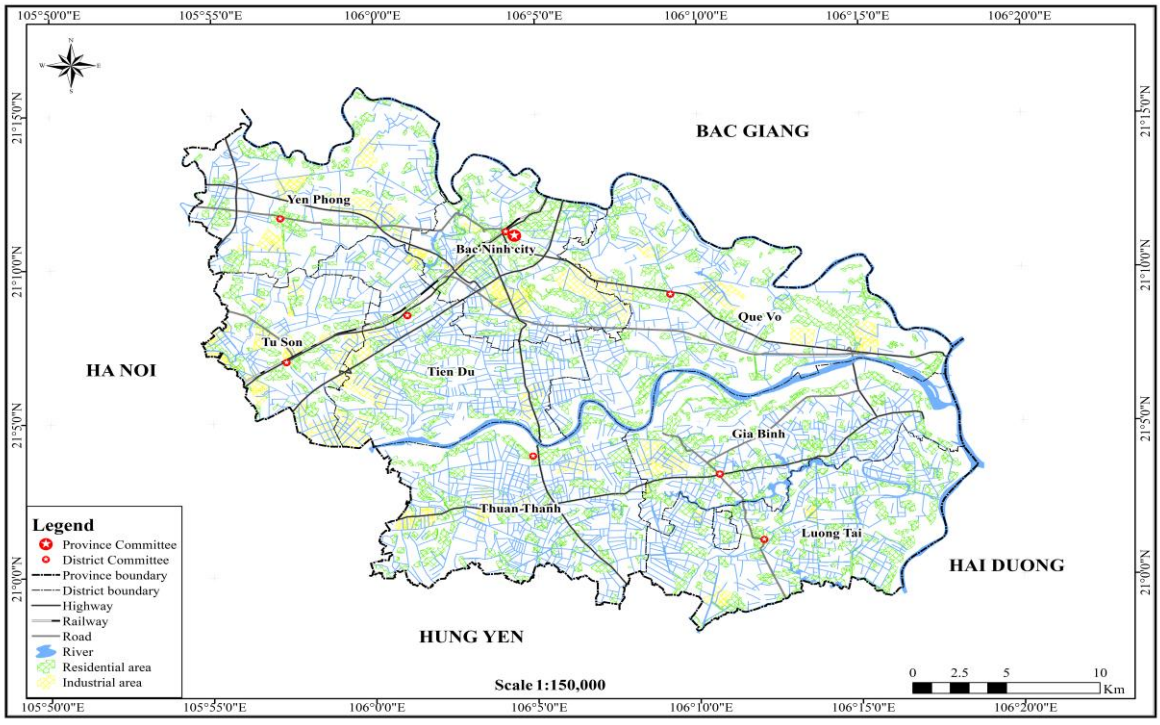

Figure 1. Map of Bac Ninh Province.

2.2. The Analytic Hierarchy Process (AHP)

AHP (Analytical Hierarchy Process) developed by Saaty is a sensitive and practical multi–criteria decision analysis method [18]. The precise presentation of decision problems in a hierarchical structure is the first and possibly the most important step. The hierarchical structure should be constructed so that elements (elements) at the same level have the same magnitude (quantity) and must be related to some or all of the elements at the same level. higher level. In a typical hierarchy, the top level reflects the objective overview (concentration) of the decision problem. The factors influencing the decision are placed at intermediate levels. The lowest level are decision–making options. Accordingly, this form of hierarchy provides a clear and simple view of all the factors influencing the decision and the relationships between them. Once the hierarchy is built, decision makers begin to prioritize the prerequisite decisions that have important correlations among the factors at each level of the hierarchy. Factors at each level are compared in pairs corresponding to their importance in consideration–based decision–making. The comparison is made in the following manner: how important is the relative importance of factor 1 when compared to factor 2 for each particular factor in the higher intermediate level? For each level, starting at the top level of the stratification system and continuing down to the lower levels, a number of square matrices is formed from the results of comparisons between the elements in that level corresponding to an element at the upper intermediate level. Elements are arranged into homogeneous groups according to each layer. The decision maker can express preference between each pair of 2 factors in the following common way: equally (or important, or relevant), moderate priority, high priority, extreme priority period or overriding priority. These preferred descriptors will then be reduced to the form numbers 1, 3, 5, 7 and 9 respectively; where 2, 4, 6, and 8 are intermediate values to satisfy between two consecutive qualitative assessments. The real scope used in AHP allows decision makers to combine subjectivity, experience, and knowledge in an intuitive and natural way [14, 19–21].

The desired outcome is calculated through the matrix's preference vector, which is done by increasing the matrix A with increasing step k. The k increment of matrix A is iterated until the difference in the weights of the vector preference vector for the last two iterations is less than the allowable error of 0.00001. In each iteration, the weights are always normalized so that the sum of the components equals 1. Finally, the maximum characteristic value (k_{max}) of the matrix A is determined. Priority factors are checked for consistency through the consistency ratio (CR), which is the ratio of the random inconsistency index (RI) to the consistency index (CI). CRs below 0.1 are generally considered acceptable but higher values require reconsideration as they are highly inappropriate. The CI coefficients are synthesized from the k_{max} and the order of the matrices (n). RI is a function of n in the relationships between the elements X_1, X_2, …X_n. The questions asked are X_1 is more profitable, more satisfying, contributing more, surpassing, … than X_2, X_3, X_n … X_1, X_2, X_3, …, X_n are factors affecting the object. The questions are very important, they reflect the relationship between the components of one level with the properties of the higher level. Use a rating scale from 1 to 9 as shown in the table below:

Table 1. The classification of Saaty's importance [18].

Level	Definition	Explanation
1	Equally important	Two activities with equal contributions
3	Moderately important	Experience and judgment have a moderate influence on an activity
5	Relatively important	Experience and judgment have a strong influence on an activitv
7	Very important	A very important activity
9	Extremely important	The highest priority
2, 4, 6, 8	Intermediate level between the above levels	Need a compromise between two levels of perception

Matrix of Expert's Opinion

$$\begin{array}{c} \\ x_1 \\ x_2 \\ \\ x_n \end{array} \begin{array}{c} \begin{array}{cccc} x_1 & x_2 & & x_n \end{array} \\ \begin{bmatrix} a_{11} & a_{12} & \dots & a_{1n} \\ a_{21} & a_{22} & \dots & a_{2n} \\ \dots & \dots & \dots & \dots \\ a_{n1} & a_{n2} & \dots & a_{nn} \end{bmatrix} \end{array} \quad (1)$$

where a_{ij} is the rating between the i and j criterion $a_{ij} > 0$, $a_{ij} = 1/a_{ji}$, $a_{ii} = 1$. Choosing w_{ii} be the vector weight of the i factor, w_{ii} is calculated according to the equation 2.

$$w_{ii} = \frac{a_{ii}}{\sum_{i=1}^{n} a_{ni}} \quad (2)$$

AHP multi–criteria method is presented a flowchart of the steps to calculate the damage assessment (Figure 2).

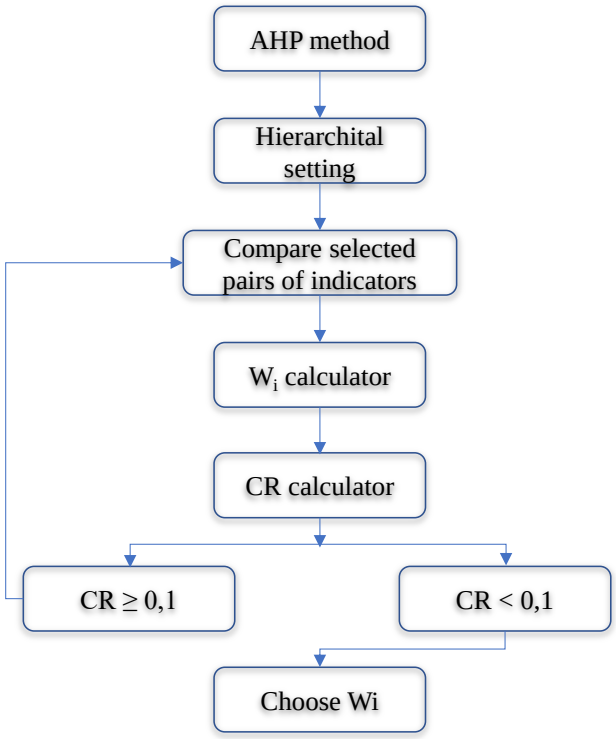

Figure 2. The diagram of multi–criteria method.

3. Results and discussion

3.1. Evaluation of the assessment of vulnerability due to flooding for industrial areas

Using the AHP method, the exposure indices E, susceptibility S and tolerance A of the land use groups in the project area were calculated. In order to be able to classify the vulnerability of land use to inundation, it is necessary to develop a flood risk map of the area. From the flood risk map of the project area, a vulnerable area map will be built based on the superposition of map layers: topographic map layer, current land use map layer and flood map layer. With the data source collected, analyzed and evaluated, the article assesses the extent of inundation vulnerability based on the current state of land use in Bac Ninh province, which is a characteristic factor for both nature and purpose. intended use by humans. Based on the current land use map in 2019 of Bac Ninh province, the article classifies and groups land into 05 types of land, including: land use group for industrial zones, group of traffic

land, group of urban land , group of rural land and group of agricultural land. Rain scenarios are developed corresponding to rain cases according to Decision 18/2021/QD–TTg Regulations on forecasting, warning, communication of natural disasters and disaster risk levels [22], including:

- Scenario 1: Rainfall in 24 hours from 100 mm lasting for 2 days;
- Scenario 2: Rainfall in 24 hours from 100 mm lasting for 4 days;
- Scenario 3: Rainfall in 24 hours from 200 mm lasting for 2 days;
- Scenario 4: Rainfall in 24 hours from 200 mm lasting for 4 days;
- Scenario 5: Rainfall in 24 hours from 500 mm lasting for 1 day;
- Scenario 6: Rainfall in 24 hours from 500 mm lasting for 2 days.

From the rainfall data according to the above scenarios, the article analyzed satellite images taken during the period with equivalent rainfall to determine the flooded area of each land use group corresponding to each rain scenario. Below is the statistics of flooded area of Bac Ninh province according to the rainfall scenarios corresponding to the rain cases according to Decision 18/2021/QD–TTg Regulations on forecasting, warning, communication of natural disasters and risk levels natural disasters, specifically as follows:

Table 1. Area of soil affected by inundation scenario 1 [13].

No	Land use group	Flooded area (km^2)					
		Scenario 1	**Scenario 2**	**Scenario 3**	**Scenario 4**	**Scenario 5**	**Scenario 6**
1	Transportation	158.7	305.88	504	523.3	723.1	927.5
2	Industrial zone	79.29	109.89	108.99	123.3	255.35	278.7
3	Urban land use	104.3	124.2	167.2	252.1	458.7	559.3
4	Rural land use	51.84	156.51	188	270.9	576.4	983.2
5	Agricultural land use	1647.18	3738.97	5407.26	5538.01	12897.1	20256.1

Table 1 shows that the agricultural land group in Bac Ninh is the most vulnerable group because the it is mainly used with major food crops such as rice, maize, potatoes and vegetables; When heavy rain occurs, the agricultural land area is flooded causing a decrease in the yield of food crops and vegetables, even the possibility of losing everything. The second vulnerable group of land users is the group of rural land, because at present the rural population still accounts for the majority, when inundation occurs, the rural land group will suffer significant damage. The third group of land users affected by inundation when heavy rains occur is the group of urban land users because the assets of households in urban areas are relatively high and urban inundation can cause delays. production activities in the economic centers of the province. The fourth vulnerable group is land used for industry because this area has equipment and machinery with high investment costs, but industrial parks have high leveling foundation along with standard drainage systems. standard, so it is less affected by flooding. The last vulnerable group is the group of roads and major national highways with the ability to quickly drain water, less affected by heavy rain causing flooding. For each group of land use status, the analysis is carried out according to the percentage of the area affected by inundation and divided into 5 levels: Very low, low, medium, high and very high.

3.2. Assessment of vulnerability due to inundation according to land use groups of Bac Ninh Province

The table assesses the vulnerability of groups of soil on a scale showing the vulnerability of those factors under the impact of inundation. In fact, the vulnerability of different types of land use is not similar. This difference is reflected in the determination of the weight of each factor. Below is the matrix to determine the vulnerability of land use groups calculated by the AHP method.

Table 2. Matrix of determining the impact of vulnerability of groups of land use.

Land use group	Land for transportation	Land for industry	Land for urban use	Land for rural use	Land for agriculture
Land for transportation	1	3	5	7	9
Land for industry	1/3	1	4	5	7
Land for urban use	1/5	1/4	1	3	5
Land for rural use	1/7	1/5	1/3	1	4
Land for agriculture	1/8	1/7	1/5	1/4	1

Synthesize data from the table of the level of damage caused by inundation with the accessing matrix, build a table to evaluate the level of vulnerability under the influence of inundation for different land use groups.

Table 3. Summary table of inundation vulnerability for land use group.

Land use group	Land for transportation	Land for industry	Land for urban use	Land for rural use	Land for agriculture
Extremely low	< 0.2	< 0.4	< 0.1	< 0.08	< 0.05
Low	0.2–0.4	0.4–0.6	0.1–0.2	0.08–0.15	0.05–0.15
Average	0.4–0.6	0.6–0.75	0.2–0.4	0.15–0.25	0.15–0.25
High	0.6–0.8	0.75–0.85	0.4–0.6	0.25–0.4	0.25–0.35
Extremely high	> 0.8	> 0.95	> 0.6	>0.4	> 0.35
Weight	0.03	0.05	0.17	0.30	0.45
Vulnerable degree	**Extremely low**	**Low**	**Average**	**High**	**Extremely high**

The groups of vulnerable land use types are determined through the establishment of a matrix to compare the correlation between factors and calculate the weight of each factor. After decentralizing and calculating the weights corresponding to the vulnerability of different types of land use, the article has built a vulnerability map of inundation for Bac Ninh Province according to scenarios corresponding to rain cases. Figures 3a–3f is these maps of flood vulnerability and a detailed assessment of flood damage to urban industrial areas in Bac Ninh province.

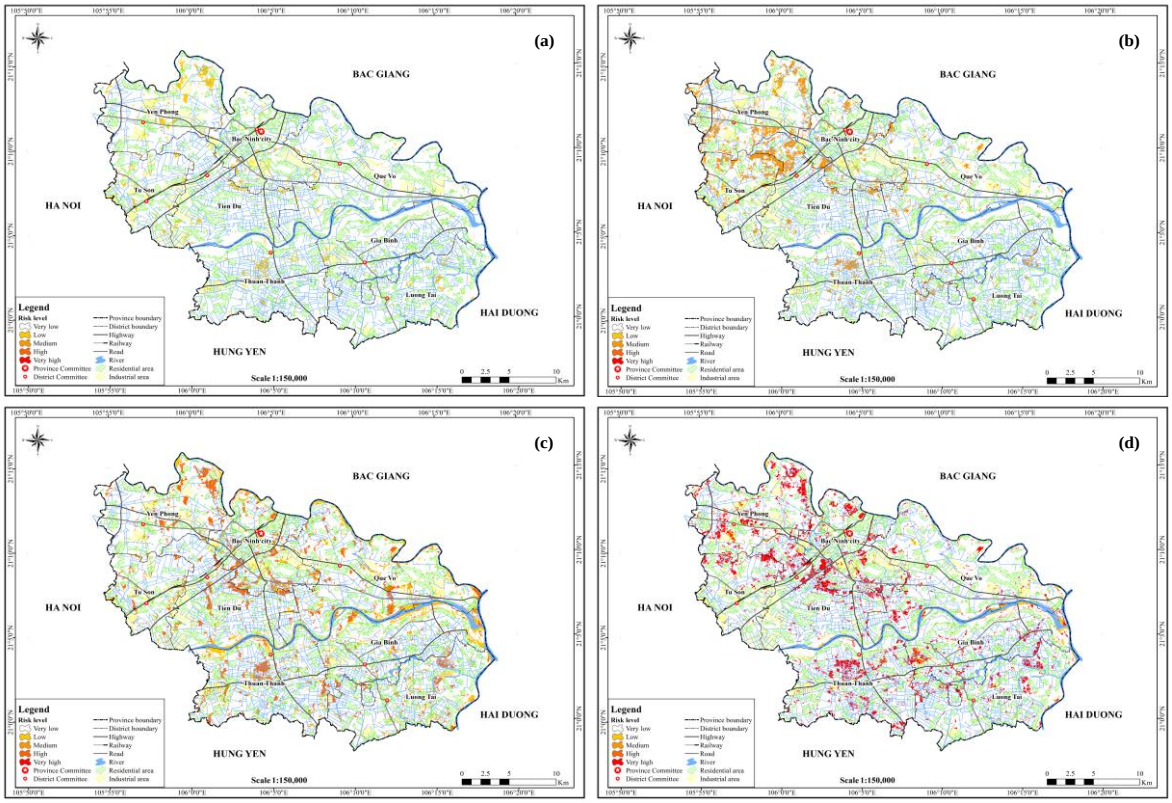

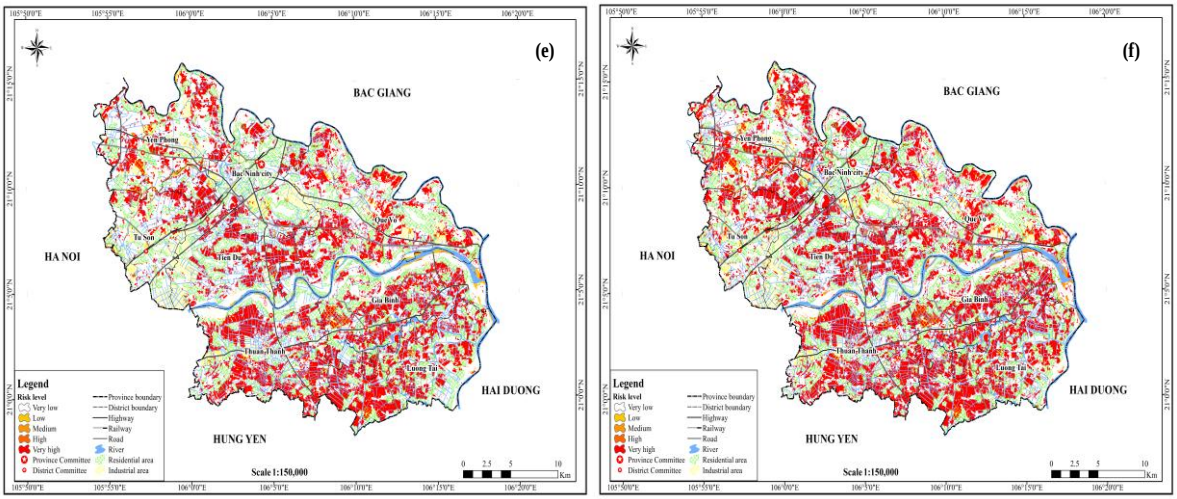

Figure 3. Maps of inundation vulnerability in Bac Ninh province: (a) Scenario 1; (b) Scenario 2; (c) Scenario 3; (d) Scenario 4; (e) Scenario 5; (f) Scenario 6.

The area of industrial parks and urban land in Bac Ninh Province is statistically shown in figures 4a–4h.

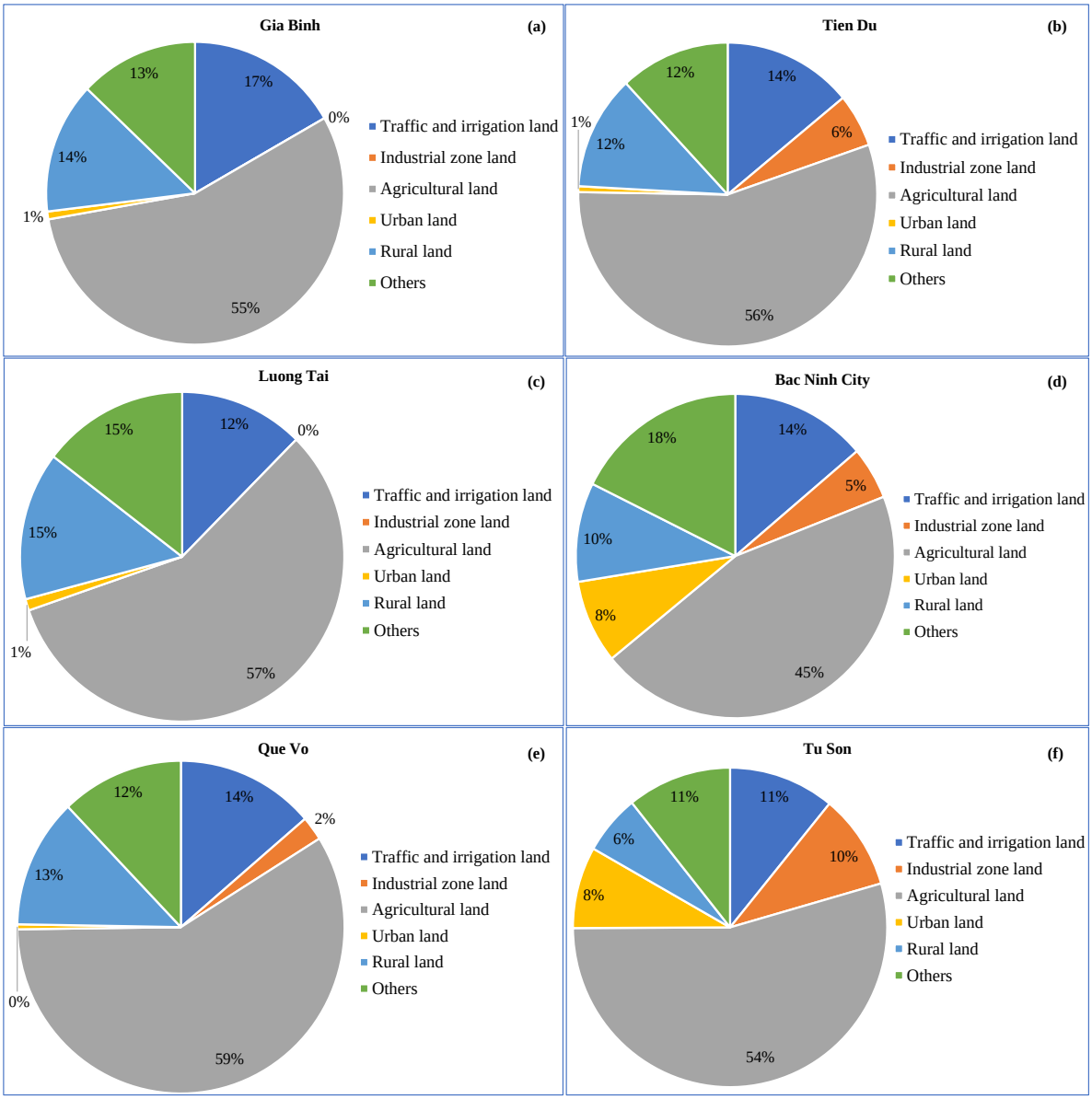

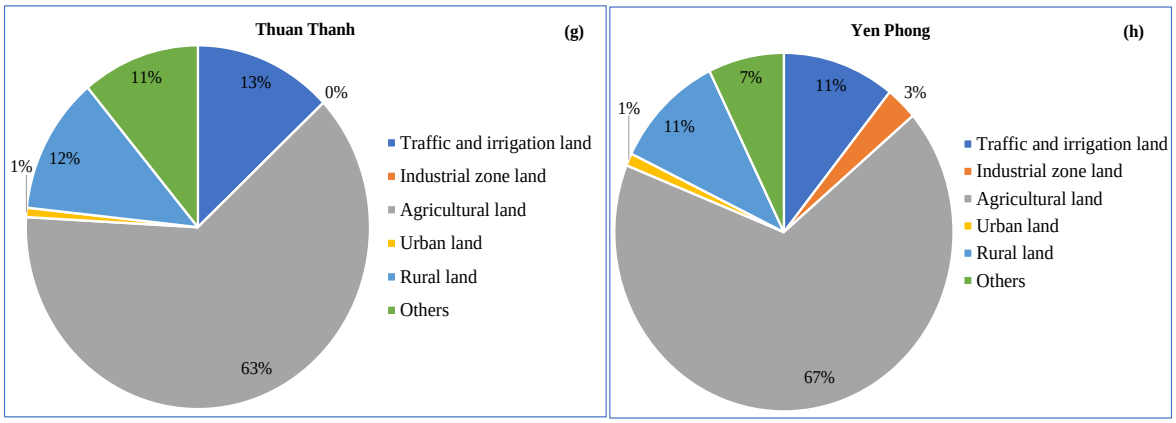

Figure 4. Proportion of urban and industrial land areas: (a) Gia Binh District; (b) Tien Du District; (c) Luong Tai District; (d) Bac Ninh City; (e) Que Vo District; (f) Tu Son District; (g) Thuan Thanh District; (h) Yen Phong District.

Overlapping the weighted layers of vulnerability due to flooding in Bac Ninh province, inundation map in Bac Ninh Province, land use map in Bac Ninh province with statistical charts of the area of damage caused by flooding in urban and industrial areas of districts Bac Ninh Province are presented in Figures 5a–5f.

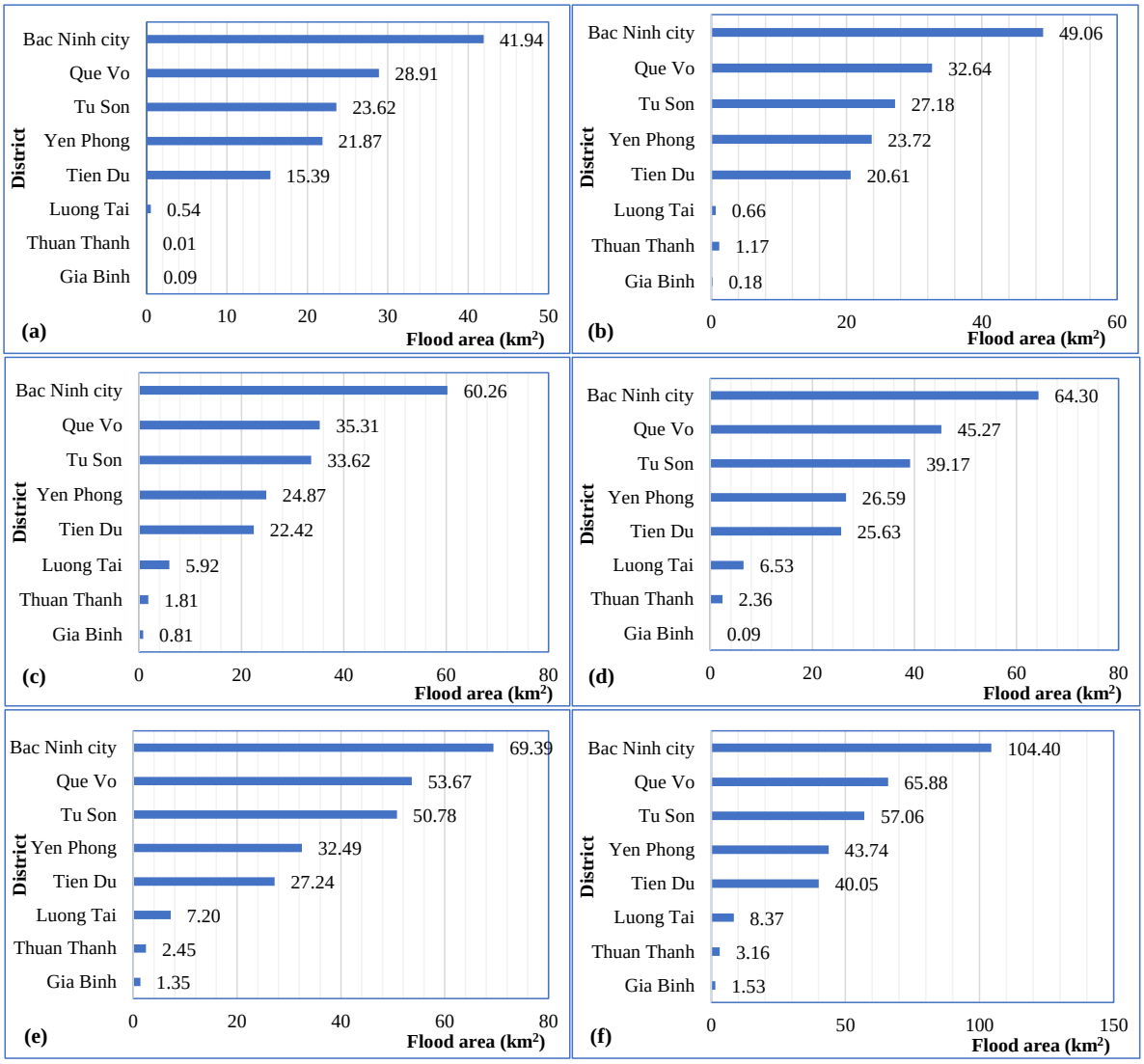

Figure 5. Area affected by flooding in industrial areas: (a) Scenario 1; (b) Scenario 2; (c) Scenario 3; (d) Scenario 4; (e) Scenario 5; (f) Scenario 6.

Analysis of the aggregate results from the above graphs shows that:

Scenario 1: The area of industrial urban land damaged by flooding in Bac Ninh is 42 km^2, in Que Vo is 29 km^2, Tu Son is 24 km^2, Yen Phong is 22 km^2, Tien Du is 15.4 km^2, Luong Tai is 0.54 km^2, Thuan Thanh and Gia Binh areas are insignificant.

Scenario 2: The area of industrial urban land damaged by flooding in Bac Ninh is 49 km^2, in Que Vo is 33 km^2, Tu Son is 27 km^2, Yen Phong is 23.7 km^2, Tien Du is 20.6 km^2, Luong Tai is 0.66 km^2, Thuan Thanh is 1.17 km^2 and Gia Binh is 0.18 km^2.

Scenario 3: The area of industrial urban land damaged by flooding in Bac Ninh is 60 km^2, in Que Vo is 35 km^2, Tu Son is 333 km^2, Yen Phong is 25 km^2, Tien Du is 22.4 km^2, Luong Tai is 5.9 km^2, Thuan Thanh is 1.8 km^2 and Gia Binh is 0.8km^2.

Scenario 4: The area of industrial urban land damaged by flooding in Bac Ninh is 64.3 km^2, in Que Vo is 45 km^2, Tu Son is 39 km^2, Yen Phong is 27 km^2, Tien Du is 26 km^2, Luong Tai is 6 km^2, Thuan Thanh is 3 km^2 and Gia Binh is 0.1 km^2.

Scenario 5: The area of industrial urban land damaged by flooding in Bac Ninh is 70 km^2, in Que Vo is 54 km^2, Tu Son is 51 km^2, Yen Phong is 33 km^2, Tien Du is 27 km^2, Luong Tai is 7.2 km^2, Thuan Thanh is 2.5 km^2 and Gia Binh is 1.35 km^2.

Scenario 6: The area of industrial urban land damaged by flooding in Bac Ninh is 104.4 km^2, in Que Vo is 66 km^2, Tu Son is 57 km^2, Yen Phong is 44 km^2, Tien Du is 40 km^2, Luong Tai is 8.4 km^2, Thuan Thanh is 3.16 km^2 and Gia Binh is 1.53 km^2.

4. Conclusion

The study results show that in different rain scenarios, Bac Ninh Province has the most vulnerable industrial areas to flooding, followed by Que Vo district, Tu Son district, Yen Phong district, Tien Du district, Luong Tai district, but Thuan Thanh district and Gia Binh district are least vulnerable to flooding.

It can be seen that the area of urban industrial land in Bac Ninh occupies a relatively low proportion in most districts, only Que Vo, Tu Son and Bac Ninh city have a similar proportion of land used for industrial urban areas. relatively high (Tu Son is 18% and Bac Ninh city is 13%). Combined with the injury map of Bac Ninh province built from the results of the multi–criteria method and overlapping the map, the vulnerability of the industrial area and urban land are 0.05 and 0.17 respectively, which are low and moderate damage. This is appropriate, because the main area in Bac Ninh is still agricultural and rural areas, so when flooding occurs, these are the most vulnerable site. The area of industrial parks and industrial clusters is increasingly being planned to expand in Bac Ninh, although the equipment of industrial parks is of high value, but when it rains heavily, the possibility of damage from rainwater flooding to industrial parks increases, most industrial zones are designed with standard rainwater collection and drainage systems. Statistics show that there much heavy rains causing urban flooding in Bac Ninh, but they do not occur much in the urban area, the water is flooded for a short period of time, so the impact on the city is only moderate.

The limitation of the article is that have no flood data about inundation area and amount of inundation. The study also only assesses the damage caused by flooding to land use group in Bac Ninh province.

Author contribution statement: Author contribution statement: D.Q.T.; Q.T.T.T.; Analyzed and interpreted the data; Materials, analysis tools and data; Calculation, analyzed and interpreted the results: N.V.N., Q.T.T.T.; Wrote the draft manuscript: Q.T.T.T., N.V.N.; Materials, manuscript editing: D.Q.T.

Acknowledgement: The article was completed thanks to the results of the project: “Mapping disaster risk in Bac Ninh Province”.

Competing interest statement: The authors declare no conflict of interest.

References

1. AHA Centre, JICA. Natural Disaster Risk Assessment and Area Business Continuity Plan Formulation for Industrial Agglomerated Areas in the ASEAN Region, Risk Profile Report - Hai Phong of Vietnam, 2015, pp. 140.
2. Gharbi, M.; Soualmia, A.; Dartus, D.; Masbernat, L. Floods effects on rivers morphological changes application to the Medjerda River in Tunisia. *J. Hydrol. Hydromechanics* **2016**, *64*, 56–66. https://doi.org/10.1515/johh-2016-0004.
3. Ryu, J.; Lee, D.K.; Park, C.; Ahn, Y.; Lee, S.; Choi, K.; Jung, T. Assessment of the vulnerability of industrial parks to flood in South Korea. *Nat. Hazards* **2016**, *82*, 811–825.
4. Mavhura, E. Analysing drivers of vulnerability to flooding: a systems approach. *S. Afr. Geog. J.* **2019**, *101(1)*, 72–90. Doi:10.1080/03736245.2018.1541020.
5. Luu, C.; Tran, H.X.; Pham, B.T.; Al-Ansari, N.; Tran, T.Q.; Duong, N.Q.; Dao, N.H.; Nguyen, L.P.; Nguyen, H.D.; Ta, H.T.; Le, H.V.; von Meding, J. Framework of spatial flood risk assessment for a case study in Quang Binh province Vietnam. *Sustainability* **2020**, *12(7)*, 3058. https://doi.org/10.3390/su12073058.
6. Sood, S.K.; Sandhu, R.; Singla, K.; Chang, V. IoT, big data and HPC based smart flood management framework, Sustain. *Comput. Informatics Syst.* **2018**, *20*, 102–117. https://doi.org/10.1016/j.suscom.2017.12.001.
7. Dimitrova, A.; Muttarak, R. After the floods: differential impacts of rainfall anomalies on child stunting in India. *Global Environ. Change* 2020, 64, 102130. https://doi.org/10.1016/j.gloenvcha.2020.102130.
8. Ahmed, F.; Moors, E.; Khan, M.S.A.; Warner, J.; Van Scheltinga, C.T. Tipping points in adaptation to urban flooding under climate change and urban growth: the case of the Dhaka megacity. *Land Use Policy* **2018**, *79*, 496–506.
9. Kumar, S.; Agarwal, A.; Ganapathy, A.; Villuri, V.G.K.; Pasupuleti, S.; Kumar, D.; Kaushal, D.R.; Gosain, A.K.; Sivakumar, B. Impact of climate change on stormwater drainage in urban areas. *Stoch Environ Res Risk Assess* **2022**, *36*, 77–96. https://doi.org/10.1007/s00477-021-02105-x.
10. Kryvasheyeu, Y.; Chen, H.; Obradovich, N.; Moro, E.; Hentenryck, P.V.; Fowler, J.; Cebrian, M. Rapid assessment of disaster damage using social media activity. *Sci. Adv.* **2016**, *2*, e1500779. https://doi.org/10.1126/sciadv.1500779.
11. Batica, J.; Gourbesville, P.; Hu, F.Y. Methodology for flood resilience index. International Conference on Flood Resilience Experiences in Asia and Europe – ICFR, 5-7 September, Exeter, United Kingdom, 2013.
12. Hammond, M.; Chen, A.S.; Batica, J.; Butler, D.; Djordjević, S.; Gourbesville, P.; Manojlović, N.; Mark, O.; Veerbeek, W. A new flood risk assessment framework for evaluating the effectiveness of policies to improve urban flood resilience. *Urban Water J.* **2018**, *15(5)*, 427–436. https://doi.org/10.1080/1573062X.2018.1508598.
13. Bac Ninh Statistical Yearbook.
14. Downing, T.E.; Patwardhan, A.; Klein, R.J.T.; Mukhala, E.; Stephen, L.; Winograd, M.; Ziervogel, G. Assessing Vulnerability for Climate Adaptation; In Adaptation Policy Frameworks for Climate Change: Developing Strategies, Policies and Measures. Lim, B.; Spanger–Siegfried, E.; Burton, I.; Malone, E.; Huq, S. (Eds), Cambridge University Press, Cambridge, 2005.
15. Patwardhan, A.; Narayanan, K. Assessment of Vulnerability of Indian Coastal Zones to Climate Change. Proceeding of the conference on Water Resources, Coastal Zones and Human Health, 2003.
16. Iyengar, N.S.; Sudarshan, P. A Method of Classifying Regions from Multivariate Data. *Econ. Political Weekly* **1982**, *17*, 2047–2052. https://www.jstor.org/stable/4371674.

17. Kurek, K.A.; Heijman, W.; van Ophem, J.; Gędek, S.; Strojny, J. Measuring local competitiveness: comparing and integrating two methods PCA and AHP. *Qual. Quant.* **2022**, *56*, 1371–1389. https://doi.org/10.1007/s11135-021-01181-z.
18. Saaty, T.L. How to make a decision: The Analytic Hierarchy Process. *Eur. J. Oper. Res.* **1990**, *48*, 9−26.
19. Balica, S.F. Development and Application of Flood Vulnerability Indices for Various Spatial Scales. Master of Science Thesis, UNESCO–IHE, Institude for water education, 2007, pp. 157.
20. Edwards, J. Handbook for Vulnerability Mapping. EU Asia ProEco project, 2007.
21. Watts, M.J.; Bohle, H.G. The space of vulnerability: The causal structure of hunger and famine, Progress in Human Geography, 1993.
22. Decision 18/2021/QD–TTg Regulations on forecasting, warning, communication of natural disasters and disaster risk levels.

VIETNAM JOURNAL OF HYDROMETEOROLOGY

Research Article

Exploiting SEAFFGS to determine threshold runoff and bankfull discharge – pilot application for Quang Nam province

Trinh Thu Phuong[1*], Tran Tuyet Mai[1], Nguyen Thi Nhu Quynh[1], Nguyen Tien Kien[1], Luong Huu Dung[2]

[1] National Centre for Hydro–Meteorological Forecasting; trinhphuong2010@gmail.com; tuyetmai1110@gmail.com; quynh.ntn.1984@gmail.com; kien.wrs@gmail.com
[2] Vietnam Institute of Meteorology, Hydrology and Climate Change; dungluonghuu@gmail.com

*Corresponding author: trinhphuong2010@gmail.com; Tel.: +84–912967014
Received: 05 November 2022; Accepted: 12 December 2022; Published: 25 December 2022

Abstract: Flash flood is a natural disaster occurring in a short time due to heavy rainfall combined with topography, geomorphology, economic growth in the basin. Although it happens on a small scale but it leaves far–reaching destruction in its wake. Recent years have recorded, several consecutive flash flood events causing great damage in the mountainous area of Quang Nam province. For example, in 2020, the successive flash floods and landslides occurring in October and November has been a pressing disaster problem which causes great loss of life and property. Flash flood prediction poses a big challenge for not only Vietnamese but also international scientists. The general method of flash flood prediction is based on threshold runoff and bankfull discharge. Currently, the Viet Nam Meteorological and Hydrological Administration is selected as Regional Centre for supporting flash flood warning by the World Meteorological Organization, has received the "Southeast Asia Flash Flood Guidance System (SEAFFGS)" developed by the U.S Hydrological Research Center and initially applied in flash flood and landslide warning. This paper presents the results of a methodological application for determining the guidance threshold runoff and bankfull discharge for flash flood warning in the SEAFFGS, which will be applied for the mountainous area of Quang Nam province as a pilot study area. The research results will be the first step for studies to determine the threshold runoff formed for flash flood warnings and can be referred for other mountainous regions of Vietnam.

Keywords: Flash Flood; SEAFFGS; Bankfull discharge; Threshold runoff.

1. Introduction

Flash flood is considered as one of the disasters causing the most terrible loss of human lives and properties because of their occurrence on a small scale, rapid development when there is heavy rainfall combined with triggering factors related to topography, geology and land cover. The concept of flash flood is defined differently due to various studies approaches, but they overlap when describing a flood that forms quickly after heavy rainfall with high intensity. According to WMO [1], a flash flood is a flood occurring in a short period of time with a relatively high flood peak. The American Meteorological Society (AMS) [2] defines that flash flood as a flood event with very short duration of rising and falling and with little to no forewarning, it is a result of highly intense rainfall events across the small basin. The US National Weather Service (US NWS) [3] also defines a flash flood

as a rapid and intense flow which is caused by high water mass reaching a frequently dry area or a very high–water level rise in streams, canals, rivers exceeding the predetermined flood level and usually occurring within 6 hours of the incident (heavy rain, dam breaking, ice melting). Flash flood thresholds may vary from regions to regions and basins to basins. Besides, [4] states that flash floods often occur in mountainous basins with catchment areas ranging from a few tens of square kilometers to several hundred square kilometers. Flash floods with a peak time of less than 3 hours in a 5–10 km^2 basin in the United Kingdom while in the US, a peak time of up to 6 hours for a 400 km^2 basin is considered a potential flash flood basin.

Vietnamese Scientists have also introduced many different concepts of flash floods in order to express the fast and intense characteristics of this type of disaster. [5] said that Flash flood is a type of big flood which occurs suddenly and lasts for a short time (fast up and down quickly) with great destructive power. [6] gave the definition: Flash flood is a type of flood with rapid speed (sweeping which occurs suddenly (usually appears at nights where it rains small–flood pipes) on a small or large scale, maintained for a short or long period of time (depending on the rainfall–flood event), carries a lot of mud and sand and has great destructive power. According to [7] flash flood is a flood formed by rainfall combined with unfavorable combinations of buffer surface conditions (topography, geomorphology, cover, etc.) to produce mud, rock flows on the steep slopes (basins, rivers and streams) and propagate very quickly downstream, causing sudden and terrible destruction in the mountainside areas and along the rivers and streams through which it overflows.

Currently, following the functions and tasks prescribed by the Government, flash flood warnings are carried out at the Viet Nam Meteorological and Hydrological Administration (VNMHA and implemented directly at the National Center for Hydro–Meteorological Forecasting (NCHMF), Regional Hydro–Meteorological Centers and Provincial Hydro–Meteorological Centers. The Early Warning Systems (EWS) are considered the key to reducing the impacts of flash floods.

For the purpose of enhancing the capacity of warning small–scale natural disasters such as flash floods, the World Meteorological Organization (WMO) cooperates with the United States Agency for International Development/Office of U.S. Foreign Disaster Assistance (USAID/OFDA), the National Oceanic and Atmospheric Administration/National Weather Service (NOAA/NWS) and the Hydrological Research Center (HRC) are collaborating to develop a supporting system. Flash Flood Guidance System with Global Coverage (GFFGS) for the benefit of the community with multi–stakeholder coordination. Flash flood guidance system (FFGS) is developed to provide a system of tools to support hydrometeorological forecasters around the world in operational work, analysis, monitoring and warning of flash flood disasters through observed data, real–time model data, and real–time information on guidance rainfall thresholds capable of generating flash floods in a certain area [8].

In 2019, the first FFGS system was established for Vietnam under the name of VNFFGS within the framework of the project “Investigation, survey, and mapping of flash flood risk zoning for the Central and Highland regions, and develop a pilot system of flash floods warning for high–risk localities in order to serve planning, directing and operating disaster prevention and climate change adaptation” implemented by the Viet Nam Institute of Meteorology, Hydrology and Climate Change [9].

In 2022, the Southeast Asia Flash Flood Guidance System (SeAFFGS) funded by WMO was transferred to the Viet Nam Meteorological and Hydrological Administration (VNMHA) for management as the representative role of SeAFFGS’s Regional Center. SeAFFGS is the first flash flood warning supporting system using extremely short–term forecast data and integrating a large number of different data sources from Southeast Asian

countries including: satellite and radar estimate rainfalls, telemetry rainfall, 04 quantitative precipitation forecast products, real–time and historical data received from member countries, products of Flash Flood Risk with warning time up to 36 hours. In this system, Vietnam provides and shares data including: 10 radars, 1500 automatic rain gauges, and administrative maps of districts, communes, and extremely short–term forecasting products (Nowcasting), quantitative precipitation forecast products from radar and from numerical weather forecast model WRF with coverage for 04 countries Laos, Cambodia, Thailand, Viet Nam. The sub–basins divided in SeAFFGS have an average area of about 20 km^2 with a total of over 71,000 sub–basins for 4 member countries in Southeast Asia, of which 18,345 sub–basin are in Vietnam. The FFG approach implements flash flood warnings based on the comparison of observed or forecast rainfall over a certain period of time in a watershed with the estimated Q_{bf} (FFG) rainfall generation for Vietnam only.

The SEAFFGS system has been tested, evaluated and applied in the flash flood warning service for mountainous areas of Vietnam. The purpose of the study will be: (1) Presenting the method of determining threshold runoff for FFGS oriented warning; (2) Applying this method to calculate threshold runoff and bankfull discharge in the SEAFFGS, pilot application in the mountainous area in Quang Nam province.

2. Materials and Methods

2.1. Description of study site

The Central region has been facing natural disasters such as flooding, flash flood that occur frequently with enormity. Most of the provinces of this region recorded flash floods which cause great loss of life and property. Quang Nam is one of the central coastal provinces that suffer from many types of disasters, including flooding and flash flood. The topography of Quang Nam province features many areas with a combination of several disadvantages such as: steep terrain, strong cleavage forming narrow V–shaped stream, slope of 30–45 degrees, two walls in both sides of the stream with the condition of breakable soil structure, bedrock lying leading to landslides situation [10]. The short and steep characteristics of the stream networks as well as narrow valleys in the upstream are the basic factors for high–risk of flash floods and landslides.

In October 2020, 4 communes in Quang Nam face landslides, flash floods, and tube floods which cause great destruction. Districts where flash floods often occur are Bac Tra My, Nam Tra My, Phuoc Son, and Tam Giang. The study selects Quang Nam province which has many high–risk points for flash floods in recent years, to pilot the application of the threshold runoff generating flash floods and the bankfull discharge in mountainous areas.

2.2. Data used in the study

Observed data: Hourly and daily rainfall from 150 rain gauges, flood peak records of 60 hydrological stations in the whole country.

Model data: The catchment data of the Southeast Asia flash flood guidance system (SEAFFGS); Survey data on flash floods (rainfall, causes) of the Viet Nam Institute of Meteorology, Hydrology and Climate Change, Viet Nam Institute of Geosciences and Minerals Resources, Provincial Hydro–Meteorological Center in Quang Nam province.

Map data: DEM (Digital Elevation Model) map (30m×30m) scale obtained from free website of United States Geological Survey–USGS at http://gdex.cr.usgs.gov/gdex/.

2.3. Calculation methods of flash flood formed rainfall threshold and bankfulldischarge threshold

Threshold Runoff is an important factor which is widely used worldwide in flash flood warning methods. However, determining the exact threshold runoff in different areas is a

big challenge because flash floods are caused by many factors including hydro–meteorology, topography, land cover, and human activities. The approachable SEAFFGS flash flood warning system is based on several concepts of FFG, FFT and Q_{bf} [9], providing users the necessary information to assess the potential of flash floods in areas, including:

(1) Flash Flood Guidance (FFG) is the volume of rainfall over a given duration in a small catchment which is required for the occurrence of a Bankfull discharge at the river basin outlet. The FFG is an indicator of the volume rainfall needed to overcome the soil water storage and streambed, causing minor flooding in the basin. The FFG is continuously updated based on current soil saturation water deficits (as determined by previous soil moisture conditions), precipitation, evaporation, and infiltration losses.

(2) Flash Flood Threat (FFT) is the mean precipitation of a basin in a certain period exceeding the corresponding FFG value. The Flash Flood Threat index is determined according to the difference (or percentage) between the cumulative rainfall during the forecast period and the corresponding FFG.

(3) Bankfull discharge (Q_{bf}) is the discharge in a river/canal that is just enough to cause flooding to the entire riverbed at the same level as the bankfull channel [10].

2.3.1. Q_{bf} determination in the FFGS

Bankfull discharge is an important parameter that determines the volume of guidance rainfall capable of generating flash floods (FFG). The method of determining the bankfull discharge is based on the geometrical features of the basin or riverbed where the bankfull discharge occurs. The method of determining Q_{bf} based on cross–sectional geometry is only suitable for rivers and streams condition with clear banks and riverbeds. In mountainous areas, many river sections have a V–shaped cross–section with two steep banks, not separating the riverbed and the riverbank [9].

The determination of bankfull discharge based on topography requires a lot of surveys and measurement albeit with irregular sufficient data for calculation. Many researches have stated that Qbf is usually a peak flood discharge with a return period of about 1–2 years [10–12]. So, in the FFGS system, Q_{bf} is also defined according to $Q_{max50\%}$. Thus, each sub–basin has a Q_{bf} value, and the FFG of different periods will be different to the form the Q_{bf}. When establishing the FFGS, the bankfull discharge is determined by the HRC based on the relationship between the bankfull discharge at hydrological stations with a catchment area of less than 2000 km^2 and the basin characteristics in Table 1. This method has been implemented in many US states such as California, Iowa and Oklahoma,... The regression equation is built in the following 3 types [9]:

$$Q_{bf} = bA^{a} \quad (1)$$

$$Q_{bf} = bA^{a1}R^{a2} \quad (2)$$

$$Q_{bf} = bA^{a1}S^{a3} \quad (3)$$

where Q_{bf} is the bankfull discharge; A is the catchment area; R is the mean annual precipitation; S is the catchment slope; b, a, a_1, a_2, a_3 are calculated coefficients.

Table 1. Correlation of bankfull discharge with area A, basin slope S, and annual precipitation R in Iowa and Oklahoma (US) [14].

State	Correlation function
Iowa	$Q_{bf}= 20,4*A^{0,0607}S^{0,44}$
Oklahoma	$Q_{bf}= 0,03*A^{0,59}R^{1,84}$

Inheriting research results from the project “Investigation, survey, and mapping of flash flood risk zoning for the Central and Highland regions, and develop a pilot system of flash floods warning for high–risk localities in order to serve the purpose of planning,

directing and operating disaster prevention and climate change adaptation" [9] conducted by the Viet Nam Institute of Meteorology, Hydrology and Climate Change in 2019, analyzed the relationship Q_{bf} according to formulas (1), (2) and (3). Vietnam is divided into 4 regions for analysis and identification based on rainfall and flood characteristics, including the Northern, Northeast and Middle North, the Northwest, the North Central and Highlands. The calculation results are in Table 2.

Table 2. Relationship Q_{bf} with basin features [9].

Region	No station	$Q_{bf}= bA^a$			$Q_{bf} = bA^{a1}S^{a2}$				$Q_{bf} = bA^{a1}R^{a3}$			
		a	b	R^2	a_1	a_2	b	R^2	a_1	a_3	b	R^2
Whole VN	60	0.844	2.44	0.616	0.0790	0.40	18	0.670	0.9	1.9	0.31	0.725
Northern	34	0.765	3.60	0.600	0.0760	0.33	15	0.602	0.9	2.0	0.26	0.737
NorthEast &Middle North	14	0.768	6.01	0.724	0.0778	0.45	20	0.796	0.9	1.4	0.44	0.810
NorthWest	20	0.721	2.27	0.536	0.0770	0.47	15	0.537	0.9	3.1	0.38	0.768
Central&Highland	27	0.871	4.90	0.729	0.0629	0.47	16	0.735	0.9	1.1	0.27	0.772

Through the analysis results, the addition of mean annual precipitation and catchment slope as independent variables to determine runoff showed an improvement albeit insignificant, while uncertainty increases in all sub–catchment.

2.3.2. Determination of rainfall threshold causing flash flood

The rainfall threshold causing flash floods or the threshold of bankfull precipitation can be determined by the following formula [14]:

$$R_{thr} = A*Q_{bf}/q_{dv} \quad (4)$$

where A is the catchment area (km^2); Q_{bf} is the bankfull discharge (m^3/s); q_{dv} is the unit hydrograph peak for a specific duration ($m^3/(s.km^2.mm)$).

The unit flood hydrograph peak can be determined by measured data. However, this method will not be feasible in the case of limited hydrological time series. The unit flood peak is calculated by using the Geomorphological Unit Hydrograph method. Accordingly, the peak flood discharge in the time period t_R is determined by the formula:

$$Q = 2.42iAt_R/\Pi^{0.4}(1– 0.218t_R/\Pi^{0.4}) \quad (5)$$

where $\Pi=L^{2.5}/(iAR_L\alpha^{1.5})$; $\alpha = S_c^{0.5}/nB^{2/3}$; t_R is the duration of effective rainfall (h); L is the main stream length (km) ; i is the effective rainfall intensity (cm/h); R_L is the Horton's length ratio. Assign n as the corresponding river level of the tributary in which the precipitation threshold for bankfull is to be calculated, n+1 is the river level of the tributary and the pour into river, the R_L ratio determined by the total length of the n–level rivers divided by the total length of (n+1) level rivers (in the same main river system); Sc is the local channel slope; n is the Manning roughness coefficient; B is the channel top width at bankfull (m).

The top width (B), hydraulic depth (D) at bankfull and local channel slope (Sc) can be determined according to the relationship between basin area characteristics. The relations between features B, D and Sc has been developed for some US states. In Iowa and Oklahoma in the US, sets of channel cross–sectional data were available and utilized to develop these regional relationships:

Table 3. The relation between B, D Sc and A corresponding Qbf in some states of US.

California	Iowa	Oklahoma
$B = 3.29A^{0.3714}$	$B = 2.8A^{0.363}$	$B = 2.33A^{0.542}$
$D = 0.3A^{0.261}$	$D = 0.82A^{0.160}$	$D = 1.03A^{0.198}$
$Sc = 0.006A^{-0.385}$	$Sc = 0.045A^{-0.203}S^{0.564}$	$Sc = 0.006A^{-0.385}$

Threshold runoff R_{thr} equal to the rainfall intensity times its duration tR(i×tR). We have:

$$Q = 2.42RA/\Pi^{0.4}(1 - 0.218tR/\Pi^{0.4}) \quad (6)$$

Thus, the threshold runoff with different time can be calculated based on the basin characteristics such as: catchment area, local chanel slope, the top width, Manning roughness coefficient, Horton's length ratio and bankfull discharge. The parameters of the relations of B, D, Sc with the basin characteristics is taken according to the relation of the state of California, where the climate and rainfall conditions are similar to Vietnam. The formulas to calculate B, D, Sc are as follows:

$$B = 3.29A^{0.3714} \quad (7)$$

$$D = 0.3A^{0.261} \quad (8)$$

$$Sc = 0.006A^{-0.385} \quad (9)$$

where B is the top width at bankfull; D is the hydraulic depth at bankfull; Sc is the local channel slope.

According to [14] gave the formula for calculating Manning's roughness coefficient (for cases with roughness coefficient higher than 0.035) as follows:

$$n = 0.43\,Sc^{0.37}/D^{0.15} \quad (10)$$

where n is the Manning's roughness coefficient; Sc is the local channel slope; D is the hydraulic depth.

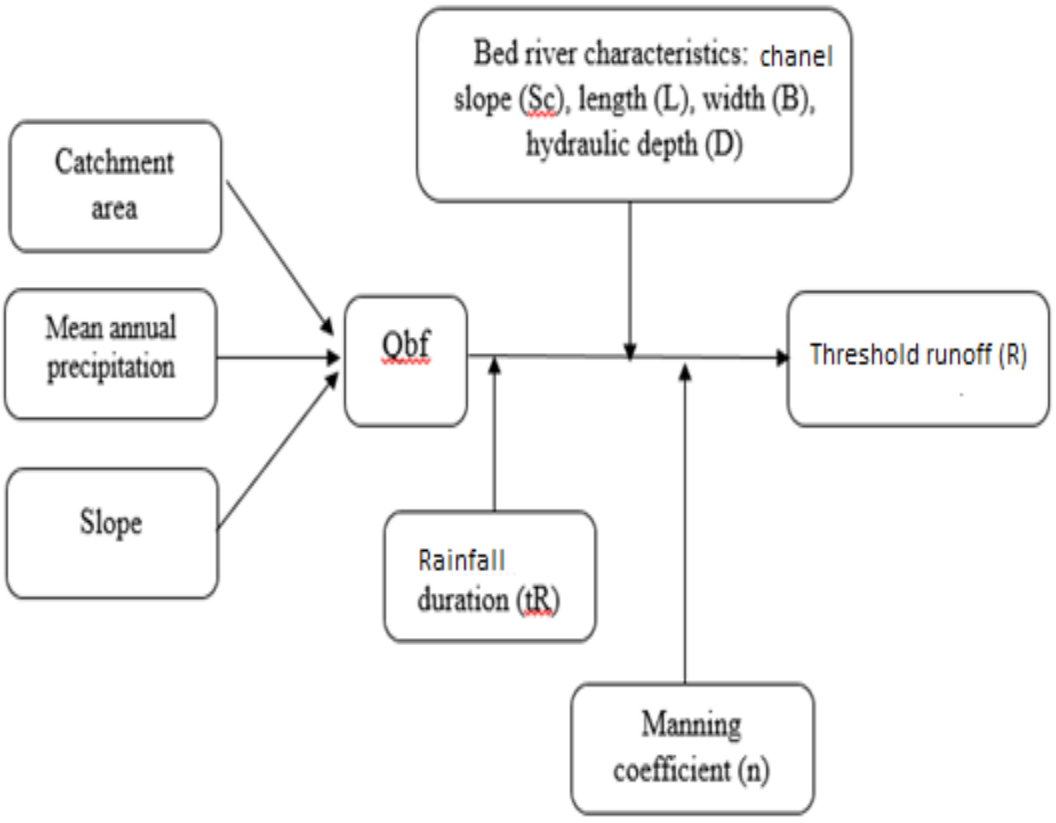

Figure 1. Diagram of bankfull discharge and threshold runoff for flash flood warning.

3. Results and Discussion

3.1. Division of sub–basins of Quang Nam province

Mapping data for dividing sub–basins in Quang Nam province is extracted from the sub–basin division map layer for the entire Southeast Asia region in the SEAFFGS system (source: https://222.255.11.76/SEAFFGS_MAPSERVER/). Using QGIS software, Clip tool to separate sub–basins in Quang Nam province with 643 sub–basins in total (Figure 1).

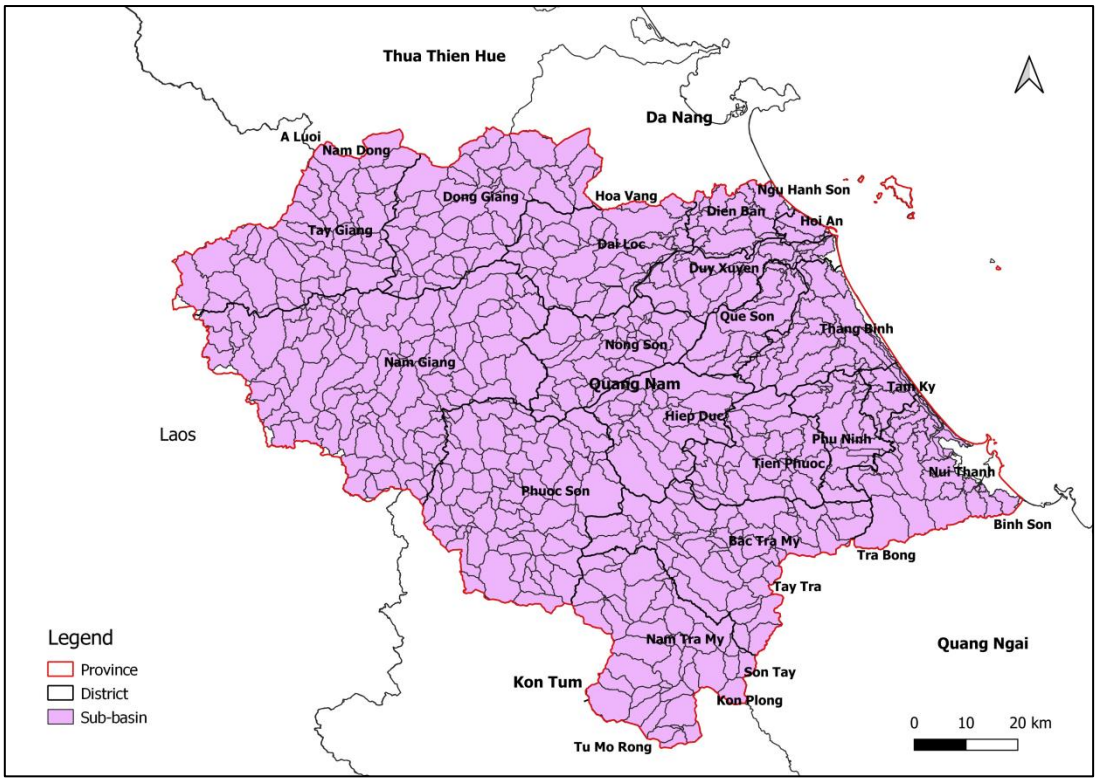

Figure 1. Sub–basins devided in Quang Nam Province.

3.2. Calculating the length of rivers and streams in Quang Nam province

Using ArcGIS software, Flow Accumulation and Flow Direction tools create a network of rivers and streams in Quang Nam province. Using the Calculate Geometry tool in ArcGIS calculate the river length (Figures 2a–2b).

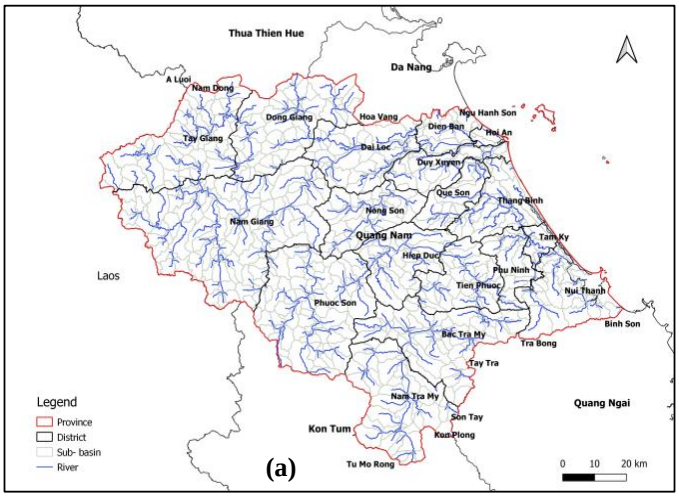

Table

SongQuangNam

FID	Shape *	cat	value	Length
0	Polyline	91792	2054203379	2.26146
1	Polyline	91793	2054203380	4.87376
2	Polyline	91838	2054203368	1.94134
3	Polyline	91856	2054203378	0.385475
4	Polyline	91895	2054203368	1.11259
5	Polyline	92057	2054203368	3.50754
6	Polyline	92061	2054203368	0.042797

(b)

Figure 2. (a) River network used in calculations in Quang Nam province; (b) Example of calculating river length in sub–basins of Quang Nam province.

3.3. Calculation results of bankfull discharge in Quang Nam

Applying the method of calculating the bankfull discharge (Q_{bf}) following the method of the SEAFFGS system, the bankfull discharge will be calculated for the sub–basins with an area less than 2000 km^2. The study will not calculate Q_{bf} for areas which cover rivers, lakes, ponds, etc. Using the calculating Q_{bf} formula in Table 2 for the Central and Highlands's regions [9] apply for sub–basins in Quang Nam province:

$$Q_{bf} = 4.9\ A^{0.871} \quad (11)$$

Calculation results show that: The Q_{bf} discharge value of sub–basins range from 10–130 m^3/s: with sub–basins less than 20 km^2, the Q_{bf} value is below 60 m^3/s; with sub–basin with area of 20–50 km^2, the Q_{bf} value ranges from 60–130 m^3/s (Figure 3).

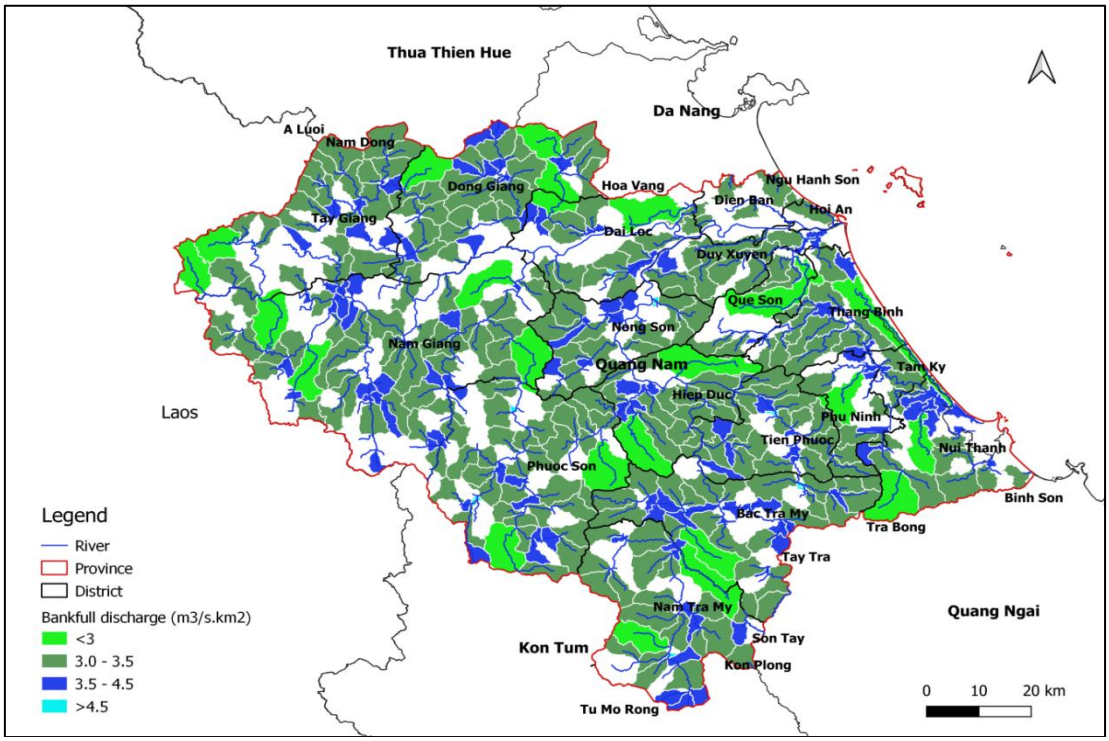

Figure 3. Module of bankfull discharge in the sub–basins of Quang Nam province.

3.4. Calculation results of the threshold of rainfall causing flash floods in Quang Nam

The rainfall threshold causing flash flood or the threshold runoff generating Q_{bf} in the duration of 3 hours and 6 hours is calculated by formulas (5) and (6). Calculation results of Q_{bf} will be the basis for calculating the threshold runoff. According to formulas (5) and (6), intermediate features B, D, Sc, Manning roughness coefficient will be intermediately calculated according to formulas (7), (8), (9), (10). The R_L index, which is the ratio of the Horton length taken as a reference from the calculated value following the river basin characteristics of the state of California with a climate similar to that of Vietnam, is 1.9 [14].

The results show that the threshold runoff with duration of 3 and 6 hours in upstream areas such as Phuoc Son, Nam Tra My, Bac Tra My, Nam Giang and Tay Giang tends to be higher than in the downstream districts such as Nui Thanh, Nong Son, Hiep Duc, Dong Giang. Threshold runoff values for basins less than 20 km^2 in 3 hours or 6 hours are equal or less than 20 mm; for basins of 20–50 km^2, the common threshold runoff is from 20–35 mm in 3–6 hours; for basins with an area larger than 50–80 km^2, the threshold runoff varies widely from 35–80 mm; for basin larger than 80 km^2, the threshold runoff for flash flood generation is greater than 80 mm in 3–6 hours (Figures 4–5).

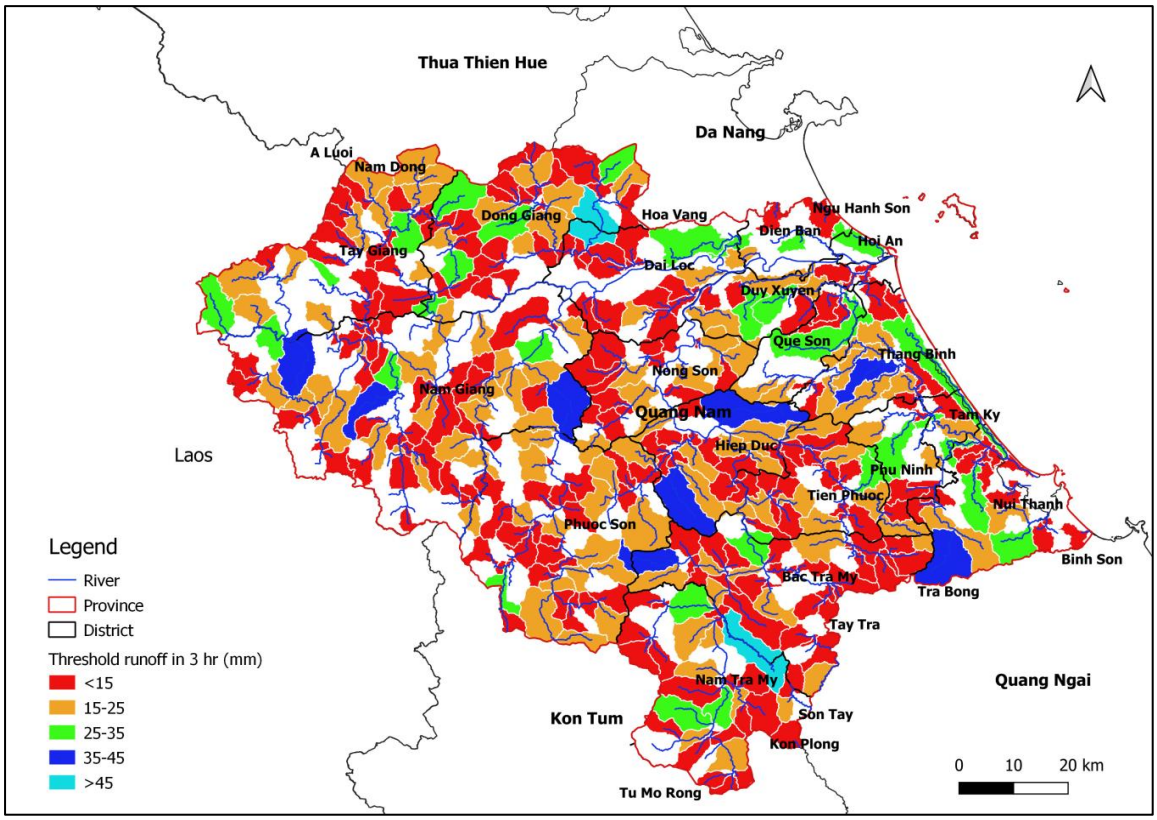

Figure 4. Threshold runoff in the 3–hour period in sub–basins of Quang Nam province.

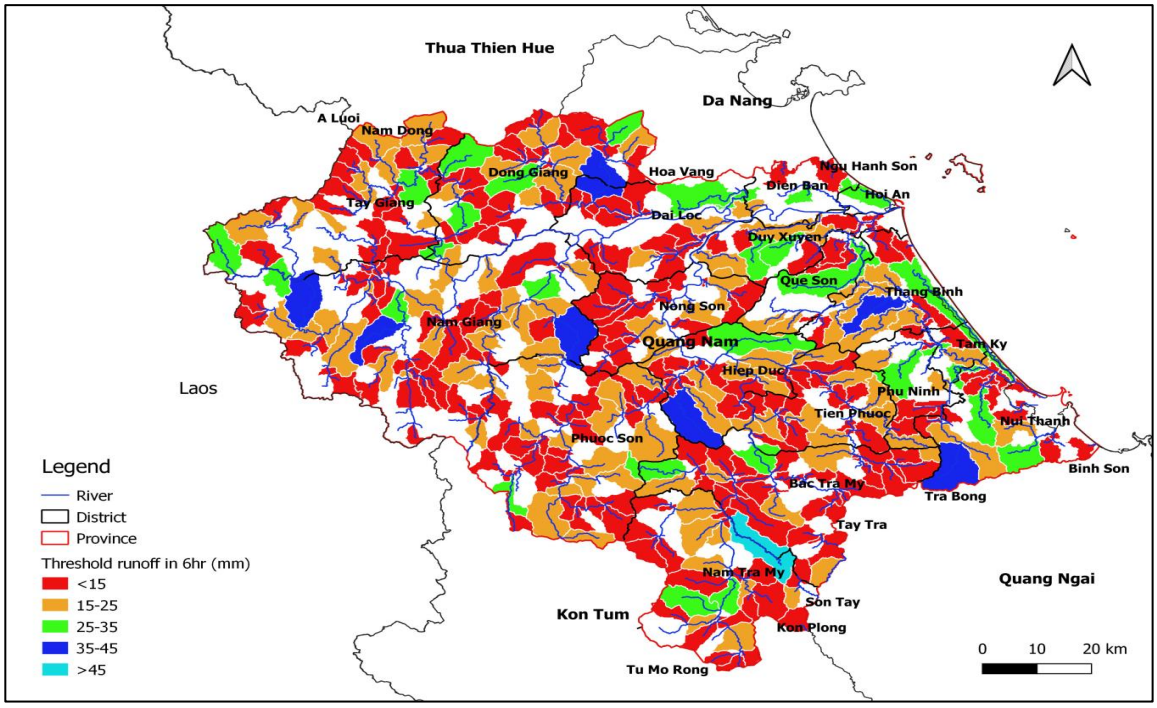

Figure 5. Flash flood generating rainfall threshold in the 6–hour period in sub–basins of Quang Nam province.

3.5. Experimental application ofthreshold runoff for some flash flood events in Quang Nam

Currently, monitoring data on flash floods in disaster–prone areas is limited. Statistical data and detailed monitoring data on flash floods such as time of occurrence, hourly rainfall accumulation, current status of the basin...have not been systematically collected and stored in uniformed database. The information is mainly collected scatteredly from many sources

such as: the Central Steering Committee on Natural Disaster Prevention and Control, the Provincial Committees for Natural Disaster Prevention and and Rescue, the Regional and Provincial Hydro–Meteorological Centers, other sources from media or broadcast. The calculation and experimental application of the flash flood generation rainfall thresholds require a lot of detailed information for testing and evaluating.

In Quang Nam, the stored data on the flash flood situation in the past is limited with a lack of detailed information except in recent. According to statistics from the Quang Nam province Hydro–Meteorological Center, there have been 4 flash floods in Nam Tra My and Bac Tra My districts (Table 3) in the year 2020–2021. As a result of the influence of storm No. 9, heavy rainfall occurred in Quang Nam province especially on October 28th when the rainfall was extremely high with the total precipitation recorded at 320 mm. During the occurrence time of historical flood in October and November, 2020, recorded rainfall for 3 and 6 hours before flash flood apparency is relatively large, from 146–259 mm in 3–6 hours; for flash flood event in the November 2021, recorded rainfall of 34 mm/3 hours and 80 mm/6 hours. During the flash flood events in October and November 2020, rainfall occurred a few days earlier. When compared, the calculation results in section 3.4 show that the threshold value of flash flood generating rainfall for the basin over 50 km^2 is quite consistent with 3 flash flood events on 28/10/2020, 6/11/2020 and 18/11/2021. Particularly for flash flood No. 4 in Tra Bui commune, the rainfall threshold for generating flash floods is high.

In general, the reliability of flash flood warning depends on rainfall forecast. The main basis for determining rainfall threshold is based on statistical data on rainfall, basin–specific data. The exact determination of the flash flood generation rainfall thresholds depends on the length and wholeness of time series of survey and investigation data, flash flood events in order to analyze and experimentally adjust. During the warning implementation, the forecasters have to refer to the actual rainfall information measured in the previous period, analyze the future precipitation trend and catchment information, etc. to identify the possibility of flash floods.

Table 3. Statistical data of sseveral flash floods in Quang Nam in 2020–2021.

Position	Area (km^2)	Occurrence time	Precipitation before flash floods (mm)	
			3h	6h
Commune Tra Leng, Nam Tra My, Quang Nam	116.53	15h 28/10/2020	146	195
Commune Tra Leng, Nam Tra My, Quang Nam	116.53	16h 6/11/2020	216	259
CommuneTra Đoc, Bac Tra My, Quang Nam	54.37	06h18/11/2021	34	80
Commune Tra Bui, Bac Trà My, Quang Nam	137.2	09h/29/11/2021	10	34

4. Conclusion

The problem of flash flood warning is associated with determining the thresholds for rainfall and flow that cause this disaster. Currently, according to different research approaches, many scientists have come up with different methods to calculate these thresholds. In Vietnam, the FFG system in the Southeast Asia Flash Flood Guidance System Project (SEAFFGS) has been transferred by the World Meteorological Organization to be used in flash flood, landslide warning that integrates multiple local data sources [15]. Approaching this warning system, the research presents a method to calculate the flash flood generating guidance rainfall threshold and bankfull discharge in the FFGS system of flash flood generation, pilot application for mountainous areas in Quang Nam province.

The characteristics of the basin such as local channel slope, river length, basin area is calculated by ArcGIS software, which are necessary parameters to calculate the threshold

runoff. The relationship between basin characteristics for excess rainfall formed flood in small basins tends to be closer than that in large basins [16]. In many watersheds, the cross–section of rivers and streams have a lot of variations over short distances and over time according to the flood situation. Therefore, it is difficult to determine the bankfull discharge in areas with unstable channel cross–section. On the other hand, the method of applying the bankfull discharge occurs in a period of 1–2, the frequency of 50% may be underestimated in many basins. Hence, the threshold runoff calculated from the formula with the bankfull discharge parameters may alsobe underestimated. Determining the frequency of bankfull discharge depends a lot on the length of the river, and the historical time series of flow monitoring at the outlet of the basins. Understanding the methods and knowledge of these limitations is crucial in selecting a method for calculating flow threshold, in interpreting and applying flow threshold estimates.

In the current situation, there is almost no monitoring data at the outlet of small sub–basins (around 20 km^2), and very little monitoring data on the mainstream and tributary with a much larger area. In addition, it is necessary to have a lot of detailed data on rainfall, time of flash flood events, flow...in order to test the threshold runoff and bankfull discharge with highest reliability. Currently, this data source is limited and not fully stored. Therefore, the calculation and experimental application of flash flood thresholds still have gaps that cannot fully reflect the level and threshold of flash flood risk of the basin.

In the condition of limited monitoring data, simple and straight forward methods are still the priority in selecting practical applications. The calculation results of this study combined with the warning products from the SEAFFGS system will lay a foundation assessing the possibility of flash flood risk in Quang Nam area, creating a reference premise for other studies to determine the threshold runoff in other mountainous areas of Vietnam. In the near future, when the automatic rain gauge network is expanded and the observation time series is much longer extended, the flash flood data stored in detail will be a valuable data source for updating and developing more the flash flood generating thresholds runoff and bankfull discharge. Moreover, proactive preventative measures in addition to early warning system should be implemented in order to alleviate the loss caused by flash flood.

Author's contribution: Developing research ideas: T.T.P., T.T.M; L.H.D.; Data processing: T.T.M., N.T.N.Q., N.T.K.; Draft of the article: T.T.P.; T.T.M.; Editing: T.T.P.

Acknowlegment: The article was completed thanks to the results of the task: "Research on design, develop an information system – early warning of landslides, flash floods in mountainous and midland areas of Vietnam", grand number: TNMT. 2021.04.06.

Disclaimer: The authors declare that this article is the work of the authors, has not been published anywhere, and has not been copied from previous studies; there is no conflict of interest in the author group.

References

1. Hall, J.. Flash flood forecasting. World Meteorological Organization, 1981.
2. National Research Council. Flash Flood Forecasting Over Complex Terrain: With an Assessment of the Sulphur Mountain NEXRAD in Southern California. Washington, DC: The National Academies Press, 2005. https://doi.org/10.17226/11128.
3. Philadelphia/Mt Holly. What is flash flooding. 2018. Available online: https://www.weather.gov/phi/FlashFloodingDefinition.
4. Georgakakos, K. On the Design of National, Real–Time Warning Systems with Capability for Site–Specific, Flash–Flood Forecasts. *Bull. Am. Meteorol. Soc.* **1986**, *67*, 1233–1239.
5. Cao, D.D.; Le, B.H. Pipe floods and flash floods. Causes and solutions. *Agricultural Publisher*, **2000**, *1*, p. 96.

6. Ngo, D.T. Flash flood and mitigating flash floodst. Agricultural Publisher, 2006.
7. La, T.H.; Nguyen, T.T. Necessary knowledge about flash floods. Map Publisher, 2009.
8. https://public.wmo.int/en/projects/ffgs.
9. Viet Nam Institute of Meteorology, Hydrology and Climate Change, Ministry of Natural resources and Environment. Project report Investigation, survey, and mapping of flash flood risk zoning for the Central and Highland regions, and develop a pilot system of flash floods warning for high–risk localities in order to serve the purpose of planning, directing and operating disaster prevention and climate change adaptation, 2019.
10. Viet Nam Institude of Geosciences and Mineral Resources, Ministry of Natural resources and Environment. Report Current status map of landslides at scale 1:50,000 in Quang Nam province, Project on Investigating, evaluating and zoning the risk of landslides in mountainous areas of Vietnam, 2019.
11. Riggs, H.C. Estimating flow characteristics at ungaugedsites. In: Beran, M.A., Brilly, M., Becker, A., Bonacci, O. (Eds.). Regionalization in Hydrology, IAHS, **1990**, *191*,150–161.
12. Nixon, M. A study of bankfull discharges of rivers inEngland and Wales. *Mm. Preo. Instn. Civ. Engrs.* **1959**, *6322*, 157–174.
13. Williams, P. Bankfull Discharge of rivers. *Water Resour. Res.* **1978**, *6*, 1–14.
14. Carpenter, T.M.; Sperfslage, J.A.; Georgakakos, K.P.; Sweeney, T.; Fread, D.L. National threshold runoff estimation utilizing GIS in support of operational flash flood warning systems. *J. Hydrol.* **1999**, *224*, 21–44.
15. SEAFFGS. 2022. https://222.255.11.111/SEAFFGS_CONSOLE/.
16. Wang, C.T.; Gupta, V.K.; Waymire, E. A geomorphologicsynthesis of nonlinearity in surface runoff. *Water Resour. Res.* **1981**, *17(3)*, 545–554.
17. Georgakakos, K.P.; Unnikrishna, P.V.; Bravo, H.R.; Cramer, J.A. A national system for determining threshold runoff values for flash–flood prediction. Issue Paper, Department of Civil and Environmental Engineering and Iowa Institute of Hydraulic Research, The University of Iowa, Iowa City, IA, 1991.
18. Georgakakos, K.P. Modern Operational Flash Flood Warning Systems Based on Flash Flood Guidance Theory: Performance Evaluation. Proceedings of International Conference on Innovation, Advances and Implementation of Flood Forecasting Technology, Bergen–Tromsø, Norway, 2005, pp. 1–10.
19. Georgakakos, C.R.; Shamir, E.; Randall, B. Sothesast Asia Flash Flood Guidance System (SEAFFGS) system Administration User's Guide. Hydrologic Research Center, 2002.
20. Shamir, E.; Ben-Moshe, L.; Ronen, A.; Grodek, T.; Enzel, Y.; Georgakakos, K.; Morin, E. Geomorphology–based index for detecting minimal flood stages in arid alluvial streams. *Hydrol. Earth Syst. Sci. Discuss.* **2012**, *9*, 12357–12394.
21. Zhai, X.; Guo, L.; Liu, R. et al. Rainfall threshold determination for flash flood warning in mountainous catchments with consideration of antecedent soil moisture and rainfall pattern. *Nat. Hazards* **2018**, *94*, 605–625.

VIETNAM JOURNAL OF HYDROMETEOROLOGY

Research Article

Assessment of water environmental carrying capacity of Thuy Trieu lagoon, Cam Ranh, Khanh Hoa

Hanh Hong Thi Pham[1,2], Diem Hong Thi Luong Tran[1,2], Long Ta Bui[1,2*]

[1] Ho Chi Minh City University of Technology; longbt62@hcmut.edu.vn; diemtran.nyim0120@gmail.com; hanhpth99@hcmut.edu.vn
[2] Vietnam National University Ho Chi Minh City

*Corresponding author: longbt62@hcmut.edu.vn; Tel.: +84–918017376
Received: 13 November 2022; Accepted: 12 December 2022; Published: 25 December 2022

Abstract: In recent years, the socio-economic development of two districts of Cam Lam and Cam Ranh city of Khanh Hoa province has taken place strongly. This process has affected the environment of Thuy Trieu lagoon (TTL), leading to the need to assess the lagoon water environmental carrying capacity (LECC). Based on survey data in the years 2019–2021, this study has the objective of assessing the environmental capacity of the Thuy Trieu lagoon. Three substances are selected: Ammonia, Phosphate, and Nitrate. In this study, we use a MIKE 3 model with a Hydrodynamic module (HD) combined with a 3D numerical lab for ecological modeling (ECOLab), then extract the results and calculate the environmental carrying capacity load for the Thuy Trieu lagoon in the wet and dry seasons. The results showed that in the dry season, the residual carrying capacity of the water body $LECC_{RM}$ of substances such as Ammonia is 104.81 tons/month, Phosphate 193.18 tons/month, and Nitrate 2,294.91 tons/month. During the wet season, the $LECC_{RM}$ capacity in the water body also increased compared to the dry season with the $LECC_{RM}$ values of the following substances: Ammonium 165.33 tons/month, Phosphate 311.41 tons/month, and Nitrate 3,629.60 tons/month. This result complements the results already done, helping to have a more scientific basis for lagoon management and planning.

Keywords: Lagoon water quality; 3D hydrodynamic model; Ecological model; LOICZ; Thuy Trieu lagoon.

1. Introduction

Vietnam's coast has a total sea surface area of nearly 4,000 km^2 with all three types of water bodies, typically bays (gulf, bay, bight), estuary, and coastal lagoons [1]. The problem of lagoon pollution and marine environmental carrying capacity posed a science for the first time in [2]. From the initial concepts of ecological carrying capacity and environmental capacity assessment methods, up to now, related concepts and methods of assessing marine environmental capacity have become more and more complete. Environmental capacity helps to define sustainable limits for sustainable development action; rationally distribute activities taking place on and around water bodies to achieve the highest economic efficiency and maintain environmental quality within allowable limits and develop solutions to maintain and restore environmental capacity [3]. This is not only a theoretical development of marine environmental capacity but is mainly based on the practice of marine environmental pollution occurring in many parts of the world.

According to research by [4], most of the coastal areas worldwide have been ruined by pollution. As a result, coastal fisheries and marine-related industries are significantly affected [5]. In order to sustainably manage the coast and protect fishery resources, pollution of the

aquatic environment needs to be controlled. In the control of marine pollution, a series of programs such as the total daily maximum tonnage of the United States and the European Framework of Marine Strategic Indicators, the carrying capacity of the marine environment for pollutants must be estimated because it is important for coastal water management, as well as sustainable use of coastal areas [6–8]. From there, the discharge, transport, and transformation of pollutants must be analyzed and their effects assessed on the respective ecosystems [5]. To carry out this analysis and assessment, water quality modeling can make a powerful contribution to the necessary scientific basis of coastal zone management [9–10].

Increasing population density, and rapid developing socio-economic in the past centuries have led to increased discharge of pollutants from the landmass into these coastal seawaters [11–13]. These coastal environmental problems are mostly related to inland inputs, which are recognized to contribute to more than 75% of marine pollutants [14–15]. Therefore, it is very important to identify and estimate the pollutant load on land flowing to the coastal area and this is also the basis for pollution control and reduction. The US National Oceanic Development Policy and the European Union (EU) maritime strategy emphasize the use of integrated ecosystem-based management to maintain a healthy marine environment. China has established a "monitoring and forecasting system of natural resource-environmental capacity" based on land and sea assessment to promote ecological civilization-building [7].

Since the late 1970s, many research efforts have been made to estimate the terrestrial pollutant discharge to coastal areas around the world [16–17]. Based on the research findings, a range of policy instruments, such as the Total Maximum Daily Load (TMDL) program, the Best Management Practices, the Directive the European Water Framework Directive, etc., has been adopted to control soil pollution in developed countries such as the United States, Canada and the countries of the European Union.

In recent years, the process of socio-economic development of the central coastal region, including two districts of Cam Lam and Cam Ranh city of Khanh Hoa province, has firmly increased pressure on the environment, including the Thuy Trieu lagoon. Against that background, several studies have been conducted to assess marine environmental capacity (EC). The first study on the marine capacity in Vietnam was carried out in 2001 [18]. Recent years have been followed by studies [3, 19 – 21]. In that context, research has been carried out for this area, especially [19] presented the results of the environmental capacity assessment of Thuy Trieu lagoon from 2011 to 2012. However, this work is only based on monitoring data from some periods to estimate the average concentration for the whole lagoon. This leads to a non-accurate calculation. Therefore, our team continues to study this area by adopting a different approach, namely modelization. The modeling results, in the opinion of the authors, will give the average concentration over the entire lagoon more accurate, especially the model that has passed the calibration and verification steps. Therefore, it can be said that this study will supplement the results already done, and provide a better scientific basis for the management and planning of the lagoon.

Although environmental capacity has been considered for many coastal areas, when applied to specific coastal lagoons, it is still necessary to consider the possibility of communication between the lagoon and the open sea, namely the effects of hydrodynamic factors on LECC must be noticed. In this study, the authors use the method in [21] to calculate the LECC for the selected water body. The object of the study is Thuy Trieu lagoon, Khanh Hoa province. The steps in this study include hydrodynamic calculation, lagoon water quality assessment, and LECC calculation with clarification of semi-enclosed factors.

2. Materials and methodology

2.1. Study area

The scope of the study is the Thuy Trieu lagoon area, in Cam Lam district and Cam Ranh city. This is a prison lagoon and it seems that there is only water exchange through Cam Ranh

Bay, so the study extends to Cam Ranh Bay and creates an open boundary at the mouth of the bay (Figure 1).

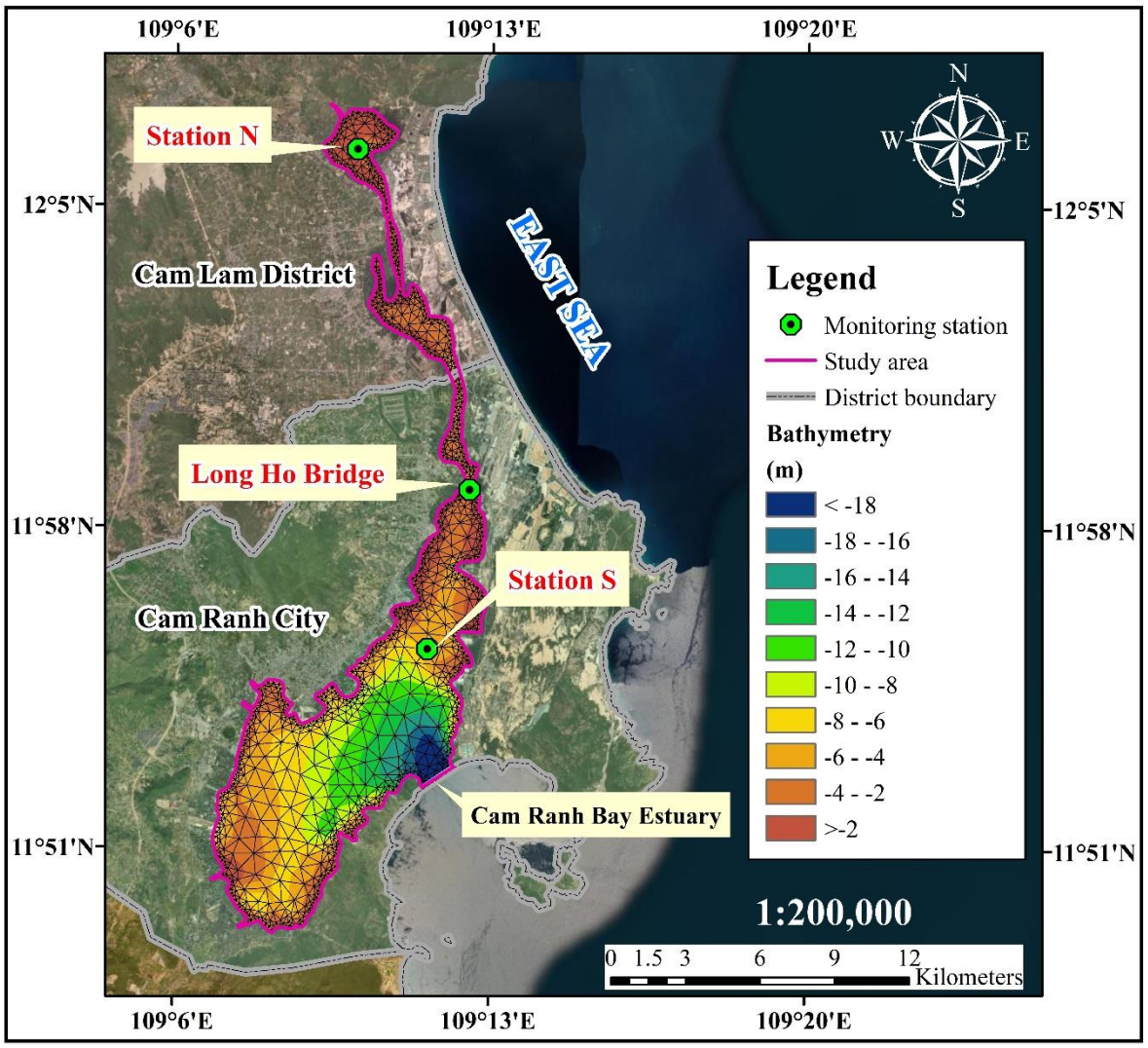

Figure 1. The study area, computation mesh, bathymetry, and monitoring stations.

2.2. Data

2.2.1. Bathymetry data

Bathymetry data Thuy Trieu Lagoon (from the top of Thuy Trieu Lagoon to Long Ho Bridge – the contiguous position between Thuy Trieu Lagoon and Cam Ranh Bay) in this study are measured data provided by Khanh Hoa Environmental and Resource Monitoring Cente. The bathymetry of Cam Ranh Bay is taken from General Bathymetric Chart of the Oceans (GEBCO) data. The computation mesh is set up with 2,195 nodes and 3,317 triangular elements, the minimum allowed angle is 26^o.

2.2.2. Meteorological data

The study took into account the area's meteorology. These data are extracted from Danish Hydraulics Institute (DHI) global data. Velocity (m/s) and wind direction (degrees) data are the time series from January 1, 2019 to December 31, 2020, and the time step is 1 hour. Besides, the evaporation data are calculated as an average annual value to calculate the water retention time.

2.2.3. Hydrological data

The water level boundary data at the inlet of Cam Ranh Bay was established with tidal data extracted from the MIKE Toolbox. Water level data measured at Long Ho Bridge station (Fig. 1) from January 1, 2019 to December 31, 2020, the time step 1 hour is used to calibrate – validate the Hydrodynamic (HD) module.

In addition, annual average rainfall data is collected to calculate the retention time of water.

2.2.4. Measured water quality data

Measured water quality data at Station N, Station S, and Station M locations (Figure 1) is provided by Khanh Hoa Environment and Natural Resources Monitoring Center. The pollutants noted are BOD_5, DO, NH_4^+, NO_3^-, PO_4^{3-}, Ecoli, and Coliforms. The value of the data is the average of the month in 2020. Data at Station S and Station M are used to calibrate the ECOLab model.

In this paper, the water quality data from the model is compared with the National Water Quality Standard (NWQS) from QCVN 10-MT:2015/BTNMT (National technical regulation on marine water quality – NMWQ) and QCVN 08-MT:2015/BTNMT (National technical regulation on surface water quality – NSWQ) (Table 1).

Table 1. National Water Quality Standard (Unit: mg/L).

Parameter	**NWQS**		
	NMWQ	**NSWQ**	
	Aquaculture areas, aquatic conservation	**A1**	**A2**
DO	≥ 5	≥ 6	≥ 5
BOD_5	-	4	6
Ammonia	0.1	0.3	0.3
Nitrate	-	2	5
Phosphate	0.2	0.1	0.2

2.2.5. Land-based pollution source data

In this study, we pay attention to 3 sources of waste collected from documents of the Khanh Hoa Center for Natural Resources and Environment Monitoring, in which industrial wastewater is Khanh Hoa sugar factory (NMD), domestic wastewater is residential near Cam Hai bridge (T1) and residential near sugar factory (C5). Detailed information about waste sources is shown in Table 2 below.

Table 2. Land-based pollution source information.

Name	**X**	**Y**	**Discharge (m^3/s)**	**DO**	**NH_4^+**	**NO_3^-**	**BOD_5**	**PO_4^{3-}**	**Total P**	**Coliform**
NMD	303050	1330967	0.105	5.73	0.35	1.25	23.08	0.96	2.23	7000.00
T1	301657	1335928	0.014	5.73	0.18	0.24	6.80	0.04	0.39	9300.00
C5	302648	1331095	0.014	5.73	0.21	0.28	17.72	1.29	2.91	6800.00

2.3. Methodology

In this study, our team approaches the calibrated and verified MIKE 3 with hydrodynamic and ECO Lab modules. Then, simulate advection-dispersion. Next, extract values from the model such as lagoon volume, flow velocity, area, and discharge,… combined with meteorological data such as precipitation and evaporation to calculate the water retention time using the LOICZ model. Finally, extract the concentration of substances from the model results combined with NWQS, and lagoon volume to calculate LECC. This process is shown in Figure 2.

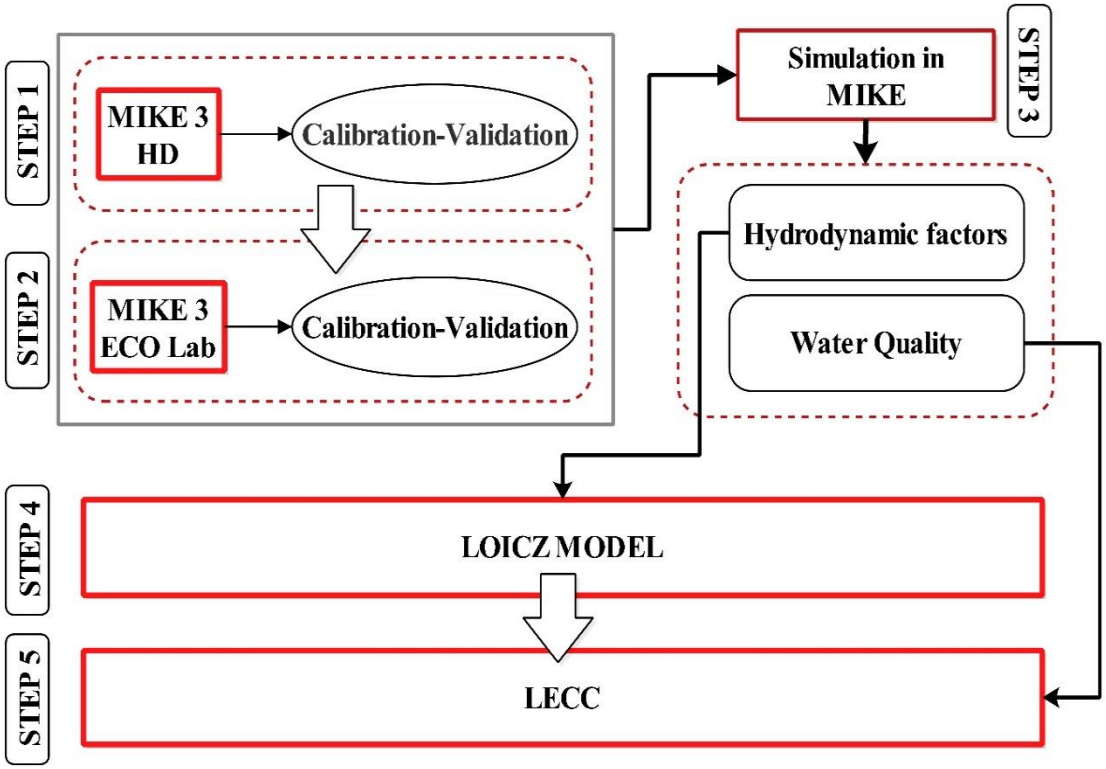

Figure 2. The flow chart of study structure.

2.3.1. Hydrodynamic model

MIKE 3 HD developed by DHI is used to simulate the flow and tidal regime [22]. This model is built from the solution of the three-dimensional incompressible Reynolds averaged Navier-Stokes equations, subject to the assumptions of Boussinesq and hydrostatic pressure.

The local continuity equation is written as

$$\frac{\partial u}{\partial x}+\frac{\partial v}{\partial y}+\frac{\partial w}{\partial z}=S \tag{1}$$

The two horizontal momentum equations for the x- and y- components respectively as below:

$$\frac{\partial u}{\partial t}+\frac{\partial u^2}{\partial x}+\frac{\partial vu}{\partial y}+\frac{\partial wu}{\partial z}=fv-g\frac{\partial \eta}{\partial x}-\frac{1}{\rho_0}\frac{\partial p_a}{\partial x}-\frac{g}{\rho_0}\int_z^\eta \frac{\partial \rho}{\partial x}-\frac{1}{\rho_0 h}\left(\frac{\partial s_{xx}}{\partial x}+\frac{\partial s_{xy}}{\partial y}\right)+F_u +\frac{\partial}{\partial z}\left(v_t\frac{\partial u}{\partial z}\right)+u_sS \tag{2}$$

$$\frac{\partial v}{\partial t}+\frac{\partial v^2}{\partial y}+\frac{\partial uv}{\partial x}+\frac{\partial wv}{\partial z}=fu-g\frac{\partial \eta}{\partial y}-\frac{1}{\rho_0}\frac{\partial p_a}{\partial y}-\frac{g}{\rho_0}\int_z^\eta \frac{\partial \rho}{\partial y}-\frac{1}{\rho_0 h}\left(\frac{\partial s_{yx}}{\partial x}+\frac{\partial s_{yy}}{\partial y}\right)+F_v +\frac{\partial}{\partial z}\left(v_t\frac{\partial v}{\partial z}\right)+v_sS \tag{3}$$

$$F_u=\frac{\partial}{\partial x}\left(2A\frac{\partial u}{\partial x}\right)+\frac{\partial}{\partial y}\left(2A\left(\frac{\partial u}{\partial y}+\frac{\partial v}{\partial x}\right)\right) \tag{4}$$

$$F_v=\frac{\partial}{\partial y}\left(2A\frac{\partial v}{\partial y}\right)+\frac{\partial}{\partial x}\left(2A\left(\frac{\partial u}{\partial y}+\frac{\partial v}{\partial x}\right)\right) \tag{5}$$

where t is the time; x, y and z are the Cartesian co-ordinates; η is the surface elevation; d is the still water depth; h= η+d is the total water depth; u, v and w are the velocity components in the x, y and z direction; f=2Ω sinΦ is the Coriolis parameter (Ω is the angular rate of revolution and ϕ the geographic latitude); g is the gravitational acceleration; ρ is the density of water; s_{xx} s_{xy} s_{yx} and s_{yy} are components of the radiation stress tensor; ν_t is the vertical turbulent (or eddy) viscosity; p_a is the atmospheric pressure; ρ_0 is the reference density of water. S is the magnitude of the discharge due to point sources and (u_s v_s) is the velocity by which the water is discharged into the ambient water. F_u, F_v are horizontal stress terms, A is horizontal viscous turbulence. The MIKE 3 HD module allows to calibrate two main parameters, namely the viscosity coefficient (eddy viscosity, ν, m^2/s) and the roughness height (roughness height, k_s, m) [22–25].

2.3.2. Ecological model

The biochemically coupled advection–diffusion model was developed to evaluate the physical–biological interactions in estuarine tropical ecosystems on nutrient and oxygen cycling:

$$\frac{\partial C}{\partial t}+\frac{\partial uC}{\partial x}+\frac{\partial vC}{\partial y}+\frac{\partial wC}{\partial z}=\frac{\partial}{\partial x}\left(K_x\frac{\partial C}{\partial x}\right)+\frac{\partial}{\partial y}\left(K_y\frac{\partial C}{\partial y}\right)+\frac{\partial}{\partial z}\left(K_z\frac{\partial C}{\partial z}\right)+F_{Ecolab}(C,t) \quad (6)$$

The compartments of the ecological model are dissolved oxygen (DO), biological oxygen demand (BOD), Ammonia (NH_4^+), and Phosphate (PO_4^{3-}) for the water quality factors. The variation concentrations at a given time in the ecological model is described by the equation (7-10).

$$\frac{dDO}{dt}=K_2(C_s-DO)-K_3.BOD.\theta_3^{(T-20)}.\frac{DO}{DO+[HS\_BOD]}-K_4.NH_3.\theta_4^{(T-20)}.\frac{DO}{DO+[HS\_nitr]} \quad (7)$$
$$+P_{max}.F_1(H).\cos 2\pi(\tau/\alpha).\theta_1^{(T-20)}-R_1.F_1(H).\theta_1^{(T-20)}-R_2.\theta_2^{(T-20)}-SOD$$

$$\frac{dBOD}{dt}=-K_3.BOD.\theta_3^{(T-20)}.\frac{DO}{DO+HS\_BOD} \quad (8)$$

$$\frac{dNH_4^+}{dt}=Y_{BOD}.K_3.BOD.\theta_3^{(T-20)}.\frac{DO}{DO+HS\_BOD}-K_4.NH_3.\theta_4^{(T-20)}-UN_p.(P-R_1.\theta_1^{(T-20)}) \quad (9)$$
$$-UN_b.K_3.BOD.\theta_3^{(T-20)}.\frac{NH_3}{NH_3+HS\_NH_3}+UN_p.R_2.\theta_2^{(T-20)}$$

$$\frac{dPO_4}{dt}=Y_2.K_3.BOD.\theta_3^{(T-20)}.\frac{PO_4}{PO_4+HS\_PO_4}-UP_p.(P-R_1.\theta_1^{(T-20)}) \quad (10)$$
$$-UP_b.K_3.BOD.\theta_3^{(T-20)}.\frac{PO_4}{PO_4+HS\_PO_4}-UP_p.R_2.\theta_2^{(T-20)}$$

The coefficients in equations (1) to (10) are shown in Table 3.

Table 3. Coefficients in the Ecological model.

No.	Parameter	Unit
1	Oxygen Processes: Respiration of animals and plants (R_1 = R_2)	(/d)
2	Oxygen Processes: Respiration temperature coefficient (q_1) = (q_2)	dimensionless
3	Sediment processes: Sediment oxygen demand (SOD)	$g/m^2/day$
4	Nitrogen Content: Ratio of ammonia released at BOD decay (Y_{BOD})	$gNH_4/gBOD$
5	Nitrogen Content: Uptake of ammonia in plants (UN_p)	Dimensionless
6	Nitrogen Content: Uptake of ammonia in bacteria (UN_b)	Dimensionless

No.	Parameter	Unit
7	Nitrification: Ammonia decay rate at 20 deg Celcius (K_4)	(/d)
8	Nitrification: Temperature coefficient for nitrification (q_4)	Dimensionless
9	Denitrification: Half saturation constant (HS_denitr = HS_PO_4 = HS_NH_3 = HS_nitr)	mg/l
10	Denitrification: Denitrification rate, conversion of nitrate into free nitrogen N_2 (K_6)	1/day
11	Denitrification: Temperature coefficient for denitrification (q_6)	Dimensionless
12	Coliforms: 1. Order decay Faecal coliforms (K_{dF})	(/d)
13	Coliforms: Arrhenius temperature coefficient (q)	Dimensionless
14	Phosphorus content: Ratio of phosphorus released at BOD decay (Y_2)	gP/gBOD
15	Phosphorus content: Uptake of P in plants (UP_p)	Dimensionless
16	Degradation: 1. order decay rate at 20 deg. C (K_3)	(/d)
17	Degradation: Temperature coefficient for decay rate (q_3)	Dimensionless
18	Degradation: Half-saturation oxygen concentration (HS_BOD)	mg/l

2.3.3. The Land Ocean Interactions in the Coastal Zone (LOICZ) model

This study used the wide model applied in coastal water bodies - the LOICZ to estimate the retention time of water, material balance, and nutrient status [25–27]. The retention time τ of water in a water body is expressed in equation (11):

$$\tau = \frac{V_{Sys}}{\left(V_X + |V_R|\right)} \tag{11}$$

where V_{sys} is bay volume, V_X is the exchange flow between the system and the sea, V_R is a residual flow to the sea [25].

2.3.4. LECC model

In this study, as applied to TTL, based on volumetric data and water retention time combined with data on pollutant content in water bodies and national water quality standards, the LECC is calculated as follows:

$$LECC = V_{sys}\left(1+1/\tau\right)\times\left(C_{ST} - C_{CR}\right) \tag{12}$$

where C_{CR} is the average concentration of pollutants, which is extracted from the results of running the eco-hydrodynamic model, considering the water body's self-cleaning process; C_{ST} is the allowable concentration of pollutants in National Water Quality Standards (NWQS); V_{sys} is the average water body volume in wet and dry seasons [19, 21].

$LECC_{PT}$ is potential LECC, the threshold amount of a pollutant that the water body, can hold according to the norm; τ is an important parameter that considers the water exchange between the Thuy Trieu lagoon and the open sea determined according to the LOICZ model. $LECC_{CR}$ is the current amount of a pollutant that the water body can hold, and C_{CR} is obtained from the seasonal average modelling results. $LECC_{RM}$ is the remaining amount of a pollutant that the water body can accept with that pollutant, in other words, $LECC_{RM}$ is the residual amount of pollutants that can be accepted by the water body. $LECC_{AU}$ is the residual safe threshold amount of pollutants that can be accepted by the water body, in other words, $LECC_{AU}$ is the remaining safe amount of a pollutant that the water body can accept.

2.4. Method to evaluate model accuracy

To evaluate the reliability of the model, the study uses the following four statistical criteria to evaluate: R^2, NSE, RSR, and PBIAS. R^2 is calculated directly from Excel, other formulas (13) to (15) include:

$$NSE = 1 - \frac{\sum_{i=1}^{n}\left(Q_i^{obs} - Q_i^{sim}\right)^2}{\sum_{i=1}^{n}\left(Q_i^{obs} - \bar{Q}\right)^2} \tag{13}$$

$$RSR = \frac{RMSE}{STDEV_{obs}} = \frac{\sqrt{\sum_{i=1}^{n}\left(Q_i^{obs} - Q_i^{sim}\right)^2}}{\sqrt{\sum_{i=1}^{n}\left(Q_i^{obs} - \bar{Q}\right)^2}} \quad (14)$$

$$PBIAS\% = \frac{\sum_{i=1}^{n}\left(Q_i^{obs} - Q_i^{sim}\right)\times 100}{\sum_{i=1}^{n}\left(Q_i^{obs}\right)} \quad (15)$$

where Q_i^{obs} is the measured value, Q_i^{sim} is the value from the model, and $\bar{Q}$ is the measured average value.

2.5. Model setup

2.5.1. Module HD

The Hydrodynamic model is set from January 1, 2020 to December 31, 2020, with a time step of 30 seconds. The viscosity coefficient with eddy type according to the Smagorinsky formula is 0.28, roughness coefficient with the Roughness height formula is 0.05m. The wind is also noted in the model. The module calibration time is selected from 1 January 2020 to 30 June 2020, with a time step of 1 hour at Long Ho Bridge station. Similarly, the validation period is from 1 July 2020 to 31 December 2020. The results of calibration and validation show that the water level data from the simulation and the measurements have a very good correlation for all four statistical criteria. This proves that the simulated Hydrodynamic model meets the requirements for simulation (Table 4).

Table 4. Water level correlation between model and measurement.

	R^2	NSE	RSR	PBIAS%
Calibration	0.976	0.974	0.162	1.388
Validation	0.983	0.980	0.140	0.220

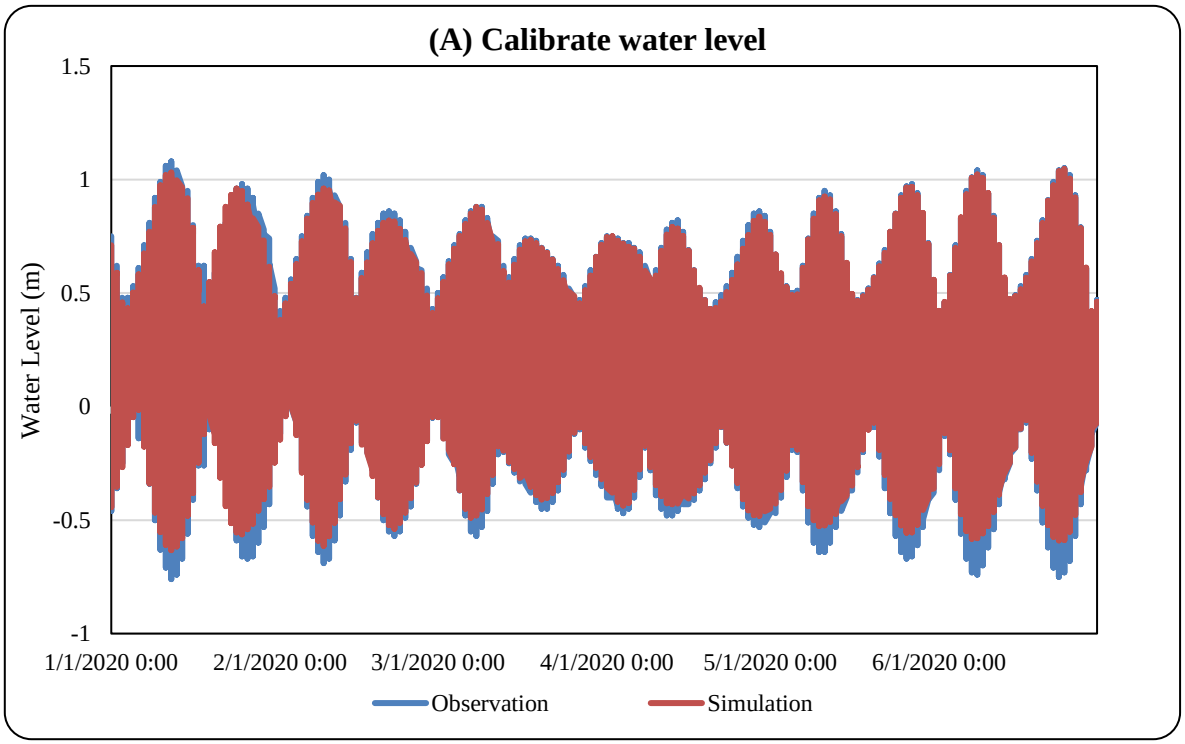

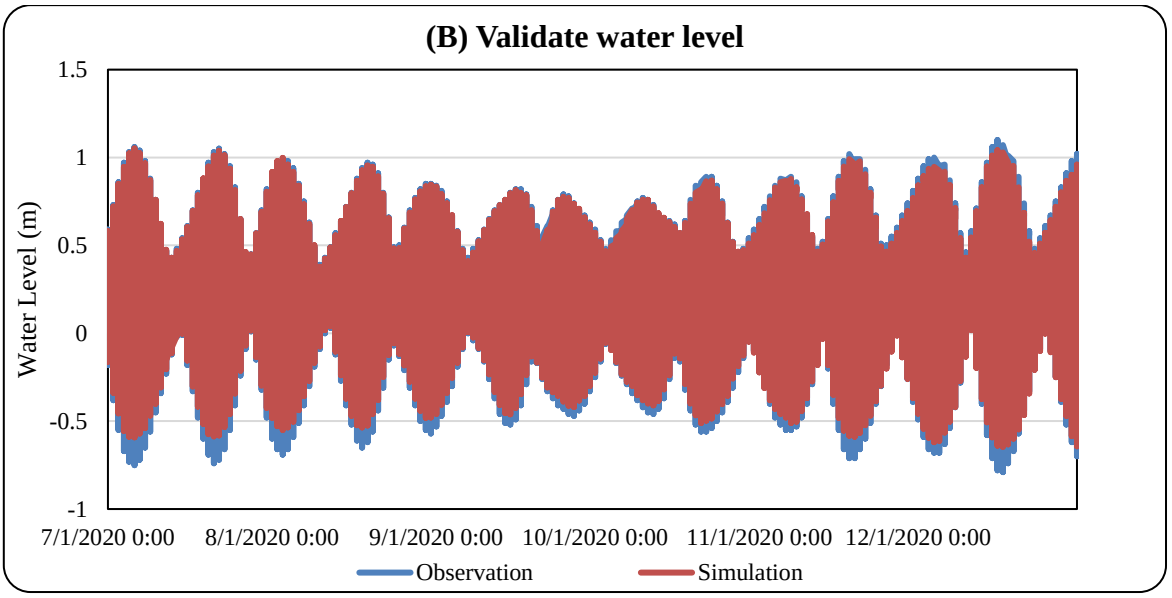

Figure 3. Water level between model and real measured (A) calibration (B) validation.

2.5.2. Module ECO Lab

The ECO Lab module is set up based on the calibrated HD module. Set up time is 1 year–2020, water quality parameters of boundary, initial, and discharge source are included in the model. Other parameters in ECOLab are set to default and adjusted gradually. The ECO Lab model used is MIKE WQ Level 4 and Coli + P. The dispersion coefficient is used according to the Scaled Eddy Viscosity formula, with the horizontal diffusion coefficient being 1, and the vertical being 0.01 (m^2/s). The set of parameters after calibrating is shown in Table 5. The comparison of the measured concentration and the simulation is shown in Table 6. The comparison results show that at Station S, 89.7% of the data has an accuracy of > 0.5, and Station M has 64.1% data with an accuracy of > 0.5 (Table 6). Since the data provided is a monthly average, only observed once a month, and taken as a representative of the month, it is difficult to correlate with the model.

Table 5. ECOLab parameter datasets applied in this model.

No.	Description	Value	Unit
1	Temperature: Latitude		
2	Temperature: Maximum absorbed solar radiation	4992	(/d)
3	Temperature: Displacement of solar radiation max. from 12 pm	0	hours
4	Temperature: Emitted heat radiation	1608	(/d)
5	Oxygen Processes: No. of reaeration expression	4	dimensionless
6	Oxygen Processes: Reaeration temperature coefficient	1.02	dimensionless
7	Oxygen Processes: Respiration of animals and plants	3	(/d)
8	Oxygen Processes: Respiration temperature coefficient	1.05	dimensionless
9	Oxygen Processes: Max. oxygen production by photosynthesis	2	(/d)
10	Oxygen Processes: Production/respiration per m^2 (=1) or per m^3 (=2)	1	
11	Degradation: 1. order decay rate at 20 deg. C	0.1	(/d)
12	Degradation: Temperature coefficient for decay rate	1	dimensionless
13	Degradation: Half-saturation oxygen concentration	2	mg/l
14	Oxygen Processes: Own #1 Reaeration constant	1	(/d)
15	Oxygen Processes: Own #1 Exponent, flow velocity	0	dimensionless
16	Oxygen Processes: Own #1 Exponent, water depth	0	dimensionless
17	Oxygen Processes: Own #1 Exponent, river slope	0	dimensionless
18	Oxygen Processes: Own #2 Reaeration constant	1	(/d)

No.	Description	Value	Unit
19	Oxygen Processes: Own #2 Exponent, flow velocity	0	dimensionless
20	Oxygen Processes: Own #2 Exponent, flow velocity	0	dimensionless
21	Oxygen Processes: Own #2 Exponent, river slope	0	dimensionless
22	Oxygen Processes: Own #3 Reaeration constant	1	(/d)
23	Oxygen Processes: Own #3 Exponent, flow velocity	0	dimensionless
24	Oxygen Processes: Own #3 Exponent, flow velocity	0	dimensionless
25	Oxygen Processes: Own #3 Exponent, river slope	0	dimensionless
26	Sediment processes: Sediment oxygen demand	2	$g/m^2/day$
27	Sediment processes: Temperature coefficient SOD	1	Dimensionless
28	Sediment processes: Resuspension of organic matter	0.5	$g/m^2/day$
29	Sediment processes: sedimentation rate for organic matter	0.8	m/day
30	Sediment processes: Critical flow velocity	1	m/s
31	Nitrogen Content: Ratio of ammonia released at BOD decay	0.2	$gNH_4/gBOD$
32	Nitrogen Content: Uptake of ammonia in plants	0.2	dimensionless
33	Nitrogen Content: Uptake of ammonia in bacteria	0.1	dimensionless
34	Nitrification: Reaction order 1 = first order process 2 = half order process	1	dimensionless
35	Nitrification: Ammonia decay rate at 20 deg Celcius	0.5	(/d)
36	Nitrification: Temperature coefficient for nitrification	1.13	dimensionless
37	Denitrification: Oxygen demand by nitrification	4.47	gO_2/gHN_4
38	Denitrification: Half saturation constant	0.5	mg/l
39	Denitrification: Reaction order 1 = first order process 2 = half order process	1	dimensionless
40	Denitrification: Denitrification rate, conversion of nitrate into free nitrogen N_2	0.1	1/day
41	Denitrification: Temperature coefficient for denitrification	1.2	dimensionless
42	Coliforms: 1. Order decay Fecal coliforms	0.2	(/d)
43	Coliforms: 1. Order decay Total coliforms	0.3	(/d)
44	Coliforms: Arrhenius temperature coefficient	1.09	dimensionless
45	Coliforms: Salinity coefficient of decay rate	1.01	dimensionless
46	Coliforms: Light coefficient of decay rate	1	dimensionless
47	Coliforms: Light Extinction Coefficient	1	1/m
48	Phosphorus content: Ratio of phosphorus released at BOD decay	0.01	gP/gBOD
49	Phosphorus content: Uptake of P in plants	0.009	dimensionless
50	Phosphorus exchange with bed: Resuspension of particulate phosphorus	0.5	$g/m^2/day$
51	Phosphorus exchange with bed: Deposition of particulate phosphorus	0.8	m/day
52	Phosphorus exchange with bed: Critical velocity of flow	1	m/s
53	Phosphorus processes: Decay constant for particulate phosphorus	0.1	(/d)
54	Phosphorus processes: Temperature coefficient for decay	1	dimensionless
55	Phosphorus processes: Formation constant for particulate phosphorus	0.1	(/d)
56	Phosphorus processes: Temperature coefficient for formation	1	dimensionless

Table 6. Comparison of the measured and modeled concentration outcomes.

		Station S			Station M		
	Time	**Observation**	**Simulation**	**Accuracy**	**Observation**	**Simulation**	**Accuracy**
DO	Jan-20	5.9000	5.2476	0.8894	6.1000	4.1351	0.6779
	Feb-20	6.2000	5.1659	0.8332	5.7000	3.9923	0.7004
	Mar-20	6.3000	5.3073	0.8424	5.8000	3.9906	0.6880
	Apr-20	6.2000	5.0487	0.8143	6.4000	3.9213	0.6127
	May-20	6.3000	5.4326	0.8623	5.3000	3.4940	0.6592
	Jun-20	5.7000	5.6636	0.9936	5.9000	3.3585	0.5692
	Jul-20	5.8000	5.7289	0.9877	6.0000	3.4604	0.5767
	Aug-20	5.7000	5.8867	0.9683	6.0000	3.5476	0.5913
	Sep-20	5.9000	6.0362	0.9774	5.7000	3.8990	0.6840
	Oct-20	6.0000	5.8649	0.9775	6.2000	4.0122	0.6471

		Station S			Station M		
	Time	**Observation**	**Simulation**	**Accuracy**	**Observation**	**Simulation**	**Accuracy**
Ammonium	Nov-20	5.8000	5.4402	0.9380	5.1000	4.1449	0.8127
	Dec-20	5.0000	5.2640	0.9499	4.6000	4.0684	0.8844
	Jan-20	0.0200	0.0251	0.7957	-	-	-
	Feb-20	0.0330	0.0237	0.7167	-	-	-
Nitrate	Feb-20	-	-	-	0.0200	0.0284	0.7045
	May-20	0.0260	0.0427	0.6085	0.0220	0.0289	0.7617
	Jun-20	0.0540	0.0364	0.6734	0.0230	0.0357	0.6450
	Jul-20	0.0260	0.0366	0.7096	-	-	-
	Aug-20	0.0260	0.0260	0.9981	0.0220	0.0243	0.9045
	Sep-20	0.0420	0.0354	0.8433	-	-	-
	Oct-20	0.0500	0.0424	0.8487	-	-	-
	Nov-20	0.0470	0.0603	0.7791	0.0530	0.0270	0.5089
	Dec-20	0.0620	0.0690	0.8984	0.0490	0.0289	0.5892
BOD	Jan-20	3.1200	2.8048	0.8990	-	-	-
	Feb-20	3.9000	2.6245	0.6729	-	-	-
	Mar-20	3.3000	1.7853	0.5410	-	-	-
	Apr-20	3.3000	1.6542	0.5013	-	-	-
	Nov-20	3.3000	2.4562	0.7443	-	-	-
	Dec-20	3.3000	3.0596	0.9271	-	-	-
Phosphate	Jan-20	0.0320	0.0541	0.5911	-	-	-
	Feb-20	-	-	-	0.0300	0.0424	0.7072
	Mar-20	0.0590	0.0531	0.9002	0.0520	0.0427	0.8204
	Apr-20	0.0300	0.0504	0.5956	0.0400	0.0375	0.9381
	May-20	-	-	-	0.0300	0.0412	0.7276
	Jun-20	0.0270	0.0452	0.5967	-	-	-
	Jul-20	0.0230	0.0451	0.5094	-	-	-
	Aug-20	0.0270	0.0430	0.6274	0.0230	0.0367	0.6267
	Sep-20	0.0350	0.0446	0.7845	0.0320	0.0329	0.9731
	Oct-20	-	-	-	0.0200	0.0383	0.5225

2.6. Conceptual model

The model of integrating information and data with mathematical models (presented above is named LECC) LECC includes a database bank, a model bank shown above Figure 4. The database block consists of 7 components: meteorology; hydrology; oceanography; surface water quality, waste source; Tide Prediction of Height dataset, and Vietnamese standards; model bank block includes 4 models: hydraulic, water quality model, residual time model, load calculation model. The LECC operation is carried out as follows: First, calibrate and verify the hydrological model; Second, the hydraulic model and water quality model simulate the concentration of selected substances, at the same time, in this step, NWQS block on water quality standards and results Retention time calculation results are performed to move to step 3; Third, calculate $LECC_{PT}$, $LECC_{CR}$, $LECC_{RM}$, and $LECC_{AU}$; Step four, verify LECC calculation results are transferred back to Step 2 to test whether when adding a calculated load $LECC_{RM}$ or $LECC_{AU}$, the water quality in the study area meets NWQS. The results outputted by LECC include flow simulation results in 3 layers, results on water quality modeling in 3 floors, $LECC_{RM}$ and $LECC_{AU}$ capacity calculation results Figure 4.

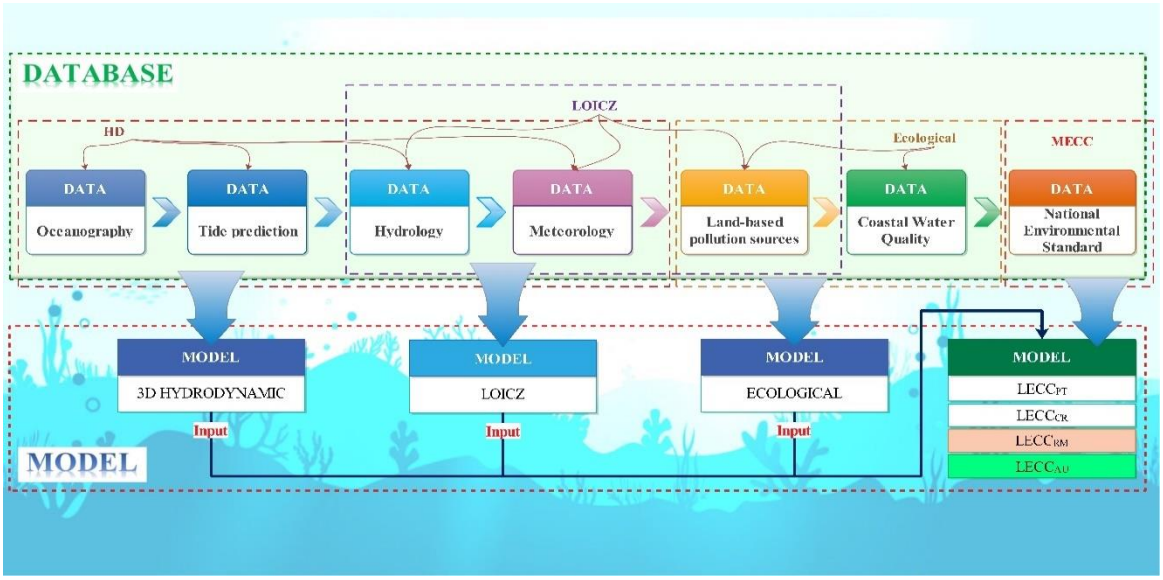

Figure 4. Conceptual model LECC.

3. Results and discussion

3.1. Hydrodynamic simulation

The hydraulic regime of Thuy Trieu lagoon is affected by the tides. The division of Thuy Trieu lagoon into 2 parts that can be clearly seen based on the water level. The North region from Thuy Trieu Lagoon Peak to Moi Bridge belongs to the commune and the South region from Moi Bridge to Long Ho Bridge. The study runs a hydrodynamic for the whole of 2020; Figure 4 represents April (dry season) and November (wet season). The water level in the wet season is higher than that in the dry season, the peak and the bottom of the tide in the wet season are 0.5 m different from that in the dry season. This shows that in the wet season, the water level in the lagoon increases rapidly due to the inflow of Cam Ranh Bay, presented in Figure 5.

In general, the flow velocity in the lagoon does not change much because it is a stagnant lagoon that only exchanges water through Cam Ranh Bay, so it is less affected by hydrodynamic factors from other regions. The flow velocity in the lagoon ranges from 0 to 0.15 m/s, the velocity is small at the shoreline and higher in the middle of the lagoon. Strong currents >0.4 m/s occur at the waists connecting the regions (at Moi Bridge and Long Ho Bridge) (Figure 6).

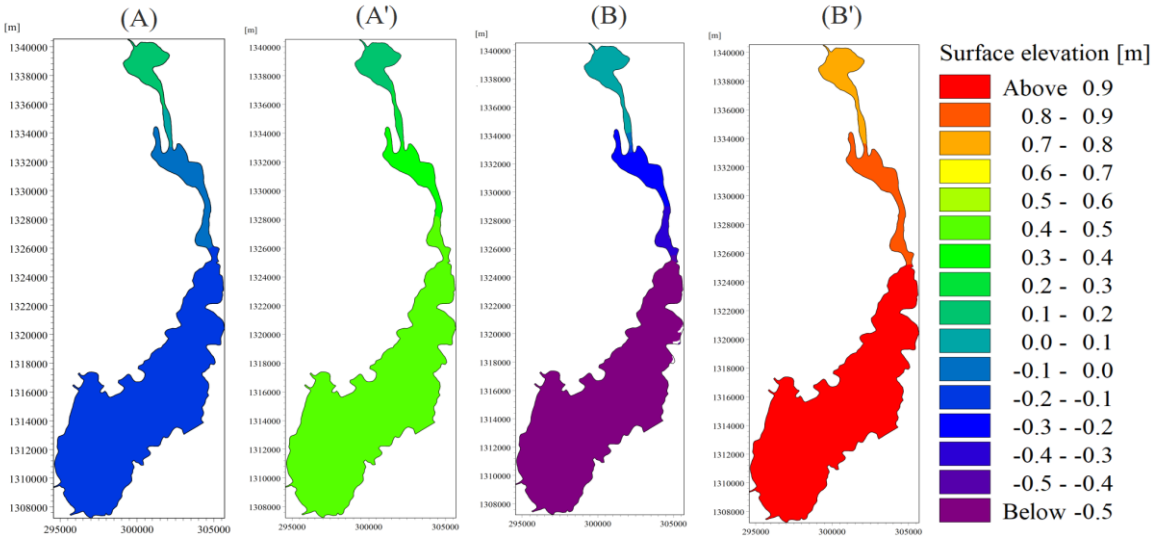

Figure 5. The water level at (A) the low tide, and (A') high tide in the dry season; (B) low tide, and (B') high tide in the wet season.

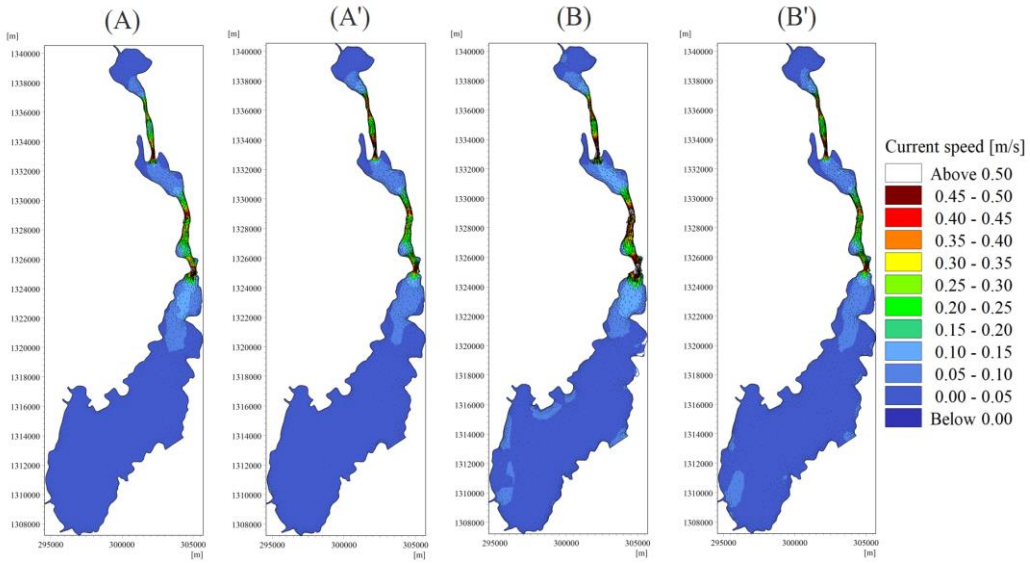

Figure 6. Current velocity at (A) low tide, (A') high tide in the dry season; (B) low tide, (B') high tide in the wet season.

3.2. Water quality modelling

The results of the substance advection-dispersion simulation for 2020 indicate that most of the parameters meet NWQS (Table 1) except for Ammonia not meet the NMWQ (the limit for it is ≤ 0.1 mg/l), but this parameter meets the NSWQ (the limit for it is ≤ 0.3 mg/l). This can be explained as the monitoring results of all parameters that meet NWQS, the model is calibrated by this data, so most substances meet NWQS.

Figure 7. Diagrams of NH_4^+, NO_3^-, and PO_4^{3-} changes in 2020 of TTL.

In terms of concentration distribution, most of the concentrations in the TTL did not change much, only increased during high tide and increased sharply in the wet season, with pollution from Cam Ranh Bay pushed in plus pollution from the South of the Lagoon to the North of the Lagoon and leaving it there, Figure 7. This is proven when considering the concentration of substances at the top of the Thuy Trieu Lagoon, they increase in the middle of the wet season, increase from November to February next year and decrease gradually from March, then fluctuate stably from April to October.

3.3. Retention time

The method of assessing water exchange capacity by the LOICZ model calculates the retention time of the tidal lagoon area as 28.11 days for the dry season and 14.01 days for the wet season (Table 7).

Table 7. The results of the calculation for the retention time.

	Unit	Wet	Dry
Precipitation (V_p)	10^6m^3/month	7.9510	3.8960
Evaporation (V_e)	10^6m^3/month	0.0005	0.0013
River (V_q)	10^6m^3/month	0	0
Groundwater flow volume (V_g)	10^6m^3/month	0	0
Other sources (V_o)	10^6m^3/month	0.1328	0.1328
Area	10^6m^2	96.9498	
System volume (V_{sys})	10^6m^3	566.3063	566.1567
Residual flow volume (V_r)	10^6m^3/month	–8.0833	–4.0275
System salinity (S_{sys})	‰	26.4	26.4
Oceanic salinity (S_{ocean})	‰	33	33
The salinity flux (V_x)	10^6m^3/month	32.3331	16.1101
The retention time (τ)	Day	14.0118	28.1143

3.4. LECC calculation

The results of calculating capacity are shown in Table 8 and Table 9. Note that the dry season of the study area lasts from January to August and the wet season is mainly from September to December.

Table 8. The load capacity of Thuy Trieu lagoon in the dry season.

Pollutant	$LECC_{PT}$ (ton/month)	$LECC_{CR}$ (ton/month)	$LECC_{RM}$ (ton/month)	$LECC_{AU}$ (ton/month)
Ammonia	115.01	10.21	104.81	70.30
Phosphate	230.03	36.85	193.18	124.17
Nitrate	2300.30	5.39	2294.91	1604.82

Table 9. The load capacity of Thuy Trieu lagoon in the wet season.

Pollutant	$LECC_{PT}$ (ton/month)	$LECC_{CR}$ (ton/month)	$LECC_{RM}$ (ton/month)	$LECC_{AU}$ (ton/month)
Ammonia	181.92	16.59	165.33	110.75
Phosphate	363.84	52.44	311.41	202.25
Nitrate	3638.43	8.83	3629.60	2538.07

From the simulation results, it is found that the considered that 2 indicators have concentrations that meet NMWQ and NSWQ except for Ammonia only meets the NSWQ, so the environmental capacity in this area is still high with Phosphate and Nitrate, and

Ammonia is the lowest. These are shown in Table 8 and Table 9. Specifically, during the dry season, the study area's volume is 566.1567 million m^3, so the remaining capacity of Ammonia, Phosphate, and Nitrate indicators is 104.81 tons/month, 193.18 tons/month, and 2,294.91 tons/month, respectively. For the wet season, the volume of the area increased by 0.1496 million m^3, so the remaining capacity of Ammonia, Phosphate, and Nitrate substances also increased, followed by 60.52 tons/month, 118.23 tons/month, and 1,334.69 tons/month, respectively.

3.5. Discussion

In the study [19] based on the observed data of the Thuy Trieu lagoon to calculate the load, this approach may lead to errors when choosing the average concentration of pollutants in the study water body C_{CR}. Meanwhile, this study is based on the method of using the MIKE 3 model to calculate the concentration of substances present in the area, then using the results of the load bearing model. There are also differences in the method of calculating the retention time between the two studies. At the time of implementation, the study [19] calculated the retention time to be 18.90 days for the dry season and 16.02 days for the wet season, while this study team calculated the retention time in the dry season to be 28.1143 days and in the dry season is 14.0118 days, this explains the difference in the relevant parameters in 2 different periods: 2011–2012 and 2019–2020 at present. At the same time, in the process of calculating the retention time for the area in the study of the team, only for the whole area of Thuy Trieu lagoon – Cam Ranh Bay, while the research team [19] divided into 3 areas: the peak area Thuy Trieu lagoon, Thuy Trieu lagoon estuary and Cam Ranh Bay.

There are also differences in the results of the calculation of the load between the two studies: based on the input data and the calculation results from the model, the Ammonium, Phosphate and Nitrate considered substances in this study are still capable of being considered. load capacity, > 70 tons/month, while in the study of [19], the indicators of Ammonium and Nitrate were close to the useful capacity, and the indicator of Phosphate reached the potential carrying capacity of the region.

4. Conclusion

Based on survey data, collected during 2019–2021, together with the socio-economic development plan in Thuy Trieu – Cam Ranh lagoon area, the article presents the results of the assessment of the environmental capacity of the lagoon. The research results showed that the water bodies are still capable of receiving wastewater containing Ammonium, Phosphate, and Nitrate substances in both dry and wet seasons. Specifically, in the dry season, the residual capacity of water bodies ($LECC_{RM}$) of substances such as Ammonium 104.81 tons/month, Phosphate 193.18 tons/month, Nitrate 2,294.91 tons/month. During the wet season, the volume of water bodies increased by 0.1496 million m^3 compared to the dry season, the total volume of the water body in the wet season was 566.3063 million m^3, resulting in an increase in the $LECC_{RM}$ in the water body compared to the dry season with the $LECC_{RM}$ values of the water bodies. Substances are as follows: Ammonia 165.33 tons/month, Phosphate 311.41 tons/month, and Nitrate 3,629.60 tons/month.

Since our team aims to use modeling to calculate the substance advection-dispersion and then extract the values to calculate LECC, it is easy to apply to other lagoons and bay areas if there is a full set of data for the model. The study makes it easier to assess when a new waste source appears to assess the impact of this source on the regional environmental capacity, by just adding the waste source and running the simulation. Thereby helping the manager make it easier to make decisions about whether this project will be implemented. This is an easy path for environmental managers in the future. The next research direction is to collect more information on water quality, and forecast pollution concentrations in the area to optimize the

established model. Collect more waste source information and evaluate if this calculation is correct.

Author contribution statement: Conceived and designed the experiments; Analyzed and interpreted the data; contributed reagents, materials, analysis tools, or data; module HD calibration/validation: H.H.T.P.; Performed the experiments; contributed reagents, materials, analyzed and interpreted the data; running ECOLab and LECC models: D.H.T.L.T.; wrote the manuscript: L.T.B.

Acknowledgments: We acknowledge the support of time and facilities from Ho Chi Minh City University of Technology (HCMUT), VNU-HCM for this study.

Competing interest statement: The authors declare no conflict of interest.

References

1. Tran, D.T. Classification and general features of coastal bays in Vietnam. *Vietnam J. Mar. Sci. Technol.* **2006**, *6(2)*, 38–51.
2. GESAMP. Environmental Capacity – An approach to marine pollution prevention, *Rep. Study GESAMP* **1986**, *30(80)*, 49.
3. Luu, V.D. Environmental capacity of typical water bodies along Vietnam's coast. Publishing house for natural sciences and technology, 2016, pp. 356.
4. Li, K.; Zhang, L.; Li, Y.; Zhang, L.; Wang, X. A three-dimensional water quality model to evaluate the environmental capacity of nitrogen and phosphorus in Jiaozhou Bay, China. *Mar. Pollut. Bull.* **2015**, *91(1)*, 306–316.
5. Islam, M.S.; Tanaka, M. Impacts of pollution on coastal and marine ecosystems including coastal and marine fisheries and approach for management: A review and synthesis. *Mar. Pollut. Bull.* **2004,** *48(7–8)*, 624–649.
6. Borja, Á.; Elliott, M.; Carstensen, J.; Heiskanen, A.S.; Van de Bund, W. Marine management – Towards an integrated implementation of the European marine strategy framework and the water framework directives. *Mar. Pollut. Bull.* **2010**, *60(12)*, 2175–2186.
7. Han, H.; Li, K.; Wang, X.; Shi, X.; Qiao, X.; Liu, J. Environmental capacity of nitrogen and phosphorus pollutions in Jiaozhou Bay, China: Modeling and assessing. *Mar. Pollut. Bull.* **2011**, *63(5–12)*, 262–266.
8. Linker, L.C.; Batiuk, R.A.; Shenk, G.W.; Cerco, C.F. Development of the Chesapeake Bay watershed total maximum daily load allocation. *J. Am. Water Resour. Assoc.* **2013**, *49(5)*, 986–1006.
9. Lung, W.S. *Water Quality Modeling for Wasteload Allocations and TMDLs*. Wiley, New York, 2001.
10. Nobre, A.M. et al. Assessment of coastal management options by means of multilayered ecosystem models. *Estuar. Coast. Shelf Sci.* **2010**, *87(1)*, 43–62.
11. Jickells, T.D. Nutrient Biogeochemistry of the Coastal Zone. *Science* **1998**, *281*, 217–222.
12. Syvitski, J.P.M.; Kettner, A.J.; Green, P. Impact of Humans on the Flux of Terrestrial Sediment to the Global Coastal Ocean. *Science* **2005**, *308(2005)*, 376–380.
13. Smith, S.V.; Swaney, D.P.; Talaue-mcmanus, L. Carbon – Nitrogen – Phosphorus Fluxes in the Coastal Zone : The LOICZ Approach to Global Assessment. Carbon and Nutrient Fluxes in Continental Margins, Springer-Verlag Berlin Heidelberg, 2010, 575–586.
14. Pravdlc, V. The scientific basis of marine pollution prevention strategies. *Chem. Ecol.* **1995**, *10(1–2)*, 25–31.
15. Williams, C. Combatting marine pollution from land-based activities: Australian initiatives. *Ocean Coast. Manag.* **1996**, *33(1–3)*, 87–112.
16. Jarvie, H.P.; Neal, C.; Tappin, A.D. European land-based pollutant loads to the North Sea: An analysis of the Paris Commission data and review of monitoring strategies. *Sci. Total Environ.* **1997**, *194–195*, 39–58.

17. Tuncer, G. et al. Land-based sources of pollution along the Black Sea coast of Turkey: Concentrations and annual loads to the Black Sea. *Mar. Pollut. Bull.* **1998**, *36(6)*, 409–423.
18. Vo, D.S.; Nguyen, T.A. Assessment of environmental capacity of Thuy Trieu – Cam Ranh waters. *Vietnam J. Mar. Sci. Technol.* **2001**, *1(4)*, 4–20.
19. Thu, P.M.; Huan, N.H.; Long, B.H. Assessment of Environmental Capacity of Thuy Trieu – Cam Ranh Waters. *Vietnam J. Mar. Sci. Technol.* **2013**, *13(4)*, 371–381.
20. Long B.T.; Khanh, H.T.P.; Thuy, V.T.A. Environmental capacity assessment for Amoni and TSS in Dung Quat bay, Viet Nam. *IOP Conf. Ser. Earth Environ. Sci. (EES).* **2019**, *344*, 1–8.
21. Bui, L.T.; Tran, D.L.T. Assessing marine environmental carrying capacity in semi-enclosed coastal areas – Models and related databases. *Sci. Total Environ.* **2022**, *838*, 156043.
22. DHI. MIKE 21 & MIKE 3 flow model FM, Hydrodynamic and Transport Module, Scientific Documentation, 2018.
23. DHI. MIKE 21 - Spectral Wave Module - Scientific Document, 2007.
24. DHI. MIKE 21 & MIKE 3 flow model FM, Mud Transport Module Scientific Documentation, 2012.
25. DHI. MIKE 21/3 coupled model FM, User guide, 2009.
26. Gordon, D.C., Boudreau, Jr.P.R., Mann, K.H., Ong, J.E., Silvert, W.L., Smith, S.V., Wattayakorn, F.W.A.T.Y. LOICZ BIOGEOCHEMICAL Modelling Guidelines, 1996.
27. Kiwango, H.; Njau, K.N.; Wolanski, E. The application of nutrient budget models to determine the ecosystem health of the Wami Estuary, Tanzania. *Ecohydrol. Hydrobiol.* **2018**, *18(2)*, 107–119.

VIETNAM JOURNAL OF HYDROMETEOROLOGY

Research Article

Potential Sections for The Development of Solar Energy Using Remote Sensing Data and GIS in Dak Nong Province, Viet Nam

Nga Pham–Thi–Thanh[1*], The Doan–Thi[1], Cong Nguyen-Tien[2]

[1] Vietnam Institute of Meteorology, Hydrology and Climate Change, Hanoi, Vietnam; doanthe00@gmail.com; pttnga.monre@gmail.com

[2] Vietnam National Space Center, Vietnam Academy of Science and Technology; tiencongn@gmail.com

*Corresponding author: pttnga.monre@gmail.com; Tel.: +84–945803088

Received: 13 November 2022; Accepted: 13 December 2022; Published: 25 December 2022

Abstract: For promoting the development of renewable energy in Vietnam, in 2015 the Government approved the "Strategy for the development of renewable energy in Vietnam to 2030, with a vision to 2050" intending to gradually increase the proportion of renewable energy in national energy production and reduce dependence on fossil energy sources, contribute to ensuring energy security, mitigating climate change, and sustainable socio–economic development. In recent decades, remote sensing and Geography information of system (GIS) have been able to build thematic maps with high accuracy for managing and monitoring natural resources and the environment, including the solar radiation potential. Establishing solar potential maps from satellite data combined with natural conditions, topography, and land cover will effectively assist in planning solar energy development while helping to identify the appropriate technology and lowest cost. Therefore, this paper presents the zonalization of the solar energy potential based on its calculations from Himawari–8 satellite and elevation from The Shuttle Radar Topography Mission data applied for Dak Nong province. The results show that only about 18% of land in Dak Nong province is suitable for solar energy development. The appropiate sites for the development of solar energy are distributed in different regions of the Dak Nong province.

Keywords: Surface solar irradiation; Himawari–8 Satellite; K–mean cluster, zonalization.

1. Introduction

Vietnam has a vast potential for solar resources that could be tapped for solar energy development using solar photovoltaic (PV) and solar thermal (ST) applications for the hot water, commercial heat and industrial generation. Current scientific estimates of total solar resources in Vietnam give an average of 4–5 kWh/m^2/day in most parts of southern, central and even partly northern Vietnam (total 1,460–1,825 kWh/m^2/year) and an average maximum irradiance of up to 5.5 kWh/m^2/day in some southern regions (total up to 2,000 kWh/m^2/year [1–2]. The rapid growth in electricity demand is challenging Vietnam's energy sector and green growth strategy. In response to this, the Government of Viet Nam has prioritized a development of the renewable energy in the National Power Development Plan VII with a share about 6% of the total energy production by 2030. In detail, the solar power was expected to reach 850 MW (0.5%) by 2020, about 4,000 MW (1.6%) in 2025 and about 12,000 MW (3.3%) by 2030 [3]. A report implemented by Vietnam Electricity (EVN) shows a rapid development of the renewable energy in Viet Nam (Figure 1).

In order to enhance this rapid development of the renewable energy, it is urgent to study, evaluate, and regionalize its potential for every energy source, including the irrandicance energy. However, the barriers to solar energy development are production costs, policies, database information for planning and policy; technology, and ancillary services [4]. Which, there are three difficulties related to planning issues: 1) Lack of reliable assessments of potential renewable energy sources; 2) lack of terrestrial data series with appropriate distribution for trend and reliability studies; 3) limited understanding of the variability and relationships of renewable energy potential with other variables such as climate, topography, and human impact on the environment [5].

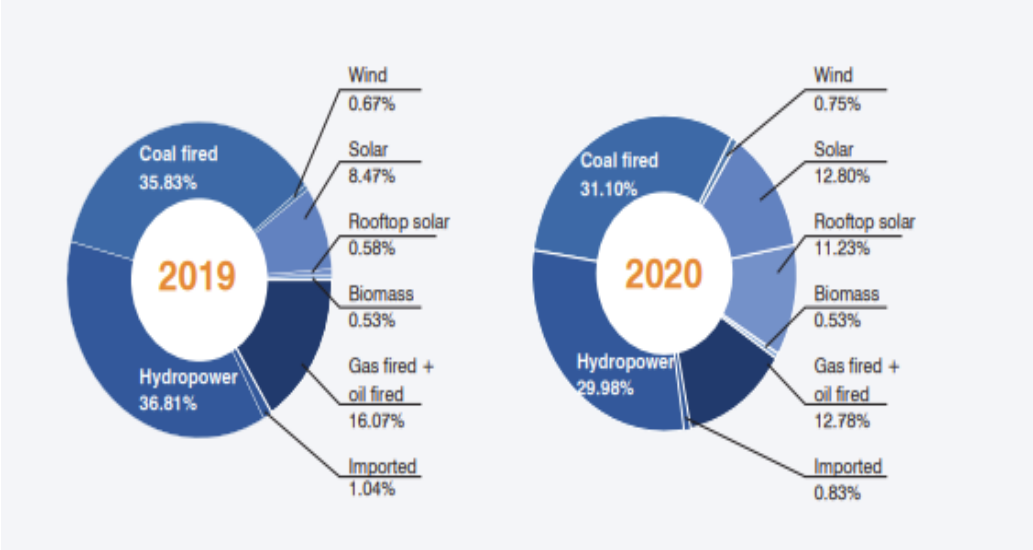

Figure 1. Renewable Energy Productivity Growth 2019–2020 by Vietnam Electricity [25].

Solar energy estimation using satellite data has been studied and applied very early in countries such as the USA, EURO, Brazil, China, Iran, India, and Vietnam [5–8]. With outstanding advantages in terms of coverage, spatial resolution, and monitoring frequency, satellite data has become a useful alternative for large–scale extraction of surface radiant energy parameters, especially for areas without hourly frequency measurement stations [9]. The satellites commonly used for irradiance calculations are Geostationary Satellites like MGS (Meteosat Second Generation) – SEVIRI, GOES-USA, INSAT-India, FY-2-China, and MTSAT/ Himawari-8 (Japan). Vietnam is in the best coverage of satellites GMS/Himawari-8 (Japan), Elecktro–Russia, and FY-2 (China). However, from 1997 until now, Vietnam's Ministry of Natural Resources and Environment has only collected Himawari–8 data for weather forecasting. Therefore, this study also used this data to estimate the value of solar energy in Vietnam

The concept of zoning is quite broad, including natural geographic zoning, landscape geography, ecological zoning, climatic zoning, economic zoning, and cultural zoning. However, the principle of zoning is to divide the territory into regions with similar and homogenous characteristics. From there, serving the planning for each object or the overall development [10–15]. The objective of radiation zoning is a combination of radiation characteristics and many other factors such as topography, land use, etc. to study zoning for the development of solar energy [16]. For example, the study [17] presented the development zoning for solar power plants with a capacity of 1MWe or more over Vietnam. The research [7] has also performed solar energy potential zoning for the solar power plant using terrestrial PV technology with a capacity of more than 1MWe. However, there has been no research on solar zoning at the provincial level. Therefore, this study implements zoning of the solar potential for Dak Nong province, contributing to the formulation of a solar energy development strategy in the Dak Nong province.

2. Data and Methodology

2.1. Data

Solar radiation data: The Himawari 8 satellite was launched in 2014 and became commissioned by the Japan Meteorological Agency (JMA) in July 2015. The Himawari–8 features the new 16–band Advanced Himawari Imange (AHI), covering visible, shortware–IR and thermal–IR spectra. A high–speed algorithm to estimate solar radiation using HIMAWARI–8/AHI data was developed by the Oceanic and Atmospheric Research Institute (AORI) of Japan. The goal of satellite–based irradiance estimation models is to use information about irradiance at the top of the atmosphere and albedo to calculate total Global horizontal irradiance (GHI) and Direct Normal Irradiation (DNI). In this study, we used the GHI data as detaily described in our previous publications [18–19] for radiation potential zoning in Dak Nong province, and the average GHI value is calculated from data of three years from 2016 to 2019.

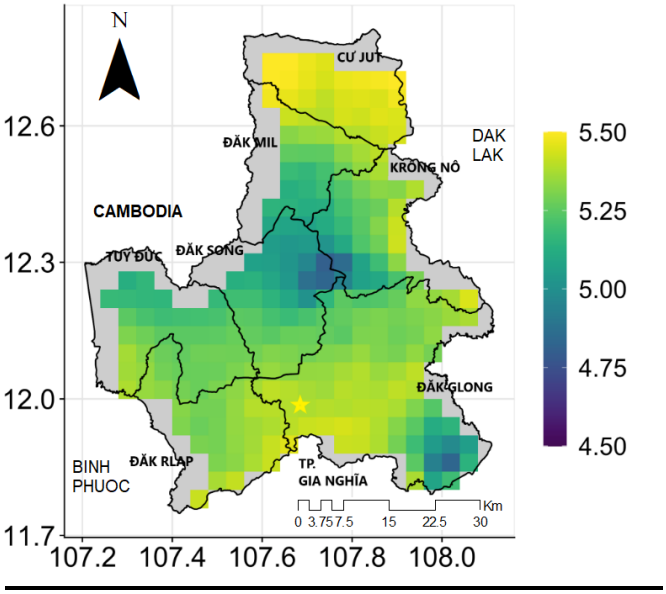

Figure 2. Average surface radiation in the period 2016–2018 in Dak Nong province (kWh/m^2/day).

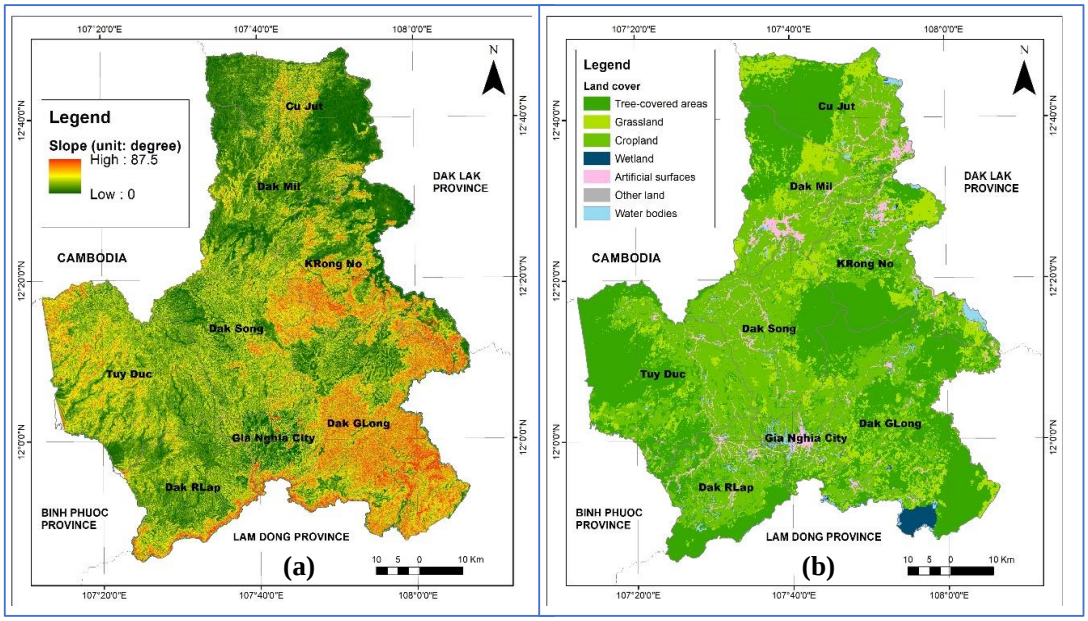

Figure 3. The slope map of Dak Nong province is built from DEM–SRTM30M; Land cover map in Dak Nong province.

Digital elevation model and slope: DEM–Digital Elevation Model of Dak Nong province is the 30meter resolution SRTM (The Shuttle Radar Topography Mission). This data is avaiable on the USGS Earth Explore and from the site: https://gisgeography.com/free-global-dem-data-sources/ (Figure 3a).

Land–use and land cover data: Land use data for 2014 of Dak Nong province (Figure 3b) was collected from the Department of Natural Resources and Environment of Dak Nong province. This study uses Sentinel–2 satellite data in 2019 to update the landcover in Dak Nong.

2.2. Methodology

The GIS technology has been widely used to integrate spatial data analysis and mapping to assess solar energy potential in the world. We also applied the GIS technique for solar energy potential zoning in this study for Dak Nong province and the process consists of 6 following steps:

Step 1: Data collection.

Step 2: Estimation of GHI using

Step 3: Updating and classifying land use 2019.

Step 4: Classification of slope criteria, suitable land use for PV power development

Step 5: Theoretical Potential Mapping: Partition of GHI data using K–means algorithm.

This method has also been presented in our previous studies [18, 23]. The K–means clustering algorithm belongs to the class of unsupervised learning methods (Machine Learning) that groups the unlabeled data set into different clusters. Firstly, it determines the best value for K centers or centroids through an iterative process.

Then, it assigns each data points its nearest k center data points close to the respective center k form a cluster. Therefore, each cluster has data points with some similarities and is separate from the othe clusters. Figure 4 explains how the K-mean clustering algorithm works:

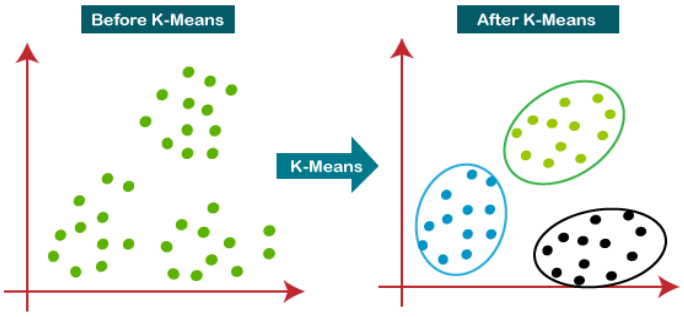

Figure 4. The diagram of the K–mean clustering algorithm.

A diagram of the K–means algorithm used in the study is presented in Figure 5.

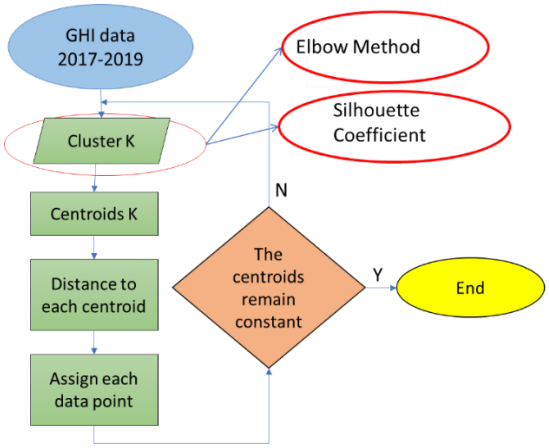

Figure 5. The Diagram of the K–means algorithm for GHI data.

Step 6: Mapping geographic potential using multi–criteria spatial analysis method by combining zoning results with groups of geographical criteria (land use, topography) that promote or limit the development of solar energy.

3. Results and Discussion

The results obtained from the GHI solar irradiance zoning by the K–means method show that for the GHI surface radiation annual process in Dak Nong area, the division into 4 clusters is reasonable. This is shown by the similarity in the results of both Elbow method and Silhouette coefficient. Therefore, in this study, the number of "optimal" clusters selected is 4. Figure 6 below shows the results of GHI zoning in Dak Nong province and Table 1 shows the solar radiation characteristics by months and years of the clusters.

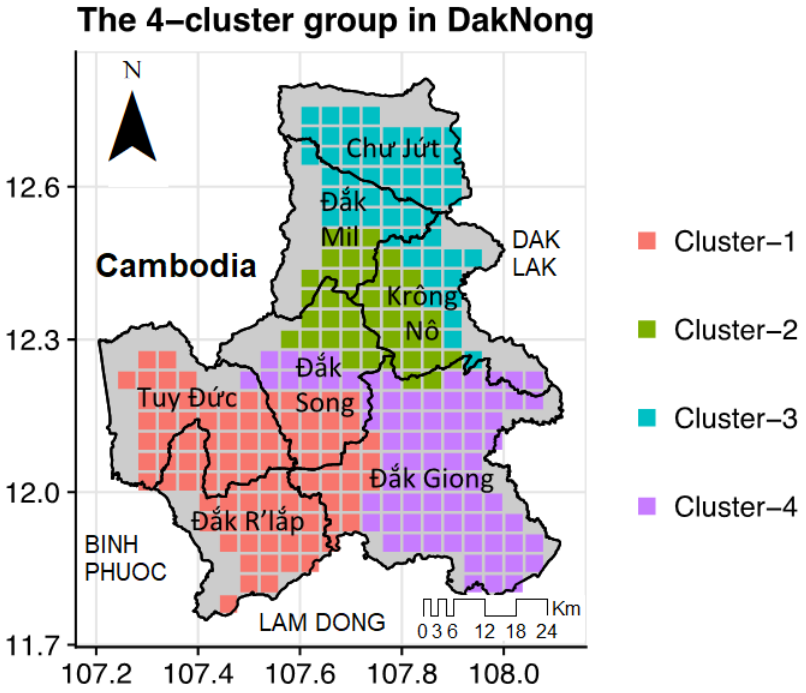

Figure 6. Radiation zoning in Dak Nong province.

In general, the radiation shows the maximum in March and the minimum in December. For cluster 1, cluster 3, and cluster 4, the annual radiation process has 2 peaks with the maximum being in March and the sub–max in September and 2 times being the minimum. Particularly for cluster 2, during the period from June to September, the average monthly radiation volume is almost unchanged. Compared with the average annual radiation value of the whole province, the months with significantly lower average radiation amounts are July–August in cluster 1 and cluster 4; November–December in all 4 clusters, and January in clusters 2 and 3. Months with significantly higher mean radiation values are from February to May (in clusters 1, 3, and 4), and from March to May (in clusters 2). The period with a large amount of radiation usually falls in the dry period before the rainy season begins in the Central Highlands.

Table 1. Average radiation value by month ($kW/m^{-2}day^{-1}$).

	Jan	Feb	Mar	Apr	May	Jun	Jul	Aug	Sep	Oct	Nov	Dec	Mean
Cluster–1	5.18	6.20	6.58	6.31	5.67	5.05	4.62	4.63	5.15	5.07	4.83	4.36	5.30
Cluster–2	4.22	5.31	6.78	6.32	5.57	5.15	5.11	5.14	5.29	4.86	3.97	3.21	5.09
Cluster–3	4.64	5.67	6.96	6.57	6.08	5.37	5.43	5.44	5.59	5.07	4.29	3.60	5.39
Cluster–4	5.04	6.08	6.83	6.33	5.72	5.05	4.64	4.69	5.25	5.00	4.57	4.04	5.27

The geographic potential is a combination of geographical criteria such as land use and topography. The criteria of land use and topography are only to exclude areas that are not allowed or cannot develop Solar Energy according to the following criteria:

Topographic standard: Considering the slope criteria suitable for solar PV development as studied [17, 24] are below 15^o. For terrain elevation, the solar development standard is lower than 2000 m. Therefore, this study uses an area that encourages solar development with an altitude below 2000 m and a slope lower than 15^o (Figure 7a). The optimal slope direction for solar PV development is the South direction and is flat, so the aspect for solar PV development in Dak Nong is where the aspect is < 1^o and from 112.5^o (southeast) to 292.5^o (west) (Figure 7b).

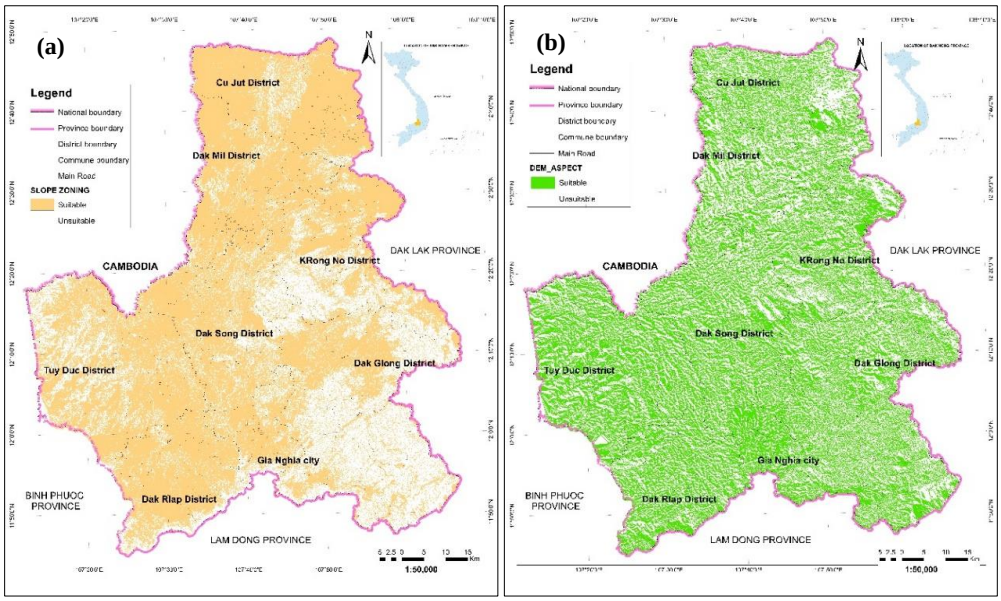

Figure 7. (a) Elevation and slope zoning (Orange is the promotion zone and white is the unsuitable zone for Solar PV Development); (b) The Aspect zoning (Green is the promotion zone and white is the unsuitable zone for Solar PV Development.

Land–use standard: Figure 8 and Table 2 lists the types of land use suitable for solar power development in Dak Nong province. Including 31 types of land use suitable for solar energy development with a total area of 158,528.21 ha, equivalent to 22.9% of the province's area.

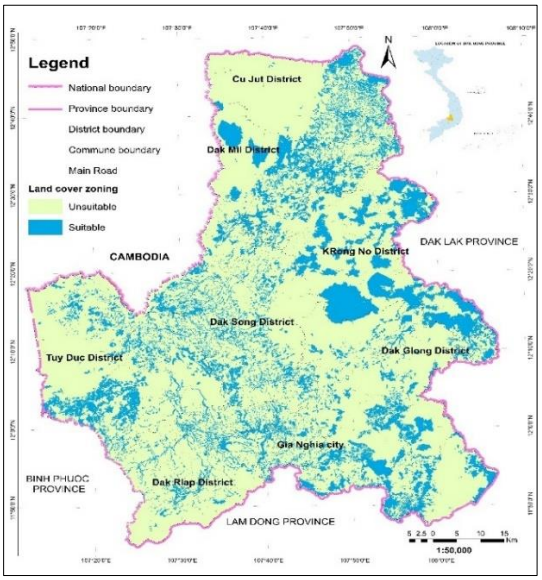

Figure 8. Land cover zoning (blue is the promotion zone and green is the unsuitable zone for Solar PV Development.

Table 2. Lists of types of Land use suitable for solar power in Dak Nong province.

Code	Land use type	Area (ha)
BCS	Unused flat land	51.05
CAN	Security land	1,213.09
CDG	Specialized land	779.88
CQP	Defense land	2.885.65
DBV	Land for post and telecommunications works	6.82
DCH	Market land	33.36
DCK	Land for other public works	1.55
DCS	Unused hilly land	18,065.93
DDT	Land with historical and cultural relics	17.56
DGD	Land for construction of educational and training institutions	412.92
DNL	Land for energy works	8,344.65
DRA	Land for landfill, waste treatment	45.40
DSH	Land for community activities	49.31
DTS	Land for construction of headquarters of non–business organizations	31.86
DTT	Land for construction of sports facilities	83.13
DVH	Land for construction of cultural facilities	32.39
DXH	Land for construction of social service establishments	7.39
DYT	Land for construction of medical facilities	70.64
NHK	Upland land for planting other annual crops	104,671.34
NKH	Other agricultural land	108.38
ODT	Land in urban areas	2,115.60
ODT+CLN	Land in urban areas + Land for perennial crops	553.30
ONT	Land in countryside	15,730.46
ONT+CLN	Land in countryside + Land for perennial crops	2,240.67
ONT+NHK	Land in countryside + Upland land for planting other annual crops	57.19
PNK	Other non–agricultural land	235.96
SKC	Land for non–agricultural production facilities	6.71
SKS	Land used for mineral activities	385.49
TIN	Land of faith	0.87
TMD	Commercial and service land	15.65
TON	Land for religious facilities	130.51
TSC	Land to build office headquarters	197.50

The zoning result is an integration of the criteria of solar irradiance and geographical criteria (slope and land use) using GIS tools. Thus, the zoning results show that Dak Nong province is divided into four potential solar energy zones, with average radiation values ranging from 5.09 to 5.39 kW/m^2/day. The selection of numerical partition value ranges is to help users use solar radiation data in choosing solar power technologies suitable for use purposes (Figure 9). The detailed results of the area suitable for solar energy development in Dak Nong province are presented in Table 3 and Figure 10.

Table 3. The area suitable for solar power by districts in Dak Nong province.

Name of Districts	Unsuitable	Under 5.09 kM/m^2/day	5.09–5.27 kM/m^{2}2/day	5.27–5.30 kM/m^2/day	5.30 –5.39 kM/m^2/day
Cu Jut Dist.	59905.67	0.00	0.00	**11659.70**	0.00
Dak Mil Dist.	55824.77	0.00	3781.53	**7610.32**	0.00
Krong No Dist.	67295.40	0.00	5357.16	**7027.33**	1780.47
Dak Song Dist.	74102.14	2111.35	1685.93	0.00	2741.61
Gia Nghia City	24217.52	3750.01	0.00	0.00	252.10
Dak Rlap Dist.	57400.41	6018.93	0.00	0.00	0.00
Tuy Duc Dist.	98839.62	**11454.87**	0.00	0.00	393.91
Dak Glong Dist	133661.17	299.37	47.27	0.00	**10541.00**
Total Area	**571246.70**	**23634.53**	**10871.89**	**26297.36**	**15709.09**

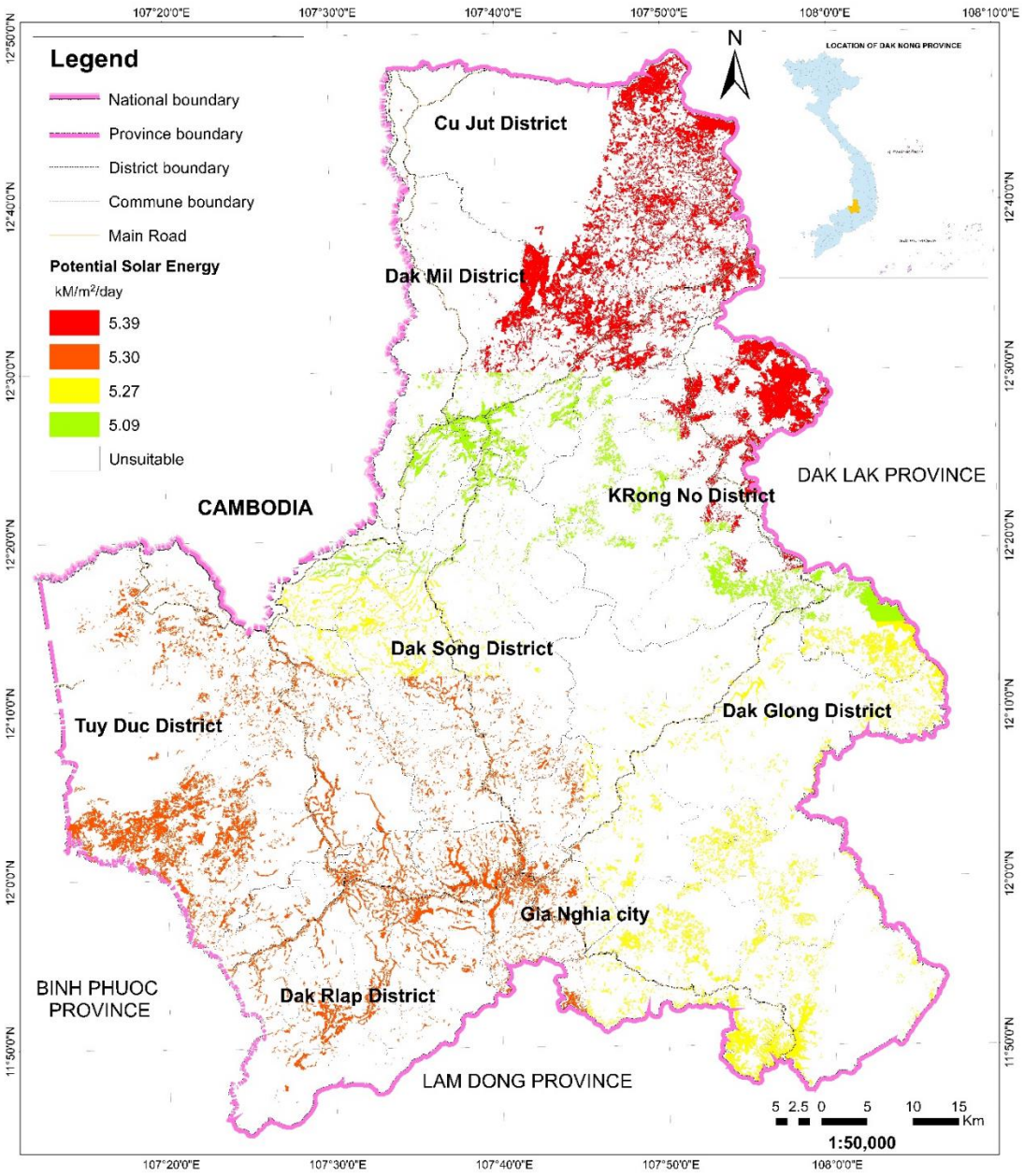

Figure 9. Map of potential zoning for solar energy development.

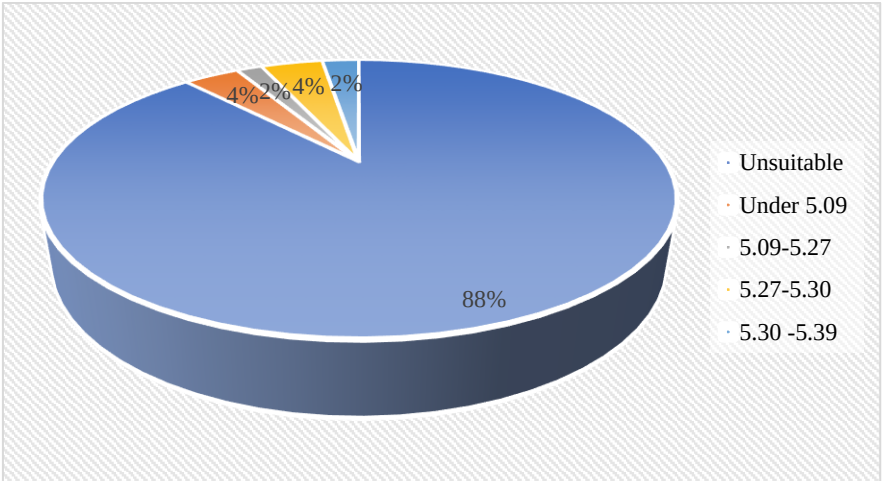

Figure 10. The ratio of the area suitable for developing solar energy (Unit: kM/m^2/day).

The results show that only about 18 percent of the entire area of Dak Nong province is suitable for solar power development. Distributed in different areas of the province. Solar energy development potential is highest in the northeast of Dak Nong province in Cu Jut district (total suitable area is 11.659 ha), then in some southwestern areas of the province in Tuy Duc district is 11.454 ha, and Dak GLong district is 10.541 ha.

4. Conclusions

This study has provided a scientific basis for potential zoning for solar energy development planning in Vietnam, applied as a pilot for Dak Nong province. The theoretical potential is partitioned by the k-means clustering method, then the geographic potential is the combination of zoning results with criteria to exclude areas that are not suitable for solar PV development. The standard land use thresholds and slope criteria are used as the basis for excluding areas that are not permitted or unsuiable for solar PV development.

Remote sensing data and and GIS are useful for site assessment in zoning mapping for the solar energy development in Dak Nong province, determining specific thresholds for each criterion. We used the 3-year average of solar radiance from the Himawari-8 estimation and the K-means method for clustering. The results of clustering solar radiation in Dak Nong province are divided into 4 clusters. The land use map in 2014 year in Dak Nong province has been updated with satellite images from 2014 to 2020. The types of land use that are considered unsuitable for development solar energy are rice, land for growing perennial trees and forest. The total area suitable for the development of solar energy potential in Dak Nong province is 76.512 ha, which accounts for 18% of the total area of the province.

In this study, disaster risk and future climate factors, and the opinions of users such as planners, politicians and engineers have not been clarified. Nevertheless, the constructed map of solar energy potential zonalization is likely a useful information for development planning of solar power and similar maps are possibly developed for other provinces to assisst solar potential zoning in the future.

Author contribution statement: Conceived and designed the study: P.T.T.N.; Selection of research methods: P.T.T.N., N.T.C.; Analyzed and interpreted the data; analysis tools and mapping: P.T.T.N., N.T.C., D.T.T.; wrote the manuscript: P.T.T.N., D.T.T.

Acknowledgement: This study was conducted under the National Space Technology Program for the period 2016–2020 (Grant number: VT–CB.14/18–20).

Competing interest statement: The authors declare no conflict of interest.

References

1. Toan, D.V. Renewable energy at sea and development orientation in Vietnam. Collection of scientific reports National scientific conference Natural resources and green growth, 2013.
2. GIZ Deutsche Gesellschaft für Internationale Zuammenarbeit. Subsector Analysis: Vietnam. Solar PV Rooftop Investment Opportunities in Vietnam, (Eds). N.T.H.T., Peter Cattelaen, D–11019 Berlin, Germany: Federal Ministry for Economic Affairs and Energy (BMWi) Public Relations, 2016.
3. Prime Minister's Decision. PM Decision 428/QĐ–TTg on the Approval of the Revised National Power Development Master Plan for the Period of 2011–2020 with the Vision to 2030. Vietnam Goverment Division, 2016.
4. Do, T.M.; Sharma D. Vietnam's energy sector: A review of current energy policies and strategies. *Energy Policy* **2011**, *39(10)*, 5770–5777.
5. Martins, F.R.; Pereira E.B.; Abreu S. Satellite–derived solar resource maps for Brazil under SWERA project. *Solar Energy* **2007**, *81(4)*, 517–528.

6. Gastli A.; Charabi Y. Solar electricity prospects in Oman using GIS–based solar radiation maps. *Renewable Sustainable Energy Rev.* **2010**, *14(2)*, 790–797.
7. Polo, J. et al. Maps of solar resource and potential in Vietnam. 2015.
8. Mahtta R.; Joshi, P.K.; Jindal, A.K. Solar power potential mapping in India using remote sensing inputs and environmental parameters. *Renewable Energy* **2014**, *71*, 255–262.
9. Zelenka, A. et al. Effective accuracy of satellite–derived hourly irradiances. *Theor. Appl. Climatol.* **1999**, *62(3)*, 199–207.
10. Hai, P.H. et al. Landscape zoning of Vietnam territory. in Proceedings of the Geoscientific Conference, University of Natural Sciences. Vietnam Geographic Society, Hanoi, Vietnam, 2000.
11. Hai, P.H. Methodology, principles and methods for building a Vietnamese landscape classification system. Journal of Science, University of Natural Sciences. Vietnam National University, Hanoi, 1996.
12. Hai, P.H. Territorial planning and organization on the basis of landscape studies. Vietnam Journal of Earth Sciences, 1998.
13. Hai, P.H. Natural geographical zoning of the territory of Vietnam (Russian). Geography Journal of Ucraina, Kiev, Ucraina, 1999.
14. Cuong, H.D. et al. Research on climate zoning of the Central Highlands. *VN J. Hydrometeorol.* **2014**, *647*, 5–8.
15. Ha, T.T. Some issues about Vietnam's economic zoning, in International Conference of the Institute of Vietnam Studies, Institute of Vietnamese Studies and Development Science: Vietnam, 2015.
16. Le Sam, et al. Ecological zoning, scientific basis for researching and building ecological lake system in Central region. Collection of results of Science and Technology Vietnam, 2008.
17. Tuan, N.A. et al. Workshop report "Evaluating the potential development of solar power projects connected to the national grid in Vietnam to 2020, vision to 2030". 2018.
18. Nga, P.T.T. et al. Assessment of solar radiation estimated from Himawari–8 satellite over Vietnam region. *VN J. Sci. Technol.* **2020**, *58(3A)*, 20–32.
19. Nga, P.T.T. et al. Comparative Assessment of Solar Radiation by Satellite–Based and Reanalysis Products Over Vietnam Regions. In IGARSS 2020–2020 IEEE International Geoscience and Remote Sensing Symposium, 2020, 6702–6705.
20. Takenaka, H.; Nakajima, T.Y.; Higurashi, A.; Higuchi, A.; Takamura, T.; Pinker, R. T.; Nakajima, T. Estimation of solar radiation using a neural network based on radiative transfer. *J. Geophys. Res.: Atmos.* **2011**, *116*, D08215.
21. Kawamoto, K.; Nakajima, T.; Nakajima, T.Y. A global determination of cloud microphysics with AVHRR remote sensing. *J. Clim.* **2001**, *14(9)*, 2054–2068.
22. Nakajima, T.Y.; Nakajma, T. Wide–area determination of cloud microphysical properties from NOAA AVHRR measurements for FIRE and ASTEX regions. *J. Atmos. Sci.* **1995**, *52(23)*, 4043–4059.
23. Nga, P.T.T.; Ha, P.T.; Hang, V.T. Satellite–Based Regionalization of Solar Irradiation in Vietnam by K–Means Clustering. *J. Appl. Meteorol. Climatol.* **2021**. *60(3)*, 391–402.
24. Effat, H.A. Mapping Solar Energy Potential Zones, using SRTM and Spatial Analysis, Application in Lake Nasser Region, Egypt. *Int. J. Sustainable Land Use Urban Plann.* **2016**, *3(1)*, 1–14.
25. Vietnam Electricity. Annual Report, 2021.

VIETNAM JOURNAL OF HYDROMETEOROLOGY

Research Article

Probabilistic seismic hazard assessment for Da Nang city, Vietnam

Nguyen Hong Phuong[1,2*], Vo Thi Hong Quyen[3], Pham The Truyen[1, 2*], Do Van Linh[4], Vu Trong Tan[4], Nguyen Trong Hieu[1]

[1] Institute of Geophysics, Vietnam Academy of Science and Technology, 8 Hoang Quoc Viet Street, Nghia Do, Cau Giay District, Ha Noi; phuong.dongdat@gmail.com; truyentpt@igp.vast.vn; nguyenhieu200993@gmail.com

[2] Graduate University of Science and Technology, Vietnam Academy of Science and Technology; phuong.dongdat@gmail.com; truyentpt@igp.vast.vn

[3] Ho Chi Minh City Institute of Resource Geography, 01 Mac Dinh Chi Street, Ben Nghe Ward, District 1, Ho Chi Minh City; vthquyen@hcmig.vast.vn

[4] South Vietnam Geological Mapping Division, 200 Ly Chinh Thang, Ward 9, District 3, Ho Chi Minh City; dovalinh@gmail.com; vutrongtan@gmail.com

*Corresponding author: phuong.dongdat@gmail.com; truyentpt@igp.vast.vn

Received: 10 November 2022; Accepted: 19 December 2022; Published: 25 December 2022

Abstract: This paper presents the probabilistic seismic hazard assessment (PSHA) results for Da Nang city. A regional earthquake catalog was updated until 2021 and comprehensive seismic source zones within 150 km of Da Nang city were used. The PSHA results for Da Nang city are presented in the form of probabilistic seismic hazard maps, depicting peak horizontal ground acceleration (PGA) with 10%, 5%, 2% and 0,5% probability of exceedance in 50 years, corresponding to return times of 475; 975; 2,475 and 9,975 years, respectively, as well as the 5–hertz (0.2 s period) and 1–hertz (1.0 s period) spectral accelerations (SA) maps with 5–percent damping on a uniform firm rock site condition, with 2% probability of exceedance in 50 years, corresponding to a 2,475 year return period. The results show that, for the whole territory of Da Nang city, for all four return periods, the predicted PGA values correspond to the intensity of VI to VIII degrees according to the MSK–64 scales. As for the SA maps, for the 2,475–year return period, the predicted SA values at 1.0 s period correspond to the intensity of VI, while the predicted SA values at 0.2 s period correspond to the intensity of VIII to IX according to the MSK–64 scales. These probabilistic seismic hazard maps present short–and long–term forecasts of seismic hazards for Danang city.

Keywords: Probabilistic seismic hazard maps; Peak Ground Acceleration; Spectral acceleration; Seismic source zones; Ground motion prediction equations.

1. Introduction

Da Nang is located on the South-Central Coast of Vietnam, is the commercial and educational center of Central Vietnam, and is one of Vietnam's most important port cities. Da Nang is a class–1 municipality and the fifth–largest city in Vietnam by municipal population. According to the most recent population and housing census results, as of April 1, 2019, the population of Da Nang city reached 1,134,310 people, ranking 39th in the country, accounting for 1.18% of the population nationwide, with the population density reaching 740 people/km² [1]. Da Nang is also the city with the highest urbanization rate in

the country: 87.2%. The city has the highest proportion of people living in urban areas in the country. The urban population is usually concentrated in the city center. Along with the fast growth rate and high population density, Da Nang city will have to face a series of challenges and risks from natural hazards. In addition to the types of disasters that cause frequent damage, such as storms, floods and droughts, disasters with a low frequency but destructive nature, such as earthquakes and tsunamis, are also on the list of natural disasters to be avoided in the region [2].

To date, no quantitative seismic hazard assessment studies have been carried out at a detailed level for Da Nang city. The earthquake hazard map established for the whole territory of Vietnam shows that Da Nang city, in particular, and Quang Nam province in general, could be affected by the average earthquakes in the whole country, compared with the highest earthquake hazard area in the Northwest. However, the World experience of earthquake damage has shown that the damage caused by strong earthquakes to the community is not as significant as the damage caused by average earthquakes due to the frequency of occurrence of moderate earthquakes being much higher than that of strong earthquakes. Implementing science and technology tasks to assess and map earthquake hazards and anti–seismic design for big cities in Vietnam, including Da Nang city, is necessary. It should be deployed soon so that the results of seismic hazard assessment can be used effectively in a number of practical fields, such as seismic design for civil works or the development of a public transport network in the city.

This paper presents the results of applying the probabilistic method to evaluate and develop the earthquake hazard maps for Da Nang city, using the earthquake catalog updated to June 2021 and the most comprehensive knowledge on seismically active faults in Da Nang city and surrounding areas.

2. Materials and methodology

This paper uses the classical PSHA methodology proposed by Cornell and Esteva in 1968 [3–4]. In the original Cornell–Esteva approach, if the study area can be divided into seismic sources according to geotectonic considerations, it can be assumed that, within a seismic source, an independent earthquake occurrence process is taking place and the magnitude exceedance rates, λ(M) can be estimated through statistical analysis of earthquake catalogs. These rates are the number of earthquakes per unit of time in which magnitude M is exceeded, and they characterize the seismicity of the source.

The PSHA methodology also assumes that, within a seismic source, all points are equally likely to be earthquake hypocenters. In this case, acceleration exceedance rates due to a single source, say, the i–th source, are computed using the following expression:

$$v_i(a) = \sum_j w_{ij} \int_{M_0}^{M_u} \left(-\frac{d\lambda_i(M)}{dM} \right) \Pr(A > a | M, R_{ij}) \, dM \quad (1)$$

where M_0 and M_u are the smallest and largest magnitudes considered in the analysis, respectively, $\Pr(A > a|M, R_{ij})$ is the probability that acceleration exceeds the value at the site, given that at a distance R_{ij} an earthquake of magnitude M originates. R_{ij} is the distance between the site and the sub–elements into which the source has been divided. A weight w_{ij} has been assigned to each sub–element, and the expression above assumes that $\Sigma w_{ij} = 1$. Finally, the contributions of all N sources to earthquake hazards at the site are added:

$$v(a) = \sum_{i=1}^{N} v_i(a) \quad (2)$$

The seismicity model used in this paper is called the modified Gutenberg–Richter model, for which the earthquake magnitude exceedance rate is given by [5]:

$$\lambda(M) = \lambda_0 \frac{e^{-\beta M} - e^{-\beta M_0}}{e^{-\beta M_0} - e^{-\beta M_u}}, \; M_0 \le M \le M_u \quad (3)$$

where λ_0 is the exceedance rate of magnitude M_0; β is a parameter equivalent to the "b–value" for the source (except that it is given in terms of the natural logarithm), and M_u is the maximum magnitude for the source.

With the Poissonian assumption of earthquake occurrence within each seismic source, the probability density of the earthquake magnitude is given by:

$$p(M) = -\frac{d\lambda(M)}{dM} = \lambda_0 \beta \frac{e^{-\beta M}}{e^{-\beta M_0} - e^{-\beta M_u}}, \; M_0 \le M \le M_u \quad (4)$$

The procedure of probabilistic seismic hazard assessment for Da Nang city was carried out through the following steps: (1) Determination of seismic sources in the Da Nang region; (2) Estimation of seismicity parameters for seismic source zones; (3) Selection of ground motion prediction equations (GMPEs) for study region; (4) Calculation hazard and compilation of probabilistic seismic hazard maps.

3. Results

3.1. Seismotectonic characteristics of Da Nang city and its adjacent region

3.1.1. Seismic activity

The study area was enlarged to the entire Central Vietnam territory within 150 km around Da Nang city to incorporate all possible impacts from seismic sources to Da Nang city. Figure 1 shows the seismotectonic map of Da Nang city and surrounding areas, which was established based on up–to–date knowledge of seismically active faults and an earthquake catalog updated until 2021.

The catalog of earthquakes instrumentally observed since 1903, archived at the Institute of Geophysics, contains 13617 earthquakes with magnitudes of 2.5 and above that have been recorded in the study area. Of these, 10 have moment magnitudes exceeding 4.0. Thus, it can be generally assessed that the study area has average seismicity compared to other regions in Vietnam. However, the fact that a 4.7–magnitude earthquake was recorded in Da Nang city in 1947 shows that the possibility of earthquakes causing damage to the urban community of Da Nang city needs to be taken into account.

Based on the known seismic wave attenuation law, the research scope needs to be selected at the minimum distance where the impact of the seismic wave is still valid when traveling from the source to the site. Therefore, depending on the selected seismicity model, the study area is usually selected with a radius of 300 to 500 km around the site to assess earthquake hazards. Thus, in this work, a total of 68 earthquakes were used in the calculation to evaluate the characteristics of the study area's seismicity.

Research results show that earthquakes recently recorded in the Central Vietnam provinces mainly induce seismicity origin, which is generated due to the operation of hydroelectric power plants [5–6]. The earthquake sequences that have been recorded in Bac Tra My district from 2012 to the present, in the A Luoi district from 2014 to the present, and in the Kon Plong district from 2021 to the present are all consequences of the reservoir impoundment processes of the Tranh River 2 (Quang Nam), A Luoi (Thua Thien–Hue) and Thuong Kon Tum (Kon Tum) hydropower plants.

The results of research on stress fields and the tectonic regime of Central Vietnam also show that the study area has undergone various deformation phases, of which the sub–meridian compression phase characterized by the horizontal strike–slip movement is quite common [6]. Figures 2a–2b illustrate the focal mechanisms of two earthquakes recorded at Song Tranh 2 hydropower plant in 2015 obtained by using the moment tensor inversion method. The results show that the right–lateral strike–slip mechanism of the source faults is in the Northwest–southeast direction [7].

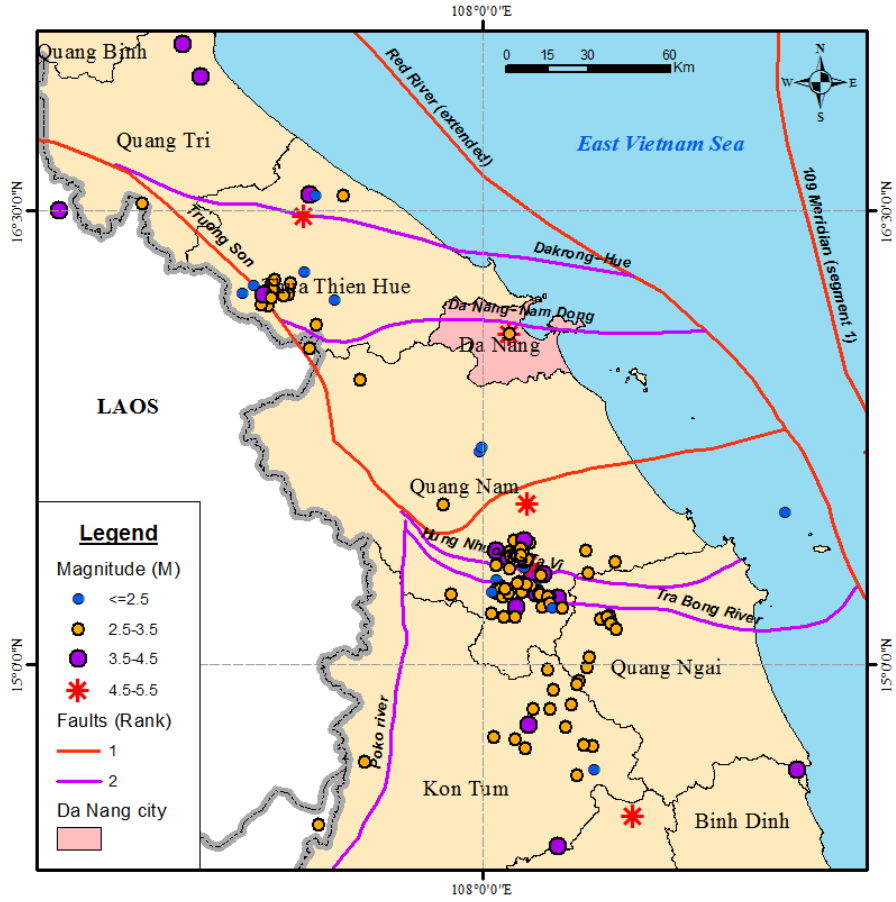

Figure 1. Seismic and tectonic map of Da Nang city and surrounding area.

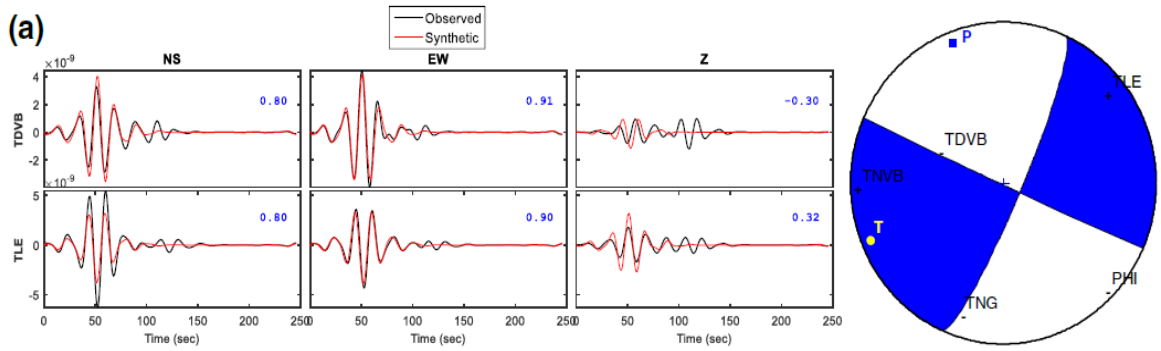

Figure 2a. Moment tensor solution of the April 2, 2015 event in the ST2 region using ISOLA. Waveform match between observed (black) and synthetic (red) seismograms in the frequency range of 0.04–0.1 Hz (left). The first motion polarities of five stations superposed on the mechanism where (+) represent compressions and (−) are the dilatations (right).

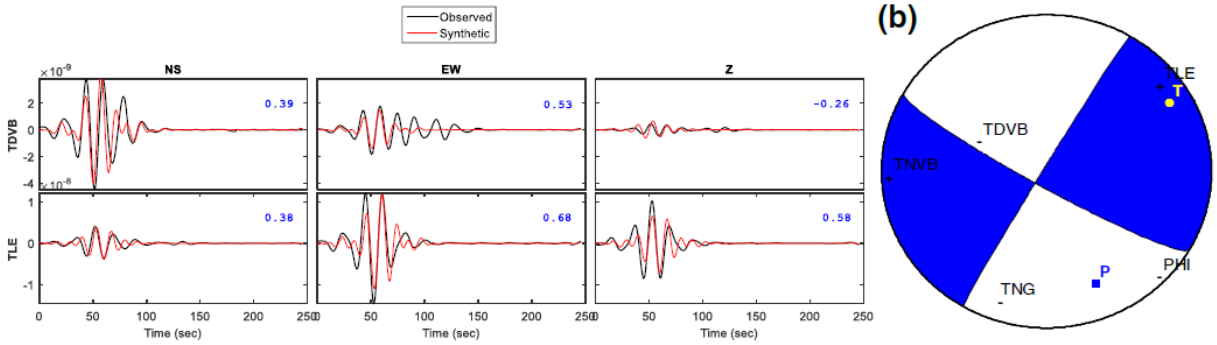

Figure 2b. Same as Figure 2a but for April 26, 2015, in the ST2 region [7].

3.1.2. Seismically active faults

The activity of the capable fault zones in Central and Southern Central Vietnam has been studied [6, 9–12]. Within a radius of 150 km around Da Nang city, 9 fault zones capable of generating earthquakes have been identified, of which 3 are of the 1st rank and 6 of the 2nd rank (Figure 1, Table 1). Below is a detailed description of each such active fault zone to decrease the impact on Da Nang city. It should be noted that the fault classification in this study is based on the seismic activity criterion, so it is different from the fault classification according to geological criterion.

Table 1. The seismically active faults in the study area.

No	Fault name	Rank	Direction	Dip	Mechanism in Pliocene–Quaternary
1	Tam Ky–Phuoc Son	1	Sub–parallel	NNW	Thrust/Right lateral Strikeslip/Normal
2	Red River (extended)	1	NW–SE	NE	Right lateral Strikeslip
3	109º Meridian (segment 1)	1	NW–SE	E	Normal
4	Da Nang–Nam Dong	2	Sub–parallel	Vertical	Thrust/Right lateral Strikeslip /Normal
5	Dakrong–Hue	2	NNW–SSE	Vertical	Thrust/Right lateral Strike-slip
6	Truong Son	2	NW–SE	SW	Right lateral Strikeslip
7	Tra Bong River	2	NNW–SSE	SSW	Right lateral Strikeslip –Thrust
8	Hung Nhuong–Ta Vi	2	Sub–parallel	Vertical	Thrust/Right lateral Strikeslip
9	Poko river	2	Sub–meridian	W	Normal

3.1.2.1. The 1st rank Tam Ky–Phuoc Son fault

The Tam Ky–Phuoc Son fault was originally a shear zone separating Vietnam–Laos and Kontum's two terrains during the Paleozoic period [13]. The main fault is about 82.9 km long, consisting of three segments with different directions (Figure 1). The results of research on fracture deformation and slip surface by different tectonophysical methods have shown that the fault has a steep slope of 70–75º to the northeast on the Northwest–southeast segment; the dip angle of 70–80º to the north on the sub–parallel segment and the dip angle of 80–85º to the Northwest on the northeast–southwest segment. In the sub–meridian compressive horizontal stress field, the fault displacement in the present time is a right–lateral strike–slip on the Northwest–southeast segment and a left–lateral on the northeast–southwest segment, thrust–left–lateral strike–slip on the northeast–southwest segment and thrust on the sub–parallel segment. The results of measuring radon gas content on 03 survey profiles crossing the northeast–southwest segment of the Tam Ky–Phuoc Son fault show 23 anomalies among 123 survey points. Notably, the anomalies on this fault are mainly concentrated at its intersections with higher–order faults. In addition, some other signs indicate the activity of the Tam Ky–Phuoc Son fault; for example, along the fault, there is a source of hot mineral water appearing in Que Tan and many landslide spots.

In general, the combination of the facts and evidence such as remote sensing, geology, geomorphology, anomalies of radon content in soil gases, hot water, and mineral water exposure, landslide, and seismic hazard allows concluding that the Tam Ky–Phuoc Son fault zone is an active one. Still, the segments' activity level varies from moderate to relatively strong.

3.1.2.2. The 1st rank Extended Red river fault

The extended Red River fault is located on the sea within the study area, with a Northwest–southeast direction. The fault is determined mainly by satellite gravity and magnetic data [9]. The fault geometry reflects the horizontal gravity gradient anomaly zone

with average intensity from 0 to 1.5 mGal/km. On the Bouguer gravity anomaly map, the northeast side of the fault is characterized by a relatively positive structure with values ranging from –14 to –22 mGal. In comparison, the southwest side is a relatively negative structure with the values of isolines from –25 to –30 mGal.

The fault is also clearly shown on the aerial magnetic map, with the northeast wing being a positive structure with values from –20 to –40 nT and the southwest side being a negative structure with values from –30 to –50 nT. The fault geometry coincides with the horizontal gradient anomaly zone on the magnetic satellite map with an average intensity of about 0 to 3 nT/km. Also, according to satellite gravity and magnetic data, the fault is inclined to the northeast with an angle of 60–80^{o}.

Although located in the sea, the 1st rank Extended Red River fault zone is considered capable of shakings affecting Da Nang city from the northeast.

3.1.2.3. The 1st rank 109^{o} Meridian fault

This fault is detected using various data, including earthquakes, seismic exploration, satellite gravity, volcanic geology, and remote sensing [10, 14]. In the study area, the fault continues the Extended Red River fault on the continental shelf of Central Vietnam in the Northwest–southeast direction.

The fault has a depth of up to 60 km, cutting through the Earth's crust and reaching the lithosphere. This fault zone consists of 3 main and many minor faults running roughly parallel to and close to the 109^{o}E and 110^{o}E meridians. Based on the research results on sedimentation – geodynamics in sedimentary basins along the 109^{o} Meridian fault zone, it can be confirmed that this fault was strongly active at the beginning of the Cenozoic but weakened until the end of the Late Miocene.

During the Pliocene–Quaternary period, the 109^{o} Meridian fault has the right–lateral strike–slip mechanism, coupled with subsidence in steps to the east, creating a sedimentary layer of this age to 4000m thick. Then follows a weakened period of this fault. During the Holocene–Present, much evidence shows that it was reactivated again with the bloom of volcanic eruptions in Phu Quy and Hon Tro islands and seismic activity in the Phan Thiet–Vung Tau Sea area.

Up to now, not so many earthquakes have been recorded along the 109^{o} Meridian fault. However, two earthquake sequences were instrumentally observed along the fault at two different times. The first sequence consists of medium–magnitude earthquakes between August 1963 and January 1965 and clustered along the fault segment bounded by latitudes 10–120. This earthquake series was recorded at the Nha Trang seismic station, but the magnitude is mostly unknown. The second series of earthquakes occurred off the coast of Ba Ria–Vung Tau and Binh Thuan provinces starting in 2005 and lasting until 2017. In this second series of earthquakes, the most notable are two events with Moment magnitudes of 5.2 and 5.3 that occurred on November 8, 2005 [15].

On the continental shelf of Vietnam, N2–Q1 age volcanic eruptions and modern volcanic eruptions are observed along the 109^{o} and 109^{o}30’ meridian. These activities extend from Quang Binh, and Vinh Linh provinces down to Da Nang, Quang Ngai, Ninh Thuan, and Binh Thuan provinces, especially in the Phu Quy, Hon Tro, and the southeastern part of these islands [16]. Even though only a part of the northern segment of the 109^{o} Meridian fault appears in the study area, the impact of this 1st rank fault needs to be considered in assessing seismic hazards for Da Nang city.

3.1.2.4. The 2nd rank Da Nang–Nam Dong fault

The 2nd rank Danang–Nam Dong fault, also known as Nam Dong–Nam O fault, is the boundary dividing the North Truong Son block into the Nam Dong block in the north and the P'Rao–Thanh My block in the south. The analysis of the fault relationship with the geological

formations and its fracture deformation shows that the main fault plane dips almost vertically with a slight inclination to the Northwest and north [5]. The evidence of satellite images, geology–geomorphology, landslides, riverbank erosion along the fault, and earthquake activity has shown that the modern activity of sections of the Nam Dong–Nam O fault zone is mostly moderate, except for the western segment, which shows relatively strong activity. However, this is the most dangerous seismic source affecting Da Nang city, as this fault segment runs through the city.

3.1.2.5. The 2nd rank Dakrong–Hue fault

On the Bouguer gravity anomaly map, the Dakrong–Hue fault is shown as the boundary dividing structural blocks with different anomalies, according to which the gravity field value varies in the range –12 ÷ –24 mGal in the south and –30 ÷ –40 mGal in the north. The gravity anomaly horizontal gradient coincides with the fault with an average value of about 1.0 ÷ 2.0 mGal/km. On the aeromagnetic anomaly map showing the ΔTa component, the Dakrong–Hue fault is clearly the boundary of the blocks with different structures. The northern part is a relatively positive structure, with field values in the range –20 ÷ –30 nT, while this value at the south wing is –30 ÷ –40 nT. The fault zone coincides with the anomalous aeromagnetic horizontal gradient with an average intensity of about 2÷3 nT/km [9].

The Dakrong–Hue fault has a depth of about 15÷20 km, with the mechanism changing from right–lateral strike–slip in the northwest segment, reverse in the middle segment and left–lateral strike–slip in the eastern segment. The analysis of geological maps, geomorphological characteristics, and fracture deformation documents related to the fault shows that the main fault plane is vertically dipped in the segments with the west–Northwest–southeast and inclined to the north at parallel and sub–parallel segments with a plug angle of 70–80^o. The analysis of geological data also shows that during the Pliocene–Quaternary period, the fault had the right–lateral strike–slip mechanism, impacted by the shear stress field with the near–horizontal compression axis in the equatorial direction. The modern activity of the Dakrong–Hue fault is demonstrated by instrumentally–recorded medium–magnitude earthquakes along the fault, hot mineral water sources at Thanh Tan and My An, and soil cracks occurring in Huong Ho, Thien Mu areas, and the inner citadel of Hue.

3.1.2.6. The 2nd rank Truong Son fault

The Truong Son fault acts as the north-eastern boundary of the Indosini block. The fault has the main direction of the Northwest–southeast, starting from Vientiane, where it meets the Dien Bien–Lai Chau fault, to the area of Kham Duc town in Phuoc Son district, then ends when it encounters the Po Co River and the Tam Ky–Phuoc Son faults. The fault is clearly shown on topographic maps, satellite images and aero–photos. The study of geomorphologic data has shown that the Truong Son fault has a steep slope of 70–80^o to the northeast. In the modern tectonic stress field, the kinematic mechanism of the Truong Son fault zone is the right–lateral strike–slip for the Northwest–southeast segment and the normal–right–lateral strike–slip for the sub–a meridian segment in the sub–meridian compression stress field.

The modern activity of the fault is shown through the phenomenon of cracking – landslide, which is quite common and often occurs in the weathered crust, on steep slopes, in the territory of Huong Phong, Hong Thuong and Hong Van communes (A Luoi district, Thua Thien–Hue province) and Huc Nghi and Ta Long communes along Ho Chi Minh Road in Dak Rong district, Quang Tri province. In addition, the modern activity of the fault zone might cause the cracks in basaltic eruption rocks of the Late Miocene – Pleistocene age, and the emergence of hot mineral water in Lang Eo and Lang Ruo areas (Dak Rong commune, Dak Rong district, Quang Tri province) as well as earthquakes in A Luoi, Thua Thien Hue province.

3.1.2.7. The 2nd rank Tra Bong River fault

The Tra Bong River fault appears at the northern edge of the Kon Tum block, with a convex arc to the south, and the dominant direction is sub–latitude. The fault is clearly shown in satellite images. The results of the analysis of fracture data show that the fault has a slope of about 70–90^o to the south on the sub–latitude segment, 80–90^o to the south–southwest on the Northwest–southeast segment, inclined 85–90^o to the southeast on the northeast–southwest segment and has a vertical dip angle on the northeast–southwest segment. The results of the telluric magnetic survey on the Nam Tra My–Bac Tra My profile show that the Tra Bong River fault has a depth of more than 30 km in an almost vertical direction. On the Tra Bong–Nui Thanh profile, the Tra Bong River fault also has an almost vertical dip angle to a depth of more than 30 km. In the tectonic stress field from the Pliocene up to now, the Tra Bong River fault has the following mechanism: right–lateral strike–slip in the Northwest–southeast segment, reverse and strike–slip in the sub–parallel and Northwest–southeast segments, left–lateral and reverse in the northeast–southwest and northeast–southwest segments. The modern activity of the fault is best shown through the series of medium and small–magnitude earthquakes recorded along the fault (Figure 1). This also promotes the Tra Bong River fault up to the 2nd rank in terms of seismic activity.

3.1.2.8. The 2nd rank Hung Nhuong–Ta Vi fault

The Hung Nhuong–Ta Vi fault has a total length of 131.3 km, playing the role of the boundary between the Tra My–Tra Bong block (the northern edge of the Kontum block) in the north and the Ngoc Linh block (the center of the Kontum outcrop) in the south. This fault is very clearly shown on the Landsat 5–TM satellite image as a line that coincides with the boundary between regions with different structures, or as a zone with a relatively high density of linear textures, especially in the Northwest–southeast segment. In the field, the fault is clearly shown by the valleys stretching along the Northwest–southeast and sub–parallel segments, separating the mountain ranges that stretch in the same direction but differ in elevation and slope steepness.

The results of research on rupture characteristics along the fault through the tectonophysical method have shown that the fault is inclined 75–90^o to the northeast on the sub–parallel segment and dipping vertically on the Northwest–southeast segment. The results of magnetotelluric measurements on the Nam Tra My–Bac Tra My and Tra Bong–Nui Thanh profiles show that the Hung Nhuong–Ta Vi fault has a nearly vertical dip angle, cutting through the Earth's crust to a depth of 20 to more than 30 km. Along the Hung Nhuong–Ta Vi fault, some hot and mineral water sources are also sources (Phuoc Cong, Ban Co, Phuoc Tho, Nghia Ky). Along the fault, there are 33 earthquakes instrumentally recorded on the segment from Tra Leng to Tra Ka, of which the largest event is the M = 3.6 earthquake on March 2, 2012 in the Tra Giac commune area. The evidence and data of geology, topography, remote sensing, hot water, mineral water, earthquakes, and fractures allow assessing that the Hung Nhuong–Ta Vi is an active fault and can be classified into a group of 2nd rank faults.

3.1.2.9. The 2nd rank Po Co River fault

The Po Co River fault extends 119.7 km in the sub–meridian direction in the study area. Starting from the area of Kham Duc town, the Po Co River fault runs south along the Dak Se stream valley, through Lo So pass, then along the Po Co River valley, through Dak Glei town, Plei Can town (Ngoc Hoi district, Kon Tum province), then runs south along Sa Thay stream for about 60 km more. The Po Co River Fault has many high–rank faults in the same direction, with a length extending up to several tens of kilometres developing along the flanks. A series of parallel lineaments on the satellite images and topographic maps show the Po Co River fault.

In the neo–tectonic framework, the fault acts as the boundary between the Kon Tum block in the east and the Sekong block in the west. The fault zone appeared in the early Paleozoic, closely related to the pre–Cambrian crust–breaking process in the west of the Kon Tum outcrop, creating a large spreading zone to reveal the oceanic crust. Therefore, along the fault zone, many formations belong to the early Paleozoic phyolite complex. Magmatic activity along the fault zone developed through many stages until Quaternary, leaving intrusive bodies of different compositions, ages, and sizes.

The results of analysis by the tectonophysical method along the Po Co River fault show that the main fault plane dips to the west with an angle of 60–70^{o}, and the displacement mechanism is dominantly normal in the Pliocene–Quaternary period, causing a drop of steps from the wings to the centre with a vertical amplitude of about 800–1300 m, and the estimated speed of 0.16–0.26 mm/year [6].

3.2. Seismic source model

One of the important inputs for earthquake hazard calculations is the seismic source model of the study area. In this study, an aerial source model is used, assuming that an earthquake is caused by a source whose boundary encloses a zone of one or more seismically active faults or a zone of concentrated seismicity [17].

The seismic sources of Da Nang city and its vicinity were determined based on known seismicity and seismotectonic characteristics. A seismic source zone is defined along seismically active faults by summing all the possible rupture zones caused by maximum earthquakes which might occur within the given zone. In another word, this is the projection of tectonic fault plans counting from the lowest active layer to the Earth's surface. However, while delineating a seismic source zone boundary, this rule can be extended, depending on certain observed earthquake epicentre distribution, a set of faults in cases

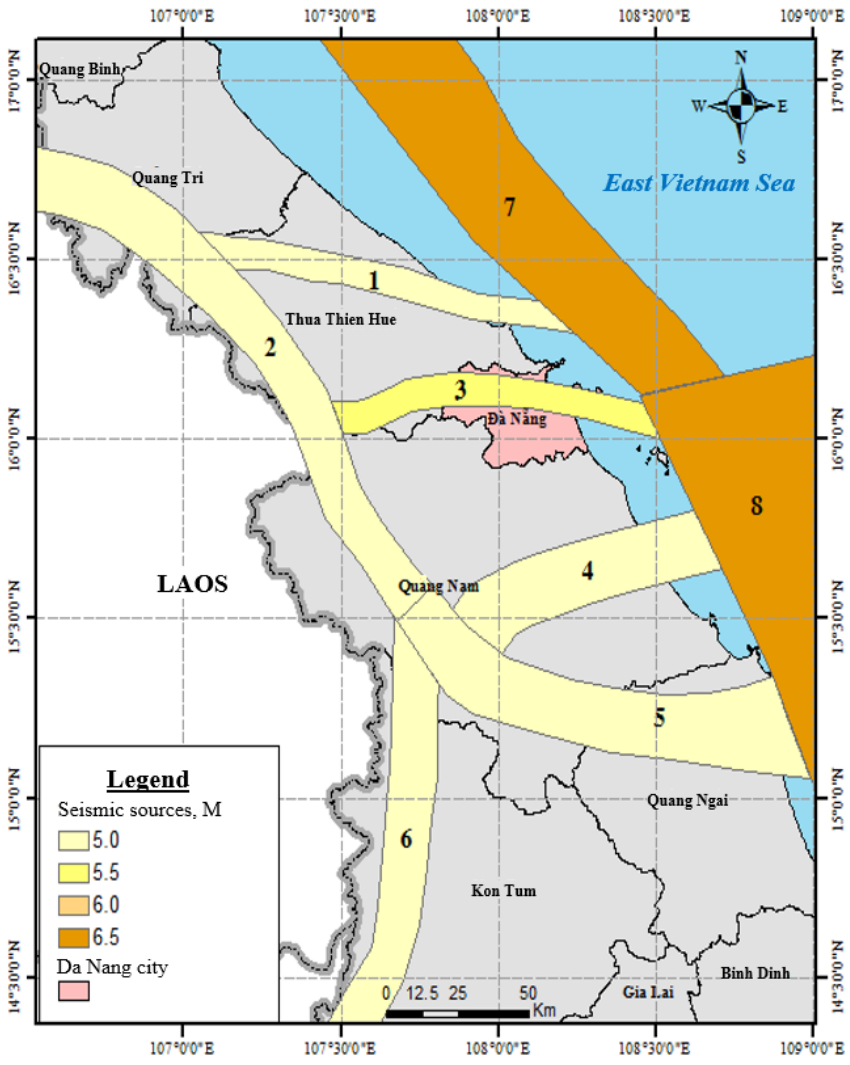

Figure 3. Map of the earthquake source zones in Da Nang city and its vicinity. The numbers on the map coincide with the ordinal numbers of the source zones given in Table 2.

of scattered earthquake data. The acceptable boundary for a seismic source zone has to maintain all seismotectonic characteristics of the zone as a whole, namely the azimuthal location, direction of main geologic structures and cluster of earthquake epicentres.

An important basis for reference and identification of areal sources in the study area is the seismotectonic model of the territory of Vietnam and the East Vietnam Sea region, built on the basis of inheriting the previous research results as well as updating new earthquake and tectonic data [18–21]. Earthquake data, including historical earthquakes, earthquakes collected from field investigations, and instrumentally recorded earthquakes, were collected in the study area within a radius of 150 km from the Da Nang city center and used with the active faults data to delineate seismic source zones. A total of 8 source zones considered to have seismic impacts on Da Nang city are identified using this approach, including (Figure 3): 1) Dakrong–Hue; 2) Truong Son; 3) Danang; 4) Tam Ky–Phuoc Son; 5) Hung Nhuong–Ta Vi; 6) Po Co River; 7) Red River–Chay River; 8) The 109^o Meridian (Segment 1).

3.3. Earthquake catalog

The earthquake catalog of the study area was established, covering the observation period from 1903 to 2021, based on the earthquake database of archived at the Earthquake Information and Tsunami Warning Center, Institute of Geophysics, Vietnam Academy of Science and Technology. The catalog contains 136 earthquakes of magnitude 2.5 or greater, including historical, field investigation and instrumental earthquakes, collected from the National seismic network of Vietnam and international seismic centers such as ISC, USGS, NEIS, and BEJ. All earthquakes recorded in the area within φ = 17.5–23.5^o N; λ = 102.0–108.5^o E.

Data treatment plays an important role in a seismic hazard assessment procedure, particularly in the case of probabilistic application. One of the basic requirements of the earthquake data to be used is that they have to be statistically independent. For this reason, statistical procedures were applied to remove all foreshocks and aftershocks from the catalog. Then, the catalog was grouped by the seismic source zones into sub–catalogs prior to the hazard computation.

The principle of aftershocks removal is well–known and can be expressed simply as follows. Let t be the origin time of earthquake occurrence, h is a focal depth, M is the magnitude, i and j be the order numbers of these earthquakes in a catalog, and j > i. The second event can be considered as the aftershock of the first one if the following conditions are satisfied: the epicentral distance between the two events is less than a given value $R(M_i)$, $h_j - h_i \leq H(M)$; and $M_j \leq M_i$, where T(M), R(M) and H(M) are empirical functions [7, 22]. The algorithm of foreshock removal is similar.

Foreshocks and aftershocks were removed from each source zone's earthquake sub–catalog. The earthquake sub–catalogs used for the calculation contain main shocks only to ensure the reliability of the calculation results. In addition, only earthquakes of magnitude 4.0 and above are used for the calculations to ensure the completeness of the earthquake catalog.

3.4. Estimation of seismic hazard parameters for the seismic source zones

To calculate and map the seismic hazard of the study region, the following seismic hazard parameters, characterizing the level of seismicity, were estimated for each seismic source zone:

- Expected maximum magnitude M_{max};
- Constants a, b in the Gutenberg–Richter magnitude–frequency relation and their deductive values λ, β;
- Mean return period T(M) of the strong earthquakes with magnitude M.

Detail description of the seismicity parameters estimation methods for a seismic source can be found in previously published documents [7, 10, 19–21, 23]. In this study, the Maximum likelihood method proposed by Aki and Utsu is applied to estimate the parameters a and b for each seismic source zone [24–25]. The parameter estimation algorithms always consider the error of determining the earthquake magnitude M [26–27]. The lower bound of the magnitude value $M_0 = 4.0$ is selected for all source zones to conform to the unified scaling law of earthquakes throughout the territory of Vietnam [7].

In practice, applying statistical methods to estimate the seismicity parameters for a seismic source zone is often difficult in case the zone contains too few earthquakes. In many cases, the only solution suggested by seismologists is to apply the rule of "seismotectonic similarity" [28]. In this study, the Poko River fault is similar to the Truong Son fault since it was previously named Poko–Kham Duc and is connected to the Truong Son fault from the Laos territory [28]. Since 2015, within the framework of a national research project, Vu Van Chinh has renamed this fault the Poko River [6]. The results of the estimation of earthquake parameters for source zones in Da Nang city and surrounding areas are listed in Table 2.

Table 2. Seismic hazard parameters were estimated for the seismic source zones of Da Nang city and the surrounding area.

N_0	Seismic source zone	λ_0	M_0	M_{maxML}	$M_{max.obs}$	B_{ML}	H (km)
1	Dakrong–Hue	0.02	4.0	5.3	4.8	1.0	10
2	Truong Son	0.02	4.0	5.0	4.0	0.84	12
3	Danang	0.02	4.0	5.3	4.8	1.0	12
4	Tam Ky–Phuoc Son	0.02	4.0	5.2	4.7	1.0	10
5	Hung Nhuong–Ta Vi	0.02	4.0	5.0	4.7	1.0	12
6	Po Co river	0.02	4.0	5.0	2.6	1.0	10
7	Red river–Chay river	0.36	4.0	6.3	4.9	0.89	17
8	The 109^o Meridian (segment 1)	0.02	4.0	6.6	4.8	0.86	12

Note: λ_0 is an annual exceedance rate corresponding to M_0; M_{max}.obs. is an observed maximum magnitude; M_{maxML} is the maximum earthquake value estimated by the maximum likelihood method; M_0 is the lower threshold of magnitude value used; b_{ML} is the b value (in the Gutenberg–Richter relationship) derived from the maximum likelihood results; H is the thickness of the active layer of each source zone.

3.5. Ground motion prediction models

Although more than half a century has passed since the first seismic hazard map of Vietnam was published, until now, no ground motion prediction equation (GMPE) has been developed for the territory of Vietnam. It is simply because of the lack of strong ground motion data recorded strong earthquakes in Vietnam's territory. Although the seismic hazard map of Vietnam has been updated to the 5^{th} generation, with different GMPEs have been applied to the Vietnamese territory so far, the choice of the most suitable GMPE out of hundreds of the published ones, built for different regions around the world, could not avoid the uncertainty.

Since 2019, a new approach to selecting GMPE for Vietnam has been used based on the results of testing the theoretical GMPEs worldwide with earthquake data recorded throughout the territory of Vietnam. In the testing process, the broadband seismic data of 39 earthquakes with magnitudes in the range of 3.5 M 4.5 observed at 55 seismic stations throughout Vietnam in the period 2010–2017 are used to test the suitability with 28 published GMPEs of the world. Note that 39 selected earthquakes are distributed in all 4 seismic tectonic zones in the territory of Vietnam [6]. The testing process includes the following steps [29]:

(1) Processing of earthquake data: observational data, including 665 seismograms of 39 earthquakes, were converted into accelerograms;

(2) Calculation of acceleration values for each GMPE: using the parameters such as earthquake magnitude, hypocentral distance, coordinates of the epicenter, V_{S30} value at stations, the values of peak ground acceleration (PGA) at stations corresponding to each earthquake were calculated corresponding to the 28 selected theoretical GMPEs;

(3) Comparison of the calculated and the observed PGA values at the stations: To evaluate the fit for each GMPE, the mean deviation value X_k^j for each GMPE was calculated (j = 1÷4 is the seismotectonic province index; k = 1÷28 is the index corresponding to the ordinal number of the GMPE to be evaluated).

(4) Selection of the GMPE that is most suitable for the study area: The selected GMPEs are those with the lowest deviation value.

It should be noted that the approach as mentioned above is also applied in building the sixth-generation probabilistic seismic hazard maps for the territory of Vietnam, which have been put into application in the new "National Regulation on data of natural conditions for use in construction" QCVN 02:2020/BXD issued by the Ministry of Construction of Vietnam [23, 30].

According to the test result, the model of [31] proved to be the most suitable for the tectonic seismic zone 3 – Central Vietnam [23]. This is the basis for applying the model of [31] in calculating earthquake hazards for Da Nang city [31]. The ground motion attenuation model of [31] can be written as:

$$\ln(Y) = \ln[Y_{REF}(M_w, R, SoF)] + \ln[S(V_{s30}, PGA_{REF})] + \varepsilon\sigma \quad (5)$$

where

$$\ln(Y_{REF}) = \begin{cases} a_1 + a_2(M_w - c_1) + a_3(8.5 - M_w)^2 + [a_4 + a_5(M_w - c_1)]\ln(\sqrt{R^2 + a_6^2}) + a_8F_N + a_9F_R + S \\ \quad for\ M_w \le c_1 \\ a_1 + a_7(M_w - c_1) + a_3(8.5 - M_w)^2 + [a_4 + a_5(M_w - c_1)]\ln(\sqrt{R^2 + a_6^2}) + a_8F_R + a_9F_R + S \\ \quad for\ M_w > c_1 \end{cases} \quad (6)$$

and

$$\ln(S) = \begin{cases} b_1 \ln\left(\frac{V_{S30}}{V_{REF}}\right) + b_2 ln\left[\frac{PGA_{REF} + c(\frac{V_{S30}}{V_{REF}})^n}{(PGA_{REF} + c)(\frac{V_{S30}}{V_{REF}})^n}\right] & for\ V_{S30} \le V_{REF} \\ b_1 ln\left[\frac{\min(V_{S30}.V_{CON}}{V_{REF}}\right] & for\ V_{S30} > V_{REF} \end{cases} \quad (7)$$

where ln(Y) is the median spectral acceleration; $\ln(Y_{REF})$ is the reference ground–motion model through the nonlinear site amplification function ln(S); Mw is moment magnitude; R is the source–to–site distance measure, (km), for which R_{JB}, R_{epi}, R_{hyp} are used for different models; F_N and F_R are the style–of–faulting dummy variables, that are unity for normal and reverse faults, respectively, and zero otherwise. The parameter c1 in the reference ground–motion model is the hinging magnitude and it is taken as Mw 6.75; σ is the total aleatory variability of the model, which is composed of within–event (φ) and between–event (τ) standard deviations (SDs); b_1 and b_2 are the period–dependent estimator's parameters of the nonlinear site function; c and n are the period–independent coefficients of the reference ground–motion model. The reference V_{S30} (V_{REF}) is 750 m/s in the nonlinear site model and V_{CON} = 1,000 m/s that stands for the limiting V_{S30} after which the site amplification is constant. PGA_{REF} is the reference rock site PGA calculated from the reference ground–motion model. The R_{jb} model calculates the distance from the source to a location in this study. The values of parameters a_1, a_2, a_3, a_4, a_6, a_9, b_1, b_2, ϕ, σ, τ are given in the paper [31].

3.6. Probabilistic seismic hazard maps of Da Nang city

The seismic hazard assessment results for Da Nang city are presented in terms of probabilistic seismic hazard maps. CRISIS2015 program was used to compute hazards [32]. The seismic source model used for computation is shown in Table 1. The lower magnitude

threshold for all seismic source zones was chosen to be $M_0 = 4.0$. The Median values of peak ground acceleration (PGA) and spectral acceleration (SA) computed at each point of a 0.01° × 0.01° grid covering the study area were used to compile seismic hazard maps.

Figures 4a–4d illustrate the probabilistic seismic hazard maps of Da Nang city, representing the spatial distribution of the median values of horizontal PGA (in the unit of % g) with 10%, 5%, 2% and 0,5% probabilities of exceedance in 50 years and V_{S30} site condition of 750 meters per second, corresponding to return times of 475, 975, 2,475 and 9,975 years, respectively. Figures 5a–5b illustrate SA maps of Da Nang city at 0.2 s and 1.0 s periods; both correspond to the return period of 2,475 years.

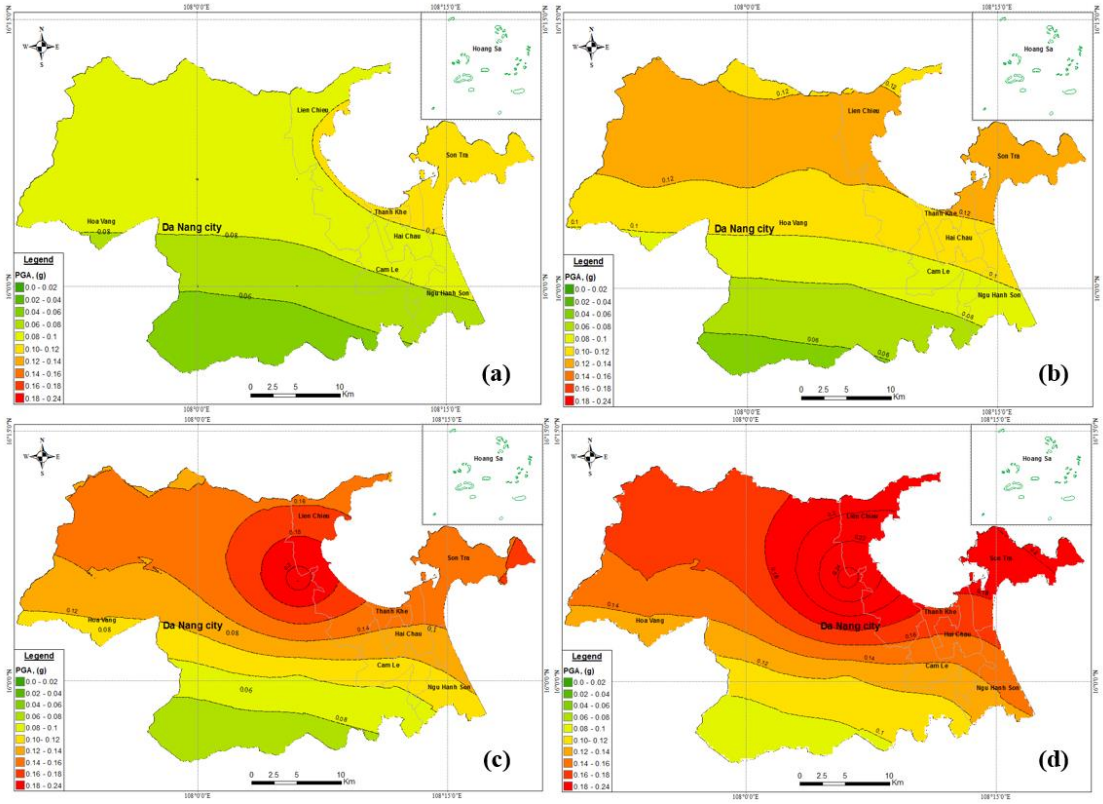

Figure 4. Maps showing peak ground acceleration (PGA) in Da Nang city: (a-d) 10%, 5%, 2%, 0.5%, respectively probability of exceedance in 50 years and V_{S30} site condition of 750 meters per second.

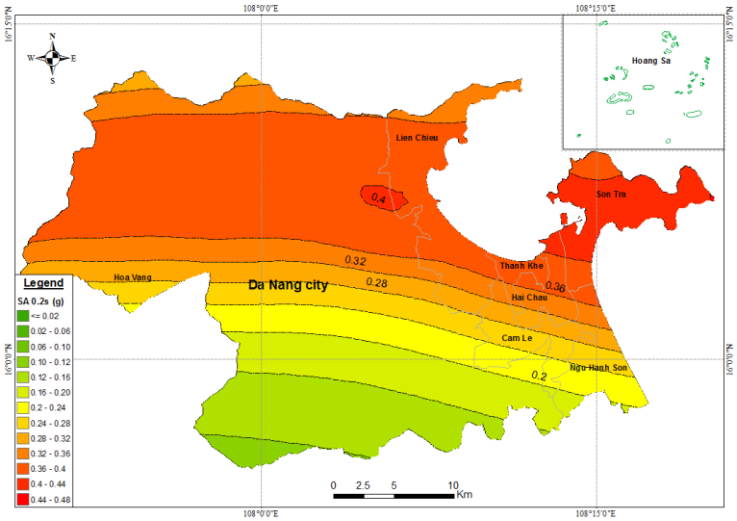

Figure 5a. Map showing 5–hertz (0.2 s period) spectral acceleration in Da Nang city for 2% probability of exceedance in 50 years (2,475–year return period) and V_{S30} site condition of 750 meters per second.

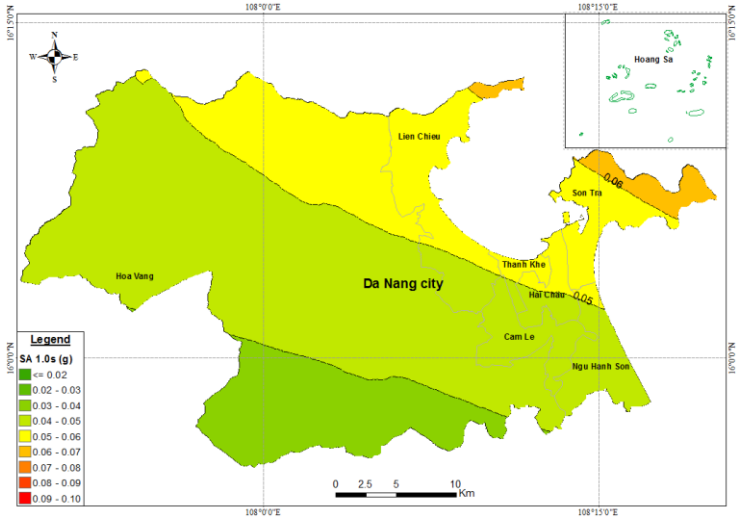

Figure 5b. Map showing 1–hertz (1.0 s period) spectral acceleration in Da Nang city for 2% probability of exceedance in 50 years (2,475–year return period) and V_{S30} site condition of 750 meters per second.

Analyzing the hazard maps of Da Nang city, the following can be concluded:

(1) The spatial distribution of PGA values reflects the resonance of seismic shakings from two 1st rank seismic sources in the sea area and the Da Nang source zone running through the city.

(2) The highest ground motion values are observed in the north and northeast of Da Nang city, in the Son Tra and Lien Chieu districts, and the Thanh Khe district. This is the urban area of Da Nang city, where many residential neighborhoods and socio–economic activities are concentrated. The intensity of shakings gradually decreases towards the south of the city.

(3) For the entire Da Nang city, PGA values are in the range of 0.04–0.1 g, 0.05–0.12 g, 0.06–0.2 g, and 0.08–0.24g corresponding to a return period of 475, 975, 2.475, 2,475 and 9,975 years, respectively. Thus, the maximum ground motion in Da Nang city for all four return periods does not exceed the VIII intensity level according to the MSK–64 scales.

(4) For the entire Da Nang city, the 0.2 s SA values for the 2.475–year return period are in the range of 0.1–0.4 g, equivalent to the intensity from VIII to IX, according to the MSK–64 scale. Meanwhile, the 1.0 s SA values for the same 2.475–year return period are in the range of 0.03–0.06 g, which are equivalent to an intensity VI according to the MSK–64 scales.

4. Discussion

During the last decade, coupled with updating input data, Vietnam's earthquake hazard assessment techniques have continuously upgraded. Previously, several studies related to the seismic assessment of the Da Nang area [19–21]. Although aiming at different goals, these works use the same methodology that is widely applied today [3–4]. In addition, using the same seismotectonic model for the territory of Vietnam and the East Vietnam Sea region provided consistency in the seismic source zones used [18].

On the other hand, updating input data and improving computational techniques also lead to differences in the input data used in the above works. The main differences are discussed below.

1) Different attenuation equations reflect advanced techniques for calculating seismic hazards over time. In the works published before 2016, the GMPEs were selected based on the assumption that the study area has a stable tectonic regime. Since 2016, the logic tree technique has been applied in hazard calculation, allowing us to consider both the

assumptions about the study area's stable and active tectonic regime. Therefore, the selected GMPEs represent both regimes of tectonic activity.

2) The use of different M_{max} values for the 109^o Meridian source zone. According to seismic data, the 109^o Meridian source zone consists of two segments with different seismic activity. Usually, the value M_{max} = 6.1 is assigned to the segment north of the Tuy Hoa shear (segment 1), while the value M_{max} = 6.6 is assigned to the southern one (segment 2). Depending on which part of the fault is nearest to the site to be assessed, the M_{max} values will be assigned accordingly. In case the study area covers the entire fault, the source region is assigned the maximum value of M_{max} = 6.6. In this work, seismic effects on Da Nang city are assumed to be caused by the entire 109^o Meridian source zone.

To investigate the variation of ground shaking values obtained from different studies, the spatial query was carried out at the same place, namely the People's Committee of An Hai Tay Ward, Son Tra District, Da Nang city on the maps published in the studies mentioned above. Except for the maps published in 2013 and 2014 in which Da Nang city is out of the mapping scope, couples of the PGA and I (MSK–64) values with the same return period calculated from the works published in 2015, 2016 and this study are compared in Table 3.

The difference between the corresponding peak ground acceleration (PGA) values is not significant, while there is a consistency between the seismic intensity values I (MSK64 scale) (Table 3). The 2016 map shows higher intensity values than the two other maps due to the favor of the GMPE representing a seismically stable region to those representing a seismically active region. Overall, the variation of ground motion parameters does not change the general picture of the seismic hazard in the Da Nang area.

Table 3. Results of the spatial query at the People's Committee of An Hai Tay Ward, Son Tra District, Da Nang city, from different studies.

Long	Lat	The PGA/I–MSK64 values										Version
		475 years		975 years		2475 years		4975 years		9975 years		
		0.08	VII	0.10	VII	0.12	VIII	–	–	0.13	VIII	2015
108,232	16,064	0.11	VII	0.16	VIII	–	–	0.28	IX	0.33	IX	2016
		0.10	VII	0.12	VIII	0.14	VIII	0.16	VIII	0.17	VIII	2022

5. Conclusion

In this study, the probabilistic approach is applied to assess the earthquake hazard for Da Nang city, using an updated earthquake catalog up to 2021 and a model of seismic source zones in Central Vietnam and adjacent sea areas. The earthquake catalog is processed to ensure completeness and statistical independence of the events. The maximum likelihood method is applied to estimate the Gutenberg–Richter earthquake recurrence law parameters for each seismic source zone. The ground motion prediction model of [31] was selected for the seismic hazard calculation.

The results are presented in the form of probabilistic seismic hazard maps, depicting peak horizontal ground acceleration (PGA) with 10%, 5%, 2%, and 0,5% probability of exceedance in 50 years, corresponding to return times of 475; 975; 2,475 and 9,975 years, respectively, as well as the 5–hertz (0.2 s period) and 1–hertz (1.0 s period) spectral accelerations (SA), maps with 5–percent damping on a uniform firm rock site condition, with 2% probability of exceedance in 50 years, corresponding to a 2,475 year return period. The results show that, for the whole territory of Da Nang city, for all four return periods, the maximum predicted PGA values are not exceeding the intensity of VIII according to the MSK–64 scales. As for the SA maps, for the 2,475–year return period, the predicted SA values at 1.0 s period correspond to the intensity of VI, while the predicted SA values at 0.2 s period are not exceeding the intensity of IX according to the MSK–64 scales.

These are the first detailed probabilistic seismic hazard maps established for Da Nang city, which have many advantages. In addition to using the last–update input data, the advantages in methodology and technique are also applied in the analysis process. The first novelty to be mentioned in this study is the application of a new ground motion prediction model, which has proven to be the most suitable for Vietnamese conditions. It is worth mentioning that this is the first-time spectral acceleration (SA) maps have been compiled for Da Nang city. The probabilistic seismic hazard maps provide short–, medium– and long–term quantitative forecasting information on earthquake hazards. They can be used as a reference in antiseismic design and many earthquake engineering applications for Da Nang city.

Author contribution statement: Conceived and designed the study; Selection of research methods: N.H.P., V.T.H.Q., P.T.T.; Analyzed and interpreted the data; analysis tools and mapping: N.H.P., V.T.H.Q., P.T.T., D.V.L., V.T.T., N.T.H. wrote the manuscript: N.H.P., V.T.H.Q., P.T.T.

Acknowledgment: This research is funded by the People's Committee of Da Nang city.

Competing interest statement: The authors declare no conflict of interest.

References

1. Completed results of the 2019 Vietnam population and housing census. Statistical publishing house, 2020.
2. Prime Minister of Vietnam. The Decision No. 18/2021/QD–TTg Regulation on forecasting, warning, communication of natural disasters and disaster risk levels, April 22, 2021.
3. Cornell, C.A. Engineering seismic risk analysis. *Bull. Seismol. Soc. Am.* **1968**, *58(5)*, 1583–1606.
4. Esteva, L. Bases para la formulación de decisiones de diseño sísmico. Instituto de Ingeniería, Universidad Nacional Autónoma de México, 1968.
5. Cornell, C.A.; Vanmarcke, E.H. The Major Influences on Seismic Risk. Proceeding of the 4th World Conference on Earthquake Engineering, Santiago, Chile, 1969.
6. Minh, L.H. Study of the seismotectonic impact to the stability of the Tranh River hydropower plant No. 2, Bac Tra My region, Quang Nam province. Final report of the National scientific research project, Institute of Geophysics, Hanoi, 2016. (in Vietnamese)
7. Nguyen, H.P.; Pham, T.T.; Nguyen, T.N. Investigation of long–term and short–term seismicity in Vietnam. *J. Seismol.* **2019**, *23*, 951–966.
8. Tuan, T.A.; Purnachandra Rao, N.; Gahalaut, K.; Trong, C.D.; Dung, L.V.; Chien, C.; Mallika, K. Evidence that earthquakes have been triggered by reservoir in the Song Tranh 2 region, Vietnam. *J. Seismol*. **2017**, *21*, 1131–1143.
9. Duong, N.A. Assessment of seismic hazard for development planning, ensuring the safety of hydropower and irrigation works and cultural relics of Thua Thien–Hue province. Final report of the ĐTL.CN.51/16 independent project, 2020. (in Vietnamese)
10. Phuong, N.H. Assessment of earthquake and tsunami hazards in the Ninh Thuan province for site approval of the NPPs. Final report of the National level project, Institute of Geophysics, Institute of Science and Technology (in Vietnamese), 2013.
11. Phuong, N.H.; Truyen, P.T. Analysis of earthquake data to assess the stability of the present tectonic regime", thematic report within the KC09.38/16–20 project "Study of the tectonic characteristics and the impact of the human activities capable of changing the tectonic stress field related to the seismic hazard in the sea area from Tuy Hoa to Vung Tau", 2020. (in Vietnamese)

12. Linh, D.V. Study of the tectonic characteristics and the impact of the human activities capable of changing the tectonic stress field related to the seismic hazard in the sea area from Tuy Hoa to Vung Tau, Final report of the KC.09.38/16–20 National level project, 2020. (in Vietnamese)
13. Tri, V.T.; Michel, F.; Vuong, V.N.; Hoang, H.B.; Michael, B.W.F.; Tuan, Q.N.; Claude, L.; Tonny, B.; Thomsen, K.T.; Punya, C. Neoproterozoic to Early Triassic tectono–stratigraphic evolution of Indochina and adjacent areas: A review with new data. *J. Asian. Earth. Sci.* **2020**, *191*, 104231.
14. Linh, D.V. History of the Cenozoic tectonic evolution of the Southern Central Vietnam and relationship with earthquakes. Ph.D. thesis in Geology, the Ho Chi Minh city Institute of Technology, 2009. (in Vietnamese)
15. Phuong, N.H.; Truyen, P.T. Analysis of earthquake data to assess the stability of the present tectonic regime", thematic report within the KC09.38/16–20 project "Study of the tectonic characteristics and the impact of the human activities capable of changing the tectonic stress field related to the seismic hazard in the sea area from Tuy Hoa to Vung Tau" (in Vietnamese), 2020.
16. Vu, P.N.; Vu, P.N.H.; Binh, N.X. Young Volcanic Eruption (Pliocene-Quaternary) Activities on the Southern continental Shelf of Vietnam (According to Geophysical Data). *VN J. Earth Sci*. **2008**, *30*, 289–301.
17. Budnitz, R.J.; Apostolakis, G.; Boore, D.M.; Cluff, L.S.; Coppersmith, K.J.; Cornell, C.A.; Morris, P.A. Recommendations for Probabilistic Seismic Hazard Analysis: Guidance on uncertainty and use of experts. NUREG/CR-6372 UCRL-ID-122160, 1997, 1, pp. 280.
18. Nguyen, H.P.; Pham, T.T. Development of a fault–source model for earthquake hazard assessment in Vietnam. *VN J. Earth Sci.* **2007**, *29*, 228–238.
19. Probabilistic seismic hazard assessment for the South Central Vietnam Central Vietnam. *VN J. Earth Sci*. **2014**, *36*, 451–461.
20. Phuong, N.H.; Truyen, P.T. Probabilistic seismic hazard maps of Vietnam and the East Vietnam Sea. *VN J. Mar. Sci. Technol.* **2015**, *15(1)*, 77–90. Doi:10.15625/1859-097/15/1/6083.
21. Phuong, N.H.; Truyen, P.T.; Nam, N.T. Probabilistic seismic hazard assessment for the Tranh river hydropower plant No2 site, Quang Nam province. *VN J. Earth Sci*. **2016**, *38(2)*, 188–201.
22. Keilis–Borok, V.I.; Knopoff, L.; Rotwain, I.M. Burst of aftershocks, long–term precursors of strong earthquakes. *Nature* **1980**, *283*, 259–263.
23. Phuong, N.H. Earthquake Hazards in the territory of Vietnam and adjacent seas. Natural science and technology Publishing house, **2021**, pp. 314. (in Vietnamese)
24. Aki, K. Maximum likelihood estimate of b in the formula log N = a–bM and its confidence limits. *Bull. Earthq. Res. Inst*. **1965**, *43*, 237–239.
25. Utsu, T. A Method for Determining the Value of b in a Formula log n = a – bM showing the Magnitude–Frequency Relation for Earthquakes. *Geophys. Bull. Hokkaido Univ*. **1965**, *13*, 99–103.
26. Amorese, D. Applying a Change–Point Detection Method on Frequency–Magnitude Distributions. *Bull Seismol. Soc. Am.* **2007**, *97*, 1742–1749.
27. Amorese, D.; Rydelek, P.A.; Grasso, J.R. Package "GRTo" – Tools for the Analysis of Gutenberg–Richter Distributions of Earthquake Magnitudes. **2015**. https://cran.r–project.org/package=GRTo.
28. Xuyen, N.D. Study on earthquake prediction and ground motion in Vietnam. Final report of the National level project, Institute of Geophysics, Institute of Science and Technology (in Vietnamese), 2004.

29. Khoi, L.Q. Verification of the Ground Motion Prediction Models using broadband seismic data collected in Vietnam. Final report of a research project on basical level. Institute of Geophysics, 2018. (in Vietnamese)
30. Minh, N.D. National Regulation on data of natural conditions used in construction (Draft). Appendix 4 – The earthquake data for QCVN 02:2020/BXD, Institute of Construction Science and Technology, Ministry of Construction, 2020.
31. Akkar, S.; Sand, I.M.A.; Bommer, J.J. Empirical ground–motion models for point– and extended–source crustal earthquake scenarios in Europe and the Middle East. *Bull. Earthq. Eng.* **2014**, *12*, 359–387.
32. Ordaz, M.; Martinelli, F.; Aguilar, A.; Arboleda, J.; Meletti, C.; Amico, D.; Crisis, V. Program for computing seismic hazard. 2015. Online available: http://www.r-crisis.com/download/binaries/.

VIETNAM JOURNAL OF HYDROMETEOROLOGY

Research Article

The research on electrodialysis model to treat brackish water in Ben Tre province

Ton That Lang[1*], Nguyen Phan Thai Vy[1]

[1] Ho Chi Minh City University of Natural Resources and Environment; ttlang@hcmunre.edu.vn; vy.npt251@gmail.com

*Corresponding author: ttlang@hcmunre.edu.vn; Tel.: +84−903983932

Received: 13 November 2022; Accepted: 15 December 2022; Published: 25 December 2022

Abstract: Nowadays, clean water is becoming more scarce. People are getting closer to the adverse effects of climate change, especially the people of Ben Tre province those are heavily affected by seawater intrusion every year. The electrodialysis (ED) model, combined with electrostatic attraction and membrane filtration, has shown the ability to handle nearly 30% of salt concentrations of 5.5−7.9 g/L. The experiment also showed that air bubbles occur when the voltage of the model is increased higher than 26V. The model also promised a stable foundation to develop into a larger−scale model with more treatment stages and low electricity consumption. Moreover, it is possible to reuse the products produced by the ED model with two separate streams: a concentrated stream that can be applied to separate salts and a dilute stream that can be used as domestic water.

Keywords: Electrodialysis; Brackish water; Salinity treatment.

1. Introduction

The Earth is covered by 71% water, but only more than 1% can be drinkable and suitable for daily use [1–4]. In addition, the world is facing with the impact of climate change, including rising sea levels, drought, saline intrusion, and the saline boundary encroaching more profoundly into the mainland, causing severe consequences that directly affect people's lives [5–6].

The Mekong Delta has a geographical position in both directions bordering the sea, and is located in the lower Mekong River with a length of 4,800 km. The location makes the whole region a vulnerable area easily affected by the saline intrusion; many regions do not have clean drinking water. The river water in the dry season is increasingly salty, causing severe impacts on the lives and health of local people. In particular, the 2016 salinity drought caused 10% of people in Ben Tre province to have no clean water for daily activities. Domestic water in many areas still needs better quality [7]. Finding a reasonable and effective treatment method will significantly help improve the living condition of people in the Mekong Delta and Ben Tre province [8−9]. Therefore, an applicable process to desalinate the salty river water is essential. In addition, according to the report of Ben Tre province's official web portal, the salinity in their measurement points was a very high salinity for using, and the price of supplied water in dry season increased significantly. This leads to a need of indoor brackish water for this area.

Electrodialysis (ED), which is a combined process of DC application and ion exchange membranes [5−6], has been used for the desalination of brackish water and saline water. ED is designed by applying the filtering mechanism and electrostatic attraction [5, 10]. These mechanisms can reduce the number of salt ions in the water, purifying the water selectively

by changing the parameters of voltage, amperage, and flow rate. ED has become a very effective technology in ion removal applied to many majors [11−12]. Thus, using ED to treat water in Ben Tre Province could be a promised technology.

According to [12] research on the history of the formation of electrodialysis technology, the basic principles of the technology were first discovered in the 1930s. In 1903, applied scientific articles The first ED technology released research on uncharged and non−polarized membranes.

The efficiency of ED is contributed by many factors such as voltage, temperature, flow rate, and feed concentration [1, 13−14]. In this study, an ED pilot module was designed to treat the Ben Tre River water in salt intrusion areas. In this study, the pilot model was implemented in the laboratory with voltage (at 20, 22, 24, 26, 28, and 30V) and feed concentrations were modified to determine the optimal voltage for a specific NaCl concentration range from 2 g/L to 20 g/L.

2. Materials and methods

2.1. ED setup

The expected flow rate was 1 m^3/d, and the anion and cation exchange membranes are AMI−7001S and CMI−7000S, respectively. The research was implemented at a temperature of 25℃. The specifications of every element in this design are shown in Table 1.

Table 1. The specifications of every element in this design.

Element	Function	Specifications
Ion exchange membrane	Allow only the corresponding ions to pass through the membrane to prevent the tank from reacting into dense flow compartments and clean water flow 2 types: cation and anion	Height × width: 14cm × 8.8 cm. Total area/ type of membrane: 123.2 cm^2. The no. of sheets: 6 sheets of each type. The total useful area/of each type: 624 cm^2
DC power supply	Power supply to the model	Voltage limitation: 0−30V Current limitation: 0−10A Power supply: up to 300W
Electrode	Create 2 electrode ends that draw opposite ions to two ends to support dense and dilute current separation.	Titanium mesh, D1.5 mm fiber as insoluble electrode
Working tank	Contain the electrodes, ion exchange membrane and	Mica Acrylics Taiwan Thick: 15 mm L×W×H = 20cm × 10cm × 15cm
Pump	Pump the feed water into the model.	Dosing membrane pump 0−45L/h

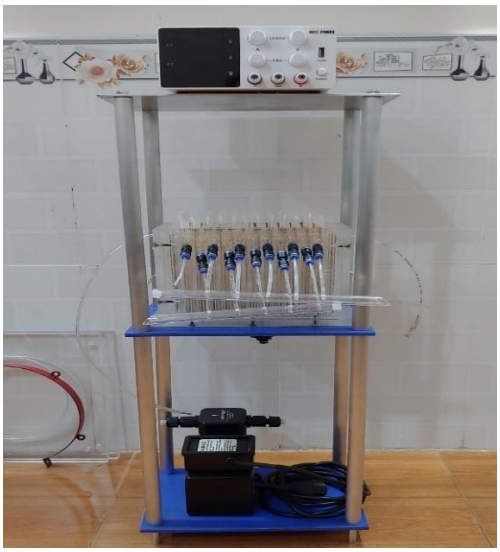

Figure 1. ED model.

2.2. Cell and membrane

In the first stage of designing, the model was arranged by layering up alternately Anion Exchange Membrane (AEM) and Anion Exchange Membrane (CEM) with a spacer between every pair. The spacers were made of mica, and the membrane was pasted on frames with silicon glue. Unfortunately, after dipping into the water, the membranes started to expand and come off the frames, leaving the water to flow freely between every stack. This condition also happened on applying the epoxy resin. Therefore, a new design was created to avoid this situation. The working tank was designed to contain 12 parallel separating trenches; every trench made room for a pair of one membrane and one spacer. The spacer was made to embrace the membrane and allow the membrane to stand without using glue; with this arrangement, the membrane could expand without leakage.

2.3. Materials

To find out the optimal voltage and other factors affecting the performance of the ED model, industrial sodium chloride produced by TRS was used in all experiments to produce feed water solutions with the concertation 2, 5, 8, 10, 15, and 20 g/L, namely. The applied voltage in treating every feed water concentration was changed at 20, 22, 24, 26, 28, and 30V.

2.4. Analytical method

The concentration of Cl^- was analyzed by following TCVN 6194:1996. Each measurement was repeated three times, and calculate the average amount to have the results. The analysis was applied to both dilute and concentrated flow.

In this study, the removal efficiency was E, which was calculated as follows:

$$E\% = (C0 - C)/C0 \times 100 \quad (1)$$

where C_0 and C are feed and dilute concentrations, respectively.

3. Results and Discussion

3.1. Optimal voltage

The processing efficiency varies proportionally to the increase in voltage. With the same retention time and resistance, while increasing the voltage, the amperage also increased, affecting the current of the ions and thereby increasing the treatment efficiency; the same result could be observed in another research [1, 15].

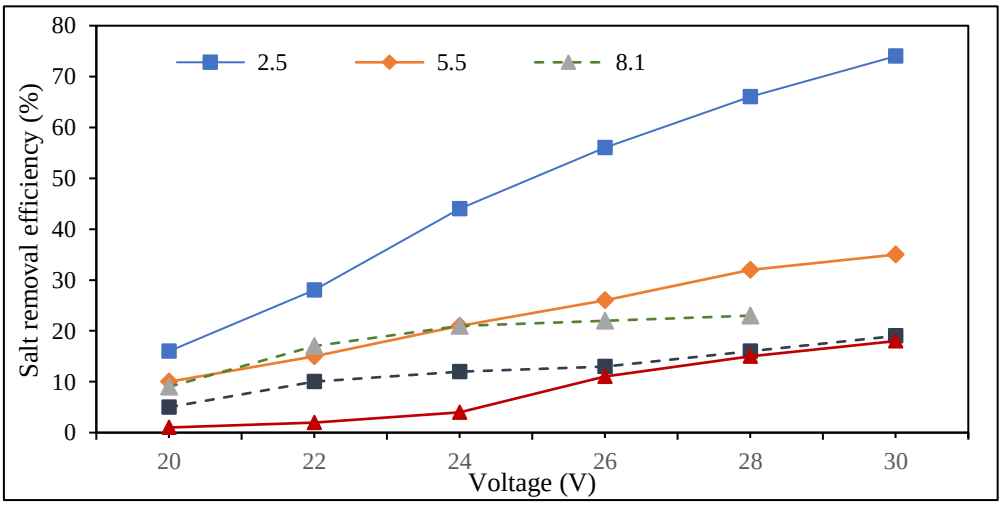

Figure 2. Processing performance at different voltages (20, 22, 24, 26, 28, and 30V) and feed brackish water concentrations (2.5, 5.5, 8.1, 10.1, 20 g/L).

After increasing the voltage to 28V, the two electrode compartments got bubble formation (Figure 3). The cause of this bubbling is the high voltage generated by the electrolysis of oxygen and hydrogen gas in water [16−17]. This phenomenon is partly due to the evaporation of Cl2 gas at the Anode [17], which is harmful to the model and the surrounding environment. To minimize this, the voltage should be kept at < 26V.

Figure 3. The bubbles formation in both electrode compartments.

In addition, on increasing the voltage, there was an upward trend in bubbles formation (which can contain Cl2) in the Anode compartment. The optimal voltage of 26V was considered a suitable application to river water; the efficiency at the 26V point tends to increase faster than the smaller voltages.

The efficiency of ED applying 26V for treating artificial salty water with concentrations 2, 5, 8, 10, 15, and 20 g/L was 56%, 26%, 21%, 13%, and 11%, respectively. It can be seen that the efficiency was not very high and decreased through the raising of NaCl concentration. This could be explained by the fact that with the flow rate of 1 m^3/day, the retention time is low, and the water velocity is too high for the ions to separate. The same result was observed by [15]. Therefore, to improve the performance of ED, the larger working tank and adding treatment stages could be applied [17−18]. Additionally, in the concentrate flow, the concentration increased by 37.5%, 22%, 22.86%, 28.87%, and 13.88% higher than the input with the concentrations 2, 5, 8, 10, 15, and 20 g/L. Thus, it is possible to produce raw salt by storing and drying this output flow [1].

According to above results, the voltage of 26V was the optimal voltage due to several reasons:

1. The removal efficiency of the higher voltage started to increase slower, which means that the higher voltage could not provide significantly higher efficiency. So, increasing the voltage could not improve the efficiency and also consume higher power.

2. From 28V, there was the bubble formation in Anode, this was Cl2 which not only toxic to the environment but also corrosive the model material.

Therefore, the efficiency could be improved by dividing the model into 2 parallel stages in order to increase the retention time.

Moreover, the ED models have a limited current density (LCD) [19], and the results of this experiment can give a correlation equation in the form of a logarithmic graph in which the increasing tendency of current density slowed down over the rising voltage (Figure 4). More specifically, the operation of the ED system should be kept lower than the LCD to ensure efficient use of amperage and no increase in resistance.

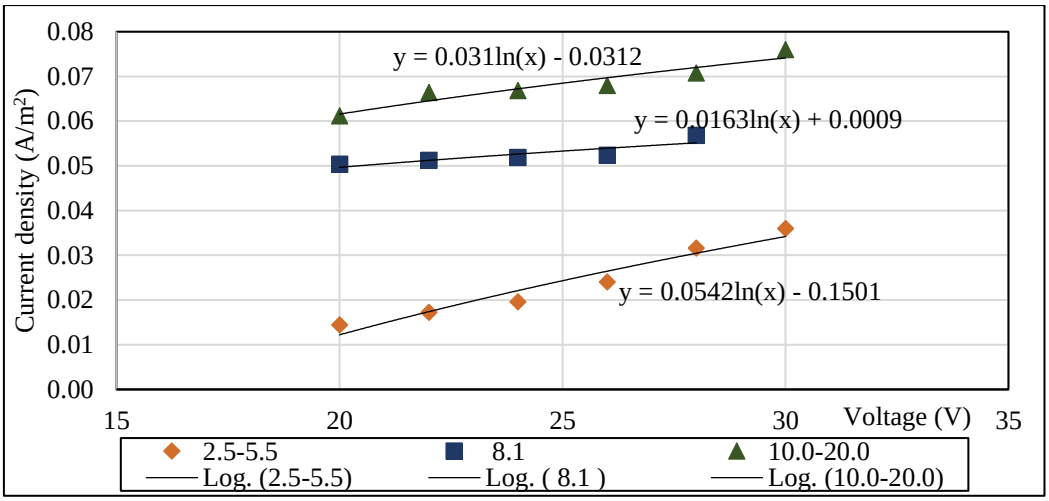

Figure 4. The current density changed over the rising voltage in 3 range of NaCl concentration (2.2−5.5, 8.1, and 10−20 g/L).

3.2. Optimal voltage

In terms of cost efficiency, power consumption was calculated.

The formula for calculating energy consumption:

$$A = P \times t = (U \text{ x } I) \times t \quad (2)$$

where A is the power consumption (kWh); P is the electrical capacity (W); U is the potential difference (V); I is an amperage (A); t is the time (h) = 24h/day.

The power consumption of the experiment was deficient (Table 2).

Table 2. The power consumption in the experiment.

Influent NaCl concentration (g/L)	Effluent NaCl concentration (g/L)	Voltage (V)	Energy (W)	Power consumption (kWh/ day)
2.5	2.10	20	3.20	0.08
2.5	1.8	22	3.96	0.10
2.5	1.4	24	5.04	0.12
2.5	1.1	26	7.28	0.17
2.5	0.85	28	9.8	0.24
2.5	0.65	30	12.3	0.30
5.5	4.95	20	4	0.096
5.5	4.7	22	5.5	0.132
5.5	4.35	24	6.72	0.16128
5.5	4.05	26	8.32	0.19968
5.5	3.75	28	12.32	0.29568
5.5	3.55	30	14.7	0.3528
8.1	7.4	20	12.8	0.31
8.1	6.75	22	13.86	0.33
8.1	6.4	24	15.552	0.37
8.1	6.35	26	17.03	0.41
8.1	6.2	28	19.88	0.48
10.1	9.6	20	16.2	0.3888
10.1	9.1	22	16.5	0.444
10.1	8.89	24	19.44	0.46656
10.1	8.79	26	21.58	0.51792
10.1	8.5	28	24.36	0.58464
10.1	8.2	30	28.5	0.684
20.0	19.8	20	15.6	0.37
20.0	19.6	22	18.48	0.44
20.00	19.15	24	20.40	0.49
20.0	17.9	26	22.62	0.54
20.0	17.05	28	25.2	0.60
20.0	16.4	30	28.5	0.68

Figure 5 showed that the power consumption increased proportionally with feed water concentration, and the highest amount of the investigation was 0.68kWh/m^3 in applying 30V to treat the 20 g/L of NaCl in the input.

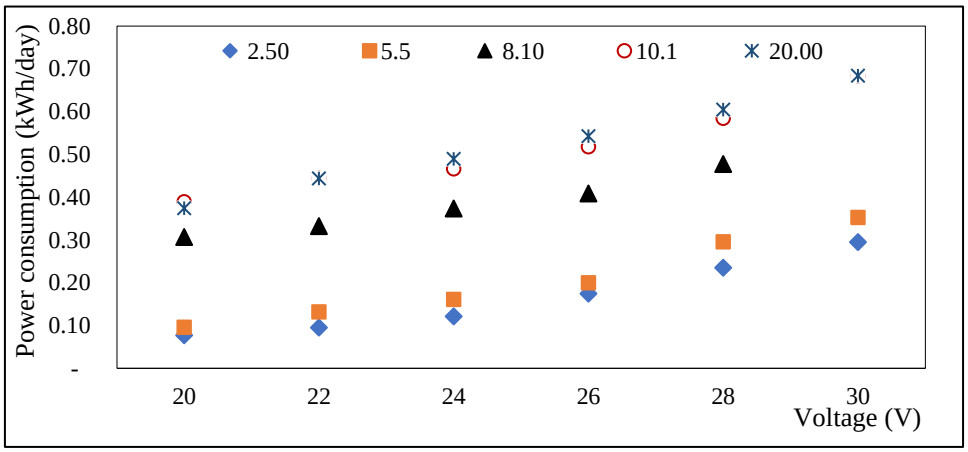

Figure 5. The power consumption trend.

For the voltage of 26V, the electrical capacity corresponding to the concentration of 2.5, 5.5, 8.1, 10, 20.1 µg/L respectively, is 0.175; 0.2; 0.409; 0.518; and 0.543 kWh/day, equivalent to 351.89−1,093.36 VND/m3/day (electricity price is 2,014VND/kWh−Ben Tre Power Company) compared to 9,600−9,900 VND/m3 in the rainy season and 27,846 − 35,581 VND/ m^3 in dry seasons and sometimes up to 150,000−200,000 VND/m^3 in drought period 2020−2021 (search on BEWACO website) when the water is treated by RO method provided by external parties. The model's application helps reduce 68−75% price compared to the water price in regular seasons, without high salinity concentration in water, and 91% compared to water supply in the salinity intrusion season. Compared with water prices, 42,000−51,500 VND/m^3 supplied by barge from the upstream, method can reduce by 94%. There is concrete proof of energy efficiency, but the cost depends strongly on the concentration of NaCl in the feed water [20]. However, counting the possibility of reusing the water in dilute and concentrated flow, this technology could serve as a chance to make a profit from producing raw salt and clean water.

4. Conclusions

The electrodialysis model can reduce down to 0.27 g/L salt concentration with low energy consumption and stable treatment performance. Although this treatment efficiency is enough to treat river water to meet QCVN 01−1:2018/BYT, more researches are needed to thoroughly treat the higher salt concentration and other pollutants in the river water. But this problem can be improved by increasing the retention time (increasing the membrane contact area or increasing the treatment steps).

The voltage of 26V was proved as the optimal voltage for the brackish water with the NaCl concentration ranging from 2g/L to have better efficiency (56%). For higher concentration, the voltage could be kept at 26V to avoid the formation of the bubble, especially Cl2.

The power consumption was very applicable whereas this technology does not cost much energy. In the voltage of 26V, the power consumption ranged only from 0.175 to 0.543 kWh/day and cost only 351.89−1,093.36 VND/m^3/day. By the results of very low power consumption, solar energy should be considered to combine with ED to create a more efficient treatment [21].

Author contribution statement: Constructing research idea: T.T.L., N.P.T.V.; Select research methods: T.T.L., N.P.T.V.; Take sample and sample analysis, data processing: N.P.T.V.; Writing original draft preparation: N.P.T.V.; Writing review and editing: T.T.L.

Competing interest statement: The authors declare that this article was the work of the authors, has not been published elsewhere, has not been copied from previous research; there was no conflict of interest within the author group.

References

1. Sadrzadeh, M.; Mohammadi, T. Sea water desalination using electrodialysis. *Desalin* **2008**, *221(1–3)*, 440–447. Doi: 10.1016/j.desal.2007.01.103.
2. Sadrzadeh, M.; Mohammadi, T. Treatment of sea water using electrodialysis: Current efficiency evaluation. *Desalin* **2009**, *249(1)*, 279–285. Doi: 10.1016/j.desal.2008.10.029.
3. Yang, Y.; Gao, X.; Fan, A.; Fu, L.; Gao, C. An innovative beneficial reuse of seawater concentrate using bipolar membrane electrodialysis. *J. Memb. Sci*. **2014**, *449*, 119–126. Doi: 10.1016/j.memsci.2013.07.066.
4. Liu, Y.; Wang, J.; Wang, L. An energy−saving 'nanofiltration/ electrodialysis with polarity reversal (NF/EDR)' integrated membrane process for seawater desalination. Part III. Optimization of the energy consumption in a demonstration operation. *Desalin* **2018**, *452*, 230–237. Doi: 10.1016/j.desal.2018.11.015.
5. Elimelech, M.; Phillip, W.A. The future of seawater desalination: Energy, technology, and the environment. *Science* **1979**, *333(6043)*, 712–717. Doi: 10.1126/science.1200488.
6. Yen, F.C.; You, S.J.; Chang, T.C. Performance of electrodialysis reversal and reverse osmosis for reclaiming wastewater from high−tech industrial parks in Taiwan: A pilot−scale study. *J Environ. Manage*. **2017**, *187*, 393–400. Doi: 10.1016/j.jenvman.2016.11.001.
7. Ministry of Science and Technology. Report on the status of drought, salinity intrusion of southern area of Vietnam 2019−2020, 2021.
8. Nguyen, L.D.; Gassara, S.; Bui, M.Q.; Zaviska, F.; Sistat, P.; Deratani, A. Desalination and removal of pesticides from surface water in Mekong Delta by coupling electrodialysis and nanofiltration. *Environ. Sci. Pollut. Res.* **2019**, *26(32)*, 32687–32697. doi: 10.1007/s11356-018-3918-6.
9. Cong, V.H. Desalination of brackish water for agriculture: Challenges and future perspectives for seawater intrusion areas in Vietnam. *J. Water. Supply. Res. Technol.* **2018**, *67(3)*, 211–217. Doi: 10.2166/aqua.2018.094.
10. Murray, P. Electrodialysis and Electrodialysis Reversal − Manual of Water Supply Practices, M38 (1st Edition). 1995. Online Available: http://app.knovel.com/web/toc.v/cid:kpEERMWSP1/viewerType:toc/root_slug:electrodialysis−electrodialysis/url_slug:electrodialysis−electrodialysis?b−q=electrodialysis and electrodialysis reversal−manual&sort_on=default&b−subscription=TRUE&b−group−by=true&b−
11. Demircioglu, M.; Kabay, N.; Kurucaovali, I.; Ersoz, E. Demineralization by electrodialysis (ED)−separation performance and cost comparison for monovalent salts. Online Available: www.elsevier.com/locate/desal.
12. Shaposhnik, V.A.; Kesore, K. An early history of electrodialysis with permit selective membranes. *J. Memb. Sci.* **1997**, *136(1–2)*, 35–39. Doi: 10.1016/S0376-7388(97)00149-X.
13. Long, R.; Li, B.; Liu, Z.; Liu, W. Reverse electrodialysis: Modelling and performance analysis based on multi−objective optimization. *Energy* **2018**, *151*, 1–10. Doi: 10.1016/j.energy.2018.03.003.

14. Chehayeb, K.M.; Farhat, D.M.; Nayar, K.G.; Lienhard, J.H. Optimal design and operation of electrodialysis for brackish−water desalination and for high−salinity brine concentration. *Desalin* **2017**, *420*, 167–182. Doi: 10.1016/j.desal.2017.07.003.
15. Mohammadi, T.; Kaviani, A. Water shortage and seawater desalination by electrodialysis. *ELSEVIER*, **2003**. Online Available: www.elsevier.com/locate/desal
16. Han, J.H. Electrode system for large−scale reverse electrodialysis: water electrolysis, bubble resistance, and inorganic scaling. *J. Appl. Electrochem.* **2019**, *49(5)*, 517−528. Doi: 10.1007/s10800-019-01303-4.
17. Shi, L. In situ electrochemical oxidation in electrodialysis for antibiotics removal during nutrient recovery from pig manure digestion. *Chem. Eng. J.* **2021**, *413*, 127485. doi: 10.1016/j.cej.2020.127485.
18. Doornbusch, G.J.; Bel, T.M.; M.; Post, J.W.; Borneman, Z.; Nijmeijer, K. Effect of membrane area and membrane properties in multistage electrodialysis on seawater desalination performance. *J. Memb. Sci.* **2020**, *611*, 118303. Doi: 10.1016/j.memsci.2020.118303.
19. Lee, H.J.; Strathmann, H.; Moon, S.H. Determination of the limiting current density in electrodialysis desalination as an empirical function of linear velocity. *Desalin* **2006**, *190(1–3)*, 43–50. Doi: 10.1016/j.desal.2005.08.004.
20. Strathmann, H.; Strathmann, H. Assessment of Electrodialysis Water Desalination Process Costs, 2004, pp. 32–54. Online Available: https://www.researchgate.net/publication/267765712.
21. Mir, N.; Bicer, Y. Integration of electrodialysis with renewable energy sources for sustainable freshwater production: A review. *J. Environ. Manage.* **2021**, *289*, 112496. Doi: 10.1016/j.jenvman.2021.112496.

VIETNAM JOURNAL OF HYDROMETEOROLOGY

Rerearch Article

Application of Exploratory Factor Analysis on assessment of the community – based survey on environmental quality in Distric 1, Ho Chi Minh City, Vietnam

Nguyen Thi Minh Thu[1*], Nguyen Thi Thu Hang[2], Phan Thanh Hai[3]

[1] Department of Environmental Science, SaiGon University; ntmthu@sgu.edu.vn
[2] Department of Environmental Science, SaiGon University; ntthang@sgu.edu.vn
[3] Department of Construction, The People's Committee of Ho Chi Minh City, Vietnam; thaiquan1@yahoo.com

*Corresponding author: ntmthu@sgu.edu.vn; Tel.: +84−938914769
Received: 2 October 2022; Accepted: 22 December 2022; Published: 25 December 2022

Abstract: Research on people's evaluations and expectations for the living environmental quality has been conducted by many studies. In Vietnam, assessing people's opinions about the quality of the living environment, especially in densely areas, are still limited. However, people's judgments about the quality of the living environment have been considered as one of the assessing methods for the regional environmental protection results, approved by the Ministry of Natural Resources and Environment in 2019. Therefore, this research was carried out to provide the evaluation and expectations of the people about the quality of their living environment in District 1, Ho Chi Minh City. The study used Exploratory Factor Analysis (EFA), a multivariate evaluation method, to group the surveyed answers that best express the respondents' evaluations and expectations. From 07 proposed groups and 26 initial variables, the analysis results have been reduced to 3 evaluation groups with 18 variables; and 2 expectation groups with 18 variables. The analysis results of influencing factors including age, survey's location, and gender showed that although there is no difference in the two groups of gender, the age groups and respondents of 10 wards of District 1 revealed significantly different answers. The results of this pilot evaluation can therefore be applied as a premise to expand more in−depth studies on a larger scale and broader scope, and also an important reference for managers in designing regional environmental management options and plans, particularly in terms of age and location.

Keywords: Living environmental quality; Exploratory Factor Analysis; Principal component analysis; Varimax; Principal Axis Factoring.

1. Introduction

The definition of human quality of life has long been studied by social scientists and managers. WHO defines the quality of life as "an individual's perception of their position in life in the context of the culture and value systems in which they live and in relation to their goals, expectations, standards and concerns" [1]. Therefore in order to quantify these factors, a set of criteria for assessing the quality of life (Quality of life index) has been proposed to build. EU mentioned that this set of indicators should include aspects of employment, health status, social relationships, leisure time, education level, environmental quality, safety security, and administration [2]. For populated environments such as urban

areas, the quality of life has been suggested as the level of happiness and quality of the place where the individual is living [3]. These indicators are a useful tool for sustainable urban development and should include environmental, economic, governance, and management aspects [4−5].

One of the very important aspects of this index is the living environmental quality. Research on environmental quality as a component of quality of life was mentioned quite early by UNESCO social scientists, in which they presented initial views on how to define the natural and man−made environment; and proposed environmental quality criteria such as purity of air, water, soil, noise level, the proportion of man−made structures such as bridges, roads, etc [6]. Studies focusing on sustainable environmental quality were also conducted, especially the Environmental Sustainability Index (ESI) consisting of 21 environmental indicators [7]; or OECD report on environmental indicators for assessing environmental quality (air, water, soil, solid waste, etc), along with assessing methods for each criterion [8]. Studies on assessing aspects of environmental quality in the context of people's quality of life have been conducted by many studies in Europe [9−12], Brazil [13], Iran [14], Malaysia [15], China [16], and Hong Kong [17].

In Vietnam, studies on quality of life have also been researched, including assessment of the quality of life of the elderly in Ho Chi Minh City [18], and comparative evaluation of the sustainability of the big cities Hanoi, Da Nang, Ho Chi Minh City, and Can Tho [19]. However, studies on assessing the quality of life of the residents, in particular the quality of the living environment in large urban areas and high population density such as Ho Chi Minh City, are still limited. In particular, the people’s opinions and evaluations of the living environmental quality in the area have received little attention and research. This is one of the major shortcomings in assessing the quality of the living environment, because the individual judgments reflect an overall environmental quality, together with the pollution conditions of the area.

Nonetheless, people’s assessments have been taken care of by managers and recognized as an important reference source. This is mentioned in Decision No. 2782/QD/BTMT dated October 31, 2019, of the Ministry of Natural Resources and Environment on promulgating a set of indicators for assessing environmental protection results of provinces and cities, which the level of people’s satisfaction is evaluated and accounted for 30% of the rating points by applying the sociological survey method. According to this regulation, the criteria are defined by ambient air, surface water, soil environment, natural landscape, and biodiversity quality [20].

Considerably, the criteria for people's quality of life may be different based on individuals’ assessment and the actual environmental quality. Therefore, this study was carried out to assess people’s satisfaction with their living environmental quality. This study was carried out on a pilot scale (small scale) in the 10 wards of District 1, Ho Chi Minh City. The results of this study are expected to contribute to the development of a set of criteria and evaluation weights suitable to the actual conditions in the locality. The results of this study can then be applied as a reference for local authorities to develop parameters and how to calculate people’s satisfaction with the quality of life, and contribute to the process of assessing the results of local environmental protection.

2. Methods and data

2.1. Study area

As a central area of Ho Chi Minh City, District 1 has an area of 7.72 km^2. According to the information on the District's web portal, the current population of the area is 142,625 people (in 2019), accounting for 1.59% of the total population of the city; population density 18,479 people/km^2; gender ratio is 86 men/100 women. The study is focused on people who

have lived or worked for more than one year in District 1, Ho Chi Minh City. Surveyed people were randomly introduced and selected by the Ward People's Committee in the area. This study, therefore, uses the questionnaire dataset answered by selected citizens for the analysis.

2.2. Research framework

The implementation process of the study is illustrated in Figure 1.

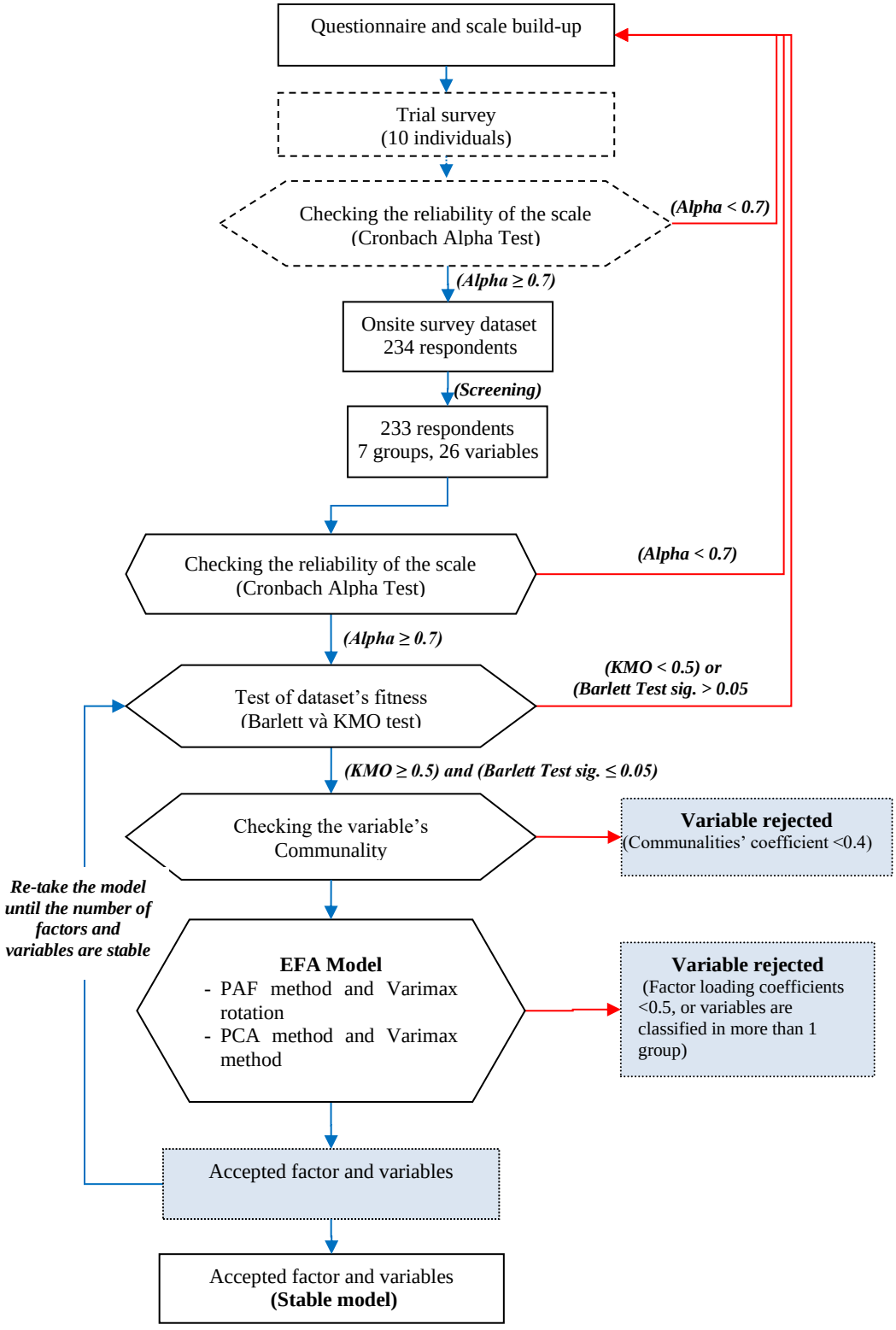

Figure 1. The study's workflow.

2.3. Methods

2.3.1. Questionnaires' development

Questionnaires' contents: The Questionnaires are designed with short questions and scoring answers to get the necessary information without causing difficulties [21]. The content of the survey focuses on two main objectives: (1) assessment and (2) expectations of the respondents for the quality of the living environment. The environmental indicators were referenced from previous studies with a research context close to Vietnam together with the practical experiences on the current situation in the area. The recommended set includes 26 evaluation indicators, divided into 07 main quality groups with 3 to 5 indicators in each group (Table 1). To facilitate the analysis of the results, the questions and scales for each question are designed unidirectionally (either positive or negative). Specifically, for the assessment purpose, the questions are designed in a negative direction (pollution is presented); and for the expectation purpose, the questions are designed in a positive direction (no pollution).

Table 1. The survey's questions.

Label	1. Personal assessment of the environmental quality	Label	2. Personal expectation of the environmental quality
Group 1: Soil [22−23]			
C11	Subsidence conditions presented	C21	Subsidence conditions not presented or limited
C12	Soil pollution presented	C22	Soil pollution not presented or limited
C13	Less percentage of green area	C23	High percentage of green area
Group 2: Water [24−25]			
C14	Poor quality of supply water	C24	Good quality of supply water
C15	Poor quality of natural water	C25	Good quality of natural water
C16	Pollution of surface water and groundwater presented	C26	Pollution of surface water and groundwater not presented or limited
C17	Poor drainage condition	C27	Good drainage condition
C18	High level of groundwater extraction	C28	Low level of groundwater extraction
Group 3: Air [26]			
C19	Pollution of dust and fine dust presented	C29	Pollution of dust and fine dust not presented or limited
C110	Pollution of vehicle smoke presented	C210	Pollution of vehicle smoke not presented or limited
C111	Pollution from business establishments presented	C211	Pollution from business establishments not presented or limited
C112	Pollution from outdoor burning of coal, garbage, or items presented	C212	Pollution from outdoor burning of coal, garbage, or items not presented or limited
Group 4: Landscape [23, 27]			
C113	Poor surrounding green area	C213	Good surrounding green area
C114	Poor surrounding ecosystem	C214	Good surrounding ecosystem
C115	The openness of the surrounding environment is not presented or limited	C215	Good openness of the surrounding environment
Group 5: Noise [23, 26]			
C116	Noise from transportation presented	C216	Noise from transportation not presented or limited
C117	Noise from business activities presented	C217	Noise from business activities not presented or limited
C118	Noise from construction activities present	C218	Noise from construction activities not presented or limited
Group 6: Odor (onsite investigation)			
C119	The odor of untreated waste presented	C219	The odor of untreated waste not presented or limited

Label	1. Personal assessment of the environmental quality	Label	2. Personal expectation of the environmental quality
C120	The odor of sewer presented	C220	The odor of sewer not presented or limited
C121	The odor of production and business activities presented	C221	The odor of production and business activities not presented or limited
C122	The odor of solid waste transfer stations and landfills presented	C222	The odor of solid waste transfer stations and landfills not presented or limited
Group 7: Solid waste [24, 25, 28]			
C123	High volume of generated waste	C223	Low volume of generated waste
C124	Waste is not fully classified	C224	Waste is fully classified
C125	Low percentage of waste not collected/recycled at home/office	C225	High percentage of waste not collected/recycled at home/office
C126	Pollution from the litter on the streets presented	C226	Pollution from the litter on the streets is not presented or limited

Questionnaires' scale: The study applies a Likert scale of 4−5 levels depending on the purpose of the question (Table 2).

Table 2. Recommended scale for the questions in the survey.

Survey's purpose	Score	Explanation
1. Individual assessment of the environmental quality	1	This occurrence does not exist
	2	I have no ideas
	3	This occurrence exists but does not affect my life
	4	This occurrence exists, and affect my life
1. Individual expectation of the environmental quality	1	Very much disagree
	2	Disagree
	3	I have no ideas
	4	Agree
	5	Very much agree

Before conducting the survey, the research team conducted a scale test by randomly surveying 10 people. The reliability results of the trial test applying Cronbach Alpla method showed that the alpha coefficient is higher than 0.7, thereby showing that the scale is reliable, and therefore can be applied to the actual survey.

2.3.2. Sample size

According to recent studies on applying Factor Analysis method, there is no exact minimum sample size because of the respondents' communiality [29−31]. The ratio of the number of surveys to the number of questions (surveyed variables) is recommended either from 2:1 to 20:1 [32−34]. Mundfrom et al (2005) recommended the number of samples from 100 to more than 1,000 [34]. Consequently, with 26 variables stated in the survey, the minimum sample size is expected from 78 to 520 respondents [34]. Because this is a small−scale investigation, the research team surveyed 234 respondents. After screening, a number of 233 were qualified to run the Explanatory Factor Analysis model.

2.3.3 The Cronbach Alpha's test

The Cronbach Alpha test was conducted to check the consistency and reliability of the survey's scale. Although there are arguments about the acceptability interval of Alpha, its application, and interpretation, this method has been widely recognized and applied. In the study, the Alpha's coefficient greater than 0.7 is acceptable [35].

2.3.4 Barlett and Kaiser−Meyer−Olkin's test

The Bartlett and Kaiser−Meyer−Olkin (KMO) test is applied to assess the fit of the data before conducting the Factor Analysis. The Bartlett test checks the correlation between the variables in the matrix. The KMO value, range from 0 to 1, checks the fit of the dataset of the model. A suggested KMO value greater than or equal to 0.5 is acceptable to run the EFA model [29]. Therefore, in the study, the acceptable requirement to conduct Exploratory Factor Analysis is KMO coefficient > 0.5 and the Barlette's p−value < 0.05.

2.3.5. Explanatory Factor Analysis

The Exploratory Factor Analysis (EFA) is one of the multivariate statistical methods used to identify hypothetical or latent constructs. The method groups structures that are related to each other among a set of variables [30, 36]. In social and behavioral science research, factors are understood as unobservable characteristics, expressed by the subjective individual assessment by scoring in a survey. The results of the EFA through the respondents' scores will test whether the questions are correlated and combined closely related questions in a group (named components or Factors in EFA). Therefore, the results reduce the dimensions (groups) of the original dataset by diminishing unnecessary irrelevant data. This analysis is performed by SPSS 16.0. The EFA features are presented as follows:

a) Factor Extraction Models

Factor extraction models are indispensable components in the EFA model. These models include Common Factor Models (including Maximum Likelyhood method and Principal Axis method) and Principal Component Analysis (PCA) [29, 37]. According to Costello and Osborne (2005), depending on the dataset distribution, the Maximum Likelyhood method or Principal Axis Factoring (PAF) method is applicable for normal or non−normal distribution [33]. Principal Component Analysis (PCA) is targeted in reducing the number of observed variables by grouping them in a linear pattern while preserving as much information from the original dataset as possible [29, 30, 36]. As the purpose of the study is to understand the latent factors in the series of observed variables, together with retain as much information as possible, these two extraction methods PAF and PCA were applied.

b) Rotation method

The purpose of the matrix rotation method is to simplify and clarify the data structure. Many methods of matrix rotation are applied, of which orthogonal and oblique rotation methods. Some studies have shown unclear differences between the results of these two rotations, and the results of the oblique rotation can be quite complicated in interpretation [33, 38]. According to [39], the Varimax rotation maximizes the variance in a factor such that larger loads are increased and smaller loads are minimized. Therefore, Varimax rotation, one of the most popular orthogonal rotation methods, is applied in the study.

c) Communality's coefficiency determination

The communalities value indicates the contribution percentage of every observed variable. Accordingly, a variable's communalities coefficient lower than 0.4 means that the variable has a weak relationship with the group of factors [33, 40]. Therefore, in this study, variables with communalities coefficients lower than 0.4 were excluded from the EFA model.

d) Eigenvalue and Factor loading's coefficients

One of the methods to determine the number of groups (factors) is to use the Eigenvalue coefficient. Eigen coefficient, which is higher than 1, is believed to meet the requirements [36]. [29] also added a condition that the total load of variance must be greater than 60%, that is, the selected groups of variables must represent more than 60% of the original group of variables. Besides, Factor loading's coefficients show the degree of

strong or weak relationship of the variable to the group of factors and are usually chosen in the range from 0.30 to 0.55 [41], in which the larger the load coefficient the stronger the correlation of the variable with the factor group. In this study, the loading factor 0.5 was chosen to group the variables into the factor group.

3. Results and discursion

3.1. Results

3.1.1. Grouped variables by EFA model

After screening, a total of 233 valid respondents were selected. The surveyors are distributed relatively evenly in 10 wards of District 1, of which the lowest number of respondents is in Ben Nghe and Da Kao wards (16 respondents) and the highest is Cau Ong Lanh ward (33 respondents). The male/female ratio of the dataset is 53.6% (male) and 46.4% (female), respectively. The average age of the surveyors is 38.7 years old (the highest is 72 years old, the lowest is 19 years old). The average working and living time is 9.73 and 19.22 years, respectively. The average income is about 455 USD per month (9.98 million VND per month).

For the question of environmental quality assessment, the average score ranged from 2.6 to 3.2, indicating that the respondents considered that pollution occurred but did not have too much impact on their lives. Regarding the question about the respondents' expectations about the quality of the living environment, the survey results showed a high level of consensus, with the average score for each question ranging from 3.76 to 4.02 points. This reflects the respondents' level of agreement, but not too high, for environmental quality improvement.

The initial input includes a total of 26 variables in two main groups: 1) The environmental quality assessment group (26 variables, labeled from C11 to C126, referred to as C1); and 2) The environmental quality expectation group (26 variables, labeled from C21 to C226, referred to as group C2). The dataset was tested for the scale's reliability by Cronbach Alpha method in the first run. In the next runnings, the data series is tested for Communality without running Cronbach Alpha again. The results after three runs are presented in Table 3.

Table 3. Summary of EFA model's results.

	1st run		**2nd run**		**3rd run**	
	C1	**C2**	**C1**	**C2**	**C1**	**C2**
No. of rejected variables	0	0	6	7	2	1
No. of tested variables	26	26	20	19	18	18
Cronbach Alpha's test	0.957	0.979	–	–	–	–
Barlett test sig.	0.000	0.000	0.000	0.000	0.000	0.000
KMO 's test	0.891	0.940	0.884	0.935	0.885	0.933
Communality's test	Pass	Reject: C21	Pass	Pass	Pass	Pass
No. of recommended factors	4	2	4	2	3	2
Total cumulative variance (%) (based on the recommended factors)	72.46	72.27	74.7	75.9	72.1	76.5
Rejected variables (PAF method)	C114,C116,C121, C125,C126	C210,C211,C212, C213,C214,C215	C19, C110	C29	None	None
Rejected variables (PCA method)	C13,C114,C116, C121,C125,C126	C210,C211,C212, C213, C214,C215	C19, C110	C29	None	None

In the three runs, the Barlett and KMO tests showed that the results of the two groups of question were satisfactory: Alpha coefficient > 0.7, KMO coefficient > 0.5, and Barlette sig coefficient < 0.05 (Table 3). The total loads of variance of the three runs were higher than 60% (total cumulative variance % in Table 3), which meets the requirement for the number of factors. In the first run, variable C21 was excluded because the test result of communalities coefficient was 0.384 and 0.398 for PAF and PCA methods, respectively. This variable thus was not satisfactory and rejected from the EFA model.

The redistribution of groups of variables (Table 3) shows an association among the variables within the same group. The average survey scores for each variable after grouping are presented in Table 4.

Table 4. Average survey score of each grouped variable.

1. Surveyors' assessment on environmental quality			
Factor 1:	**Factor 2:**	**Factor 3:**	**Rejected:**
C17: 2.94	C11: 2.59	C111: 2.66	C13: 2.95
C118: 2.90	C12: 2.67	C112: 2.57	C19: 3.20
C119: 2.80	C14: 2.60	C113: 2.75	C110: 3.24
C120: 2.81	C15: 2.77	C115: 2.78	C114: 2.62
C122: 2.78	C16: 2.78	C117: 2.70	C116: 3.02
C123: 2.84	C18: 2.82		C121: 2.56
C124: 2.94			C125: 2.63
			C126: 2.77
2. Surveyors' expectation on environmental quality			
Factor 1:	**Factor 2:**		**Rejected:**
C22: 3.91	C216: 3.80		C21: 3.88
C23: 3.84	C217: 3.76		C29: 3.82
C24: 4.02	C218: 3.77		C210: 3.80
C25: 3.96	C219: 3.85		C211: 3.90
C26: 3.85	C220: 3.86		C212: 3.90
C27: 3.82	C221: 3.89		C213: 3.90
C28: 3.88	C222: 3.89		C214: 3.91
	C223: 3.86		C215: 3.90
	C224: 3.76		
	C225: 3.81		
	C226: 3.84		

For the purpose of assessing the environmental quality, the mean score of each group is quite concentrated, which shows the similar assessments of the surveyed people for the variables of the same factor. The average scores of all three groups range from 2.59 to 2.94, showing the assessment of the occurrence of pollution but not too much impact on the people's quality of life. For the expectation purpose of environmental quality, the average score spectrum of the surveyed people for the two groups ranges from 3.76 to 4.02 which shows that people's great concern about environmental quality, especially the variables in factors 1 and 2.

The rejected variables have a fairly high mean score spectrum (from 2.56 to 3.24 for the assessment's purpose, and 3.80 to 3.90 for the expectation's purpose), which shows the respondents' opinion about the large influence of these variables. These variables are excluded due to violation of the principle of not being uploaded to more than 1 group or having unclear loading factors for different factors. Therefore, we believe that these variables should be kept in further extended studies to have a better evaluation of the model.

3.1.2. Affecting conditions including age, location and gender to the results

After conducting the normality test (Q−Q plot) which the results of all the variables are satisfactory, the chosen variables (Table 4) were then applied One–way ANOVA statistical test in term of age and location (Table 5).

Table 5. Sig. index results of One–way ANOVA statistical test of age groups and ward groups (statistically significant level α at 0.05).

Variable's label	**Sig.index of ANOVA test of the three age groups:** * Group 1: less than 30 * Group 2: from 30 to 50 * Group 3: more than 50		**Sig.index of ANOVA test of 10 ward groups** (Ben Nghe, Ben Thanh, Co Giang, Cau Kho, Cau Ong Lanh, Da Kao, Nguyen Cu Trinh, Nguyen Thai Binh, Pham Ngu Lao, Tan Dinh)	
	Statistical Differences (sig.< α)	**Not Statistical Differences (sig.> α)**	**Statistical Differences (sig.< α)**	**Not Statistical Differences (sig.> α)**
1. Surveyors' assessment on environmental quality – Factor 1				
C17		0.696	0.000	
C118		0.205	0.000	
C119		0.450	0.000	
C120		0.523	0.000	
C122		0.127	0.000	
C123		0.139	0.000	
C124	0.027		0.000	
1. Surveyors' assessment on environmental quality – Factor 2				
C11	0.003		0.000	
C12	0.000		0.000	
C14	0.040		0.000	
C15	0.033		0.000	
C16	0.005		0.000	
C18	0.002		0.000	
1. Surveyors' assessment on environmental quality – Factor 3				
C111		0.853	0.000	
C112		0.780	0.000	
C113		0.921	0.000	
C115	0.035		0.000	
C117		0.293	0.000	
2. Surveyors' expectation on environmental quality – Factor 1				
C22		0.186		0.137
C23		0.725		0.068
C24		0.127		0.098
C25		0.697	0.001	
C26		0.950	0.001	
C27		0.981	0.000	
C28		0.903	0.002	
C29		0.843		
2. Surveyors' expectation on environmental quality – Factor 2				
C216		0.437		0.099
C217		0.267	0.024	
C218		0.282	0.001	
C219		0.313		0.163
C220		0.232	0.005	
C221		0.313	0.012	
C222		0.921	0.042	

Variable's label	**Sig.index of ANOVA test of the three age groups:** * Group 1: less than 30 * Group 2: from 30 to 50 * Group 3: more than 50		**Sig.index of ANOVA test of 10 ward groups** (Ben Nghe, Ben Thanh, Co Giang, Cau Kho, Cau Ong Lanh, Da Kao, Nguyen Cu Trinh, Nguyen Thai Binh, Pham Ngu Lao, Tan Dinh)	
	Statistical Differences (sig.< α)	**Not Statistical Differences (sig.> α)**	**Statistical Differences (sig.< α)**	**Not Statistical Differences (sig.> α)**
C223		0.342		0.088
C224		0.714	0.000	
C225		0.329	0.015	
C226		0.356	0.001	

Considering the three different age groups, the results of the expectation varibles showed similarity among the groups. However, for the assessment perspective, results revealed diffences in assessment groups of factor 2, variable C124 of factor 1, and variable C115 of factor 3. For the survey location factor, the survey groups of 10 different wards of District 1 answered differently about the pollution status, as shown by the zero-sig index of all the assessment variables of the One−way ANOVA statistical test. As for the desired variables, most of the answers are significantly different among the 10 survey groups of various wards. Only a few variables showed similarity in the responses of 10 survey groups, including C22 (Soil pollution not presented or limited), C23 (High percentage of green area), C24 (Good quality of supply water). C216 (Noise from transportation not presented or limited), C219 (The odor of raw waste not presented or limited), C223 (Low volume of generated waste)

On the contrary, the results of the two independent samples t−test of the two gender groups (male and female) revealed that there was no difference among the answers in most of the questionnaires (Table 6). Statistically different responses were C12 (Soil pollution presented), C14 (Poor quality of supply water) and C113 (Poor surrounding green area). For these three variables, the female tends to give higher scores than the male, which may indicate that the female's statements about the pollution status of these variables are more severe than the male.

Table 6. Sig. index results of independent statistical t−test of male/female groups (statistically significant level α at 0.05).

Variable's label	Male (N = 108)		Female (N=125)		Statistical Differences (sig.< α)	Not Statistical Differences (sig.> α)
	Mean	StdDev	Mean	StdDev		
1. Surveyors' assessment on environmental quality – Factor 1						
C17	2.86	0.990	3.01	0.996		0.261
C118	2.78	0.931	3.01	0.875		0.053
C119	2.78	0.960	2.82	1.100		0.735
C120	2.78	0.970	2.83	0.905		0.659
C122	2.69	0.954	2.86	1.019		0.170
C123	2.78	1.017	2.90	1.030		0.381
C124	2.88	1.011	2.99	0.920		0.376
1. Surveyors' assessment on environmental quality – Factor 2						
C11	2.48	1.054	2.68	1.182		0.180
C12	2.52	1.018	2.81	1.090	0.038	
C14	2.44	1.061	2.74	1.165	0.042	
C15	2.65	1.017	2.87	10.70		0.105
C16	2.75	0.987	2.81	1.127		0.679
C18	2.76	0.906	2.87	1.047		0.384

Variable's label	Male (N = 108) Mean	StdDev	Female (N=125) Mean	StdDev	Statistical Differences (sig.< α)	Not Statistical Differences (sig.> α)
1. Surveyors' assessment on environmental quality – Factor 3						
C111	2.63	1.064	2.68	1.097		0.723
C112	2.52	1.037	2.62	1.162		0.503
C113	2.59	0.886	2.89	0.900	0.013	
C115	2.70	1.044	2.84	0.893		0.284
C117	2.69	0.891	2.70	1.064		0.990
2. Surveyors' expectation on environmental quality – Factor 1						
C22	3.90	0.723	3.93	0.825		0.771
C23	3.86	0.703	3.82	0.794		0.708
C24	4.01	0.619	4.02	0.735		0.870
C25	4.01	0.555	3.92	0.852		0.350
C26	3.87	0.685	3.83	0.905		0.719
C27	3.82	0.895	3.82	0.984		1.000
C28	3.88	0.770	3.89	0.900		0.940
C29	3.83	0.952	3.80	1.024		0.798
2. Surveyors' expectation on environmental quality – Factor 2						
C216	3.85	0.905	3.76	1.011		0.469
C217	3.81	0.866	3.71	1.030		0.415
C218	3.78	0.868	3.77	0.952		0.935
C219	3.84	0.929	3.86	0.970		0.864
C220	3.91	0.933	3.82	1.040		0.523
C221	3.95	0.813	3.83	0.922		0.290
C222	3.96	0.784	3.83	0.881		0.231
C223	3.89	0.824	3.83	0.905		0.618
C224	3.80	0.915	3.73	1.042		0.598
C225	3.86	0.841	3.78	0.966		0.485
C226	3.90	0.937	3.78	1.028		0.380

3.2. Discussion

After testing for 26 surveying variables in 7 initial groups with the EFA model, the results obtained are 18 variables categorized into 3 groups for environmental quality assessment; and 18 variables allocated into 2 groups for environmental quality's expectation. Groups of variables and interpretations are presented in Table 7.

The results of the EFA model have significantly reduced the dimension of the survey questionnaire, from initially 7 groups and 26 variables to 3 groups and 18 variables for the assessment target) and 2 groups (for expectation target). Unrelated variables have also been omitted by the model, including 8 variables in each assessment and expectation purposes. The results from the PCA extraction model always show a higher factor loading and a greater number of retained variables than PAF. However, the PAF showed a clearer distinction among groups and therefore the subgroup results were also more discriminatory.

4. Conclusion

The study results show that the EFA model have narrowed and clarified the respondents' assessments of environmental quality in the area divided into 3 groups, along with expressing people's expectations about environmental quality divided into 2 groups. The results of this model can serve as a baseline study, and as a reference for building public opinion survey models at an expanded level and more focused on variables that have been kept by EFA model. This EFA result can also serve as a theoretical model of people's evaluation factors and expectations about environmental quality, thereby becoming an

important input in a Confirmatory factor analysis model, which is a tool used to confirm or disprove a measurement theory.

Besides, although groups of gender have similarity in the responses, the influence of individual factors such as age, living and working location greatly affects the survey results. Therefore, these factors need to be considered, included in a detailed survey plan, and carefully analyzed to develop appropriate environmental protection and management strategies for the area.

Table 7. Grouping results on quality of the living environment.

1. Surveyors' assessment on environmental quality	
Factor 1	
C17	Poor drainage condition
C118	Noise from construction activities present
C119	The odor of untreated waste presented
C120	The odor of sewer presented
C122	The odor of solid waste transfer stations and landfills presented
C123	High volume of generated waste
C124	Waste is not fully classified
Factor 2	
C11	Subsidence conditions presented
C12	Soil pollution presented
C14	Poor quality of supply water
C15	Poor quality of natural water
C16	Pollution of surface water and groundwater presented
C18	High level of groundwater extraction
Factor 3	
C111	Pollution from business establishments presented
C112	Pollution from outdoor burning of coal, garbage, or items presented
C113	Poor surrounding green area
C115	The openness of the surrounding environment is not presented or limited
C117	Noise from business activities presented
2. Surveyors' expectation on environmental quality	
Factor 1	
C22	Soil pollution not presented or limited
C23	High percentage of green area
C24	Good quality of supply water
C25	Good quality of natural water
C26	Pollution of surface water and groundwater not presented or limited
C27	Good drainage condition
C28	Low level of groundwater extraction
Factor 2	
C216	Noise from transportation not presented or limited
C217	Noise from business activities not presented or limited
C218	Noise from construction activities not presented or limited
C219	The odor of untreated waste not presented or limited
C220	The odor of sewer not presented or limited
C221	The odor of production and business activities not presented or limited
C222	The odor of solid waste transfer stations and landfills not presented or limited
C223	Low volume of generated waste
C224	Waste is fully classified
C225	High percentage of waste not collected/recycled at home/office
C226	Pollution from the litter on the streets is not presented or limited

Author contribution statement: Conceived and designed the questionnaire; Analyzed and interpreted the data; contributed reagents, materials, analysis tools or data; manuscript editing: N.T.M.T; Data collection, analyzed and interpreted the data, wrote the draft manuscript: N.T.T.H, P.T.H.

Acknowledgements: The authors would like to express our sincere thanks to the Chairman/Vice Chairman and Office Managers of 10 Wards of District 1, Ho Chi Minh City; together with the great help of residents and people with the survey. We would also like to express our gratitude to Saigon University, Ho Chi Minh City for supporting the completion of this research.

Competing interest statement: The authors declare no conflict of interest.

References

1. World Health Organization WHO. WHOQOL: Measuring Quality of Life, 2021. Available online: https://www.who.int/tools/whoqol.
2. European Union EU. Quality of life: Facts and views. Luxembourg, 2015, 268p.
3. Murgas, F.; Klobucnik, M. Quality of life in the city, Quality of urban life or well−being in the city: Conceptualization and case study. *Sciendo* **2018**, *37(2)*, 183−200. https://doi.org/10.2478/eko-2018-0016.
4. Alibegović, D.J.; de Villa, Ž.K. The role of urban indicators in city management: a proposal for Croatian cities. *Transition Studies Rev.* **2008**, *15*, 63–80. https://doi.org/10.1007/s11300-008-0171-6.
5. Wang, H.; Zou, X.; Lai, K.; Luo, W.; He, L. Does Quality of Life Act as a Protective Factor against Believing Health Rumors? Evidence from a National Cross−Sectional Survey in China. *Int. J. Environ. Res. Public Health* **2021**, *18*, 4669. https://doi.org/10.3390/ijerph18094669.
6. Seashore, S.E.Al. Indicators of environmental quality and quality of life. United Nations Educational. Scientific and Cultural Organization, France. 1978, ISBN: 92-3-101539-7.
7. Yale Center for Environmental Law and Policy YCELP Environmental Sustainability Index (ESI). Palisades, NY: NASA Socioeconomic Data and Applications Center (SEDAC). 2005. https://doi.org/10.7927/H40V89R6.
8. Organisation for Economic Co−operation and Development OECD. OECD Key Environmental Indicators. Paris, France, 2008.
9. Dalia, S. Comparative assessment of environmental indicators of quality of life in Romania and Lithuania. *Econ. Sociol.* **2014**, *7(1)*, 11−21. https://doi.org/10.14254/2071-789X.2014/7-1/2
10. Dalia, S. Environmental indicators for the assessment of quality of life. *Intellectual Econ.* **2015**, *9*, 67−79. https://doi.org/10.1016/j.intele.2015.10.001.
11. Chiara, G.; Valentina, M.P. Evaluating Urban Quality: Indicators and Assessment Tools for Smart Sustainable Cities. *Sustainability* **2018**, *10*, 575. http://doi.org/10.3390/su10030575.
12. Vanessa, K.S. Amaury Labenne, and Tina Rambonilaza. Using ClustOfVar to Construct Quality of Life Indicators for Vulnerability Assessment Municipality Trajectories in Southwest France from 1999 to 2009. *Soc. Indic. Res.* **2017**, *131*, 973–997. https://doi.org/10.1007/s11205-016-1288-3.
13. Rafael, M.; Mohammad, K.; Najjar, A.; Hammad, W.A.; Assed, H.; Elaine, V. Urban Development Index (UDI): A Comparison between the City of Rio de Janeiro and Four Other Global Cities. *Sustainability* **2020**, *12*, 823. https://doi.org/10.3390/su12030823.
14. Musa, P.; Saeed, Z.S.; Niloofar, K.; Sirio, C.; Matteo, C.; Luca, S. Factors Underlying Life Quality in Urban Contexts: Evidence from an Industrial City (Arak, Iran).

Sustainability **2020**, *12*, 2274. https://doi.org/10.3390/su12062274.
15. Arif, A.; Muhammad, A.; Alias, B.A.; Ihtisham, A.M.; Anwar, K.; Tengku, A.A.T.H.; Faridullah, M.M.K.; Hina, Z.; Khalid, Z. Environmental quality indicators and financial development in Malaysia: unity in diversity. *Environ. Sci. Pollut. Res.* **2015**, *22*, 8392–8404. https://doi.org/10.1007/s11356-014-3982-5.
16. Chuan, T.; Wen−Hu, Y.; Baohong Hou. Developing an Environmental Indicator System for Sustainable Development in China: Two Case Studies of Selected Indicators. *Environ Manage.* **2006**. *38*, 688–702. https://doi.org/ 10.1007/s00267−004−0352−y
17. Chien−Tat, Low.; Robert, Stimson.; Si, Chen.; Ester, C.; Paulina Pui−Yun, W.; Poh−Chin, L. Personal and Neighbourhood Indicators of Quality of Urban Life: A Case Study of Hong Kong. *Soc. Indic. Res.* **2018**, *136*, 751–773. https://doi.org/10.1007/s11205-017-1579-3.
18. Nam, X.V.; Trung, Q.V. Somtip Watanapongvanich, Nopphol Witvorapong. Measurement and Determinants of Quality of Life of Older Adults in Ho Chi Minh City, Vietnam. *Social. Indic. Res.* **2019**, *142*, 1285–1303. https://doi.org/10.1007/s11205-018-1955-7.
19. Van, T.D.; Jianming, W.; Wilson, V.T.D. An Integrated Fuzzy AHP and Fuzzy TOPSIS Approach to Assess Sustainable Urban Development in an Emerging Economy. *Int. J. Environ. Res. Public Health* **2019**, *16*, 2902. https://doi.org/10.3390/ijerph16162902.
20. Vietnam Ministry of Natural Resources and Environment. Decision No. 2782/QD/BTMT on promulgating a set of indicators for assessing environmental protection results of provinces and central cities. 2019. Available from https://monre.gov.vn/Pages/quyet-dinh-so-2782-qd-btnmt.aspx. (Date accessed 2021 Jun 3).
21. Sreejesh, S.; Sanjay, M.; Sanjay, M.R.A. Questionnaire Design. 2014, pp. 143–159. https://doi.org/10.1007/978-3-319-00539-3_5.
22. Shathy, S.T.; Reza, M.I.H. Sustainable Cities: A Proposed Environmental Integrity Index (EII) for Decision Making. *Front. Environ. Sci*. **2016**, *4*, 82. https://doi.org/10.3389/fenvs.2016.00082.
23. Pazhuhan, M.; Shahraki, S.Z.; Kaveerad, N.; Cividino, S.; Clemente, M.; Salvati, L. Factors Underlying Life Quality in Urban Contexts: Evidence from an Industrial City (Arak, Iran). *Sustainability* **2020**, *12*, 2274. https://doi.org/10.3390/su12062274.
24. Fehr, M.; Sousa, K.A.; Pereira, A.F.N.; Pelizer, L.C. Proposal of Indicators to Assess Urban Sustainability in Brazil. *Environ. Dev. Sustainability* **2004**, *6*, 355–366. https://doi.org/10.1023/B:ENVI.0000029914.82071.6e.
25. Organisation for Economic Cooperation and Development OECD. OECD Key Environmental Indicators, France, 2008.
26. Silva, L.T.; Mendes, J.F.G. City Noise−Air: An environmental quality index for cities. *Sustainable Cities Soc.* **2012**, *4*, 1−11. https://doi.org/10.1016/j.scs.2012.03.001.
27. Garau, C.; Pavan, V.M. Evaluating Urban Quality: Indicators and Assessment Tools for Smart Sustainable Cities. *Sustainability* **2018**, *10*, 575. https://doi.org/10.3390/su10030575.
28. Sarmento, R.; Zorza, F.M.B.; Serafim, A.J.; Allmenroedr, L.B. Urban environmental quality indicator. *WIT Trans. Eco. Environ*. **2000**, *39*, 8. https://doi.org/10.2495/URS000111.
29. Shawn, L.; Talip, G. Chapter: Exploratory Factor Analysis and Principal Components Analysis. In: Luke Plonsky, Advancing Quantitative Methods in

Second Language Research, 1st edition. *Routlede* **2015**, pp. 378. https://doi.org/10.4324/9781315870908-9.
30. Marley, W.W. Exploratory Factor Analysis: A Guide to Best Practice. *J. Black Psychol*. **2018**, *44(3)*, 219–246. https://doi.org/10.1177/0095798418771807.
31. Horst, T.; Peter, F. Exploratory factor analysis revisited: How robust methods support the detection of hidden multivariate data structures in IS research. *Infor. Manage*, **2010**, *47(4)*, 107−207. https://doi.org/10.1016/j.im.2010.02.002.
32. Field, A. Discovering statistics using SPSS. London: Sage, 2009.
33. Anna, B.C.; Jason, W.O. Best practices in exploratory factor analysis: four recommendations for getting the most from your analysis. *Pract. Assess. Res. Eval.* **2005**, *10(7)*, 1-9. https://doi.org/10.7275/jyj1-4868.
34. Mundfrom, D.J.; Shaw, Dale, G.; Ke, Tian, Lu. Minimum Sample Size Recommendations for Conducting Factor Analyses. *Int. J. Testing* **2005**, *5(2)*, 159–168. https://doi.org/10.1207/s15327574ijt0502_4.
35. Keith, S.T. The Use of Cronbach's Alpha When Developing and Reporting Research Instruments in Science Education. *Res. Sci. Edu*. **2017**, *48*, 1273–1296. https://doi.org 10.1007/s11165-016-9602-2.
36. Robin, K.; Henson, J.; Kyle Roberts. Use of Exploratory Factor Analysis in Published Research Common Errors and some Comment on Improved Practice. *Edu. Psychol. Meas.* **2006**, *66*, 393−416. https://doi.org/10.1177/0013164405282485.
37. Jim, C.; Allen, H. Organizational Research Methods: A Review and Evaluation of Exploratory Factor Analysis Practices in Organizational Research. *SAGE*, **2003**, *6(2)*, 147−168. https://doi.org/10.1177/1094428103251541.
38. Osborne, J.W. What is Rotating in Exploratory Factor Analysis? *Pract. Assess. Res. Eval.* **2015**, *20(2)*, 1-8. https://doi.org/10.7275/hb2g-m060.
39. Osborne, J.W. Best Practices in Exploratory Factor Analysis. 2014.
40. Scotts, V. CA: Create Space Independent Publishing, 2014. ISBN-13: 978-1500594343, ISBN-10:1500594342.
41. Zeynivandnezhad, F.; Rashed, F.; Kaooni, A. Exploratory Factor Analysis for TPACK among Mathematics Teachers: Why, What and How. *Anatolian. J. Edu.* **2019**, *4(1)*, 59−76.
42. Laura, L.S.; Jason, W.B.; Muriel, J.B. Factor Analysis as a Tool for Survey Analysis Using a Professional Role Orientation Inventory as an Example. *Phys. Ther*. **2004**, *84(9)*, 784−99.

VIETNAM JOURNAL OF HYDROMETEOROLOGY

Research Article

Developing a 1D kinematic wave model for simulating the downstream flow of Tra Khuc river

Bui Van Chanh[1], Can Thu Van[2*], Vu Thi Van Anh[2], Nguyen Hai Au[3], Can The Viet[4], Nguyen Hong Truong[1], Tran Duc Dung[3]

[1] South Central hydrometeorological center; buivanchanh@gmail.com; truongmeteo@gmail.com
[2] HCMC University of Natural resources environment; ctvan@hcmunre.edu.vn
[3] Institute for Environment and Resources, VNU of Ho Chi Minh City; haiauvtn@gmail.com; dungtranducvn@gmail.com
[4] Institute for Water Resources and Environment research, Thuyloi university; theviet8387@gmail.com

*Corresponding author: ctvan@hcmunre.edu.vn; Tel.: +84−983738347

Received: 13 November 2022; Accepted: 15 December 2022; Published: 25 December 2022

Abstract: The nonlinear kinematic wave model is developed from the Saint Venant system of equations, which includes a nonlinear kinematic wave program that solves the system of equations by Newton's iterative method and a linear kinematic wave program for calculations initial flow value. The developed model is tested with sample problems and compared with the simulation results by Mike 11 model on Tra Khuc river. Evaluating the simulation results of these two models show that, the simulation results of the Mike 11 model are better than the kinematic wave model, not significantly in the upstream and midstream flow, but significantly in the downstream flow of the Tra Khuc river. The simultaneous results show that the 1−dimensional kinetic wave model has sufficient reliability and applicability.

Keywords: Mike 11 model; Kinematic Wave Model; Tra Khuc River.

1. Introduction

Flow analysis models play an important role in simulation and forecasting of river flow, so it is formed very early. Simple models such as SSARR, which uses the method of reserves of river sections, or Muskingum model which simulates the displacement of flood waves on a linear channel, do not simulate the motion of the flow. More general research from Cunge (1969), where the discrete Muskingum equation is considered to be a finite difference approximation of the kinematic wave model. Therefore, the Muskingum–Cunge model is a kinematic wave approximation model [1].

Hydraulic models are widely used and are quite popular today. Depending on the difference method and assumptions, there are different hydraulic models, such as: MIKE 11, HEC-RAS, KOD1, VRSAP, ISIS-1D, HydroGIS, MK4, QUAL2-E, HEC 6, IMECH-1D, DUFLOW. The dynamic wave model has a wide range of applications on tidal and non-tidal affected rivers, with good simulation quality. However, this type of model uses the river cross-section as the input, so it cannot be applied on the river section without cross-section, while lack of cross-section is quite common in upstream rivers. Therefore, the application of models capable of simulating physical nature of flow but not requiring cross-sectional data is essential. To overcome the above problem, kinematic wave model is studied and applied;

in which, some simulation components are reduced compared to the dynamic wave model, but do not use cross-sectional data. The kinematic wave model is based on a simplified form of Saint Venant's equations [2], a dynamic wave approximation [4], which simulates the process of flood propagation in rivers due to changes in discharge or water level. In addition, the simulation principle of the kinematic wave model is that the flow is generated from the slope, so it is suitable for mountainous rivers and streams, where commonly lack of cross-sectional data.

In theory, the kinematic wave model is simpler, requires less data, so the application scope and simulation quality are lower than the dynamic wave model. However, this issue needs to be verified in practice. There are many dynamic wave models today, but Mike 11 is the most commonly used. Therefore, this research evaluates the simulation ability of the kinematic wave model and the Mike 11 model.

Kinematic wave model is proposed by [3] and developed by a number of later researches, which is applied to simulate flow in canals and rivers [4–8]. The one-dimensional model in the river is later studied by [9] for riverbanks with different types of cross-sectional shapes. Nwaogazie (1978) developes a nonlinear one-dimensional model by Newton's method Raphson [10], [11] builds the model in the channel by solving finite difference. Before, the kinematic wave model is developed by many researchers to simulate flow on slopes such as: [12, 13] calculates the peak transmission time between hydrological stations, while Morel [14] builds a model combining hydraulics and statistics. In addition, the kinematic wave model is also used in the Mike-11, HEC-1 model to be used for rivers without cross-sectional data. However, these models only simulate a river tributary, using the matrix method to solve the problem. In Vietnam, the one-dimensional model on the slope has been used by [15] to simulate the slope flow in the KW1D model.

The river section applied to evaluate the simulation ability of the kinematic wave model and Mike 11 model is Tra Khuc river, Quang Ngai province. This is a large river basin of the province, where rain and flood events are very complicated. Especially, the river basin is near Ba To - a heavy rain center of the country, so floods occur harshly. The climatic changes make the flow characteristics in the river basin become complicated. In the dry season of 2015, while the central region, including the Tra Khuc river basin, deals with a severe drought and lack of water, an unusual flood occurs suddenly on March 27. This flood isolates more than 400 households with 1,000 people and submerges 100 hectares of watermelons in water. The flood in November 2009 kills 26 people, injures 6 people, destroys 10,430 houses, and causes total damage of 47.66 billion VND. After that, the flood in December 2009 makes 41 people died, 11 people missing, 21 people injured, with a total loss of 200 billion VND. The historic flood in November 2013 kills 40 people, hundreds of houses are washed away, and damage is estimated at 179 billion VND. The extremes of the flow, the fierce nature of rain and floods occur with more frequency, greater intensity and more complex development, requiring more advanced forecasting work. Therefore, it is necessary to study and apply new models and technologies for flood forecasting and water resources calculation on Tra Khuc river.

2. Materials and methods

2.1. Developed model

The Saint Venant equation has many different simplifications, each of them defines a one-dimensionally distributed unstable flow simulation model. Continuity equation, conservative momentum equation and non-conservative momentum equation neglecting lateral currents, wind resistance, and eddy losses are used to define different types of models for one-dimensionally distributed unstable flow [2, 3–9].

The equation of momentum includes the components of the physical processes that control the flow of momentum. These components are: the local acceleration component

which describes the change in momentum due to the change of velocity with time; the convective acceleration component which describes the change in momentum caused by the change in velocity along the channel; the pressure component which is proportional to the change in water depth along the channel; the gravity component which is proportional to the bottom slope S0; and the friction component which is proportional to the friction gradient Sf. The components of local acceleration and convective acceleration represent the effects of inertial forces on the flow [1−2, 16−18].

+ Continuity equation:

$$\frac{\partial Q}{\partial x} + \frac{\partial A}{\partial t} = 0 \quad (1)$$

+ Momentum equation [1]:

$$\frac{1}{A}\frac{\partial Q}{\partial t} + \frac{1}{A}\frac{\partial}{\partial x}\left(\frac{Q^2}{A}\right) + g\frac{\partial y}{\partial x} - g(S_o - S_f) = 0 \quad (2)$$

Kinematic waves dominate the flow when the forces of inertia and pressure is neglected. In kinematic waves, the forces of friction and gravity are balanced, so the water flow has no acceleration. Therefore, the energy line is parallel to the bottom of the channel and the flow in an elemental segment is a steady stream (because $S_0 = S_f$).

Kinematic waves are caused by changes in flow such as changes in water flow or wave speed which is the changing velocity along the channel. The wave speed depends on the type of wave and it can be completely different from the water velocity. For kinematic waves, the acceleration and pressure components in the momentum equation have been neglected, so the wave motion is described mainly by the continuity equation. That is why it is called kinematic wave, because kinematics studies motion in which the influence of mass and force is not taken into account. The kinematic wave model is determined by the following equations [23−26]:

+ Continuity equation:

$$\frac{\partial Q}{\partial x} + \frac{\partial A}{\partial t} = q \quad (3)$$

+ Momentum equation:

$$S_o = S_f \quad (4)$$

$$A = \alpha Q^{\beta} \quad (5)$$

In the Manning equation, $S_o = S_f$ và R=A/P, therefore:

$$Q = \frac{1.49 S_o^{1/2}}{n P^{2/3}} A^{5/3} \quad (6)$$

Rewrite equation (6) for A, from which to find α and β = 0.6 as follows [1]:

$$A = \left(\frac{n P^{2/3}}{1.49\sqrt{S_o}}\right)^{3/5} Q^{3/5} \quad (7)$$

$$A = \left(\frac{n P^{2/3}}{1.49\sqrt{S_o}}\right)^{0.6} \quad (8)$$

Equation (1) depends only on A and Q, where A is defined in equation (5). The partial derivative of equation (5) of variables A and Q with respect to t and then substituting into equation (1) to get equation (9). Substitute equation (9) into equation (3) to get equation (10). Equation (10) is converted into difference form diagrammatically linear according to equation (17), and diagrammatically nonlinear according to equation (22).

$$\frac{\partial A}{\partial t} = \alpha\beta Q^{\beta-1}\left(\frac{\partial Q}{\partial t}\right) \quad (9)$$

$$\frac{\partial Q}{\partial x} + \alpha\beta Q^{\beta-1}\left(\frac{\partial Q}{\partial t}\right) = q \quad (10)$$

2.3. Developing a 1D kinematic wave model

The model is developed on Fortran 90 programming language and consists of two main parts: linear and nonlinear kinematic wave model. In which the linear model is used as the first solution of the nonlinear model. The linear model is solved by the hidden difference diagram, the nonlinear model is solved by the Newton iterative method [2].

2.3.1. Linear kinematic wave diagramD setup

Apply the hidden difference diagram [1−2]:

$$\frac{\partial u_{i+1}^{j+1}}{\partial x} = \frac{u_{i+1}^{j+1} - u_i^{j+1}}{\Delta x} \tag{11}$$

$$\frac{\partial u_{i+1}^{j+1}}{\partial t} = \frac{u_{i+1}^{j+1} - u_{i+1}^{j}}{\Delta t} \tag{12}$$

$$\frac{\partial Q_{i+1}^{j+1}}{\partial x} \approx \frac{Q_{i+1}^{j+1} - Q_i^{j+1}}{\Delta x} \tag{13}$$

$$\frac{\partial Q_{i+1}^{j+1}}{\partial t} \approx \frac{Q_{i+1}^{j+1} - Q_{i+1}^{j}}{\Delta t} \tag{14}$$

$$Q \approx \frac{Q_i^{j+1} + Q_{i+1}^{j}}{2} \tag{15}$$

$$q \approx \frac{q_{i+1}^{j+1} + q_{i+1}^{j}}{2} \tag{16}$$

Substituting the equations from (13) to (16) into the equation (10) to get the linear kinematic wave difference equation and the hidden plot as shown in Figure 1 [1−2]:

$$\frac{Q_{i+1}^{j+1} - Q_i^{j+1}}{\Delta x} + \alpha\beta\left(\frac{Q_{i+1}^{j} + Q_i^{j+1}}{2}\right)^{\beta-1}\left(\frac{Q_{i+1}^{j+1} - Q_{i+1}^{j}}{\Delta t}\right) = \frac{q_{i+1}^{j+1} + q_{i+1}^{j}}{2} \tag{17}$$

$$Q_{i+1}^{j+1} = \frac{\left[\frac{\Delta t}{\Delta x}Q_i^{j+1} + \alpha\beta Q_{i+1}^{j}\left(\frac{Q_{i+1}^{j} + Q_j^{i+1}}{2}\right)^{\beta-1} + \Delta t\left(\frac{q_{i+1}^{j+1} + q_{i+1}^{j}}{2}\right)\right.}{\left[\frac{\Delta t}{\Delta x} + \alpha\beta\left(\frac{Q_{i+1}^{j} + Q_i^{j+1}}{2}\right)^{\beta-1}\right]} \tag{18}$$

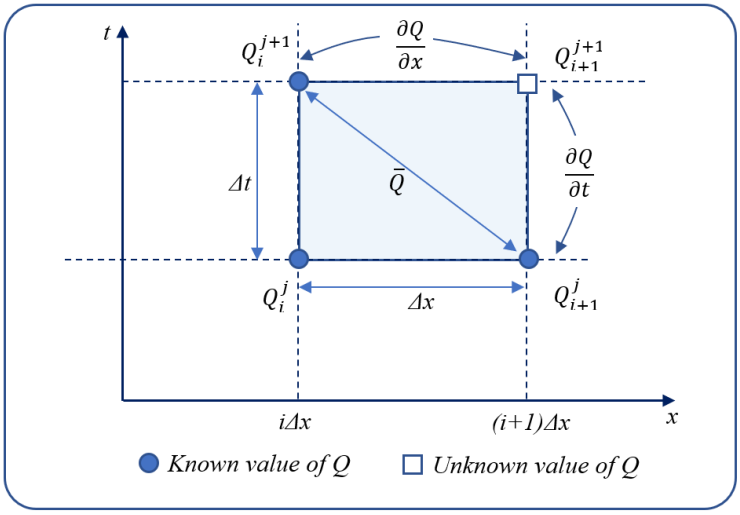

Figure 1. Hidden difference diagram solving linear kinematic wave equation.

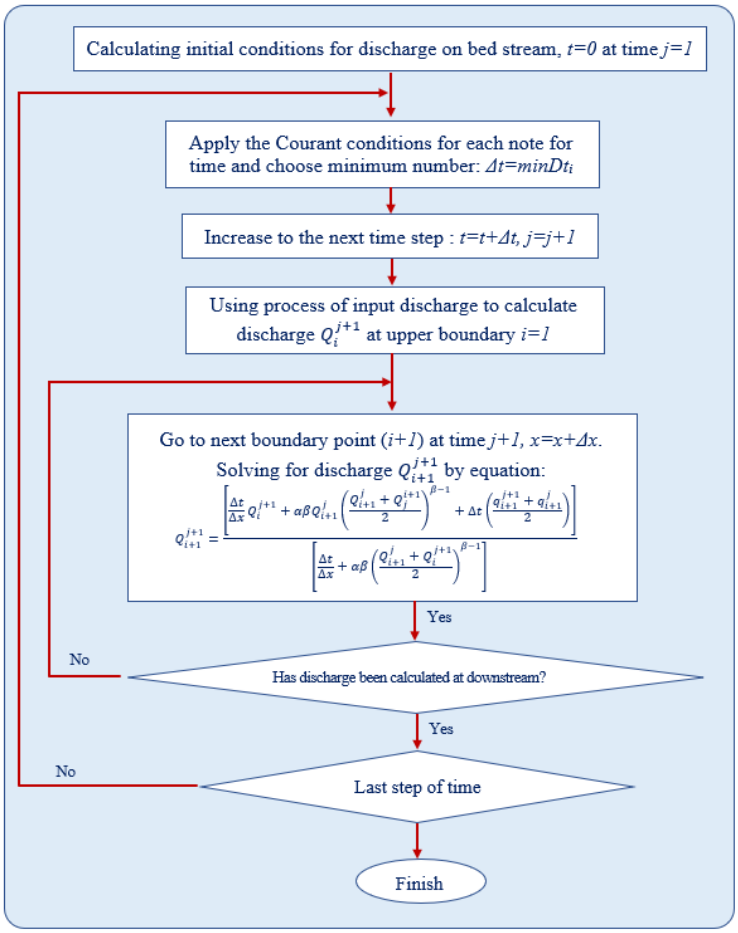

Figure 2. Linear kinematic wave calculation block diagram.

2.3.2. Nonlinear kinematic wave diagram

Equation (10) is transformed into the difference equation [1−2]:

$$\frac{Q_{i+1}^{j+1} - Q_i^{j+1}}{\Delta x} + \frac{A_{i+1}^{j+1} - A_{i+1}^{j}}{\Delta t} = \frac{q_{i+1}^{j+1} + q_{i+1}^{j}}{2} \quad (19)$$

$$A_{i+1}^{j+1} = \alpha\left(Q_{i+1}^{j+1}\right)^{\beta} \quad (20)$$

$$A_{i+1}^{j} = \alpha\left(Q_{i+1}^{j}\right)^{\beta} \quad (21)$$

Substituting equations (20) and (21) into (19):

$$\frac{\Delta t}{\Delta x} Q_{i+1}^{j+1} + \alpha\left(Q_{i+1}^{j+1}\right)^{\beta} = \frac{\Delta t}{\Delta x} Q_i^{j+1} + \alpha\left(Q_{i+1}^{j}\right)^{\beta} + \Delta t\left(\frac{q_{i+1}^{j+1} + q_{i+1}^{j}}{2}\right) \quad (22)$$

This equation is sorted so that the unknown flow Qi+1j+1 is on the left-hand side and the other known quantities are on the right-hand side. This is a nonlinear equation for $Q_{i+1_{j+1}}$ so it needs to be solved numerically. The block diagram below applies Newton's iterative method. The linear model which is developed into the nonlinear model is represented in the initial estimation block using the linear estimator 20 as shown below in Figure 3.

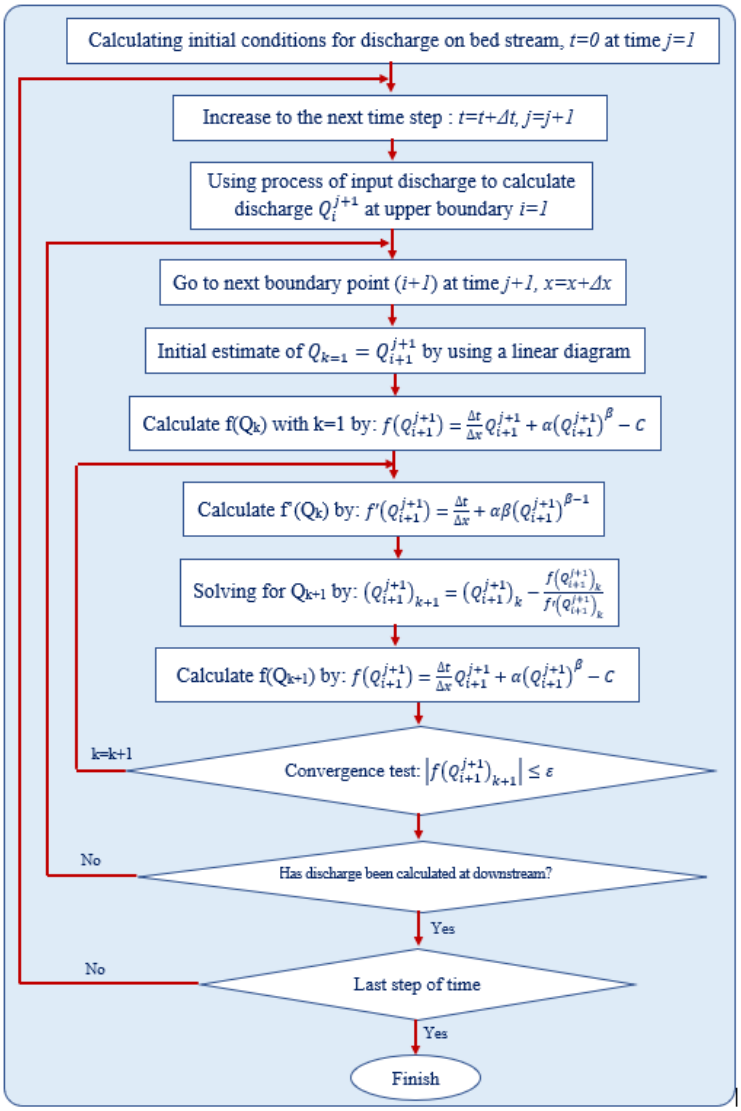

Figure 3. Block diagram for calculating nonlinear kinematic waves.

$$C = \frac{\Delta t}{\Delta x} Q_i^{j+1} + \alpha (Q_{i+1}^{j})^{\beta} + \Delta t \left(\frac{q_{i+1}^{j+1} + q_{i+1}^{j}}{2} \right) \quad (23)$$

Then a residual error $f(Q_i+1_j+1)$ is determined by equation (22).

$$f(Q_{i+1}^{j+1}) = \frac{\Delta t}{\Delta x} Q_{i+1}^{j+1} + \alpha (Q_{i+1}^{j+1})^{\beta} - C \quad (24)$$

The first derivative of $f(Q_i+1_j+1)$ is as follows:

$$f'(Q_{i+1}^{j+1}) = \frac{\Delta t}{\Delta x} + \alpha\beta (Q_{i+1}^{j+1})^{\beta-1} \quad (25)$$

The goal is to find Q_i+1_j+1 to force $f(Q_i+1_j+1)$ to zero. Using Newton's iterative method and the iteration steps k = 1, 2, 3, ...

$$(Q_{i+1}^{j+1})_{k+1} = (Q_{i+1}^{j+1})_k - \frac{f(Q_{i+1}^{j+1})_k}{f'(Q_{i+1}^{j+1})_k} \quad (26)$$

The convergence criterion for the iterative process is:

$$\left| f(Q_{i+1}^{j+1})_{k+1} \right| \le \varepsilon \quad (27)$$

Estimating the initial value of Q_i+1_j+1 in each iteration has an important influence on the convergence of the diagram. One approach is to use the solution of the linear diagram,

Equation (18) as the first approximation of the nonlinear diagram. Li Simons and Stevens (1975) [1], after conducting stability analysis, showed that the diagram using equation (22) is an unconditional stability scheme and can use values of Δ_t/Δ_x over a fairly wide range without creating large errors in the shape of the discharge process curve.

The model after programming is tested with data in example 9.6.1 in the Applied Hydrology textbook by Vente Chow [1]. The results of the model coincide with the calculation results of the above example, the calculated correlation is shown in Figure 4.

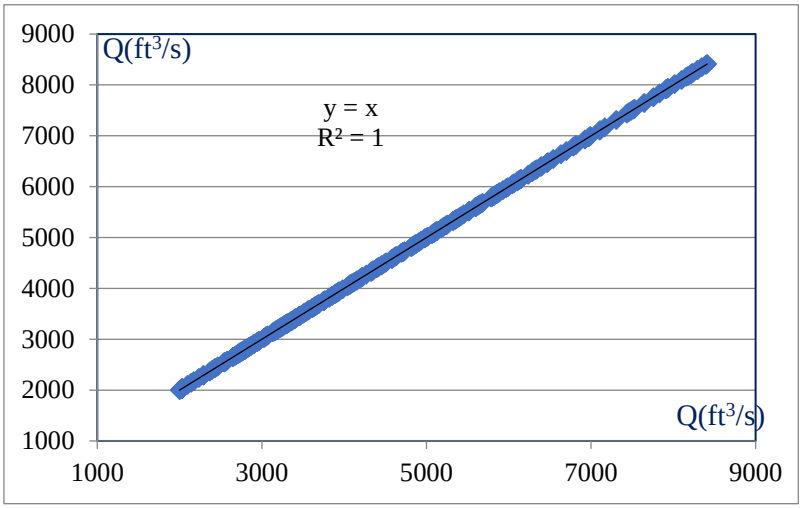

Figure 4. Correlation of results calculated by program and by Vente Chow.

3. Results and discusion

3.1. Models set up for flow simulation on Tra Khuc river

Input data for the Mike 11 and kinematic wave models are taken at the Son Giang hydrological station. The joining boundaries of the To, Son Thanh, Tam Rao, Ham Giang rivers; the position of the boundaries is shown in the model hydraulic diagram Mike 11 (Figures 6 and 8). The study uses floods that occurred from November 22 to 27, 2011 and from September 13 to 15, 2013 in the Tra Khuc river basin.

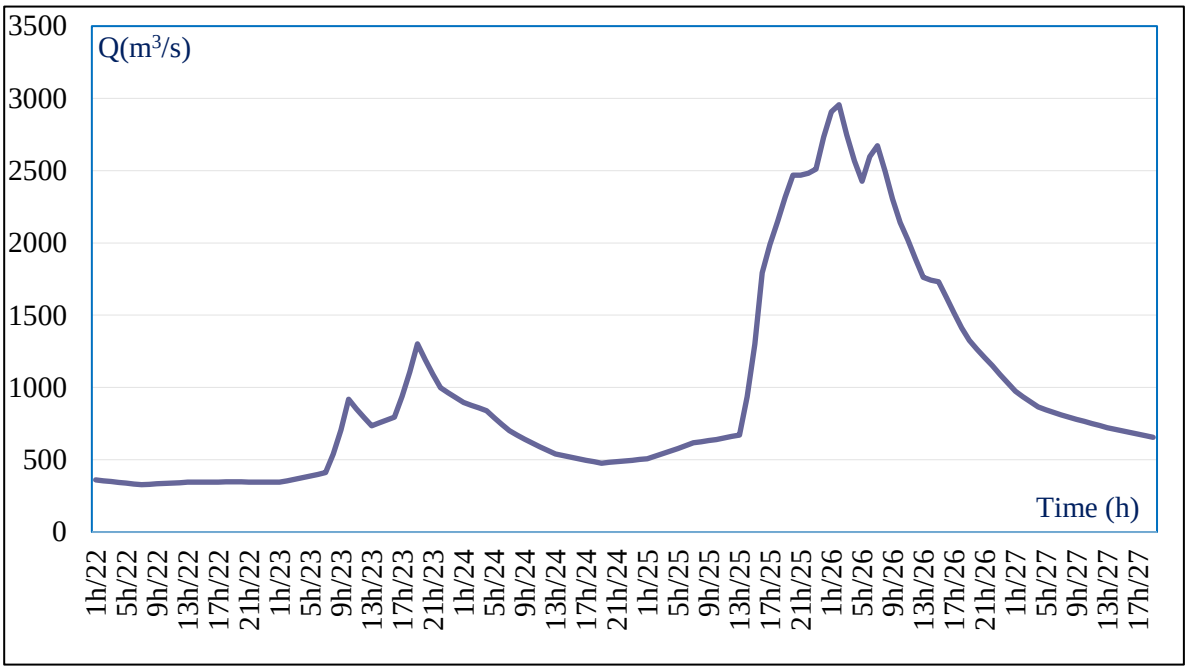

Figure 5. Discharge of Son Giang hydrological station from November 22 to 27, 2011.

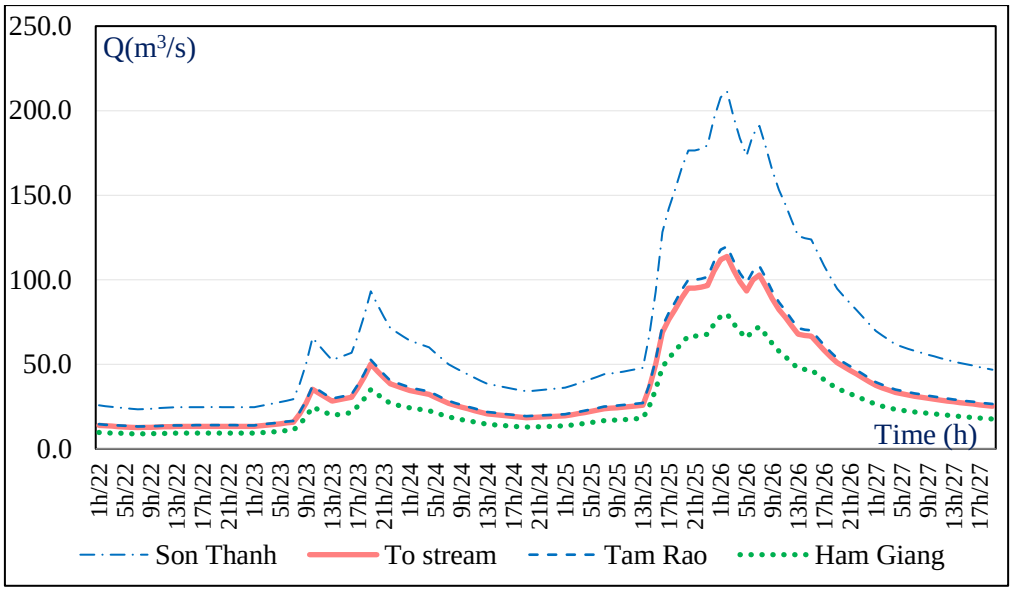

Figure 6. Entry discharge from November 22 to 27, 2011.

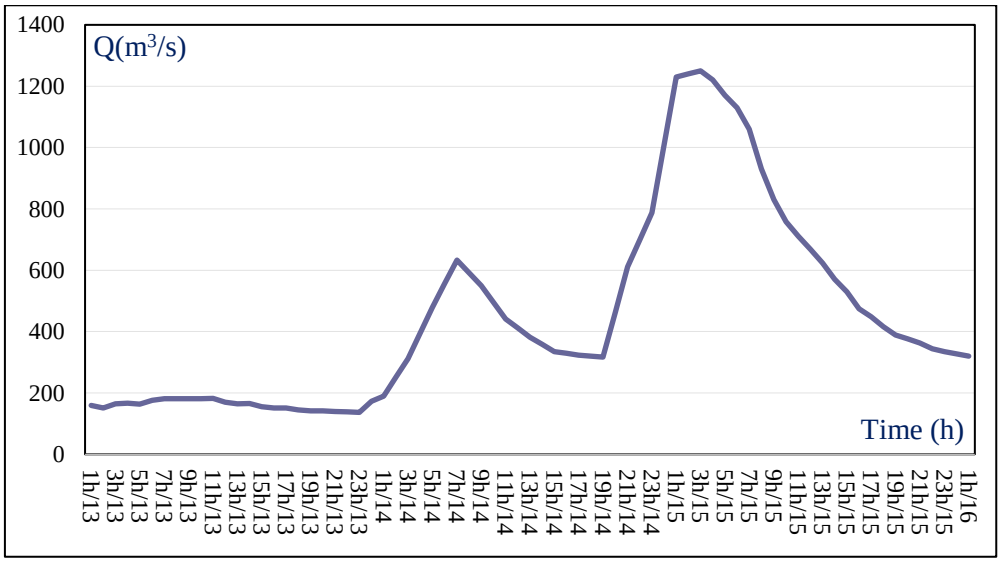

Figure 7. Discharge of Son Giang hydrological station from September 13 to 15, 2013.

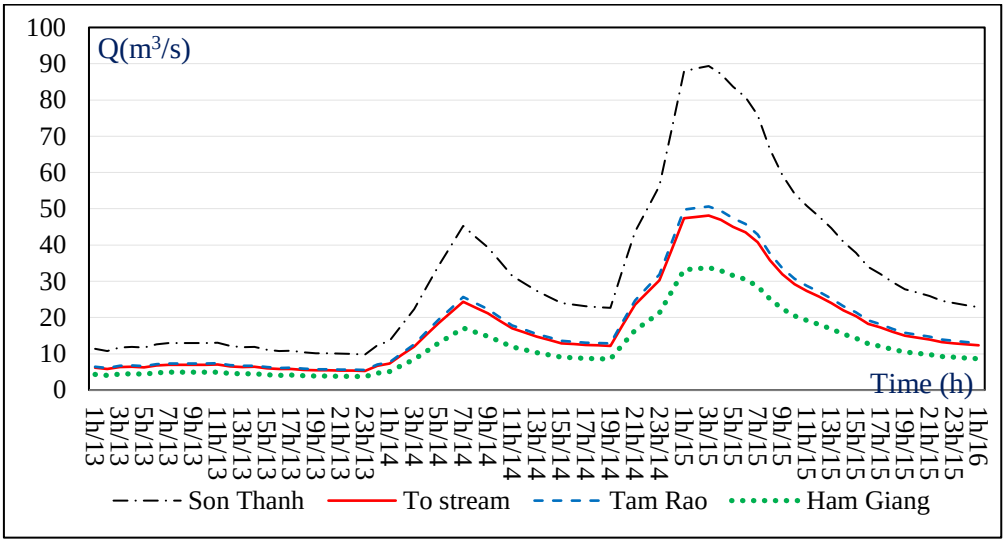

Figure 8. Discharge of Son Giang hydrological station from September 13 to 15, 2013.

3.2. One−dimensional kinematic wave model

The nonlinear one−dimensional kinematic wave model, after developing, is simulated and tested for flow on the Tra Khuc river from the Son Giang hydrological station to the outlet. The initial conditions are determined as follows: the width of the river sections is from 400 to 2200m, the slope of the river sections is from 1 to 5% and is calculated from the cross−sectional data. The hydraulic network is the same as the data in the Mike 11 model set up below, with a river length of 67,030m, 718 nodes, the simulation time step of 30 seconds, the input flow process at Son Giang station is shown in Figures 5 and 7, the Manning roughness coefficient for Tra Khuc River is from 0.032−0.037. The amount of accession to the middle zone at the tributaries of To, Son Thanh, Tam Rao and Ham Giang rivers is zoomed in proportion to the area with the Son Giang hydrological station shown in Figures 6 and 8.

The Nash indicator of the simulation results of the nonlinear one−dimensional dynamic wave model using at Tra Khuc hydrological station for the flood occurring from November 22 to 27, 2011 is 0.89. The similar simulation is implemented to the flood that occurred from 13 to 15 September 2013 which brings the Nash indicator of 0.85.

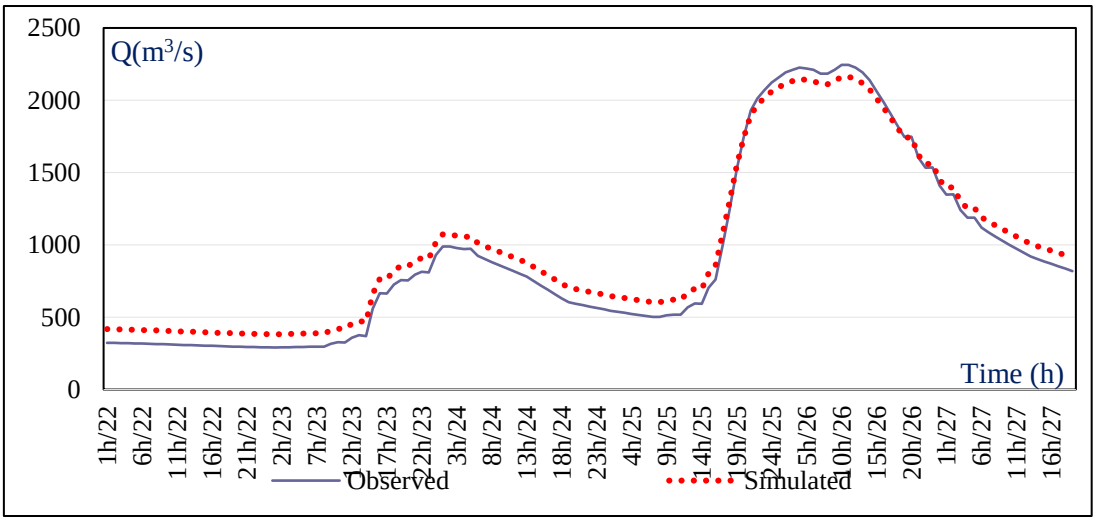

Figure 9. Observed and simulated discharge by kinematic wave model at Tra Khuc hydrological station during the flood from November 22 to 27, 2011.

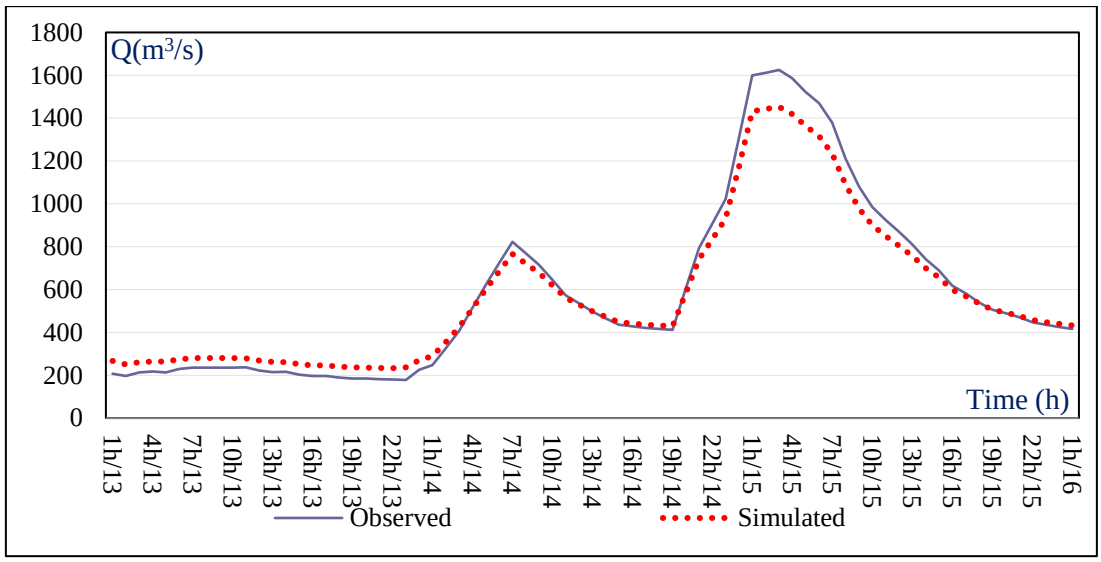

Figure 10. Observed and simulated discharge by kinematic wave model at Tra Khuc hydrological station during the flood from 13 to 15 September 2013.

3.3. Mike 11 model establishment

The river network is digitized from a map of 1/10,000 scale, using the Quang Ngai reference system with 108-degree zone 3 and then updating this reference system into the Mike 11 model. Updating 68 national standard elevation cross-sections from the Son Giang hydrological station to the sea mouth. The upper boundary is the discharge process curve at Son Giang which is shown in Figures 5 and 7, the lower boundary is the tidal water level process line. Joining the middle zone includes 4 tributaries of rivers and streams whose discharge process lines are shown in Figures 6 and 8. Manning roughness coefficients of sections on Tra Khuc river are determined as the Kinematic wave model established above, with values of river bed and banks from 0.032−0.037.

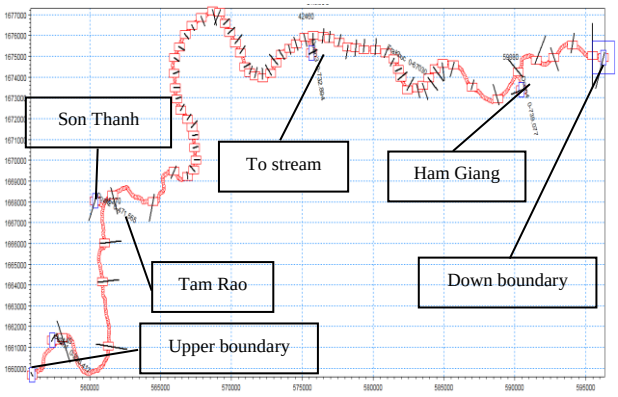

Figure 11. Hydraulic diagram at downstream of Tra Khuc river in Mike 11 model.

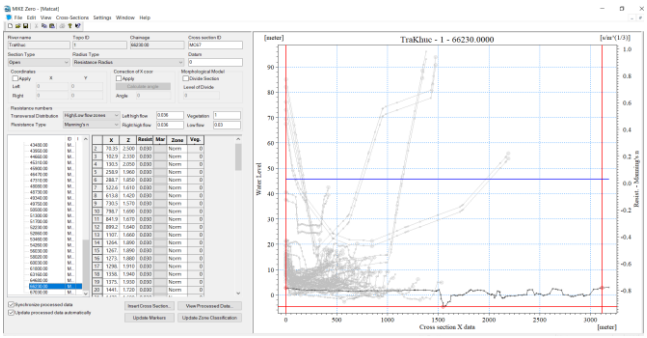

Figure 12. Cross section of Tra Khuc river downstream in Mike 11 model.

The tidal level is used as the lower boundary for the Mike 11 model, there is no tidal station at the outlet of Tra Khuc River, so the tidal boundary is determined by the tidal calculator in the Mike 21 Toolbox. The set of tidal parameters is taken from the parameter map of DHI with a resolution of 0.25° × 0.25°. The tidal water level at the mouth of Tra Khuc river is calculated at 15.15°N and 108.94°E, the parameters are shown in the figure 13 [3].

Number of 8 ...

	Name	Amplitude	Phase
1	M2	0.201654	77.01816
2	S2	0.0681956	109.7103
3	K1	0.3098014	187.8476
4	O1	0.292512	146.9564
5	N2	0.04320046	48.19024
6	P1	0.1018413	181.6318
7	K1	0.01616075	107.6501
8	Q1	0.05626091	153.8448

Figure 13. Tide model parameter set.

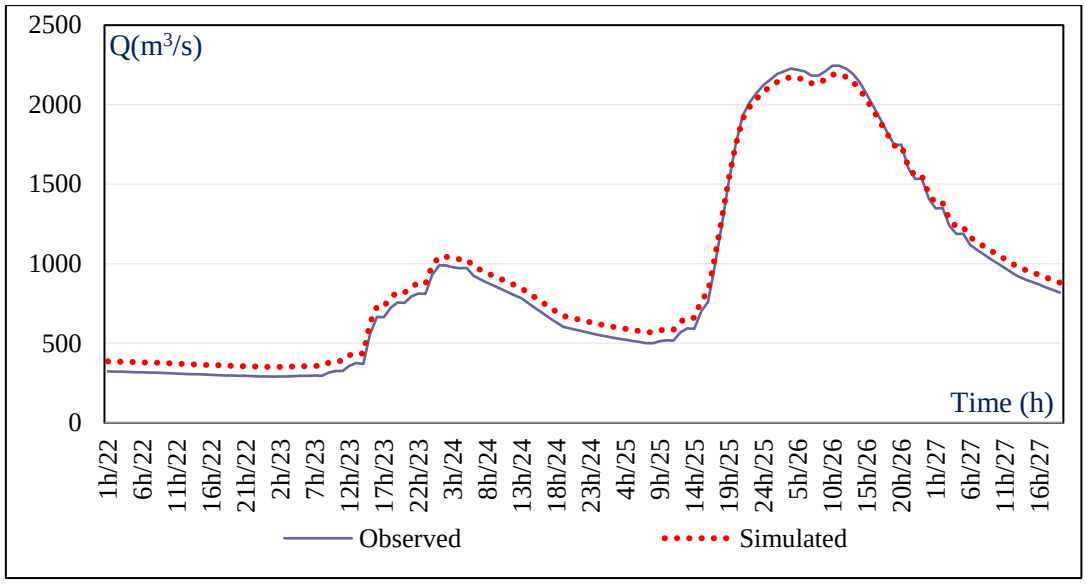

Figure 14. Observed and simulated discharge by Mike 11 model at Tra Khuc hydrological station during the flood from November 22 to 27, 2013.

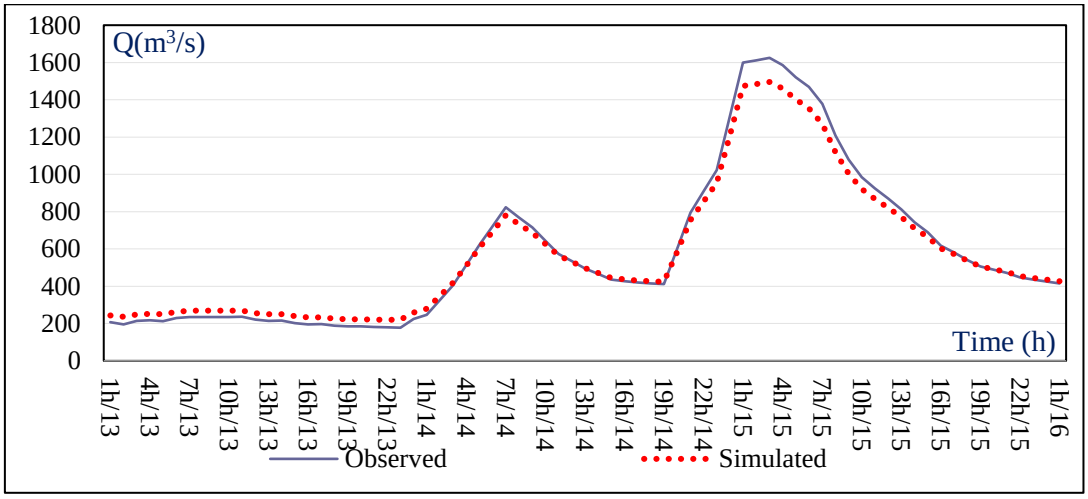

Figure 15. Observed and simulated discharge by Mike 11 model at Tra Khuc hydrological station during the flood from September 13 to 15, 2013.

The Mike 11 simulation results shows that the Nash indicator at Tra Khuc hydrological station for the flood occurring from November 22 to 27, 2011 is 0.92. Similarly, the Mike 11 simulation for the flood occurring from September 13 to 15, 2013 shows the Nash indicator of 0.88.

4. Conclusions

- The dynamic wave models has a wider simulation scope than the kinematic wave models but needs the cross-sectional data; therefore, applicability is limited in the absence of cross-sectional data.

- The simulation quality of the dynamic wave model is not much higher than that of the kinematic wave model in the upstream and middle flow where the lack of cross-sectional data is very common. Therefore, the Kinematic wave model is more likely to be applicable in mountainous rivers.

- The kinematic wave model does not use the lower boundary, so it is more suitable for forecasting than the dynamic wave model.

Author contribution statement: Constructing research idea: B.V.C., C.T.Van.; Select research methods: B.V.C., C.T.Viet., V.T.V.A., C.T.Van, T.D.D.; Take sample and sample analysis, data processing: N.H.T., N.H.A., C.T.Viet., T.D.D, V.T.V.A.; Writing original draft preparation: T.D.D, C.T.Van., B.V.C.; Writing review and editing: C.T.Van., V.T.V.A.

Competing interest statement: The authors declare that this article was the work of the authors, has not been published elsewhere, has not been copied from previous research; there was no conflict of interest within the author group.

References

1. Chanh, B.V.; Anh, T.N.; Huấn, N.Q.; Hoan, N.T. Testing the integration of Tank model and One-dimensional dynamic wave for medium-term hydrological forecasting in Ba river basin. *VN J. HydroMeteorol*. **2021**, *722*, 38−48.
2. Chanh, B.V.; Anh, T.N.; Anh, L.T. Development of nonlinear one-dimensional dynamic wave model for river network and experimental application for Dinh Ninh Hoa river basin. *VN J. HydroMeteorol*. **2017**, *684*, 41−45.
3. Chanh, B.V.; Anh, T.N.; Anh, L.T. Simulation of river flow using nonlinear 1D-kinetic waves. *J. Sci. VNU Hanoi*: *Earth. Environ. Sci*. **2016**, *32(3S)*, 14−19.
4. Lighthill, M.J.; Whitham, G.B. A Theory of Traffic Flow on Long Crowded Roads. Proceedings of the Royal Society of London A, 1955, 229, 317-345. http://dx.doi.org/10.1098/rspa.1955.0089.
5. Weinmann, P.E.; Laurenson, E.M. Approximate flood routing methods: a review. *J. Hydraul. Div. ASCE* **1979**, *105(12)*, 1521–1526.
6. Cunge, J.A. On The Subject Of A Flood Propagation Computation Method (Muskingum 2057 Method). *J. Hydraul. Res.* **1969**, *7*, 205–230.
7. Woolhiser, D.A. Simulation of unsteady overland flow. In: Mahmood, K.; Yevjevich, V (Editors), Unsteady Flow in Open Channels, Vol. II. Water Resources Publication, Fort Collins, CO, 1975, pp. 502.
8. Dawdy, D.R. et al. User's guide for distributed routing rainfall-runoff model U.S. *Geol. Surv. Water Resour. Invest.* **1978**, 78–90.
9. Jaccvkis, P.M.; Tabak, E.G. A Kinematic Wave Model for Rivers with Flood Plains and Other Irregular Geometries. *Math. Comput. Modell.* **1996**, *24(11)*, 1−21.
10. Nwaogazie, I.L. Kinematic-wave simulation program for natural rivers. *Adv. Eng. Software* **1978**, *8(1)*, 32–45.
11. Huang, H. Finite Difference Solutions of Incompressible Flow Problems with Corner Singularities. *J. Sci. Comput.* **2000**, *15(3)*, 265–292. Doi:10.1023/A:1011138516712
12. Henderson. Open chanel flow. (Eds.), Macmillan puplising Co., INC., 1966, pp. 273.
13. Woolhiser, D.A.; Liggett, J.A. Unsteady, one-dimensional flow over a plane–The rising hydrograph. *Water Resour. Res.* **1967**, *3(3)*, 753–771.
14. Hubert, J.M.S.; Fahmy, H.; Lamagat, J.P. A composite hydraulic and statistical flow-routing method. *Water Resour. Res.* **1993**, *29(2)*, 413–418. Doi:10.1029/92WR01767.
15. Anh, L.T.; Son, N.T. Applying the finite element hydrodynamic model to describe the basin flow process. *VNU J. Sci.: Nat. Sci. Technol.* **2003**, 19(1S), ISSN 2588-1140.
16. Ven, T.; David, R.M.; Larry, W.M. Applied Hydrology. New York: McGraw−Hill, 1988.
17. Chanh, B.V. Research for improvement of marine models to simulate and precaution of fluids for water basins without data − application to the south central region. PhD thesis, 2022.
18. Cuong, N.T.; Phương, T.T. Forecasting the discharge into Hoa Binh reservoir by applying the connecting model MARINE − IMECH1D. *VN J. Mech.* **2008**, *30(3)*, 149−157.

19. Chanh, B.V.; Anh, T.N. Integrated hydrological forecasting model set of Tra Khuc river basin. *J. Sci. VNU Hanoi*: *Earth Environ. Sci*: *Earth Environ. Sci.* **2016**, *32(3S)*, 20−25.
20. Chanh, B.V.; Anh, T.N.; Truong, N.H. Recovering data of Cai Phan Rang river by the method of integrating models. *VN J. Hydrometeorol.* **2016**, *668*, 39−44.
21. Chanh, B.V.; Anh, T.N. Testing the integration of MARINE model and one-dimensional dynamic wave model on Cai river basin in Nha Trang. *J. Clim. Change. Sci*. **2020**, *14*, 45−55.
22. Fattah, M.A.; Kantoush, S.A.; Saber, M.; Sumi T. Rainfall runoff Modeling for extrame flash floods in Wadi Samail (Oman). *J. Jpn. Soc. Civ. Eng. Ser. B1* **2018**, *74(5)*, I_691−I_696.
23. Ify, L.N. Kinematic−wave simulation program for natural rivers. *Adv. Eng. Software*, **1986**, *8(1)*, 32−45.
24. Lai, H.V.; Diep, N.V.; Cuong, N.T.; Phong, N.H. Coupling hydrological–hydraulic models for extreme flood simulating and forecasting on the North Central Coast of Vietnam. *WIT Trans. Ecol. Environ.* **2009**, *124*, 113−123.
25. Miller, J.E. Basic Concepts of Kinematic−Wave Models, U.S. *Geol. Surv. Prof. Pap*. **1984**, pp. 1302.
26. Nghi, V.V.; Lam, H.B.N.; Anh T.P.; Van, C.T. Development and Application of a Distributed Conceptual Hydrological Model to Simulate Runoff in the Be River Basin and the Water Transfer Capacity to the Saigon River Basin – Vietnam. *J. Environ. Sci. Eng.* **2020**, *A9*, 1−12.
27. Riccardo, R.; Giacomo, B.; Thomas, M.O. GEOtop: A Distributed Hydrological Model with Coupled Water and Energy Budgets. *J. Hydrometeorol*. **2006**, *7(3)*, 371−388.
28. Robert, M.; Jahannes, J.D. Introduction and apolication of kinematic wave routing techniues using HEC−1, Hydrologic Engineering Center, Us Army Corps of Engineers, 1993.
29. Satish, B.; Vasubandhu, M. Evaluation of dynamically downscaled reanalysis precipitation data for hydrological application. *Hydrol. Process* 2013. http://wileyonlinelibrary.com.
30. Simons, D.B.; Li, R.M.; Stevens, M.A. Development of models for prediction water and sediment routing and yield from storms on small watershed. The University of Michigan, 1975.
31. Danish Hydraulic Institute. Mike Zero Manuals, Hørsholm, Denmark, 2016.
32. MKE 21 Toolbox Reference Manual, DHI Software, 2011.

VIETNAM JOURNAL OF HYDROMETEOROLOGY

Research Article

Assessing surface water quality of main rivers in Binh Thuan province by WQI index and proposing solutions to protect water resources

Huynh Phu[1*], Nguyen Thanh Do[2], Huynh Thi Ngoc Han[3], Tran Thi Minh Ha[4]

[1] HUTECH University; h.phu@hutech.edu.vn
[2] Department of Natural Resources and Environment Binh Thuan Province; nthanhdo160@gmail.com
[3] Hochiminh City University of Nature Resources and Environment; htnhan_ctn@hcmunre.edu.vn
[4] Tay Nguyen University, Buon Ma Thuot – Dak Lak, ttmha@ttn.edu.vn

*Correspondence: htnhan_ctn@hcmunre.edu.vn; Tel.: +84–975397953

Received: 5 October 2022; Accepted: 23 December 2025; Published: 25 December 2022

Abstract: The study was conducted to evaluate 5 main river basins: Long Song River, Luy River, Cai Phan Thiet River, Ca Ty River and Phan River in Binh Thuan province has a great impact on the province's socio–economic development. By method of survey, sampling and analysis of physico–chemical parameters and WQI method with hydrological regimes, typical minimum flow, the research has carried out the following contents: (1) An overview analysis of the water quality situation in the study area in the years 2018–2020; (2) Calculating the WQI index to determine the overall status of the water environment of 5 river basins; (3) Determine the environmental flow that needs to be maintained in the river to ensure the daily activities and production of people in the area. The research results have determined the current status of the water environment in rivers and canals and assessed the responsiveness of water sources to socio–economic activities in the locality. From there, propose solutions to effectively use surface water in river basins of Binh Thuan province in the direction of sustainable development.

Keyword: Hydrological mode; Surface water quality; The main rivers of Binh Thuan; WQI index.

1. Introduction

Binh Thuan province is one of the arid regions of Vietnam [1]. Binh Thuan is also a province with quite developed agro-forestry and aquaculture industries. The current situation of drought and water shortage is complicated, which has reduced crop productivity and greatly affected people's lives. In addition to economic achievements, the regional water environment has been affected by increasing agricultural, industrial and domestic waste [2–3]. The problem of water pollution is a global problem, not just one country, or any one territory. Therefore, research and finding solutions to protect water resources are always focused. To take specific measures to protect water resources, it is essential to assess the current state of water quality. Currently, there are many ways to assess water quality, such as: modeling, environmental monitoring, WQI water quality index, etc [4–7]. In Vietnam, the application of WQI to water quality assessment is quite popular [8–9]. The study was carried out in 5 main rivers: (1) Long Song River, (2) Luy River, (3) Cai Phan Thiet River, (4) Ca Ty River, (5) Phan River. These are rivers that have a great impact on the socio–economic development of the province.

The geographical location of river basins stretches across the province, including most cities, towns and townships such as: Phan Thiet City, Ham Thuan Nam district, Ham Thuan Bac district, Tuy Phong district, Bac Binh district, Ham Tan (part of townships and communes: Tan Nghia, Song Phan, Tan Phuc), Lagi town (part of Tan Hai and Tan Tien communes), Tanh Linh district (part of Duc Binh and Duc Thuan, Suoi Kiet). Consequently, the natural and socio–economic conditions of Binh Thuan province are also the natural and socio–economic conditions of the river basins [10–11]. The scientific basis for assessing surface water quality in the main river basins of Binh Thuan province includes: physicochemical parameters, water quality index (WQI) and minimum flow, hydrometeorological factors of the water environment to ensure water quality for the existence and development of ecosystems and human activities.

2. Materials and methodology

2.1. Study area

Binh Thuan province has a geographical location [12]: The Northeast and the North borders Ninh Thuan province; The North and the Northwest borders Lam Dong province; The West borders Dong Nai province; The Southwest borders Ba Ria–Vung Tau province; The East and Southeast borders the East Sea (Figure 1).

Figure 1. Location of the study area.

2.2. Study methods

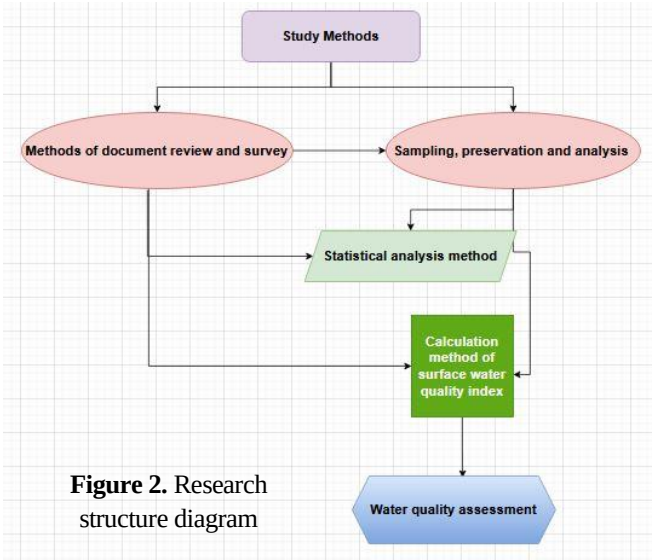

Figure 2. Research structure diagram

2.2.1. Methods of document review and survey

This method will inherit information from previous documents, investigation results or related studies to analyze and synthesize necessary information.

2.2.2. Methods of sampling, preservation and analysis of the physicochemical index composition of the sample

Sampling surface water according to Vietnam Standard (TCVN) 5996:1995 – "Water quality, sampling–Guidelines for sampling in rivers and streams". 1000 ml polyethylene, polypropylene or polycarbonate bottles for sampling were used. The dark and signed glass flasks were sterilized before sampling for microbiological analysis. Each flask was taken about 250 ml.

2.2.3. Statistical analysis method

Selectively collect and inherit documents, materials and results of domestic and international research works related to research contents applicable to river basins.

2.2.4. Calculation method of surface water quality index

The Water Quality Index (WQI) is an index calculated from the observed physicochemical parameters of water quality. The WQI is used to provide a quantitative description of water quality and its usability; represented by a scale. The WQI value scale is divided into certain intervals, each of which corresponds to a certain water quality rating. The study used the calculation of water quality index according to No. 1460/QD–TCMT dated November 12, 2019.

3. Results and discussion

3.1. Physicochemical parameters of water quality in rivers

On the basis of analysis of physicochemical criteria and comparison with national standards for each water source QCVN 08–MT:2015/BTNMT (abbreviated QC.08), the quality of water environment is assessed through physical and chemical parameters: chemical oxygen demand (COD), biological oxygen demand (BOD), dissolved oxygen (DO), Total suspended solids (TSS), Cl^-, SO_4^{2-}, PO_4^{3-}, F^-, Fe^{2+}, Mn^{2+}, Nitrogen compounds, etc.

3.1.1. Long Song River

Sampling water at 8 sites (NM–LS1–8), analysis results are as follows:

pH: The results of pH measurement at sampling sites in the Long Song River basin ranged from 7.76 to 8.35 mg.l^{-1}. The pH value at all sites reached the abbreviation QC.08–A2 and the pH value is suitable for all uses in the river basin (Figure 3a).

DO: The results of DO analysis at sampling sites in the Long River basin ranged from 4.26 to 5.18 mg.l^{-1}. In areas serving the purpose of domestic water supply: DO content measured at site NM–LS1 did not meet QC.08–A2, 0.95 times lower than the allowed standard. In areas serving irrigation and irrigation purposes: the measured DO content at all sites met QC.08, level B1 (Figure 3b).

BOD_5 and COD: The measured values of BOD_5 and COD ranged from 09–25 mg.l^{-1} and 17–47 mg.l^{-1}. In areas serving the purpose of domestic water supply: the measured organic matter content did not meet QC.08–A2, BOD_5 exceeded the permitted standard by 5.00 times, COD exceeded the permitted standard 3.13 times. In areas serving irrigation and irrigation purposes: the measured organic matter content reached QC.08–B1 (Figures 3c–3d).

TSS: The results of TSS analysis have shown that there are uneven fluctuations in the river basin. TSS values ranged from 05–132 mg.l^{-1}. The TSS values were particularly high

at sites NM–LS5, NM–LS8. In areas serving the purpose of domestic water supply: TSS value reaches QC.08–A2. In areas serving irrigation and irrigation purposes: TSS content in most sites (05/07 locations) reached QC.08 – B1. Particularly at sites NM–LS5 and NM–LS8, TSS content exceeded QC.08–B1 standards by 1.40 and 3.30 times, respectively (Figure 3e).

Coliform: According to analysis results, Coliform value ranged from 20–2400 MPN.100ml^{-1}. Coliform values at all sites reached QC.08–A2. The Coliform content is suitable for all used purposes in the river basin (Figure 2f).

Phosphate (P–PO_4^{3-}), Ammonium (NH_4^+–N): According to the analysis results, the Phosphate (P–PO_4^{3-}) and Ammonium (NH_4^+–N) values fluctuated in the range of 0.019–0.048 mg.l^{-1} and 0.047–0.184 mg.l^{-1}, respectively. Phosphate and Ammonium values at all sampling sites (08/08 sites) in the Long Song River basin reached QC.08–A2. The nutrient content is suitable for all used purposes in the river basin (Figures 3g–3h).

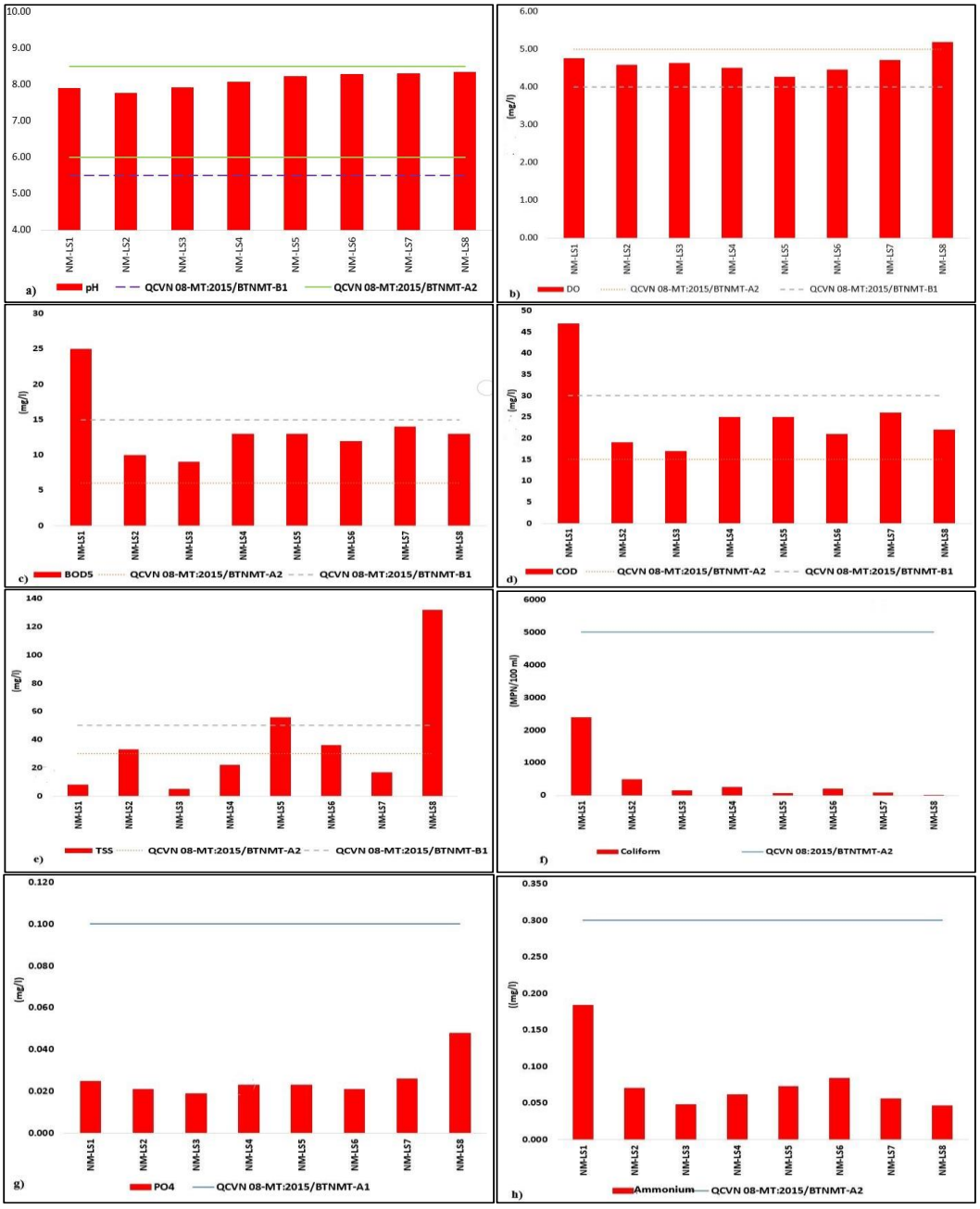

Figure 3. Measured values of water quality parameters at sampling sites on Long Song River basin: (a) pH parameter; (b) DO parameter; (c) BOD_5 parameter; (d) COD parameter; (e) TSS parameter; (f) Coliform parameter; (g) Phosphate parameter; (h) Ammonium parameter.

3.1.2. Luy River basin

Water samples were taken on the Luy River at 20 sites; (NM–L1–20). The samples were analyzed for physicochemical parameters, following results:

pH: According to the analysis results, the pH at the sampling sites on the Luy River basin ranged from 7.02 to 8.45 mg.l^{-1}. The pH value at all surface water sampling sites for domestic water supply purposes reached QC.08–A2. The pH values at all sampling sites of surface water for irrigation and irrigation purposes reached QC.08–B1 (Figure 4a).

DO: According to the analysis results, the DO concentration at sampling sites in the Luy River basin ranged from 4.52 to 5.27 mg.l^{-1}. In areas serving domestic water supply purposes: 10/14 samples did not meet QC.08, level A2. The DO value at sites NM–L2, NM–L3, NM–L6, NM–L7, NM–L8, NM–L10 and NM–L14 was lower than the allowed standard from 0.90 to 0.99 times, lowest at NM–L13–downstream of Ca Giay Lake. In areas for irrigation and irrigation purposes: DO values at all sampling sites met QCVN 08–MT:2015/BTNMT, level B1 (Figure 4b).

BOD_5 and COD: According to the analysis results, BOD_5 and COD values ranged from 07–20 mg.l^{-1}and 13–38 mg.l^{-1}, respectively. In areas serving domestic water supply purposes: the organic matter content in all sites did not meet QCVN 08–MT:2015/BTNMT–A2, the BOD_5 content exceeded the allowable standard from 1.5 to 2.83 times, the COD value exceeded the allowable standard from 1.07 to 2.07 times. In areas serving irrigation and irrigation purposes: organic matter content in most sites (04/06 sites) reached QC.08–B1. BOD_5 values at sites NM–L18 and NM–L19 exceeded the allowable standards by 1.07 and 1.33 times, respectively; COD values at sites NM–L18, NM–L19 exceeded allowable standards by 1.03 and 1.27 times, respectively (Figures 4c–4d).

TSS: The TSS value fluctuated at sites on the river basin, ranging from 04–273 mg.l^{-1}. This is consistent with the fact that the further downstream, the higher the concentration of suspended solids in the water. In which, most of the sites (16/20 sites) on the Luy River had TSS values of QC.08–A2. However, some sites at the downstream end that are in residential areas (NM–L17 and NM–L20) had significantly increased TSS values compared to other sites in the basin and all exceeded QC.08–B1 from 1.12 to 5.46 times (Figure 4e).

Coliform: According to analysis results, Coliform value ranged from 17–170 MPN.100ml^{-1}. All values of Coliform at the sites reached QC.08–A2. Therefore, the Coliform content is suitable for all water uses. By comparing the analytical criteria with the permitted standards, it shows that the water quality in the upstream and midstream on the Luy River has signs of high organic pollution, affecting the water resources and purposes of use. Further down the river, the concentration of suspended solids increases. The high concentration of pollutants in this area may be due to the concentration of many production and business activities and daily activities of people in the basin (Figure 4f).

Phosphate ($P–PO_4^{3-}$), Ammonium (NH_4^+–N): According to the analytical results, the Phosphate ($P–PO_4^{3-}$), Ammonium (NH_4^+–N) values fluctuated in the range of 0.018–0.072 mg.l^{-1} and 0.035–0.109 mg.l^{-1}, respectively. All sampling sites (20/20 sites) in Song Luy basin met QC.08–A2. The nutrient content in the river basin is therefore suitable for all used purposes (Figures 4g–4h).

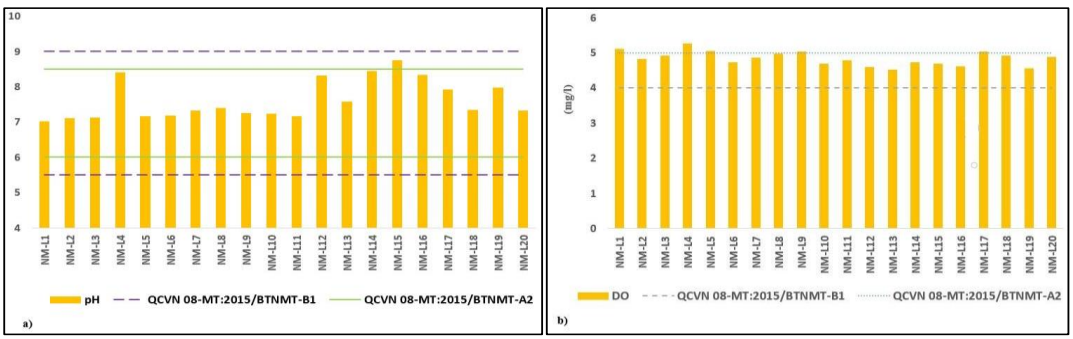

Figure 4. Measured values of water quality parameters at sampling sites on Luy River basin: (a) pH parameter; (b) DO parameter; (c) BOD_5 parameter; (d) COD parameter; (e) TSS parameter; (f) Coliform parameter; (g) Phosphate parameter; (h) Ammonium parameter.

3.1.3. The Cai River basin in Phan Thiet

Water samples were taken on the Cai River in Phan Thiet at 12 sites. The samples were analyzed for physicochemical parameters, following results:

pH: According to the analysis results, the pH at the sampling sites on the Cai River basin in Phan Thiet ranged from 6.71 to 8.41 $mg.l^{-1}$. All pH values at the sites reached QC.08–A2, pH suitable for all purposes on river basin (Figure 5a).

DO: DO at sampling sites on Cai River basin in Phan Thiet ranged from 2.17 to 5.15 $mg.l^{-1}$. In areas that serve the purpose of domestic water supply: DO content only reached QC.08–A2 at site NM–CPT3. In areas that serve irrigation and irrigation purposes: DO in most sites (07/09 sites) met QC.08–B1. Particularly at sites NM–CPT1 and NM–CPT2 that used for irrigation purposes, DO did not meet QC.08–B1 (Figure 5b).

BOD_5 and COD: According to the analysis results, BOD_5 and COD values ranged from 7–20 $mg.l^{-1}$ and 13–38 $mg.l^{-1}$, respectively. In areas serving domestic water supply purposes: the organic matter content in all sitens exceeded QC.08 – A2 from 2.00 to 4.17 times. In areas serving irrigation and irrigation purposes: organic matter content in most sites (07/09 sites) reached QC.08–B1 (Figures 5c–5d).

TSS: According to analysis results, TSS values at surface water sampling sites ranged from 02–235 mg.l^{-1}. TSS value has tended to increase gradually from upstream to downstream. In areas serving the purpose of domestic water supply: TSS values at all sites met QC.08–A2. In areas serving irrigation and irrigation purposes: TSS values exceeded the standard at sites NM–CPT1, NM–CPT2, NM–CPT10, NM–CPT11 and NM–CPT12 from 3.08 to 6.2 times (Figure 5e).

Coliform: According to the analysis results, Coliform values fluctuated unevenly at sampling sites across the basin, ranging from 70–4300 MPN.100ml^{-1}. All sites met QC.08–A2. The Coliform content was suitable for all used purposes on the river basin (Figure 5f).

Phosphate (P–PO_4^{3-}), Ammonium (NH_4^+–N): According to the analysis results, the Phosphate and Ammonium values ranged from 0.008–0.241 mg.l^{-1} and 0.072–0.254 mg.l^{-1}, respectively. In areas serving the purpose of domestic water supply: the content of nutrients in all sites reached QC.08–A2. In areas serving irrigation and irrigation purposes, the content of nutrients and nutrients reached QC.08–B1 (Figures 5g–5h).

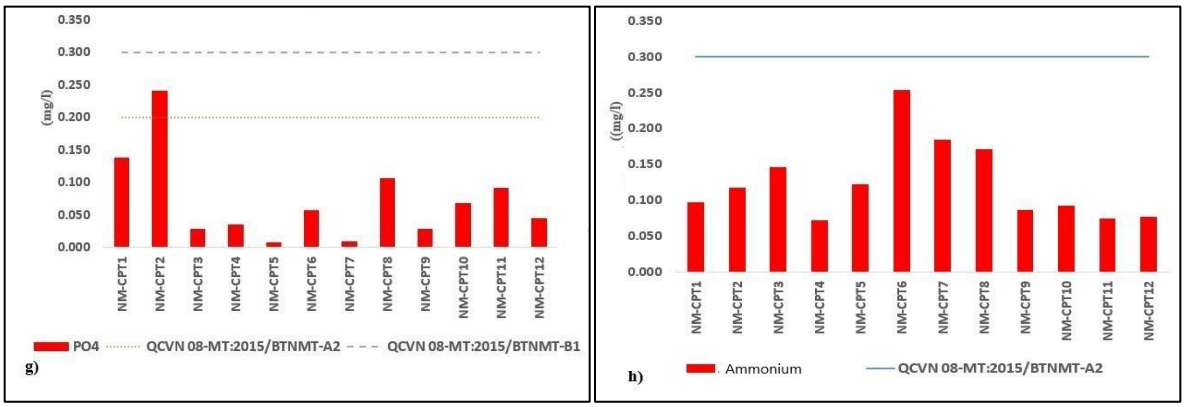

Figure 5. Measured values of water quality parameters at sampling sites on Cai River basin in Phan Thiet: (a) pH parameter; (b) DO parameter; (c) BOD_5 parameter; (d) COD parameter; (e) TSS parameter; (f) Coliform parameter; (g) Phosphate parameter; (h) Ammonium parameter.

Comment: Phan Thiet Cai River is the main river and provides water for production activities in Ham Thuan Bac district, Phan Thiet City; It also regulates the climate to create a landscape for the city center. However, the surface water quality of the Phan Thiet Cai River basin is being polluted by organic matter, with high BOD_5 and COD levels at almost all sites in the river basin, especially in the downstream area. Located in the city center location Phan Thiet City, the downstream area of Phan Thiet Cai River (from the confluence of Suoi Tien, Ben Loi river to Cau Ke bridge area, Phu Hai port) has shown signs of moderate to severe pollution (in terms of organic matter and suspended solids). The water quality in these areas is not suitable for used purposes.

3.1.4. Ca Ty River basin

Water samples were taken on the Ca Ty river at 15 sites. The samples were analyzed for physicochemical parameters, following results:

pH: According to the analysis results, the pH at sampling sites on Ca Ty River basin ranged from 6.56 to 7.77 $mg.l^{-1}$. All sites met QC.08–A2. The pH is suitable for all uses on the river basin (Figure 6a).

DO: According to analysis results, DO at sampling sites on Ca Ty River basin ranged from 1.40 to 5.18 $mg.l^{-1}$. In areas serving domestic water supply purposes: DO values achieved QC.08–A2 at sites NM–CT2, NM–CT8 and NM–CT10 (3/7 sites). In the areas serving irrigation purposes, DO in most of sites (6/8 sites) met QC.08–B1 (Figure 6b).

BOD_5 and COD: According to the analysis results, the BOD_5 and COD values ranged from 10–39 $mg.l^{-1}$ and 18–60 $mg.l^{-1}$, respectively. In areas serving domestic water supply purposes: organic matter content at all sites exceeded QC.08–A2. Specifically, BOD_5 exceeded 2.00 to 2.50 times, COD exceeded 2.08 to 2.75 times. In areas for irrigation purposes, the organic matter content exceeded at sites NM–CT6, NM–CT9, NM–CT11, NM–CT12 (4/8 sites). Specifically, the BOD_5 value exceeded 1.40 to 2.60 times and the COD exceeded 1.03 to 2.00 times (Figures 6c–6d).

TSS: According to the analysis results, the TSS values fluctuated unevenly, ranging from 04–265 $mg.l^{-1}$. In areas serving the purpose of domestic water supply: 03/07 the sites (sites NM–CT1, NM–CT5 and MN–CT10) exceeded QC.08–A2 from 1.60 (NM–CT5) to 5.13 (NM–CT10) times. In areas serving irrigation purposes: most of the TSS values (5/8 sites) exceeded QC.08–level B1 from 2.64 to 5.30 times (Figure 6e).

Coliform: According to the analysis results, the values of Coliform varied unevenly across the basin, ranging from 15–9500 $MPN.100ml^{-1}$. Most of the sites (14/15 sites) met QC.08–A2, suitable for used purposes, especially the NM–CT11 exceeded QC.08–A2 (area for the purpose of landscape conservation) 1.90 times. From the results of the assessment of

each indicator of surface water pollution in the Ca Ty River basin, it has been shown that the water quality is showing signs of organic pollution and suspended solid, especially towards the downstream of the river, from Cau Ca Ty to Phan Thiet Fishing Port, the section from Suoi Cat area, Ong Nhieu bridge flows into Ca Ty River (Figure 6f).

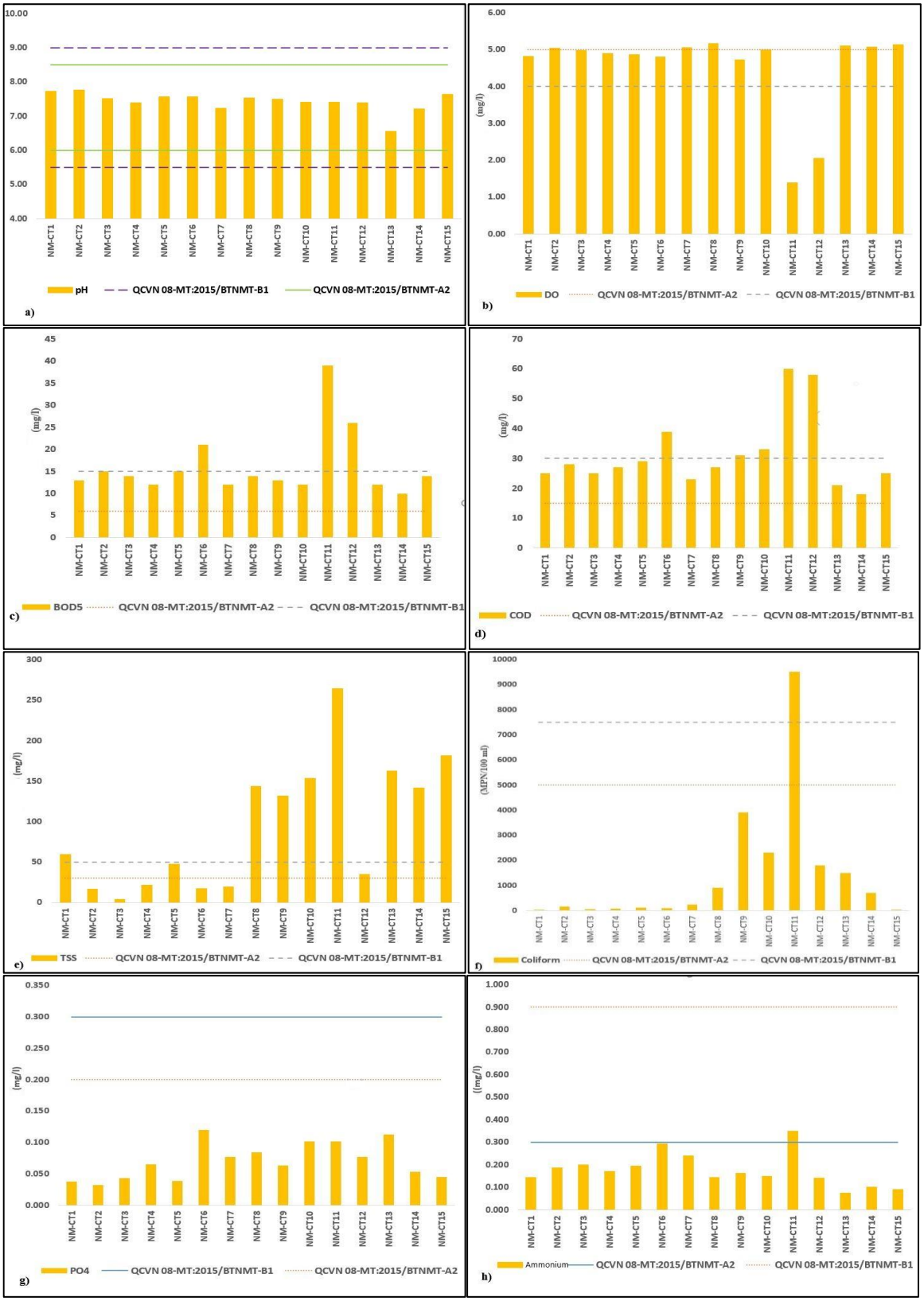

Figure 6. Measured values of water quality parameters at sampling sites on Ca Ty River: (a) pH parameter; (b) DO parameter; (c) BOD_5 parameter; (d) COD parameter; (e) TSS parameter; (f) Coliform parameter; (g) Phosphate parameter; (h) Ammonium parameter.

Phosphate ($P–PO_4^{3–}$), Ammonium ($NH_4^+–N$): According to the analysis results, the Phosphate and Ammonium values ranged from 0.032 to 0.120 mg.l^{-1} and from 0.076 to 0.350 mg.l^{-1}, respectively. In areas serving domestic water supply purposes: the nutrient content at all sites reached QC.08–A2. In areas serving irrigation purposes: the content of nutrients and nutrients reached QC.08–B1 (Figures 6g–6h).

3.1.5. Phan River basin

Water samples were taken on the Phan River at 15 sites. The samples were analyzed for physicochemical parameters, following results:

pH: According to the analysis results, the pH at sampling sites on the Phan River ranged from 7.25 to 8.12 mg.l^{-1}. All sites met QC.08–A2. The pH is suitable for all used purposes on the river basin (Figure 7a).

DO: DO at sampling sites on the Phan River ranged from 4.73 to 5.40 mg.l–1. In areas serving the purpose of domestic water supply: DO values in most sites (02/03 sites) met QC.08–A2. In the areas serving irrigation and irrigation purposes: DO values at all sites met QC.08–B1 (Figure 7b).

BOD_5 and COD: In areas serving domestic water supply purposes: organic matter content at all sites exceeded QC.08–A2; specifically, BOD_5 values exceeded 2.00 to 2.17 times, COD values exceeded 1.47 to 1.67 times. In areas serving irrigation and irrigation purposes: the organic matter content in most sites (10/12 sites) reached QC.08–B1 (Figure 7c–7d).

TSS: According to the analysis results, the TSS values increased gradually from upstream to downstream ranging from 0 –218 mg.l^{-1}. In areas serving domestic water supply purposes: all sites met QC.08–A2. In areas serving irrigation and irrigation purposes: sites from NM–P11 to NM–P15 (05/12) exceeded QC.08–B1 by 1.08 to 4.36 times (Figure 7e).

Coliform: According to analysis results, Coliform values ranged from 26–460 MPN.100ml^{-1}. All sites met QC.08– A1. Coliform within limits for all used purposes on river basin (Figure 7f).

Phosphate ($P–PO_4^{3–}$), Ammonium ($NH_4^+–N$): According to the analysis results, the Phosphate and Ammonium values fluctuated in the range of 0.024–0.153 mg.l^{-1}and 0.058 – 0.237 mg.l^{-1}, respectively. All sampling sites (15/15 sites) on Phan River met QC.08–A2. Nutrient content on river basin is suitable for all used purposes on river basin (Figures 7g–7h).

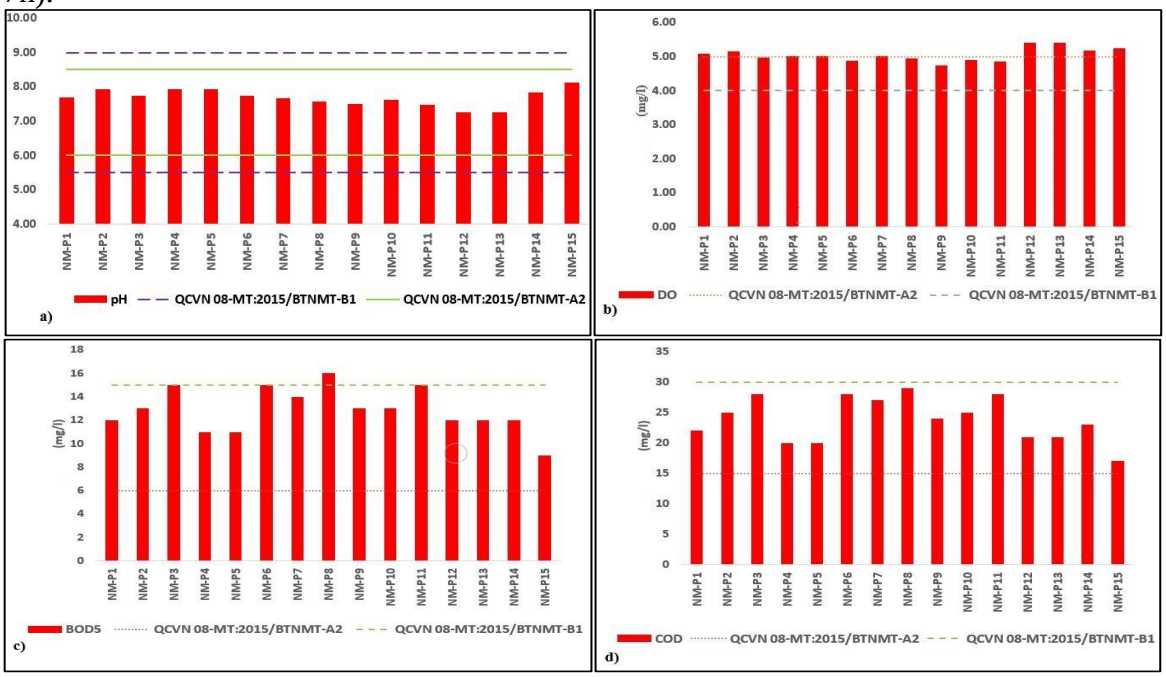

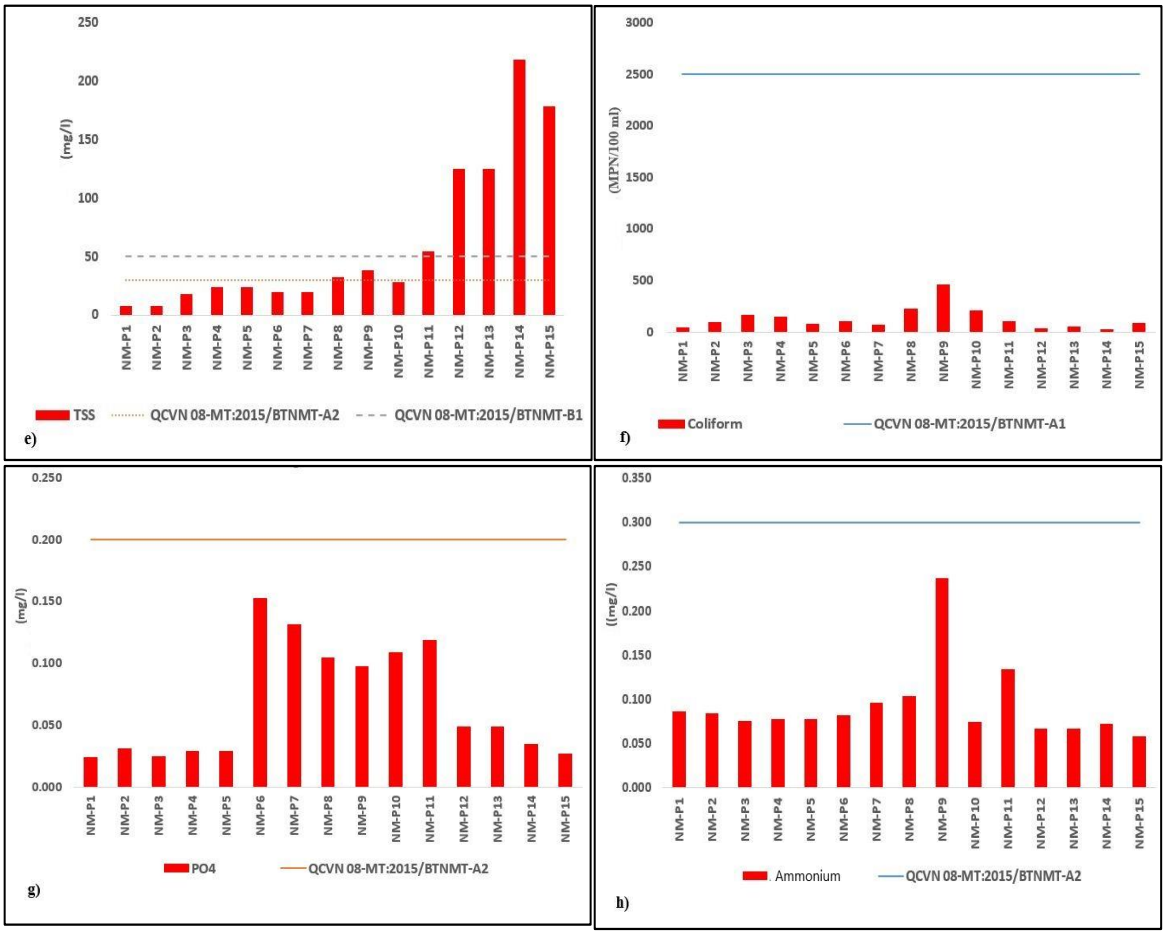

Figure 7. Measured values of water quality parameters at sampling sites on Phan River: (a) pH parameter; (b) DO parameter; (c) BOD_5 parameter; (d) COD parameter; (e) TSS parameter; (f) Coliform parameter; (g) Phosphate parameter; (h) Ammonium parameter.

3.2. Assessment of surface water quality in river basins according to the WQI index

The results of analysis of surface water quality with physicochemical parameters in river basins were carried out in February and March of the years 2018–2020. Analytical indicators: pH, DO, BOD_5, COD, TSS (Total suspended solids), N–NH_4, P–PO_4, Turbidity, Coliforms (the time of sampling surface water on the river system was taken at the same time of measuring and surveying the discharge, in accordance with No. 02/2009/TT–BTNMT of the Ministry of Natural Resources and Environment.

In order to have an objective view of the impacts of the current discharge on the investigated river and stream water quality, the consulting unit conducts an assessment of river water quality for each specific area through the analysis results. surface water samples for each river, stream and water quality index (WQI).

3.2.1. Long Song River Basin

Calculation results at sampling sites on the Long Song River showed that the WQI value does not change too much over time (Figure 8a). The water quality in the section flowing through Lien Huong town is suitable for irrigation purposes.

Water quality in the section flowing through Phong Phu in many times did not meet the purpose of domestic use. However, it is possible to ensure good use of water for irrigation (except for the dry season in 2018 which was heavily polluted due to high TSS content). The WQI index over time on the Long Song River is affected by TSS and turbidity, which makes the total WQI value quite low compared to the minimum value for domestic purposes.

3.2.2. Luy River basin

Calculation results at sites on the Luy River showed that the WQI values fluctuate greatly over time (Figure 8b). The water quality at Ca Giay reservoir location meets the purpose of using water for daily life. Water quality at locations from Xuan Quang dam to upstream is sometimes not good enough for domestic purposes, only meeting the needs of irrigation or navigation. At locations flowing through Luong Son residential area and downstream of Phan Ri Thanh, the WQI has great fluctuations; many times, the water quality is only suitable for navigation purposes. At the location of Xuan Quang dam, because it is located downstream of the agricultural area, the water quality is affected by agricultural production activities, with high TSS, organic matter and nutrients content. The WQI index is at most times only available for irrigation and navigation purposes. The WQI index over the periods on the Luy River is generally affected by TSS, turbidity and organic content due to daily activities and production of people living along the river. These parameters make the total WQI value quite low compared to the minimum value for domestic water supply purposes.

3.2.3. Cai Phan Thiet River basin

Calculation results at locations on the Cai River in Phan Thiet have shown that the WQI value has large fluctuations over time (Figure 8c). The quality of water for domestic use at the Phu Hoi dam site varies greatly between the rainy and dry seasons. In the rainy season, pollutants from agricultural production activities follow the rain to overflow into the river, making the river water quality unsuitable for domestic water use. The water quality in the downstream is only within the limits suitable for irrigation and navigation purposes. The WQI index over the period on the Cai River Phan Thiet is heavily influenced by TSS, turbidity and organic content. The total WQI value is quite low.

3.2.4. Ca Ty River basin

Calculation results at locations on the Ca Ty River have shown that the WQI values fluctuate greatly over time (Figure 8d). The water quality at the Ba Bau dam site is polluted mainly by TSS and the nutrient content is also quite high compared to the threshold for domestic water supply. The section crossing Chay bridge, the water quality in the period of 2019–2021 is good for the purpose of water supply for irrigation. The water quality in the section flowing into Phan Thiet City and Le Hong Phong bridge is only within the limits for irrigation and navigation purposes. The WQI index over the periods on the Ca Ty River is heavily influenced by TSS, turbidity and organic content, making the total WQI value quite low.

3.2.5. Phan River basin

Calculation results at locations on the Phan River show that the WQI values have large fluctuations over time (Figure 8e). The water quality at Tan Nghia dam site is suitable for the purpose of using water for irrigation. In the rainy season in 2018 and 2021, due to high TSS and turbidity, the WQI index only reached the threshold of water use for navigation. The river section passing the Vedan plant shows signs of water quality deterioration; many times, the water quality does not reach the threshold used for irrigation purposes. In the downstream (Tan Thuan and Cau Quang salt production areas) at most of the time of measurement, the WQI value is only within the limit suitable for irrigation and navigation purposes. The WQI index over the period on the Phan River is heavily influenced by TSS, turbidity and organic content, making the total WQI value at many times quite low.

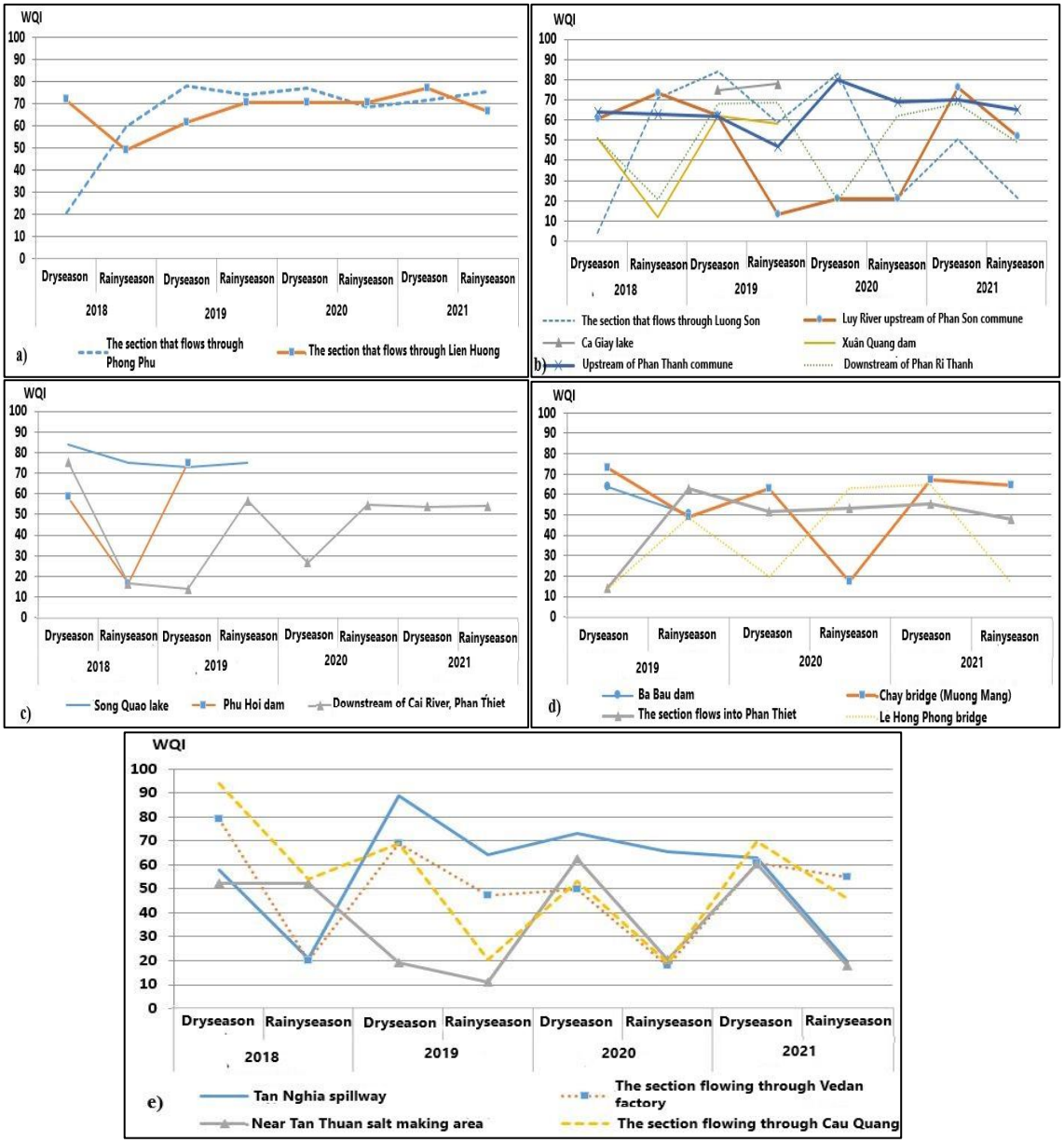

Figure 8. WQI values at sampling locations of surface water in rivers for the period 2018–2021: (a) Long Song River; (b) Luy River; (c) Cai Phan Thiet River; (d) Ca Ty River; (e) Phan River.

River water quality depends mainly on incoming flow, socio–economic development situation as well as discharge of wastewater into water sources in the basins. Usually in the flood season, the turbidity of the river is very high, the river level rises very quickly, the water overflows on the streets, alleys and concentrates on the culverts, canals, ditches and discharges into the river. At that time, the concentration of pollutants in the decreased significantly river in the rainy season because it was diluted many times compared to the dry season, typically the criteria: BOD_5, COD, SS, $N–NH_4^+$, etc.; but these parameters still exceed the water quality standards if not treated. In the dry season, the turbidity of sediment in the river is small, but the content of chemical and biological pollutants increases due to the poor dilution capacity of river water for wastewater from domestic and production activities.

The main wastewater receiving sources in Binh Thuan province within the scope of the investigation include: Nuoc Man River, Long Song River, Luy River, Cai Phan Thiet River, Ca Ty River, and Phan River. The common characteristics of rivers in Binh Thuan are short and steep. Therefore, the transport speed of pollutants that have the potential to cause water pollution after being discharged into the river is quite fast. Along the river basins, there are

many sluices with different discharges. When wastewater flows in, it will change the basic characteristics of natural water sources such as: changing the chemical composition of water, increasing the content of organic substances, mineral salts, appearance of toxic compounds, etc. changes in the ecosystem in the water, the appearance of different pathogenic bacteria and viruses. Previously, the water quality of river basins in the province was relatively good. In recent years, river water quality has been increasingly degraded due to impacts from socio–economic development activities.

3.3. Proposing solutions to protect water sources

3.3.1. Planting forests and trees

Improving land cover and rational use of land resources: The problem of water shortage in the dry season is also related to the protection of watershed forests. Binh Thuan province needs to continue to increase the area of forests and trees, restore ecosystems, and restore biodiversity. It is necessary to make use of the land fund of industrial production establishments to develop more green areas; at the same time renovating the parks to improve the quality of green areas in the area.

3.3.2. Solutions for zoning waste water in river basins

Purpose: zoning the receiving basin for different purposes of water use. From there, regulate the discharge level for each waste source to ensure the quality of water for water supply needs. For water areas used for domestic water supply purposes upstream, discharge sources in this area require mandatory wastewater treatment before discharging into the environment and meeting grade A standards compared to QCVN on waste water treatment. industrial, medical, domestic wastewater, etc. For water sources for non–domestic purposes, the discharge sources must be treated before being discharged into the environment and the quality of the wastewater is grade B compared with the current QCVN.

3.3.3. Propaganda to raise awareness of the community and businesses

Implement public and business awareness raising through the media or through actual operational models. Propagating and mobilizing people to use pesticides and chemical drugs rationally in agricultural production; do not throw plant protection drug bottles, jars and packages into canals, ditches, ponds, lakes and canals; do not discharge wastewater, domestic and production waste into the river. Organize an extensive emulation movement in the community. Implement water protection plans at all levels, branches and establishments, and all classes of people with practical actions; at the same time, take appropriate measures to sanction actions that violate the law on water source protection.

3.3.4. Encourage establishments to reduce pollution

Proposing to state levels on funding and pilot application of cleaner production program for production and business establishments in Binh Thuan province. To encourage production enterprises to invest, renew production technology and import new modern and environmentally friendly machines and equipment. Encourage voluntary establishments to relocate their production sites to the planning area. Encourage businesses to actively apply the 3Rs (Recycle – Reuse – Recovery) program. These activities are fundamental to reducing waste and optimizing the production process.

3.3.5. Management of waste sources from agricultural activities

Promote the application of technical advances in crop production. Strengthen education, propaganda and dissemination of harmful effects caused by pesticide pollution in production

to contribute to reducing environmental pollution. To build and develop the collection of used plant protection drug packages and expired veterinary drugs for communes and townships throughout the province. Organize cooperatives or teams, groups or groups of environmental sanitation in each commune/district, to collect hazardous waste in rural areas. Converting from scattered, small–scale livestock to concentrated farm farming towards industrial and semi–industrial direction to facilitate wastewater collection and treatment.

For waste from farming activities, residues of fertilizers and pesticides are lost to the environment relatively large (especially for wet rice models). In agricultural extension work, provide documents and information related to farming techniques, in which fertilization techniques and use of plant protection chemicals are based on the 4 right principles (right type, right dose, right amount) method and at the right time) is essential. Encourage the use of environmentally friendly chemicals, strictly prohibit and strictly control the use of plant protection chemicals outside the permitted list.

4. Conclusion

People's lives and socio–economic development in Binh Thuan province is associated with rivers and river basins. Nature has provided a source of water for people to live, eat, drink, and produce. But the downside is that it is humans who have put waste into the water, whether intentionally or unintentionally over the years, making the water source polluted. By traditional research methods, survey and evaluation, the authors analyzed the physico–chemical indicators of surface water quality and determined the pollution level at the measurement and monitoring locations. Through that, the authors have identified the current status of pollution caused by socio–economic activities. Moreover, the authors have calculated the WQI index to provide data for water users as well as managers to see the full picture of the extent of polluted areas. Since then, a number of practical solutions have been proposed to protect water resources, aiming to manage and use water sustainably. In addition, the research results are limited because only the WQI index is evaluated, but the correlation between the pollution components of the 5 studied river basins has not been evaluated. In addition, research is limited to only 5 main river basins of the province, it is necessary to expand some more canals and groundwater sources.

Authors contribution: Constructing research idea: H.P., H.T.N.H.; Select research methods: H.P., H.T.N.H., N.T.D., T.T.M.H.; Data processing: H.P., H.T.N.H., N.T.D.; Sample analysis: H.P., H.T.N.H., T.T.M.H.; Take samples: H.T.N.H., T.T.M.H.; Writing original draft preparation: H.P., H.T.N.H.; N.T.D.; Writing review and editing: H.P., H.T.N.H.

Acknowledgments: This study was carried out under the sponsorship of the Binh Thuan main Rivers Water Quality Research Project, under the Phu My Water Resources and Environment Technology Development Institute.

Conflicts of interest: The authors declare that this article was the work of the authors, has not been published elsewhere, has not been copied from previous research; there was no conflict of interest within the author group.

References

1. Hydrometeorological Station of the South-Central Region. Hydro–climate characteristics of Binh Thuan province, 2021.
2. Cat, L.V.; Nhung, D.T.H.; Cat, N.N. Quality aquaculture water and quality improvement solutions. Science and Technology Publishing House, Hanoi, 2006, pp. 424.
3. Boyd, C.E. Water quality for pond Aquaculture. Department of Fisheries and Allied Aquacultures. Auburn University, Alabama 36849 USA, 1998, pp. 37.

4. Wu, Z.; Zhang, D.; Cai, Y.; Wang, X.; Zhang, L.; Chen, Y. Water quality assessment based on the water quality index method in Lake Poyang: The largest freshwater lake in China. *Sci. Rep.* **2017**, *7*, 17999.
5. Phu, H.; Manh, T.X.; Huong, N.H. Research project on simulation of flood flow in Ve river basin, 2013.
6. Jena, V.; Dixit, S.; Gupta, S. Assessment of water quality index of industrial area surface water samples. *Int. J. Chem Tech Res.* **2013**, *5(1)*, 278–283.
7. Toma, J.J. Water Quality Index for Assessment of Water Quality of Duhok Lake, Kurdistan Region of Iraq. *J. Adv. Lab. Res. Biol.* **2012**, *3(3)*, 19–24.
8. Son, C.T.; et al. Assessment of water quality in some rivers in Gia Lam district using WQI water quality index. *J. Sci. Technol. Univ. Nat. Resour.* **2019**, *200(07)*, 113–140.
9. Luu, P.T. Using water quality index (WQI) and biological index of algae (BDI) to assess water quality of Saigon River. *Sci. J. Pedagogy Univ.* **2020**, *17(9)*, 1558–1596.
10. Phu, H. Research on building data sets for the application of mathematical models to simulate water quality changes in La Nga river in Binh Thuan. *J. Hydrometeorol.* **2013**, pp. 26–32. (in Vietnamese)
11. Southern Institute of Irrigation Science. Irrigation development planning in Binh Thuan province for the period 2011–2020, 2012.
12. Binh Thuan Statistical Office (2018–2021). Binh Thuan Provincial Statistical Yearbook.
13. Government. Decree No. 80/2014/ND–CP dated 6/8/2014, Decree on drainage and wastewater treatment, 2014.
14. Binh Thuan Water Supply and Sewerage Joint Stock Company. Environmental monitoring report of Binh Thuan Water Supply and Sewerage Joint Stock Company, phase 1, 2015.
15. Hydrometeorological Station of the South Central Region. Hydro–climate characteristics of Binh Thuan province, 2021.
16. Uyen, N.T.T. Research and propose steamed anchovy wastewater treatment technology at My Tan Steamed Anchovy Village, Ninh Hai District, Ninh Thuan Province. Graduation Project from Technical University, 2010.
17. Phu, H. et al. Thesis Research, application and testing of hydro–hydraulic models for flood forecasting and flood warning of La Nga river, Binh Thuan province. Ministry level project, 2014.
18. Phu, H.; Manh, T.X.; Huong, N.H. Research project on simulation of flood flow in Ve river basin, 2013.
19. Binh Thuan Provincial People's Committee. Decision No. 634/QD–UBND dated February 25, 2014 on adjustment and supplementation of industrial cluster development planning in Binh Thuan province to 2020, 2014.
20. IUCN. Flow – the essentials of environmental flows, UK. Edited by: Megan Dyson, Ger Bergkamp and John Scanlon, 2003.
21. http://ncdsnet.anu.edu.au/pdf/jbennett/chmdrr01.pdf (2004).
22. http://wwf.panda.org/about_our_earth/about_freshwater/rivers/irbm/.

Table of content